

AD A118-4

BMO-TR-82-28

SAI DOCUMENT NO. SAI-067-82R-015

**MANEUVERING AEROTHERMAL
TECHNOLOGY (MAT) PROGRAM**

**MAT PROGRAM TEST SUMMARY REPORT
BICONIC BODY WITH SLICE/FLAP**

SCIENCE APPLICATIONS, INC.
APPLIED MECHANICS OPERATION
WAYNE, PENNSYLVANIA 19087

JANUARY 1982

FINAL REPORT FOR PERIOD 16 MAY 1980 - 15 FEBRUARY 1982

CONTRACT NO. F04701-80-C-0033

APPROVED FOR PUBLIC RELEASE; DISTRIBUTION UNLIMITED.


AIR FORCE BALLISTIC MISSILE OFFICE
NORTON AIR FORCE BASE, CALIFORNIA 92409


DTIC FILE COPY

DTIC
ELECTE
S AUG 16 1982
A

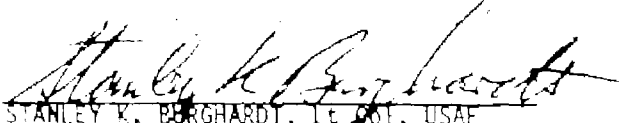
82 08 16 265

This Final Report was submitted by Science Applications, Inc.,
994 Old Eagle School Rd., Valley Forge, PA 19087 under Contract Number
F04701-80-C-0033 with the Ballistic Missile Office, AFSC, Norton AFB,
California. Capt John E. Keesee, SMC/SYMS was the Project Officer in charge.
This Technical Report has been reviewed and is approved for publication.


JOHN E. KEESSEE, Capt, USAF
Project Officer
Advanced Systems
Advanced Strategic Missile Systems


KEVIN E. YELMEISEN, Major, USAF
Chief, Advanced Systems Division

FOR THE COMMANDER


STANLEY K. BERGHARDT, Lt Col, USAF
Assistant Deputy for Advanced
Strategic Missile Systems

UNCLASSIFIED

SECURITY CLASSIFICATION OF THIS PAGE (When Data Entered)

REPORT DOCUMENTATION PAGE		READ INSTRUCTIONS BEFORE COMPLETING FORM
1. REPORT NUMBER BMO-TR-82-28	2. GOVT ACCESSION NO. AD-A118 242	3. RECIPIENT'S CATALOG NUMBER
4. TITLE (and Subtitle) MAT Program Test Summary Report -Biconic Body with Slice/Flap-		5. TYPE OF REPORT & PERIOD COVERED Final Report 16 May 1980 - 15 Feb. 1982
		6. PERFORMING ORG. REPORT NUMBER SAI-067-82R-015
7. AUTHOR(s) A. Martellucci S. Weinberg		8. CONTRACT OR GRANT NUMBER(s) F04701-80-C-0033
9. PERFORMING ORGANIZATION NAME AND ADDRESS Science Applications, Inc. 994 Old Eagle School Rd., Suite 1018 Wayne, Pennsylvania 19087		10. PROGRAM ELEMENT, PROJECT, TASK AREA & WORK UNIT NUMBERS Task 2.3
11. CONTROLLING OFFICE NAME AND ADDRESS Ballistic Missile Office/SYDT Norton Air Force Base, California 92409		12. REPORT DATE January 1982
		13. NUMBER OF PAGES 250
14. MONITORING AGENCY NAME & ADDRESS (if different from Controlling Office)		15. SECURITY CLASS. (of this report) Unclassified
		15a. DECLASSIFICATION/DOWNGRADING SCHEDULE
16. DISTRIBUTION STATEMENT (of this Report) Approved for public release; distribution unlimited. Distribution Statement "A" of AFR 80-45 applies.		
17. DISTRIBUTION STATEMENT (of the abstract entered in Block 20, if different from Report)		
18. SUPPLEMENTARY NOTES		
19. KEY WORDS (Continue on reverse side if necessary and identify by block number) Aerodynamics Shock Layer Survey Maneuvering Body Bicones Heat Transfer Sliced Body Surface Pressure Flap Hypersonic Flow		
20. ABSTRACT (Continue on reverse side if necessary and identify by block number) Detailed shock layer surveys, surface heat transfer and pressure, and force and moment data were obtained on sharp and blunted bicone models tested under laminar and turbulent boundary layer flow conditions. The objective of these tests is to obtain a basic body of data under hypersonic flow conditions, and under a variety of flow conditions and geometric parameters which would be useful for checking and validating the newly developed parabolized Navier- Stokes (PNS) codes, and other detailed flow field codes. Tests were conducted at the von Karman Facility (VKF) of the Arnold Engineering Development (over)		

DD FORM 1 JAN 73 1473 EDITION OF 1 NOV 65 IS OBSOLETE

1.

UNCLASSIFIED

SECURITY CLASSIFICATION OF THIS PAGE (When Data Entered)

SECURITY CLASSIFICATION OF THIS PAGE(When Data Entered)

This report presents a summary listing of all of the data obtained using this model, that is those data obtained at AEDC prior to the MAT program and also those data obtained under MAT program auspices. It makes no attempt to present the voluminous body of data obtained, per se, rather it is intended to provide the user with a collected detailed (including AEDC run numbers) listing of all of the data obtained including all pertinent test details and data reduction procedures inherent in the listings. Also included in this report are some limited data trends, highlights, and general observations as well as examples of data retrieved for code comparison purposes.

1

UTRE
COPY
INSPECTED

FOREWORD

This report presents the work performed for the Ballistic Missile Office (BMO) by Science Applications, Inc. (SAI) under the auspices of the Phase I part of the Maneuvering Aerothermal Technology (MAT) program (contract F04701-80-C-0033) for the period 16 May 1980 through 15 February 1982. This specific effort was accomplished under Task 2.3 (Experimental Studies) and was monitored by Capt. J. Keesee (BMO/SYDT) and D. Farlow (TRW/DSSG).

Contained in this report is a summary of all data obtained in the "HYTAC" sliced-bicone test series; that is those tests conducted by AEDC for BMO concluding with the tests run by SAI under the MAT program sponsorship.

The authors wish to acknowledge the following personnel of the von Karman Gas Dynamics Facility (VKF) of the Arnold Engineering Development Center (AEDC): D. B. Carver, S. M. Coulter, and D. L. Lanham for their assistance in the planning and conducting of the tests. The authors also wish to express their appreciation to J. T. Best (Aerodynamics Systems Division - USAF AEDC) for his assistance in the planning, scheduling, and cost maintenance of the test program.

This report has been reviewed and is approved.

J. Keesee, Capt. U.S.A.F.
Ballistic Missile Office (BMO/SYDT)
Air Force Systems Command
Norton Air Force Base, California

TABLE OF CONTENTS

	<u>Page</u>
LIST OF FIGURES	6
LIST OF TABLES	10
NOMENCLATURE	12
TABULATED DATA KEY	15
1.0 INTRODUCTION	26
2.0 APPARATUS	29
2.1 Test Facilities	29
2.2 Model Detail	31
2.2.1 Basic Body	31
2.2.2 Slice Region	33
2.2.3 Flap	33
2.2.4 Roughness/Boundary Layer Trips	36
2.2.5 Instrumentation	43
2.2.5.1 Static Force	43
2.2.5.2 Model Surface Instrumentation	44
2.3 Flow Field Survey Probes and Probe System	48
2.3.1 Pitot and Unshielded Thermocouple Probes	53
2.3.2 Preston Tube	54
2.3.3 Mach/Flow-Angularity Probe	54
3.0 SUMMARY OF TEST CONDITIONS AND DATA ACQUIRED	58
3.1 Axisymmetric Body - Turbulent Flow: $M_{\infty} = 6, \alpha = 0$ (References 4 and 5)	62
3.2 Axisymmetric Body - Turbulent Flow: Mach 8, $\alpha = 0$ (Reference 6)	67
3.3 Sliced Body w/o Flap - Laminar Flow: Mach 10, $\alpha \neq 0$ (References 2, 7)	89
3.4 Sliced Body w/Flap - Turbulent Flow: $M_{\infty} = 8, \alpha \neq 0$ (References 3 and 8)	101
4.0 SHOCK LAYER SURVEY DATA REDUCTION AND PROBE CALIBRATION ISSUES	119
4.1 Unshielded Total Temperature Probe Reynolds Number Correction	119
4.2 Angle-of-Attack Probe Calibrations	120
4.3 Boundary Layer Type-Data Reduction	124

TABLE OF CONTENTS

	<u>Page</u>
5.0 TEST DATA HIGHLIGHTS	131
5.1 Boundary Layer Trip Effectiveness	131
5.2 Limited Data Trends and Highlights	133
6.0 DATA USAGE FOR TECHNIQUE VALIDATION	152
6.1 Wall Temperature Considerations	152
6.2 Representative Comparisons of Theories with Data	153
6.2.1 Static Force and Moment	153
6.2.2 Surface Static Pressure	154
6.2.3 Surface Heat Transfer	165
6.2.4 Shock Layer Surveys	168
REFERENCES	176
APPENDIX A	179
A.1 Test Conditions	179
A.2 Surface Heat Transfer Measurements	179
A.3 Model Surface Pressure	180
A.4 Shock Layer Surveys	192
A.4.1 Preston Tube Data	192
A.4.2 Shock Layer Survey Data	194
A.5 Static Force Data	223

LIST OF FIGURES

<u>No.</u>	<u>Title</u>	<u>Page</u>
1	Tunnel Layout	30
2	Basic Model Geometry	32
3	Aft Slice Sections	34
4	Flap Details	35
5	Boundary Layer Trip Geometry [$M_\infty = 6, \alpha = 0$]	37
	a. Distributed Grit Trip	37
	b. 7-deg Grit Blasted Nose	38
	c. Grooved 7-deg Insert	38
	d. Grooved 14-deg Nose	38
	e. Spherical Element Trips	39
6	Boundary Layer Trip Geometry [$M_\infty = 8, \alpha \neq 0$]	40
	a. Machined Trips	40
	b. Grid Bonded Trips	41
7	Photograph of the Machined Boundary Layer Trip [$M_\infty = 8, \alpha \neq 0$]	42
8	Photograph of the Bicone Model Static Force Installation Viewed in the Dump Tank Below Tunnel B	45
9	Photograph of the Bicone Model Static Force Installation in Tunnel B	46
10	Photograph of the Probe Housing Assembly with the Probe Assembly Attached	49
11	Photograph of the Probe Assembly	50
12	Close-up Photograph of the Probe Assembly	51
13	Photograph of the Probe Assembly Shown in Proximity to the 10.50/70 Bicone Model	52
14	Pitot and Total Temperature Probes	55
15	Preston Tube	56
16	Mach/Flow-Angularity Probe	56
17	Probe Survey Locations	63
18	Overhead Probe Survey Locations	82
19	Model Surface Instrumentation a. Biconic Region	94
	b. Sliced Section Details	95
20	Sketch of Flow-Field Probes Mounted in Probe Holder	96
21	10.50/70 Biconic Model Surface Instrumentation-Biconic Region	103
22	Model Surface Instrumentation, Sliced Region Detail	104
23	Flap Instrumentation Details	105
24	Probe Holder Assembly with Total Temperature, Pitot and Preston Tubes	112
25	Probe Holder Assembly-Mach/Flow-Angularity Probe	113
26	Representative Total Temperature Probe Calibration	121
27	Representative Pitot and Total Temperature Probe Calibration with α	122

LIST OF FIGURES (CONT'D)

<u>No.</u>	<u>Title</u>	<u>Page</u>
28	Static Pressure Distributions Through the Shock Layer	126
29	PNS Predicted Flap Region Static Pressure Profiles Through the Shock Layer	127
30	Illustrative Example of Reduced 'HYTAC' Data - 10.50/70 Bicone $\alpha = 10^\circ$, $\delta_F = 10^\circ$, Station 76	128
31	Boundary Layer Trip Effect on 10.50/70 Bicone Surface Heat Transfer at $\alpha = 0^\circ$	132
32	Angle-of-Attack Variation of Heating at $x = 22"$ for Various Trip Heights	134
33	Axial Heating Distribution for Several Meridional Rays 10.50/70 Bicone with 13 mil Trip at $\alpha = 10^\circ$	135
34	Axial Heating Distribution for Several Meridional Rays 10.50/70 Bicone with 33 mil Trip at $\alpha = 10^\circ$	136
35	Axial Heating Distribution for Several Meridional Rays 10.50/70 Bicone with 13 mil Trip at $\alpha = 20^\circ$	137
36	Axial Heating Distribution for Several Meridional Rays 10.50/70 Bicone with 33 mil Trip at $\alpha = 20^\circ$	138
37	Schematic Location of the Profile Stations on the 10.50/70 Bicone	140
38	Representative Shock Layer Profiles on the 10.50/70 Bicone at $\alpha = 0^\circ$	141
39	Representative Flap Shock Layer Profiles on the 10.50/70 Bicone at $\alpha = 0^\circ$	142
40	Angle of Attack Variation of the 10.50/70 Bicone Slice Centerline Pressure Distribution	143
41	Slice/Flap Centerline Pressure Distribution for the 0.50" Blunted 10.50/70 Bicone at $\alpha = 0^\circ$	144
42	Chord and Spanwise Distribution of Flap Pressures for $\delta = 10^\circ$	146
43	Angle of Attack Variation of the 10.50/70 Blunted Bicone Centerline Slice Heating Distribution	147
44	Centerline Heating Distribution on the 10.50/70 Biconic Slice/Flap	148
45	Chord and Spanwise Distribution of Flap Heating on the 10.50/70 Bicone for $\alpha = 10^\circ$	149
46	Surface Shear Distribution in the Slice Region of the Blunted 10.50/70 Bicone	150
47	Surface Shear Variation with Angle of Attack - Cone and Slice Region	151
48	Force and Moment Coefficients for the 0.5"R Blunted 70° Cone	155
49	Force and Moment Coefficients for the 0.5"R Blunted 140/70 Bicone	156
50	Force and Moment Coefficient Comparisons for the Blunted 140/70 Bicone with Windward Cut	157

LIST OF FIGURES (CONT'D)

No.	Title	Page
51	Longitudinal Pressure Distribution on the Blunted 10.5°/7° Bicone at $\alpha = 0^\circ$	158
52	Longitudinal Pressure Distribution on the Blunted 10.5°/7° Bicone at $\alpha = 10^\circ$	159
53	Surface Pressure Distribution in the 10.5°/7° Blunted Bicone Control Region - $\alpha = 0^\circ$	161
54	Surface Pressure Distribution in the 10.5°/7° Blunted Bicone Control Region - $\alpha = 10^\circ$	162
55	Axial Pressure Distribution for the Blunted 10.5°/7° Bicone at $\alpha = 10^\circ$	163
56	Peripheral Pressure Distribution for the Blunted 10.5°/7° Bicone $\alpha = 10^\circ$	164
57	Axial Distribution of the Laminar Heat Transfer Results for the Blunted 14°/7° Bicone at $\alpha = 10^\circ$	166
58	Axial Distribution of the Turbulent Heat Transfer on the Blunted 10.5°/7° Bicone at $\alpha = 10^\circ$	167
59	Axial Distribution of the 3DMEIT Predicted Turbulent Heat Transfer for the 10.5°/7° Blunted Bicone at $\alpha = 10^\circ$	169
60	Peripheral Distribution of the 3DMEIT Predicted Turbulent Heat Transfer for the 10.5°/7° Blunted Bicone at $\alpha = 10^\circ$ ($s = 30''$)	170
61	Comparison of the Pitot Pressure Inviscid Predictions with Data for the 14°/7° Blunted Bicone at $\alpha = 0^\circ$	171
62	Comparison of Predicted Shock Layer Profiles with Windward Ray Data for the Blunted 7° Cone at $\alpha = 10^\circ$ ($x = 24.4''$)	173
63	Comparison of Predicted Shock Layer Profiles with Windward Ray Data for the Blunted 7° Cone at $\alpha = 10^\circ$ ($x = 34.4''$)	174
64	Comparison of Predicted Shock Layer Profiles with Leeward Ray Data for the Blunted 7° Cone at $\alpha = 10^\circ$ ($x = 34.4''$)	175
A-1	Heat Transfer Data (Leeside, $\alpha = 10^\circ$)	184
A-2	Surface Pressure Data (Windward, $\alpha = 20^\circ$)	189
A-3	Surface Pressure Data (Leeside, $\alpha = 20^\circ$)	190
A-4	Surface Pressure Data (Meridional, $\alpha = 20^\circ$)	191
A-5	Preston Tube Data Reduction Flow Chart	193
A-6	Typical Prediction Program Results (Probe Pressure)	198
A-7	Typical Prediction Program Results (Model Pressure)	199
A-8	Mach/Flow Angularity Probe Calibration Data and Curve Fits	200 201
A-9	Velocity Vector Definition with Respect to the Probe Axis System	205

LIST OF FIGURES (CONT'D)

<u>No.</u>	<u>Title</u>	<u>Page</u>
A-10	Velocity Vector Definition with Respect to the Tunnel Axis System	206
A-11	Velocity Vector Definition with Respect to the Model Axis System	207
A-12	Shock Layer Uncorrected Total Temperature Data	208
A-13	Shock Layer Corrected Total Temperature Data	209
A-14	Shock Layer Pitot Pressure Data	210
A-15	Shock Layer Pitot Pressure Data	211
A-16	Derived Local Mach Number and Velocity Data	228
A-17	Derived Local Static and Total Temperature Data	229
A-18	Derived Local Density and Reynolds Number Data	230
A-19	Mach/Flow-Angularity Probe Pressure Data	242 243
A-20	Mach/Flow-Angularity Derived Directional Data	245

LIST OF TABLES

<u>NO.</u>	<u>TITLE</u>	<u>Page</u>
1	Tunnels B and C Performance	29
2	Summary of Data Obtained on the Sharp and Blunt 7° Cones	59
3	Summary of Data Obtained on the Sharp and Blunt 10.5°/7° and 14°/7° Bicones	60
4	Surface Instrumentation Locations	64
	a. Pressure Orifices	64
	b. Heat Gages	65
5	Heat Transfer Data Summary - Mach 6, $\alpha = 0$	68
	a. Heat Transfer Data Summary - Mach 6, $\alpha = 0$	69
	b. Surface Pressure Data Summary - Mach 6, $\alpha = 0$	70
	c. Profile Data Summary - Mach 6, $\alpha = 0$	71
6	Heat Transfer Gage Locations	73
	a. 7 Degree Sharp Cone (RN = 0.0015 in.)	73
	b. 7 Degree Blunt Cone (RN = 0.50 in.)	74
	c. 10.5/7 Degree Biconic (RN = 0.50 in.)	75
	d. 14/7 Degree Biconic (RN = 0.50 in.)	76
7	Pressure Orifice Locations	77
	a. 7 Degree Sharp Cone (RN = 0.0015 in.)	77
	b. 7 Degree Blunt Cone (RN = 0.50 in.)	78
	c. 10.5/7 Degree Biconic (RN = 0.50 in.)	79
8	Test Data Summary - Axisymmetric Models @ Mach 8	83
	a. Gardon Gage Heat Transfer Data	83
	b. Coax Gage Heat Transfer Data	84
	c. Model Surface Pressure Data	85
	d. Flow Angle Sensitive Preston Tube Data	86
	e. Overhead Probe Survey Data	87
	f. Onboard Probe Survey Data	88
9	Model Instrumentation Locations	91
	a. Gardon Gage Locations	91
	b. Pressure Orifice Locations	92
	c. Coaxial Surface Thermocouple Locations	92
10	Test Data Summary - Mach 10	98
	a. Static Force Data - $Re_{\infty} = 1.0 \times 10^6/\text{ft}$	98
	b. Heat Transfer Data	99
	c. Model Pressure Data	100
	d. Flow Field Survey Data	100

LIST OF TABLES (Cont'd)

<u>NO.</u>	<u>TITLE</u>	<u>Page</u>
11	Model Instrumentation Locations	106
	a. Gardon and Coax Gage Locations	106
	b. Pressure Orifice Locations	107
	c. Orifice and Gardon Gage Locations	108
12	Flap Instrumentation Locations	110
13	Test Data Summary	116
	a. Force and Moment	116
	b. Surface Pressure Data	116
	c. Heat Transfer and Oil Flow Data	117
	d. Shock Layer Survey & Surface Shear Data	118
14	Total Temperature Probe Calibration Data from the MAT Program Test Phase	123
A-1	Heat Transfer Data	181
A-2	Surface Pressure Data	185
A-3	Shock Layer Data	212
A-4	Boundary Layer and Shock Layer Derived Data	224
A-5	Mach/Flow-Angularity Probe Measured Data	231
A-6	Mach/Flow-Angularity Derived Directional Data	240
A-7	Force and Moment Data	246

NOMENCLATURE

ALPT	Pitch angle of the overhead probe drive (Z' direction) measured from the tunnel vertical axis
C	Flap chord length
CCTV	Closed Circuit television system
C_F	Skin friction coefficient, τ_w/q_∞
C_m	Pitching moment coefficient
C_N	Normal force coefficient
D	Diameter
DX	Computation step size
H,h	Boundary layer trip height
ℓ	Axial distance from bicone-slice juncture
M	Mach number
MACS	Model Attitude Control System
MAT	Maneuvering Aerothermal Technology Program
p	Pressure
PP	Pitot pressure
PT, P_0	Tunnel stilling chamber (total) pressure
PNS	Parabolized Navier Stokes flowfield code
q	Dynamic pressure
r	Radius
Re	Reynolds number
Re_0	Local Reynolds number with viscosity based on freestream total temperature
R_N	Nose radius
S	Curvilinear surface distance from model nosetip

NOMENCLATURE (CONT'D)

s	Flap semi-span
ST_{∞} , ST(TT)	Stanton number based on freestream total temperature
T	Temperature
TG	Thermocouple gage
TT, T_o	Total temperature
TTL	Local total temperature
u	Velocity
X,Y,Z	Model axial, lateral and vertical coordinates
XF	Chordwise distance from flap leading edge
YF	Spanwise distance from flap centerline
Z'	Probe travel direction
ZP	Height of Pitot probe above model surface (Z' direction usually normal to the local surface unless otherwise specified)
α	Angle of attack
β	Angle of sideslip
γ	Specific heat ratio
δ	Flap deflection angle
δ^*	Boundary layer displacement thickness
δ_T	Thermal boundary layer thickness
δ_3	Boundary layer kinetic energy thickness
δ_4	Boundary layer total enthalpy thickness
η	Recovery factor
θ	Boundary layer momentum thickness

NOMENCLATURE (CONT'D)

θ_c	Cone half-angle
ρ	Density
τ_w	Shear stress at wall
ω	Meridian angle

SUBSCRIPTS

b	Body
c	Corrected
e	Boundary layer edge
L	Local
m	Measured
o,t	Total
REF	Reference
s	Shock
STAG	Stagnation point
W	Model wall
∞	Free-stream

TABULATED DATA KEY

A	Reference area, 75.784 in. ²
AATCA, α_T	Total pitch angle sensed by the Mach/Flow-Angularity probe, deg.
AB	Base area, 75.784 in. ² (no slices) or 69.912 in. ² (double slice)
ALPHA	Angle of attack deg
ALPHA SECTOR	Pitch angle of the tunnel sector, positive nose up, deg
ALPHAP	Model total angle of attack in the missile axis system, designated as positive for nose up attitude, deg
ALPI	Indicated pitch angle, deg
ALPO	Nominal pitch angle of the Mach/Flow-Angularity probe relative to the probe drive (Z' axis), positive nose up, deg
ALPP	Nominal pitch angle of the Mach/Flow-Angularity probe with respect to the vertical (Tunnel ZT axis), [ALPT + ALPO], deg
ALPT	Pitch angle that the overhead probe drive makes (Z' direction) with respect to the vertical (Tunnel ZT axis), deg
APP, AP(1 - 5), APRES, APPU, APW	Pressure stabilization routine slip flow coefficients for the Pitot tube, Mach/Flow-Angularity probe, Preston tube, upper Pitot, and surface pressure orifices, respectively, psia
AW	Speed of sound based on TW, ft/sec
BETA	Sideslip angle, deg
CA	Forebody axial-force coefficient, body axes, CAT-CAB
CAB	Base axial-force coefficient, body axes, -AB(PBA-P)/Q·A
CAT	Total axial-force coefficient, body axes, total axial force/Q·A

CCW	Cross-wind coefficient, wind axes
CDW	Forebody drag coefficient, wind axes
CFX	Skin friction coefficient, $[TAUX/Q]$
CLL	Rolling-moment coefficient, body axes, rolling moment/ $Q \cdot A \cdot LM$
CLLW	Rolling-moment coefficient (based on CLMF), wind axes
CLM	Pitching-moment coefficient, body axes, pitching moment/ $Q \cdot A \cdot LM$
CLMF	Forebody pitching-moment coefficient, body axes, $CLM + CAB \cdot ZB/LM$
CLMW	Pitching-moment coefficient (based on CLMF), wind axes
CLN	Yawing-moment coefficient, body axes, yawing moment/ $Q \cdot A \cdot LM$
CLNW	Yawing-moment coefficient, wind axes
CLW	Lift coefficient (based on CA), wind axes
CN	Normal-force coefficient, body axes, normal force/ $Q \cdot A$
CODE	Configuration code number
CONFIGURATION	Model configuration description (10.5/7-DEG BICONIC/SS + DS) where SS + DS = single slice and double slice
CPBA	Average base pressure coefficient, $(PBA-P)/Q$
CPHI	Local radial direction of the flow with respect to the Mach/Flow-Angularity probe, deg
C.R.	Center of rotation, axial station along the tunnel centerline about which the model rotates, in.
CY	Side-force coefficient, body axes, side force/ $Q \cdot A$
D	Preston tube outside diameter, ft

DCAT	Flap differential total axial-force coefficient, body axes, CAT(flap on) - CAT (flap off)
DCLL	Flap differential rolling-moment coefficient, body axes, CLL (flap on) - CLL (flap off)
DCLM	Flap differential pitching-moment coefficient, body axes, CLM (flap on) - CLM (flap off)
DCLMF	Flap differential forebody pitching-moment coefficient, body axes, CLMF (flap on) - CLMF (flap off)
DCLN	Flap differential yawing-moment coefficient, body axes, CLN (flap on) - CLN (flap off)
DCN	Flap differential normal-force coefficient, body axes, CN (flap on) - CN (flap off)
DCY	Flap differential side-force coefficient, body axes, CY (flap on) - CY (flap off)
DEL	Boundary-layer thickness, in.
DEL*	Boundary-layer displacement thickness, in.
DEL**	Boundar-layer momentum thickness, in.
DEL3	Boundary-layer kinetic energy thickness, in.
DEL4	Boundary-layer total enthalpy defect, in.
DEW	Free-stream flow frost point, °F
DITTE	Enthalpy difference at boundary-layer edge [ITTE - ITWX], Btu/lbm
DITTL	Local enthalpy difference [ITTL - ITWX], Btu/lbm
DPSQP	Mach/Flow-Angularity probe nondimensional parameter, $[(DP13)^2 + (DP24)^2]^{0.5} / (2 \cdot P5)$
DP13	Differential pressure measurement of the Mach/ Flow-Angularity probe in the pitch plane [P1-P3], psid

DP24	Differential pressure measurement of the Mach/Flow-Angularity probe in the yaw plane [P2-P4], psid
DTAU	Preston tube data reduction iteration parameter, lb/ft ²
DY	Lateral movement of probe assembly during Preston tube surveys, referenced to the survey station number, same sign convention as YT, in.
ETA	Effective total-temperature probe recovery factor for calibration data: $ETA = (TTLU - T)/(TT - T)$ For Survey data: $ETA = \sum_{i=0}^1 A_i \sqrt{RETD}$ where the values of A_i were determined for each thermocouple probe.
FLAP	Flap deflection angle with respect to model center-line, deg, positive down at PHI = 0
FRA	Preston tube data reduction parameter
FUN	Preston tube data reduction parameter
G	Preston tube data reduction parameter
Ġ	Preston tube data reduction parameter
GAGE NO	Identification number for Gardon gages
H(TT)	Heat-transfer coefficient, [QDOT/(TT-TW)], Btu/ft ² -sec-°R
ITTE	Enthalpy of air based on TTE, Btu/lbm
ITT	Enthalpy of air based on TT, Btu/lbm
ITTL	Enthalpy of air based on TTL, Btu/lbm

ITW	Enthalpy of air based on TW, Btu/lbm
ITWX	Enthalpy of air based on TWX, Btu/lbm
KPP, KPPU, KPRES, KPW, KP (1-5)	Coefficients obtained by the pressure stabilization routine for Pitot pressure, upper Pitot pressure, Preston tube pressure, surface pressure Mach/Flow-Angularity pressures 1-5. 1/psi-sec
KNPP, KNPPU, KNPRES, KNPW, KNP (1-5)	Nominal stabilization coefficients, evaluated by an examination of the calculated coefficients defined above. 1/psi-sec
(L/D)W	Lift-to-drag ratio (based on CA), wind axes
LM	Model reference length, in.
M	Free-stream Mach number
ME	Mach number at boundary-layer edge (ML at DEL)
ML	Local Mach number, from Pitot pressure and wall pressure measurements
MLC	Local Mach number inferred by the Mach/Flow Angularity probe
MODEL-ROLL	Model roll angle, zero for single slice on top and positive for clockwise rotation, looking upstream, deg
MT	Preston tube data reduction parameter
MU	Dynamic viscosity based on free-stream temperature, lbf-sec/ft ²
MUTE	Dynamic viscosity based on TE, lbf-sec/ft ²
MUTL	Dynamic viscosity based on TL, lbf-sec/ft ²
MUW	Dynamic viscosity based on TW, lbf-sec/ft ²
MUTTL	Dynamic viscosity based on TTL, lbf-sec/ft ²
M2	Local Mach number, from Preston tube and wall pressure measurements

NCP	Normal-force center-of-pressure location, body axes, inches from model nose, XMRP-(CLM-LM/CN)
NOSE RADIUS, RH	Model nose radius, in.
OMEGA	Radial position of gages or orifices, deg
ORIFICE	Identification number of the pressure orifices
P	Free-stream static pressure, psia
PAVG	Average pressure value of the Mach/Flow-Angularity probe "static orifices" $[(P_1 + P_2 + P_3 + P_4)/4]$, psia
PAVGP5	Ratio, PAVG/P5
PAVGP5C	PAVGP5 corrected for Reynolds number effects
	$\text{PAVGP5C} = \frac{\text{PAVGP5}_{\text{RE}} \approx 3.7}{\text{PAVGP5}_{\text{REL}}} \cdot \text{PAVGP5}_{\text{REL}}$
PBA	Average base pressure, psia
PBI	Base pressure, $i = 1$ to 4 , psia
PHI	Model roll angle, deg
PHII	Indicated roll angle, deg
PHIO	Roll alignment of the Mach/Flow Angularity probe with respect to the tunnel axis, zero for orifice P1 on top and positive for P1 rotated clockwise looking downstream, deg
PN	Data point number
PP, P(1-5), PPRES, PPU, PW	Pressure measurement for the Pitot tube, Mach/Flow Angularity pressures, Preston tube, upper Pitot, and surface pressures, respectively, psia
PP1, P(1-5)I, PPRES1, PPU1, PW1	First transducer measurement for the Pitot probe, Mach/Flow angularity pressures, Preston tube, upper Pitot, and surface pressures, respectively, psia

PPF, P(1-5)F PPRESF, PPUF, PWF	Final transducer measurement for the Pitot probe, Mach/Flow angularity pressures, Preston tube, upper Pitot, and surface pressures, respectively, psia
PPE	Pitot probe pressure at the boundary-layer edge (PP at ZP = DEL), psia
PPI	Pitot probe pressure interpolated to ZT, psia
PSIO	Yaw alignment of the Mach/Flow Angularity probe with respect to the tunnel axis, positive for the probe rotated counter-clockwise as viewed from above, deg
PT	Tunnel stilling chamber pressure, psia
PTAU	Preston tube data reduction parameter
PTM	Measured tunnel stilling chamber pressure, psia
PTP	Preston tube compressibility parameter
PT2	Free-stream total pressure downstream of a normal shock, psia
PW	Model surface pressure, psia
PWX	Model surface pressure at the location of the survey, psia
Q	Free-stream dynamic pressure, psia
QDOT	Heat-transfer rate at model surface, Btu/ft ² -sec
RE	Free-stream unit Reynolds number, ft ⁻¹
REE	Unit Reynolds number at boundary-layer edge (REL at ZP = DEL), ft ⁻¹
REL	Local unit Reynolds number, ft ⁻¹
RETD	Local "normal shock" Reynolds number based on total temperature probe reference dimension and viscosity of MUTTL
RETTE	"Normal shock" unit Reynolds number ₁ at boundary- layer edge (RETTL at ZP = DEL), ft ⁻¹

RETTL	Local "normal shock" unit Reynolds number (based on viscosity of MUTTL), ft^{-1}
RHO	Free-stream density, lbm/ft^3
RHOE	Density at boundary-layer edge (RHOL at $ZP = \text{DEL}$), lbm/ft^3
RHOL	Local density, lbm/ft^3
RHOUE	Product of RHOE and UE, lbm/sec-ft^2
RHOW	Density based on TW, lbm/ft^3
RN	Model nose radius, in.
RT	Preston tube data reduction parameter
RUN	Data set identification number
R2D	Local Reynolds number, based on Preston tube diameter
S	Curvilinear surface distance from model nosetip, in.
SLICES	Number of slices on bottom, aft portion of the model
ST(TT)	Stanton number based on TT, $ST(TT) = \frac{QDOT}{(RHO) (V) (ITT-ITW)}$
SURVEY STATION NO	Location of the survey, corresponds to the pressure orifice number above which the survey began
T	Free-stream static temperature, $^{\circ}\text{R}$
TAUX	Wall shear stress (Preston tube), lb/ft^2
TDEL	Delay time between data initiation and start of data recording, sec
TE	Static temperature of boundary-layer edge (TL at $ZP = \text{DEL}$), $^{\circ}\text{R}$

TG _i	Model surface temperature corresponding to coax gage "i", °R
THETA0	Pitch alignment of the Mach/Flow-Angularity probe with respect to the tunnel axis system, positive for probe tip rotated up, deg
TL	Local static temperature, °R
TNPP, TNP(1-5), TNPRES, TNPPU, TNPW	Nominal time constant for the Pitot probe, Mach/Flow Angularity probe, Preston tube, upper Pitot probe, and surface pressure measurement, respectively, seconds e.g., $TNPP = \frac{1}{KNPP(2 \cdot PPF + APP)}$, sec
TREC	Elapsed time to record 40 samples of pressure history for pressure stabilization routine, seconds
TRIP	Boundary-layer trip identification
TT	Tunnel stilling chamber temperature, °R
TTE	Total temperature at boundary-layer edge (TTL at ZP = DEL), °R
TTL	Local total temperature, measured by an unshielded thermocouple probe and corrected for Reynolds number effects, °R
TTLI	Local total temperature interpolated to ZP, °R
TTLU	Uncorrected (measured) probe total temperature, °R
TW	Gardon or coax gage surface temperature, °R
TWX	Temperature of coax gage nearest the survey station, °R
UE	Local velocity component parallel to model surface at boundary-layer edge (UL at ZP = DEL), ft/sec

UF, VF, WF	Local velocity vector components with respect to the tunnel axis system, ft/sec
UL	Local velocity parallel to the model surface: computed from Pitot pressure, wall static pressure and total temperature measurements, considered valid near the model (boundary layer region), ft/sec
UM, VM, WM	Local velocity vector components with respect to the model axis system, ft/sec
UP, VP, WP	Local velocity vector components with respect to the Mach/Flow-Angularity probe, ft/sec
U2	Local velocity computed from Preston tube pressure, wall static pressure and wall surface temperature measurements, ft/sec
V	Free-stream velocity, ft/sec
VL	Local total velocity at the Mach/Flow Angularity probe, ft/sec
X, Y, Z	Model instrumentation locations
XF, YF	Flap instrumentation locations
XMRP	Axial distance from model moment reference point to model virtual apex, in.
XT	Axial distance from model moment reference point to balance moment reference point, in.
XT, YT, ZT	Orthogonal tunnel axis system coordinates, tabulated values are nominal location of the probe during calibrations, in.
YCP	Side-force center-of-pressure location, body axes, inches from model nose, XMRP-(CLN-LM/CY)
ZB	Vertical distance from the model x-axis to the centroid of the base area, positive if the centroid is below the x-axis at $PH_i = 0, 0$ (no slices) or -0.348 in. (double slice)

ZM	Height of Mach/Flow-Angularity probe above model surface along a normal line, in.
ZP	Height of Pitot probe above model surface along a normal line, in.
ZPU	Height of upper Pitot probe above model surface along a normal line, in.
ZT	Height of total temperature probe above model surface along a normal line, in.
Z'	Direction of the probe travel along the Z' Drive Shaft

1.0 INTRODUCTION

Within the last decade significant advances have been made in computer architecture and in the complementary development of large scale computer programs for solving complex non-linear problems. In the field of fluid dynamics, computer programs have been developed to provide detailed properties of the flow field surrounding complex aerodynamic configurations. In addition, during this past decade, energy costs have risen so dramatically that the 'customary' use of the wind tunnel as a vehicle-configuration design aid has diminished significantly. As a result, a suitable combination of numerically generated configuration aerodynamics with experimentally generated results can lead to the desired solution in an efficient and cost effective manner.

Recognizing the advances that were being made in computational fluid dynamics, the Air Force structured the Maneuvering Aerothermal Technology (MAT) program to assess and improve the currently available technology for predicting MaRV aerothermal performance for current and next generation vehicles in flight regimes characteristic of future mission requirements. The types of computer codes that were to be evaluated in this contract ranged from the empirical methods (such as the Hypersonic Arbitrary Body Program (HABP) and the Aerodynamic Heating Program (AERHEAT)) which contain the technologies of the 60's, to the more current "sophisticated" large scale programs which numerically solve various simplified versions of the Navier Stokes equations. These include the inviscid flow field solutions, boundary layer solutions, and the more recent parabolized Navier Stokes (PNS) computer solutions.

These large scale computer codes, like newly developed wind tunnels, require a detailed "shake down" to resolve developmental difficulties in logic, numerics, grid resolution, turbulence modeling, etc. To accomplish a complete check-out of these programs, detailed "bench-mark" experimental data are required with which to resolve their predictive capabilities. The current set

of experimental data were obtained with this objective in mind. However one must recognize that the predictive ability and accuracy of any aerodynamic computer code is dependent on the vehicle configuration. Thus one must first establish systems requirements and performance goals, then consistent with these, establish the generic vehicle configuration(s) that are required to meet these requirements and goals. The MAT program has provided both the systems requirements and performance goals. The current set of experimental data satisfy one aspect of these overall objectives. Specifically, flow field data were obtained on sharp and blunt axisymmetric biconic configurations under laminar and turbulent boundary layer flow conditions over a range of hypersonic Mach Numbers and angles of attack. In addition data were also obtained on the aft section of the bicone where a slice cut was taken and where a flap was placed. This type of configuration represents one type of maneuvering reentry vehicle (MaRV) of specific interest to the Air Force. The types of data obtained are configuration force and moment, surface pressure, shear, heat transfer, and flow field surveys including pitot pressure, total temperature, and flow angularity. The force and moment data provide the resultant check-out accuracy of all of the computer codes-empirical or 'exact'. However to provide additional diagnostic detail when agreement with these data is less than satisfactory, is the specific role of the detailed data-surface and flow-field measurements. The shock layer surveys are an especially useful diagnostic tool in regions of the configuration where sudden expansions or compressions are present. For these reasons, in the current test series, the shock layer surveys were concentrated in the slice/flap regions of the vehicle along with sufficient upstream measurements on the axisymmetric surfaces to provide the 'bench-mark' reference.

This report summarized and catalogs the entire body of data obtained on the biconic configurations in the AEDC-VKF Tunnels B and C at Mach numbers of 6, 8, and 10. The test specifically sponsored by the MAT program corresponds to the Mach 8 turbulent boundary layer

experimental on the $10.5^{\circ}/7^{\circ}$ sliced bicone with flap. The remainder of the experiments referred to in this report were conducted by AEDC personnel under BMO sponsorship and Aerospace/TRW guidance. This report also provides some particulars of the data reduction details, provides typical results and limited data trends, highlights, and observations. Lastly, it contains illustrative examples of data extraction for code validation and check-out.

2.0 APPARATUS

2.1 Test Facilities

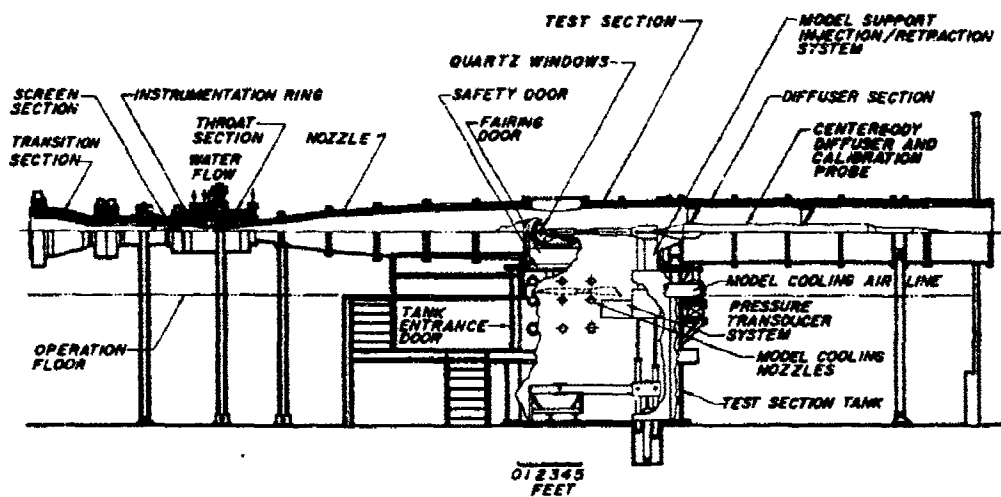
The tests were conducted in the hypersonic flow tunnels of the von Karman Facility at the Arnold Engineering Development Center; Tunnel B for Mach 6 and 8 and Tunnel C for Mach 10. Nominal tunnel performance characteristics are presented in Table 1.

TABLE 1. TUNNELS B AND C PERFORMANCE

Tunnel	Nominal Mach Number	p_o , psia		T_o , °F	q , psia		$Re/ft \times 10^{-6}$	
		Min.	Max.		Min.	Max.	Min.	Max.
B	6	20	270	390	0.3	4.1	0.3	4.7
	8	50	850	890	0.3	3.8	0.3	3.7
C	10	200	2000	1450	0.3	3.0	0.3	2.4

Both tunnels are closed circuit with axisymmetric contoured nozzles with a 50 inch diameter test section and operate continually over a range of pressure levels with air supplied by the main compressor system. Stagnation temperatures sufficient to avoid liquefaction in the test section are obtained through the use of a natural-gas-fired combustion heater in combination with the compressor heat of compression at Mach 6 and 8 and in combination with electric resistance heaters at Mach 10. Each entire tunnel (throat, nozzle, test section, and diffuser) is cooled by integral, external water jackets. Both tunnels have identical test sections equipped with model injection systems.

Directly below each test section is a tank (Figure 1) into which the model and its support can be retracted. The test section can be sealed from its tank so that the tunnel can remain running while the tank is vented to atmospheric pressure in order that personnel may enter the tank to make modifications to the model or its support system. After the desired modifications are made and the tank entrance door is closed, the tank is vented



a. Tunnel Assembly

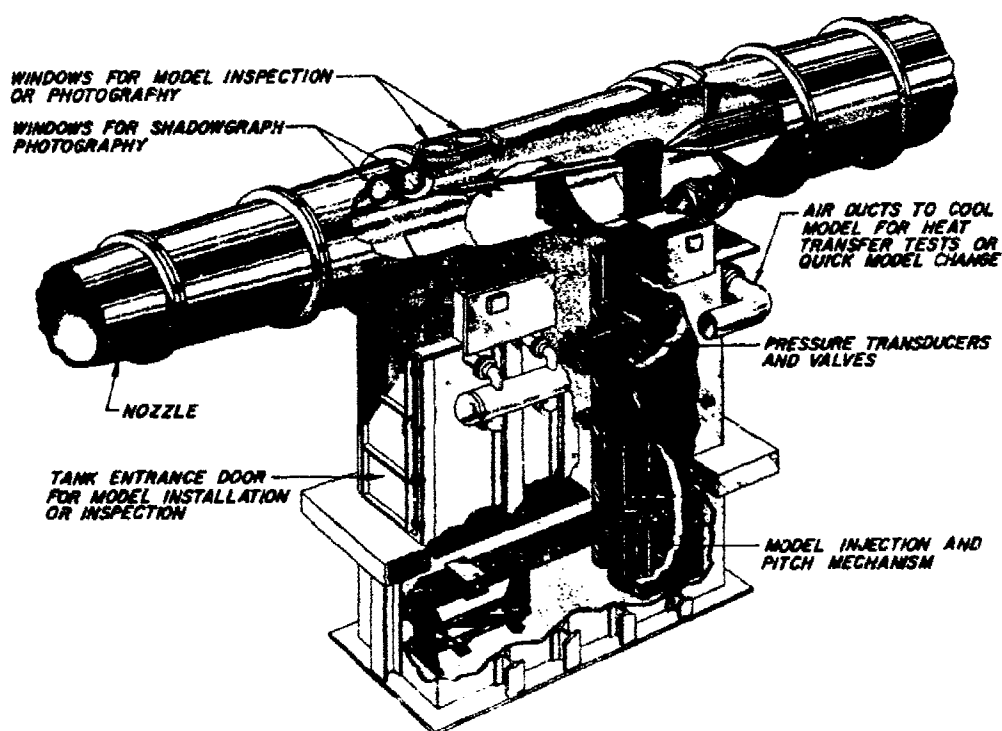


FIGURE 1. TUNNEL LAYOUT

to the test section pressure, the doors between the tank and test section are opened, and the model is injected into the airstream to obtain the desired data. Upon completion of the data acquisition, the model is retracted and the cycle completed. The injection system is also used for transient heat-transfer tests in which the model is cooled in the retracted position, set at the desired attitude, and injected into the airstream to obtain the time history of the temperatures at various locations on the model. The minimum injection time is about two seconds and the maximum acceleration or deceleration is about one g. The model is exposed to the airstream approximately 0.9 sec. prior to the injection stroke limit with the model in test position.

2.2 Model Detail

The model used for this investigation was comprised of several sections which permitted the testing of a sharp and blunt 7° cone, and sharp and blunt bicones with 10.5° and 14° forecones. All components were fabricated from type 304 stainless steel. In addition the common 7° half cone aft frustum was also sectioned to permit the inclusion of a slice/flap region. In order to provide a turbulent boundary layer for the blunted configurations, a ring of roughness trips were employed. Contained in the following sections is a detailed description of the model geometries used in this investigation including the trip geometry and the location of the surface instrumentation.

2.2.1 Basic Body

The test model used in this investigation is modular in concept, from which several bicone geometries, sharp and blunt, were assembled. The basic model components are shown in Figure 2. Exclusive of the sharp or blunt nose sections, the remainder of the model is comprised of three sections, the forecone section with half angles of 7° , 10.5° , and 14° , and the two 7° aft cone sections. For each bicone configuration, a sharp

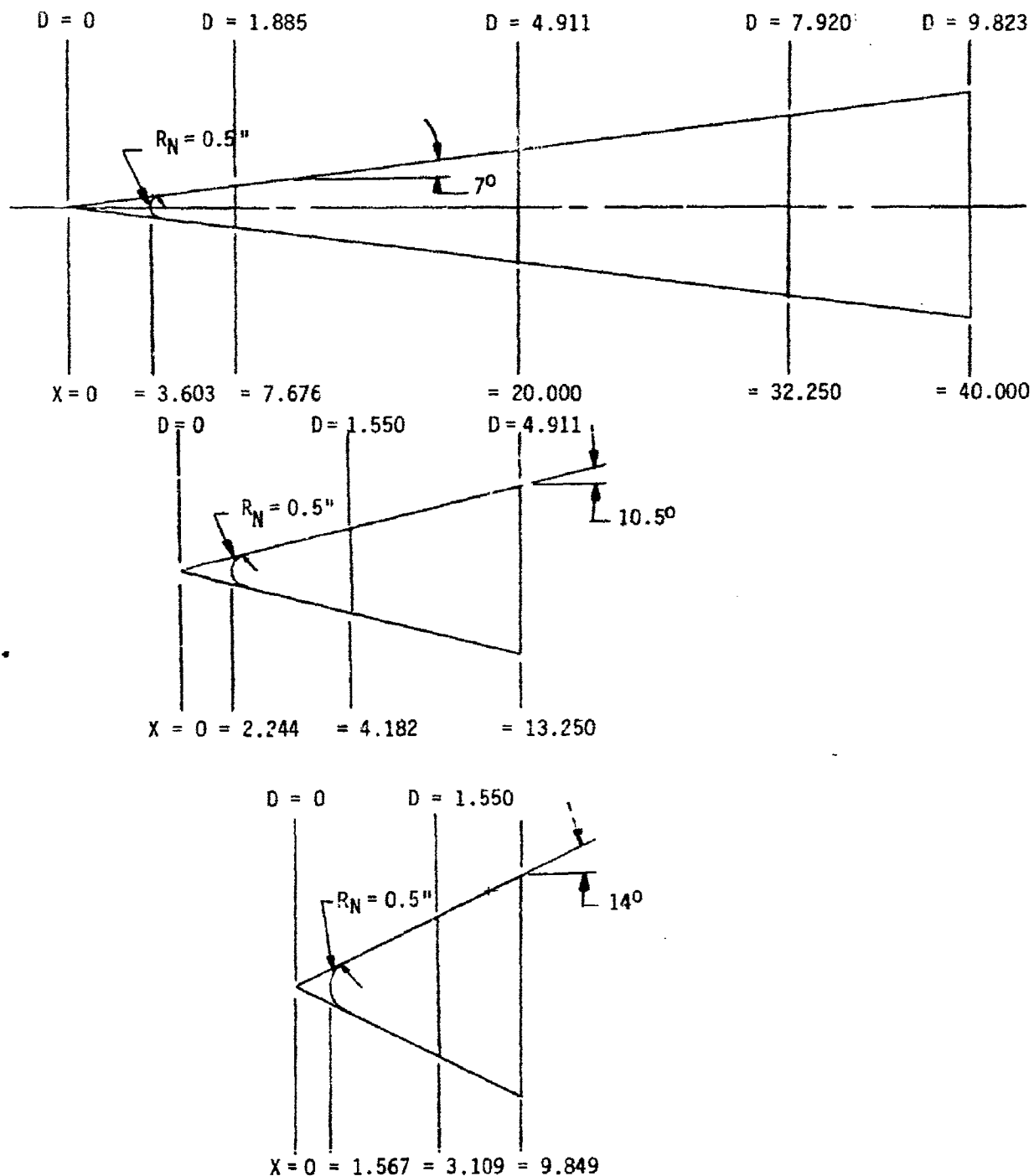


FIGURE 2. BASIC MODEL GEOMETRY

and a 0.50" R_N nosetip was tested. In summary, for this basic test series the following axisymmetric bicone configurations were tested.

<u>Nose-R_N</u>	<u>Forecone</u>	<u>Aftcone</u>	<u>Model Length</u>
0(.0015")	7°	7°	39.989
0.50"	7°	7°	36.397
0	10.5°	7°	33.250
0.50"	10.5°	7°	31.006
0	14°	7°	29.849
0.50"	14°	7°	28.282

2.2.2 Slice Region

In addition to the aft 7° conical frustum section, two additional aft sections were fabricated. One section had a double windward slice as shown in Figure 3. The first slice is parallel to the axis and starts 7.75 inches upstream of the base. The second slice on this section is inclined 7° downward, 2.75 inches upstream of the model base. This aft section was used for the force and moment test series.

The other aft cone section had an identical windward side series of slices; however, in addition it also had a single parallel slice on the leeward side as shown in Figure 3. This aft section was used for the remainder of the test series; that is the pressure, heat transfer, and shock layer profiles

2.2.3 Flap

Under MAT program sponsorship, a series of flaps were fabricated for use with the aft slice sections. Three were built, a 10° and 20° continuous span flap and a split 20°/10° flap as shown in Figure 4. The hinge line of the flaps were located at the juncture of the second windward cut,

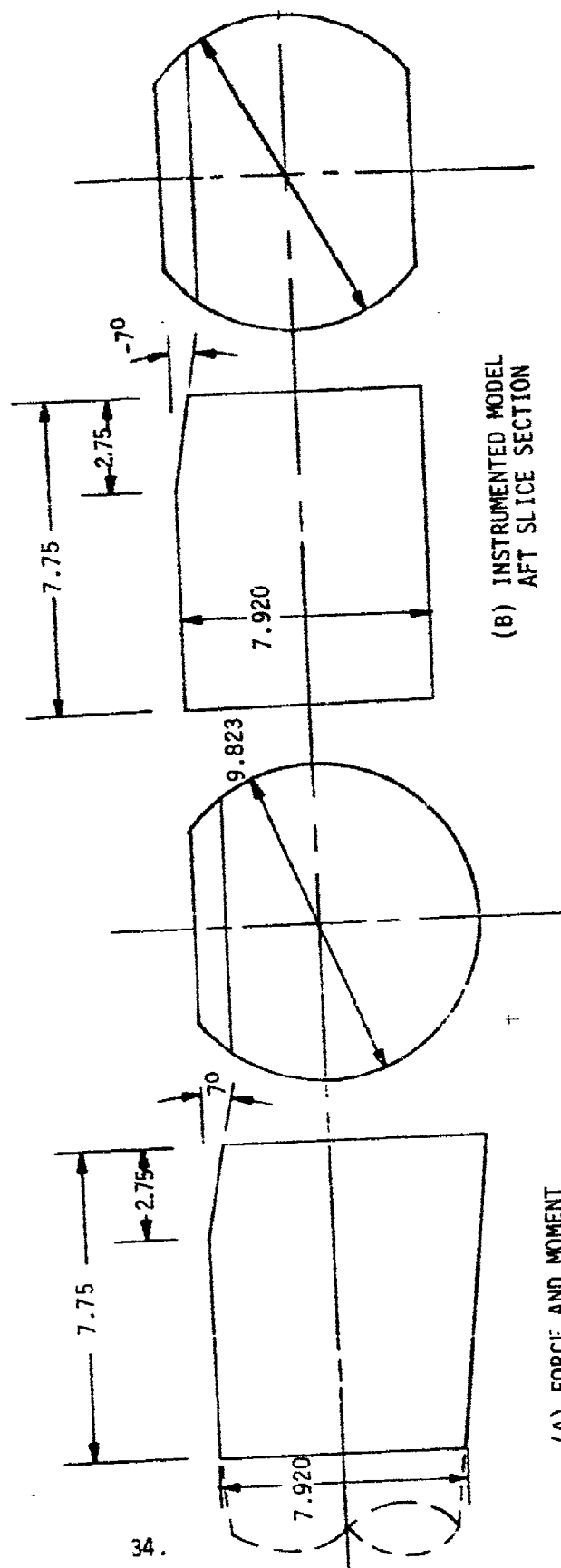
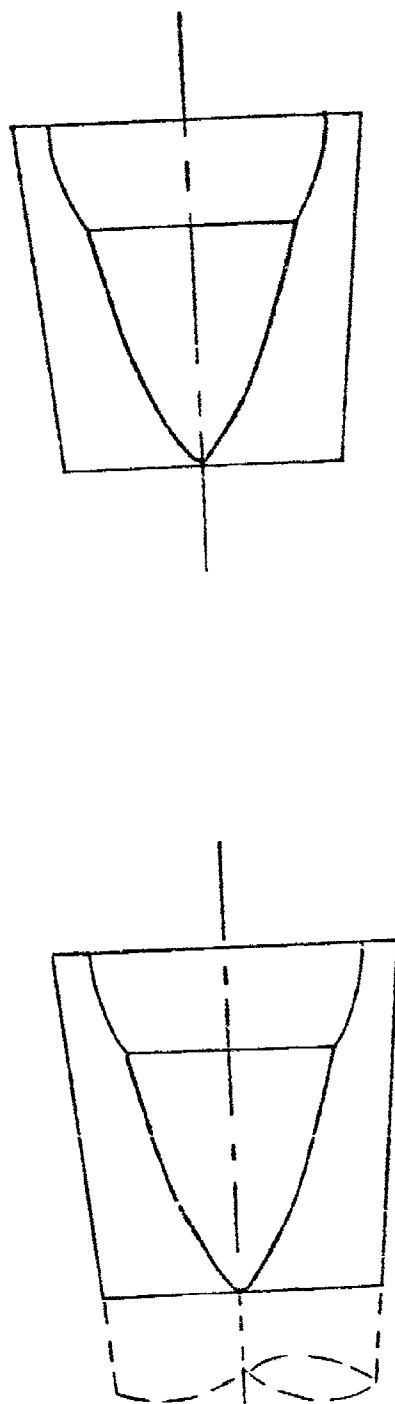


FIGURE 3. AFT SLICE SECTIONS

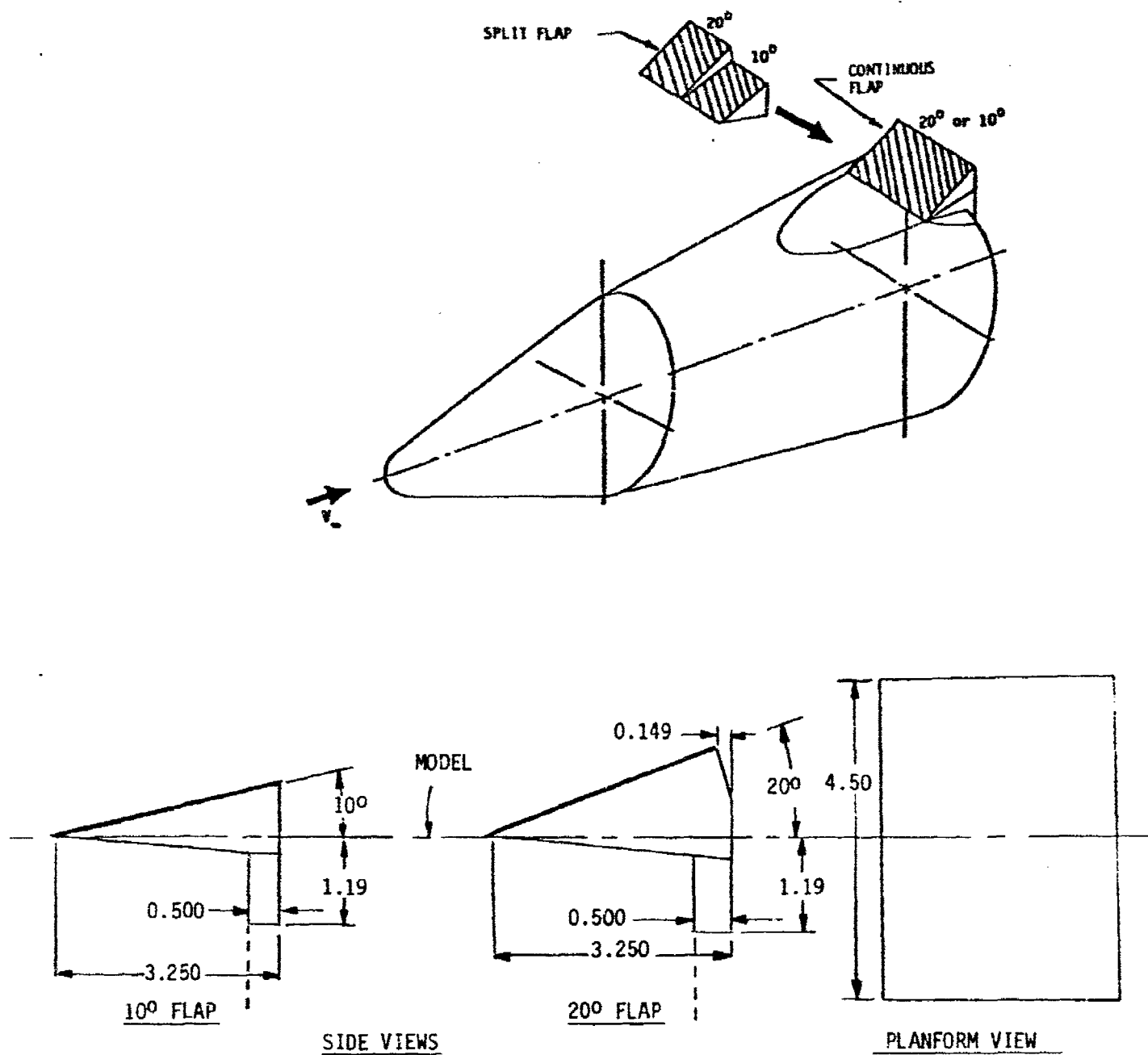


FIGURE 4. FLAP DETAILS

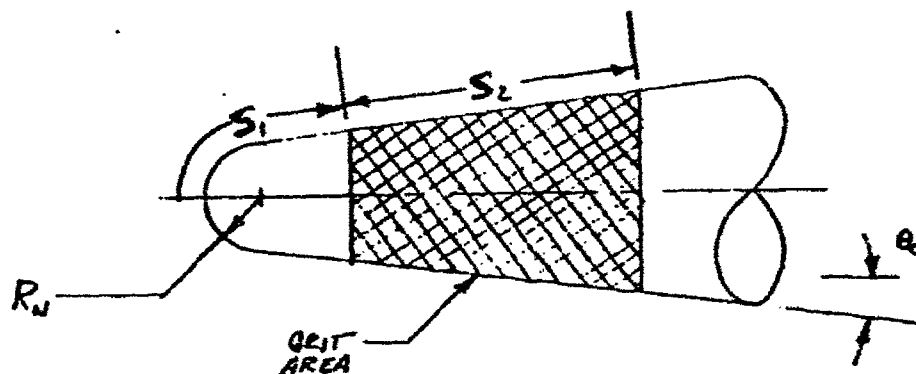
2.75 inches upstream of the base. For simplicity of installation the flaps were manufactured with a 0.50 inch overhang from the base and were attached to the basic body by fasteners into the base.

2.2.4 Roughness/Boundary Layer Trips

In the course of these experimental investigations, several test series were conducted for the primary purpose of determining the trip size - for a given model bluntness and test facility - which would provide a turbulent boundary layer (hopefully with the absence of inviscid flow disturbances). These investigations were primarily performed using the model surface heat transfer (cold wall) as the diagnostic for determining the departure from laminar flow. However, in certain cases investigations were also performed using the boundary layer portion of the shock layer survey as the diagnostic (i.e., for the hot wall case). Although the trip size, geometry, and relative placement on the models were similar, these parameters varied for several of the test series. Rather than summarize the pot-pourri of trips used, they are shown in Figures 5 and 6 for the Mach 6 and Mach 8 investigations, respectively.

The boundary layer trips consisted of distributed roughness formed by attaching Carborundum grit to the model surface, or by machining helical grooves in a spiral fashion (clockwise and counter clockwise) on the conical frustum part of the nose, or by blasting the metal surface with grit until the desired roughness was attained. The test data summarized in the following sections of this report will refer specifically to the trip used from Figures 5 and 6.

The turbulent boundary layer shock layer survey tests were performed using the machined roughness trips defined in Figure 6a and shown photographically in Figure 7.

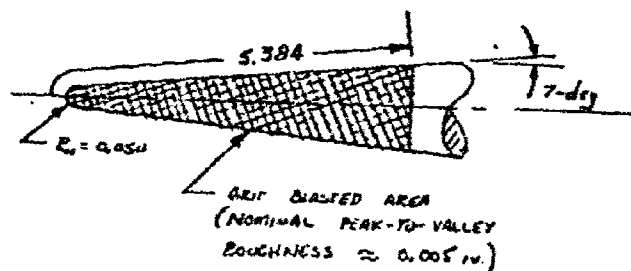


θ_c (DEG)	R_N (IN)	S_1 (IN)	S_2 (IN)	GRIT NO.	NOMINAL GRIT SIZE (IN)
7 ↓	0.05	1.481	3.900	60	0.010
	↓	↓	↓	30	0.022
	0.10	1.552	3.500	46	0.014
	0.50	1.574	0.800	80	0.0065
	↓	↓	↓	60	0.010
	↓	↓	↓	46	0.014
	↓	↓	↓	30	0.022
	↓	↓	↓	20	0.037
10.5 ↓	0.05	1.352	2.700	60	0.010
	0.50	0.949	1.300	60	0.010
	↓	↓	↓	30	0.022
14 ↓	0.05	1.069	2.000	60	0.010
	0.50	0.661	1.200	100	0.0048
	↓	↓	↓	80	0.0065
	↓	↓	↓	46	0.014

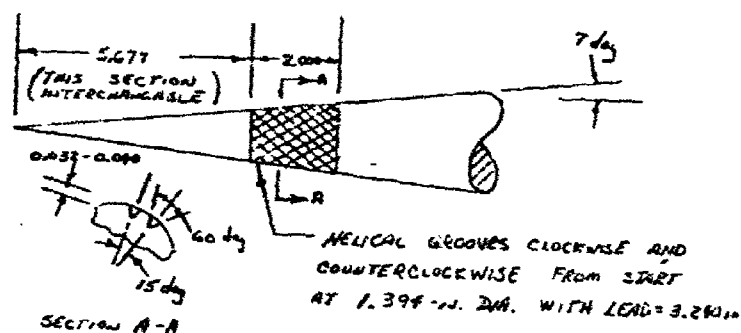
a. DISTRIBUTED GRIT TRIP

FIGURE 5. BOUNDARY LAYER TRIP GEOMETRY

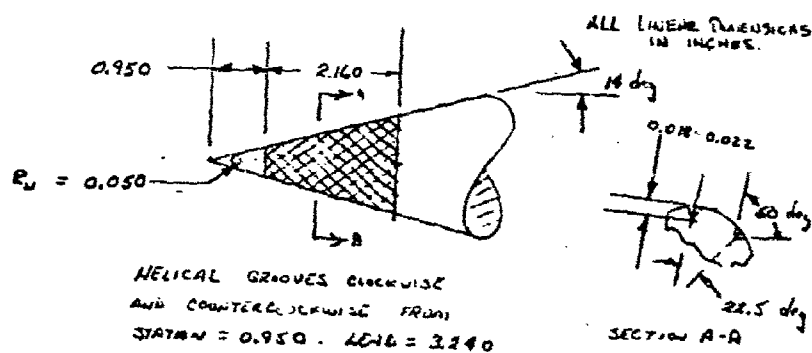
$[M_\infty = 6, \alpha = 0^\circ]$



b. 7-deg grit blasted nose



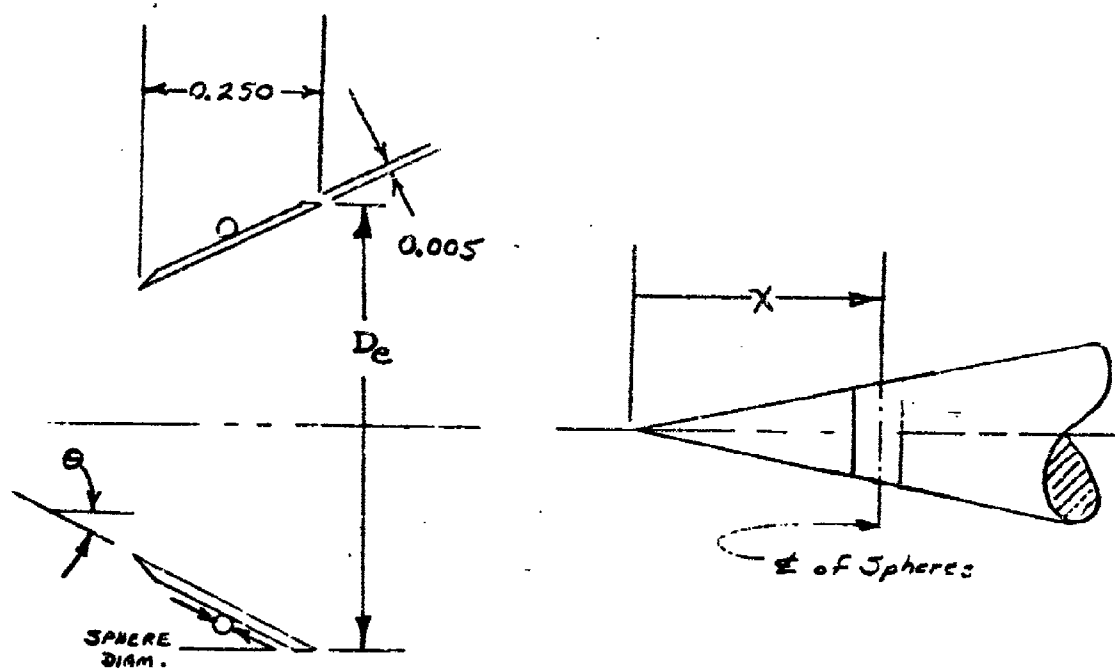
c. Grooved 7-deg insert



d. Grooved 14-deg nose

FIGURE 5. BOUNDARY LAYER TRIP GEOMETRY (CONT'D)

$$[M_\infty = 6, \alpha = 0]$$

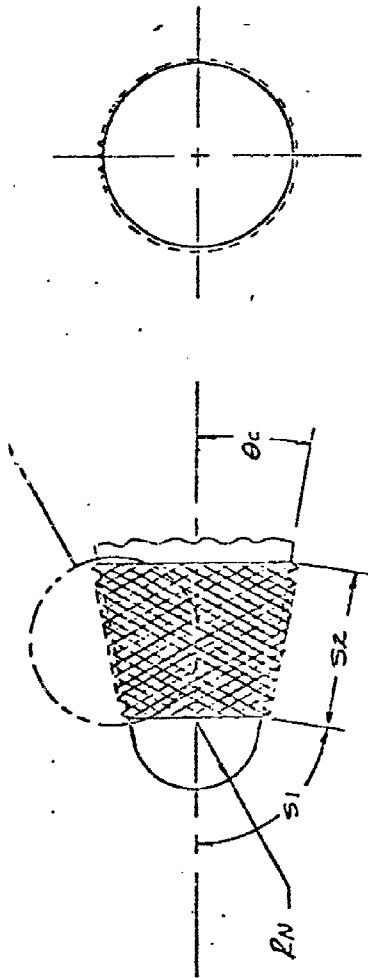
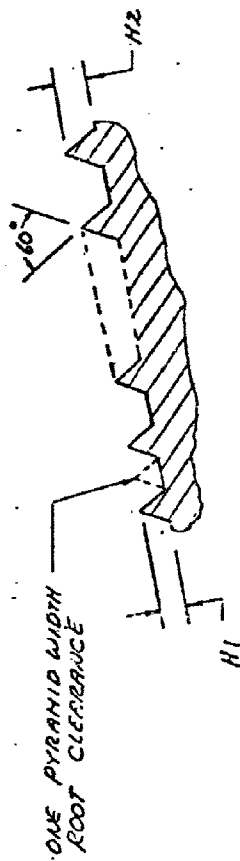


θ DEG.	X IN.	D_e IN.	SPHERE DIAM., IN.	NO. OF SPHERES
7	6.5	1.504	0.093	17
10.5	4.0	1.530	0.046	35
10.5	4.0	1.530	0.125	13
14	3.0	1.558	0.046	35
14	3.0	1.558	0.093	18

e. SPHERICAL ELEMENT TRIPS

FIGURE 5. BOUNDARY LAYER TRIP GEOMETRY (CONCLUDED)

$[M_\infty = 6, \alpha = 0]$



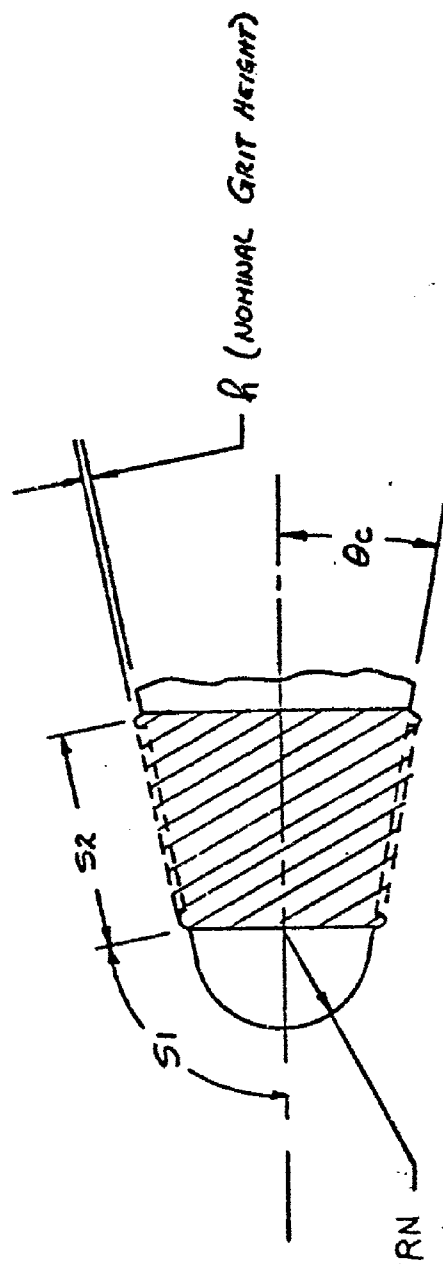
θ_c DEG.	R_N IN.	S_1 IN.	S_2 IN.	H_1 IN.	H_2^* IN.
7	0.0015	5.760	1.914	0.031	0.060
7	0.500	2.422	1.914	0.031	0.060
10.5	0.500	0.949	1.249	0.006	0.013
↓	↓	↓	↓	0.015	0.033
				0.024	0.060

*DIMENSION USED IN
TABULATED DATA FOR
IDENTIFICATION

a. MACHINED TRIPS

FIGURE 6. BOUNDARY LAYER TRIP GEOMETRY

$M_\infty = 8, \alpha \neq 0$



TRIP NO.	θ_c (DEG)	R_N (IN)	$S1$ (IN)	$S2$ (IN)	h (IN)
5	10.5	0.500	0.949	1.249	0.037
6	14.0	0.500	0.661	1.149	0.028

b. Grit Bonded Trips

FIGURE 6. BOUNDARY LAYER TRIP GEOMETRY (CONT'D) $[M_\infty = 8, \alpha \neq 0]$

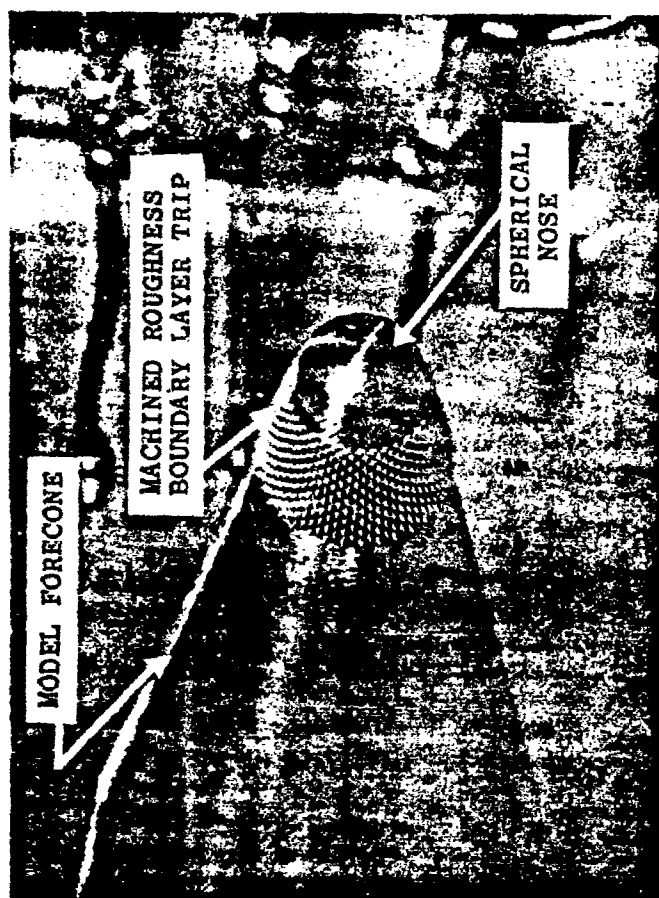


FIGURE 7. PHOTOGRAPH OF THE MACHINED BOUNDARY LAYER TRIP $[M_{\infty} = 8, \alpha \neq 0]$

2.2.5 Instrumentation

As indicated earlier, the measurements in this test series included total model static force, surface heat transfer, pressure and temperature, and also shock layer surveys (which included Pitot pressure, total temperature, Preston tube, and Mach/Flow Angularity measurements). Contained below is a summary discussion of the model surface instrumentation and locations, and the balance used for forces and moment definition. The material that is summarized below is excerpted from the appropriate AEDC Test Summary Reports (TSRs) and will be so referenced.

Model flow-field photographs were obtained with a single-pass optical flow visualization system through the two 17.25 inch diameter test sections windows.

2.2.5.1 Static Force

Static force measurements are provided using either point-pause or continuous sweep techniques. In the more conventional point-pause technique, the model support mechanism is moved to the desired model angle and stopped, measurements are taken, and then the sequence is repeated by moving to the next desired angle. In the continuous sweep technique the model is continuously varied in angle while measurements are taken, at rates of 0.5 deg/sec in pitch and 2 deg/sec in roll.

Forces and moments on models are measured with a six-component internal strain-gage balances using conventional foil and semiconductor gages. Balance details are described in Reference 1. The balance is temperature compensated over the range from 80 to 180°F. Two copper-constantan thermocouples are provided for monitoring balance temperature.

The measuring and recording devices, and the calibration methods used for all measured parameters along with the estimated measured uncertainties are provided in Reference 2 for the Mach 10 laminar static force tests and in Reference 3 for the Mach 8 turbulent tests. Model base pressure was measured in the point - pause mode of operation with the VKF standard pressure system which uses 1-psid variable capacitance transducers referenced to near vacuum.

A photograph of the model mounted for the static force series shown in the dump tank below Tunnel B is presented in Figure 8. The machined trip ring device is readily seen in this photograph. Figure 9 portrays the model assembly in the Tunnel B test section.

2.2.5.2 Model Surface Instrumentation

Surface mounted instrumentation consisted of Gardon gages, coaxial thermocouple gages, and pressure orifices. The tests were conducted in several separate entries where the model configuration varied per entry, consequently the surface instrumentation also varied. The reference for each data set and the configuration tested is listed below.

<u>Reference</u>	<u>Data Set</u>	<u>Models</u>
4	Mach 6, $\alpha = 0$ (Turbulent)	7° Cone 140/7° Bicone
5	Mach 6, $\alpha = 0$ (Turbulent)	7° Cone 10.5°/7° Bicone 140/7° Bicone
6	Mach 8, $\alpha \neq 0$ (Turbulent)	7° Cone 10.5°/7° Bicone 140/7° Bicone
7	Mach 10, $\alpha \neq 0$ (Laminar)	140/7° Bicone w/Slices
8	Mach 8, $\alpha \neq 0$ (Turbulent)	10.5°/7° Bicone w/Slice and Flap

U.S. AIR FORCE APOC
 Armed A.F. to
 Air Force 37200. Not cleared for pub
 release without prior review approved
 the Air Force Office of Public Affairs.



FIGURE 8. PHOTOGRAPH OF THE BICONE MODEL STATIC FORCE INSTALLATION VIEWED IN THE DUMP TANK BELOW TUNNEL B

4975 (7-20-81) VN2B-215 BMO/SAI MAT-1 FORCE

U.S. AIR FORCE AEC
 General A.F. St
 New York, 12/20/50. Not cleared for pub
 release without prior written approval
 the Air Force Office of Public Affairs

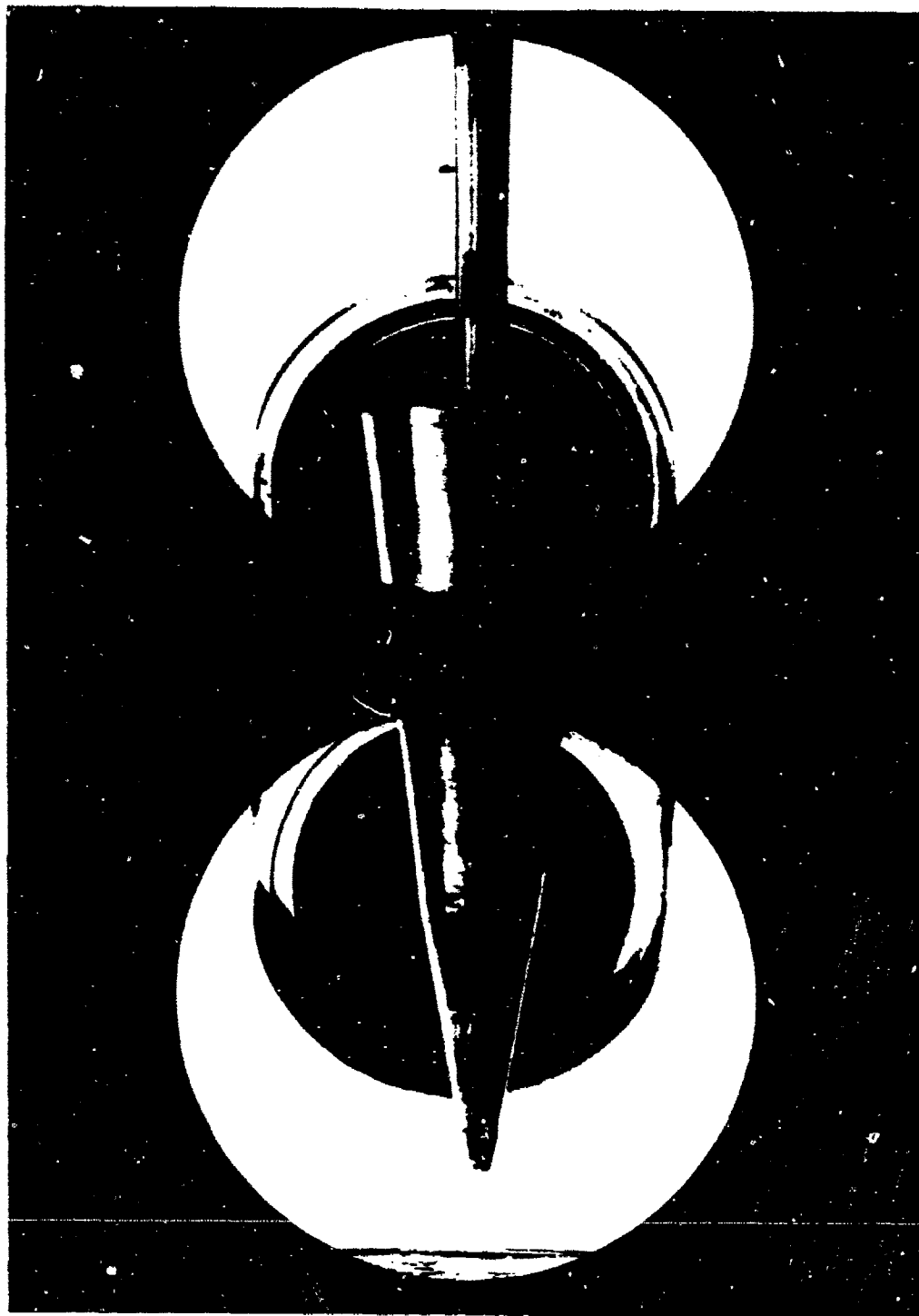


FIGURE 9. PHOTOGRAPH OF THE BICONE MODEL STATIC FORCE INSTALLATION IN TUNNEL B

4976 (7-20-51) V42B-215 BMD/SAI MAT-1 FORCE

Heat transfer data were obtained using 0.125 inch diameter Gardon-type heat flux gages with Iron-Constantan^R case thermocouples. For the Mach 6 tests where the tunnel stagnation temperature is relatively low, it was possible to use the Gardon-gage not only as a transient gage for measuring heat transfer in the pulse entry mode, but it could also be used in the steady state-long time entry (i.e., for profile measurement) mode. The case thermocouple served a dual role by providing a sensing disc edge temperature used in the evaluation of the heat-transfer coefficient and by indicating the model wall temperature during the long hot-wall runs. As an additional check on the long term wall temperature coaxial surface thermocouples were used.

In the Mach 8 and 10 tests where the tunnel stagnation temperature is significantly higher and where the Gardon-type gages would not survive a long time entry, the model was only instrumented with this type gage for short duration heat transfer tests. Prior to the survey tests, the Gardon gages were removed and the holes were plugged or replaced by coaxial gages and the afterbody was replaced with a pressure instrumented afterbody. The pressure orifices in the afterbody were located at the same locations as the Gardon gages. The coaxial gages (surface thermocouples) were added for the survey tests to provide model surface temperature. Details of both types of gages may be found in Reference 9.

Three flap assemblies were used: heat transfer, full span pressure, and split pressure as depicted in Figure 4. The heat transfer flap was a full span adjustable deflection flap instrumented with nine Gardon gages. The full span pressure flap was essentially the same as the heat transfer flap except for instrumentation. The split pressure flap had fixed deflection angles of 10 and 20-deg for its two sides and was instrumented with seven orifices and two coaxial surface thermocouples. Specific gage and orifice locations are presented in Reference 8 and Section 3.4

It should be noted that in all cases the model was instrumented with more than 75 Gardon-type gages, and more than 80 pressure orifices so that a relatively complete surface coverage was obtained. The reader is referred to Section 3 or the specific test report for detail definition and locations of the surface instrumentation.

2.3 Flow Field Survey Probes and Probe System

Two separate probing systems were used to perform the boundary layer and flow field surveys. An overhead probe system which was the primary flow field survey mechanism was instrumented with a pitot tube, unshielded thermocouple probe and a Preston tube. A second system which was used with the axisymmetric bicones was attached to the model support sting and was equipped with a Pitot tube and an unshielded thermocouple probe. A Preston tube was included on the on-board probe installation, but pressure response from this probe was not satisfactory and data from this probe are not valid.

The axial, X, lateral, Y, and vertical, Z, overhead probe drive system, is used to survey flow fields in Tunnels B and C. The positioning mechanism is mounted above a port on the top of the tunnel. The X-Y-Z mechanism has five degrees of freedom: X, Y, Z, Z' and ALPT. In addition to the X, Y, and Z controls, this mechanism has the capability for inclining the probe head by an angle ALPT relative to a vertical (from the Z axis), and then probing in the Z' direction along this tilted vertical axis. Precision surveys along the Z' axis can repeatably be made to within ± 0.005 inches. Positioning of the probe holder attachment is arbitrary in the sense that no preprogramming is required and the mechanism moves independently of the model. All stations to be sampled must remain within the mechanism traversing envelope. Shown in Figures 10 to 12 are photographs of the probe housing assembly and of the probe holder assembly. Figure 13 is a photograph of the probe holder assembly shown in proximity to the model. The flattened Pitot, upper Pitot, total temperature and Preston tube probes were mounted in one probe holder, while the Mach/Flow-

ASSEMBLY WITH THE

[illegible]

U.S. AIR FORCE
 A-10
 New York, 37200. The aircraft is a
 military aircraft and is not intended to
 be used for other than military purposes.



FIGURE 11. PHOTOGRAPH OF THE PROBE ASSEMBLY

REMOTE PITOT PRESSURE TUBE

PITOT PRESSURE TUBE

PRESTON TUBE

TOTAL TEMPERATURE

Figure 1. The effect of the concentration of the *Agaricus bisporus* spores on the growth of *Agaricus bisporus* on the substrate. The concentration of the spores was 10⁴, 10⁵, 10⁶, 10⁷, 10⁸, 10⁹, 10¹⁰, 10¹¹, 10¹², 10¹³, 10¹⁴, 10¹⁵, 10¹⁶, 10¹⁷, 10¹⁸, 10¹⁹, 10²⁰, 10²¹, 10²², 10²³, 10²⁴, 10²⁵, 10²⁶, 10²⁷, 10²⁸, 10²⁹, 10³⁰, 10³¹, 10³², 10³³, 10³⁴, 10³⁵, 10³⁶, 10³⁷, 10³⁸, 10³⁹, 10⁴⁰, 10⁴¹, 10⁴², 10⁴³, 10⁴⁴, 10⁴⁵, 10⁴⁶, 10⁴⁷, 10⁴⁸, 10⁴⁹, 10⁵⁰, 10⁵¹, 10⁵², 10⁵³, 10⁵⁴, 10⁵⁵, 10⁵⁶, 10⁵⁷, 10⁵⁸, 10⁵⁹, 10⁶⁰, 10⁶¹, 10⁶², 10⁶³, 10⁶⁴, 10⁶⁵, 10⁶⁶, 10⁶⁷, 10⁶⁸, 10⁶⁹, 10⁷⁰, 10⁷¹, 10⁷², 10⁷³, 10⁷⁴, 10⁷⁵, 10⁷⁶, 10⁷⁷, 10⁷⁸, 10⁷⁹, 10⁸⁰, 10⁸¹, 10⁸², 10⁸³, 10⁸⁴, 10⁸⁵, 10⁸⁶, 10⁸⁷, 10⁸⁸, 10⁸⁹, 10⁹⁰, 10⁹¹, 10⁹², 10⁹³, 10⁹⁴, 10⁹⁵, 10⁹⁶, 10⁹⁷, 10⁹⁸, 10⁹⁹, 10¹⁰⁰, 10¹⁰¹, 10¹⁰², 10¹⁰³, 10¹⁰⁴, 10¹⁰⁵, 10¹⁰⁶, 10¹⁰⁷, 10¹⁰⁸, 10¹⁰⁹, 10¹¹⁰, 10¹¹¹, 10¹¹², 10¹¹³, 10¹¹⁴, 10¹¹⁵, 10¹¹⁶, 10¹¹⁷, 10¹¹⁸, 10¹¹⁹, 10¹²⁰, 10¹²¹, 10¹²², 10¹²³, 10¹²⁴, 10¹²⁵, 10¹²⁶, 10¹²⁷, 10¹²⁸, 10¹²⁹, 10¹³⁰, 10¹³¹, 10¹³², 10¹³³, 10¹³⁴, 10¹³⁵, 10¹³⁶, 10¹³⁷, 10¹³⁸, 10¹³⁹, 10¹⁴⁰, 10¹⁴¹, 10¹⁴², 10¹⁴³, 10¹⁴⁴, 10¹⁴⁵, 10¹⁴⁶, 10¹⁴⁷, 10¹⁴⁸, 10¹⁴⁹, 10¹⁵⁰, 10¹⁵¹, 10¹⁵², 10¹⁵³, 10¹⁵⁴, 10¹⁵⁵, 10¹⁵⁶, 10¹⁵⁷, 10¹⁵⁸, 10¹⁵⁹, 10¹⁶⁰, 10¹⁶¹, 10¹⁶², 10¹⁶³, 10¹⁶⁴, 10¹⁶⁵, 10¹⁶⁶, 10¹⁶⁷, 10¹⁶⁸, 10¹⁶⁹, 10¹⁷⁰, 10¹⁷¹, 10¹⁷², 10¹⁷³, 10¹⁷⁴, 10¹⁷⁵, 10¹⁷⁶, 10¹⁷⁷, 10¹⁷⁸, 10¹⁷⁹, 10¹⁸⁰, 10¹⁸¹, 10¹⁸², 10¹⁸³, 10¹⁸⁴, 10¹⁸⁵, 10¹⁸⁶, 10¹⁸⁷, 10¹⁸⁸, 10¹⁸⁹, 10¹⁹⁰, 10¹⁹¹, 10¹⁹², 10¹⁹³, 10¹⁹⁴, 10¹⁹⁵, 10¹⁹⁶, 10¹⁹⁷, 10¹⁹⁸, 10¹⁹⁹, 10²⁰⁰, 10²⁰¹, 10²⁰², 10²⁰³, 10²⁰⁴, 10²⁰⁵, 10²⁰⁶, 10²⁰⁷, 10²⁰⁸, 10²⁰⁹, 10²¹⁰, 10²¹¹, 10²¹², 10²¹³, 10²¹⁴, 10²¹⁵, 10²¹⁶, 10²¹⁷, 10²¹⁸, 10²¹⁹, 10²²⁰, 10²²¹, 10²²², 10²²³, 10²²⁴, 10²²⁵, 10²²⁶, 10²²⁷, 10²²⁸, 10²²⁹, 10²³⁰, 10²³¹, 10²³², 10²³³, 10²³⁴, 10²³⁵, 10²³⁶, 10²³⁷, 10²³⁸, 10²³⁹, 10²⁴⁰, 10²⁴¹, 10²⁴², 10²⁴³, 10²⁴⁴, 10²⁴⁵, 10²⁴⁶, 10²⁴⁷, 10²⁴⁸, 10²⁴⁹, 10²⁵⁰, 10²⁵¹, 10²⁵², 10²⁵³, 10²⁵⁴, 10²⁵⁵, 10²⁵⁶, 10²⁵⁷, 10²⁵⁸, 10²⁵⁹, 10²⁶⁰, 10²⁶¹, 10²⁶², 10²⁶³, 10²⁶⁴, 10²⁶⁵, 10²⁶⁶, 10²⁶⁷, 10²⁶⁸, 10²⁶⁹, 10²⁷⁰, 10²⁷¹, 10²⁷², 10²⁷³, 10²⁷⁴, 10²⁷⁵, 10²⁷⁶, 10²⁷⁷, 10²⁷⁸, 10²⁷⁹, 10²⁸⁰, 10²⁸¹, 10²⁸², 10²⁸³, 10²⁸⁴, 10²⁸⁵, 10²⁸⁶, 10²⁸⁷, 10²⁸⁸, 10²⁸⁹, 10²⁹⁰, 10²⁹¹, 10²⁹², 10²⁹³, 10²⁹⁴, 10²⁹⁵, 10²⁹⁶, 10²⁹⁷, 10²⁹⁸, 10²⁹⁹, 10³⁰⁰, 10³⁰¹, 10³⁰², 10³⁰³, 10³⁰⁴, 10³⁰⁵, 10³⁰⁶, 10³⁰⁷, 10³⁰⁸, 10³⁰⁹, 10³¹⁰, 10³¹¹, 10³¹², 10³¹³, 10³¹⁴, 10³¹⁵, 10³¹⁶, 10³¹⁷, 10³¹⁸, 10³¹⁹, 10³²⁰, 10³²¹, 10³²², 10³²³, 10³²⁴, 10³²⁵, 10³²⁶, 10³²⁷, 10³²⁸, 10³²⁹, 10³³⁰, 10³³¹, 10³³², 10³³³, 10³³⁴, 10³³⁵, 10³³⁶, 10³³⁷, 10³³⁸, 10³³⁹, 10³⁴⁰, 10³⁴¹, 10³⁴², 10³⁴³, 10³⁴⁴, 10³⁴⁵, 10³⁴⁶, 10³⁴⁷, 10³⁴⁸, 10<

U.S. AIR FORCE JAGC
 Grand A.F. 829
 was T-28, 37309. Was shown by public
 release without press written approval of
 the Air Force Office of Public Affairs.



FIGURE 13. PHOTOGRAPH OF THE PROBE ASSEMBLY SHOWN IN PROXIMITY TO THE 10.50/70 BICONE MODEL

2763 (6-22-51) V478-115 BAK/TAI MAR. 1

Angularity probe was mounted separately. The upper Pitot was moved from 2 inches to 3 inches above the Pitot, Preston, and total temperature probes, when leeward surveys were performed. The second probe was used to minimize data acquisition time for the thick shock layers.

Probe positioning in the vicinity of the model surface, probe deflections and probe spacing are measured and monitored optically with the VKF closed circuit television (CCTV) system. The model and probes are back lighted using the collimated light beam shadowgraph system. The CCTV system can monitor the system at the rate of 30 frames/second, 1224 lines/frame, and with a magnification factor of 38. Positioning of the probes at a desired location is achieved using a graticule, marked in increments or marked to indicate stations along the model surface. Spacing between the probes and the model surface can also be measured optically. The television image is also used to verify contact between the survey probe and the model surface. The camera is isolated from the tunnel vibrations by mounting it with the optics system which has a separate foundation from the tunnels. A front lighted high magnification TV of approximately 7 power was used to view the 10 degree flap section of the split flap.

2.3.1 Pitot and Unshielded Thermocouple Probes

Total pressure (Pitot) and total temperature probe measurements were used in conjunction with the wall surface static pressure measurements to extract the total pressure and total temperature profiles, and the local Mach number in the boundary layer. To survey boundary layers, probes of small dimensions were used to minimize probe size effects on the resolution of the profiles. Boundary layer probes were designed to obtain measurements close to the surface within the boundary layers and yet remain parallel to the model surface.

The unshielded thermocouple probes were made with Chromel-Alumel thermocouples which had an estimated uncertainty of $\pm 1.5^{\circ}\text{F} + 0.375$ percent of reading. The unshielded thermocouple probe had a wire junction diameter of approximately 0.007 inches. A reference dimension of 0.005 inches was used for data reduction purposes. The time response and the resolution of the probe location are improved by using such small probes. Total temperature probe uncertainties associated with the heat transfer between the probe and environment were accounted for in the freestream probe calibration (convection and conduction effects).

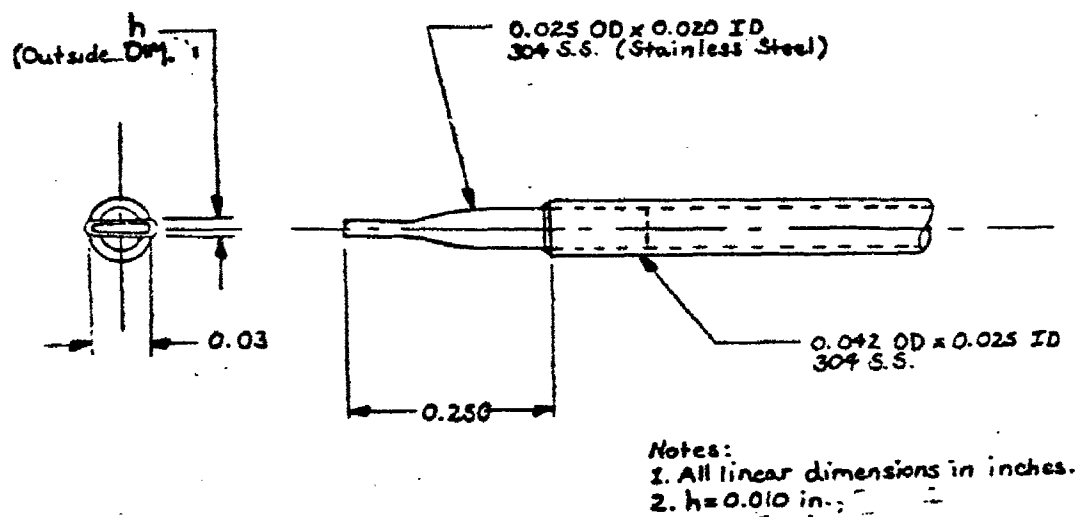
As shown in Figures 10 through 12, two Pitot tubes were attached to the probe holder assembly. Both Pitot probe pressures (on-board and overhead) and the overhead Preston tube were measured with 15-psid Druck^R transducers which had an estimated measurement uncertainty of ± 0.009 psi. A near vacuum reference pressure was used with these transducers. The near vacuum reference pressure was measured with a Hastings absolute pressure transducer. The Pitot probe used for surveys near the model surface were fabricated by flattening an 0.024 inch O.D. (0.020 I.D.) tube as shown in Figure 14. This procedure produced a probe tip thickness of 0.020 inch with an open slit of 0.005 inch height. Pitot and total temperature probes are illustrated in Figure 14.

2.3.2 Preston Tube

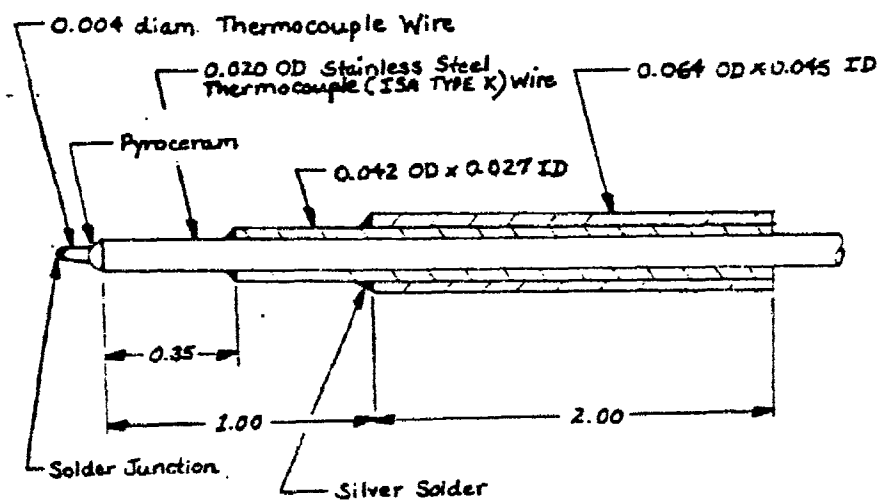
The Preston tube geometry is illustrated in Figure 15. The tube tip dimensions are consistent with those that have been used previously (References 10 and 11) for obtaining Preston tube calibration factors.

2.3.3 Mach/Flow-Angularity Probe

A Mach/flow angularity probe (Probe #5) was used to measure the local stream total pressure, local Mach number, and local flow angle. The Mach/flow angularity probe is shown in Figure 16. The probe is 0.068 inches in diameter, made up of 5 individual tubes of 0.012 inches I.D. Probes this



a. Pitot Probe



b. Unshielded Total Temperature Probe

FIGURE 14. PITOT AND TOTAL TEMPERATURE PROBES

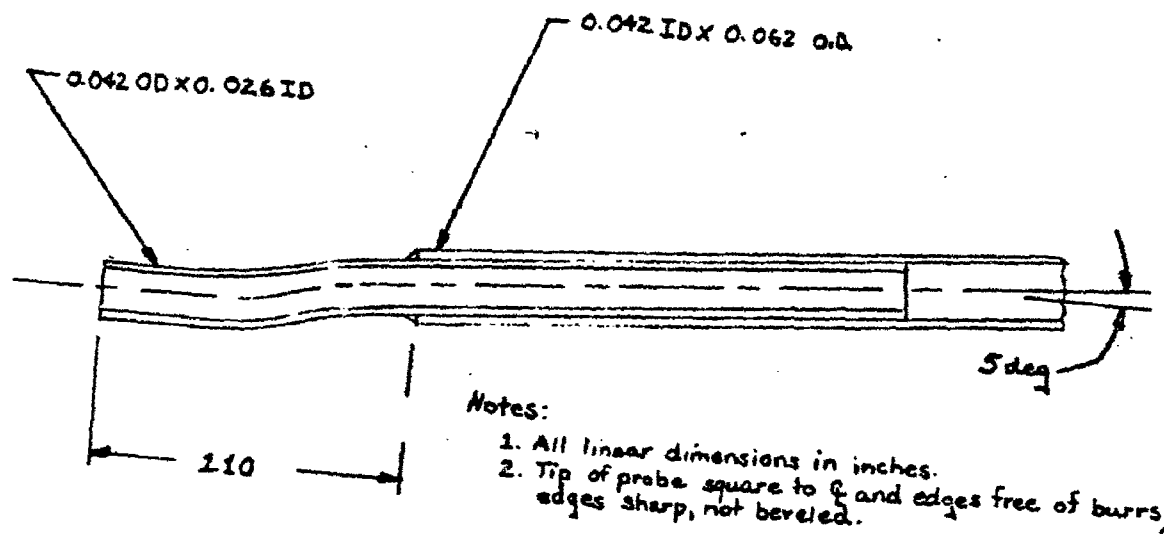


FIGURE 15. PRESTON TUBE

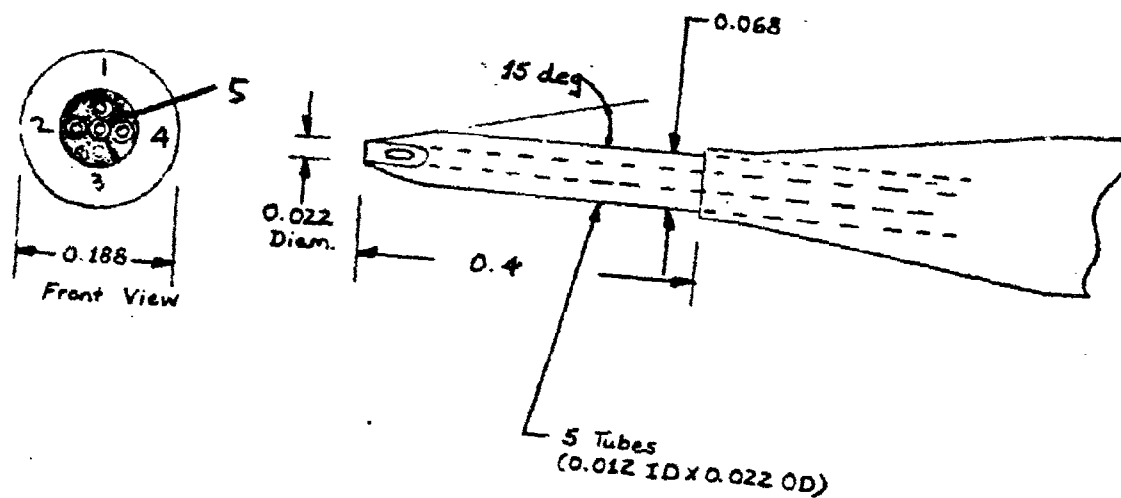


FIGURE 16. MACH/FLOW-ANGULARITY PROBE

small minimize probe interference and improve the resolution of the measurement location while mapping complex flow fields. Mach/flow angularity probes are calibrated to measure the two flow directional angles of the airstream with respect to the probe. Typically, pressure measurements in tubes 1 and 3 are in the vertical or pitch plane and tubes 2 and 4, are in the horizontal or yaw plane of the flow field.

3.0 SUMMARY OF TEST CONDITIONS AND DATA ACQUIRED

A rather large body of detailed experimental data were obtained at AEDC at Mach numbers 6, 8, and 10 on sharp and blunted $10.5^\circ/7^\circ$ and $14^\circ/7^\circ$ bicones and on a 7° cone. The data consisted of static force and moment, surface pressure - heat transfer - and shear (via a Preston tube) measurements, and lastly boundary/shock layer surveys. The survey data are composed primarily of Pitot pressure and total temperature with some limited Mach/Flow angularity measurements.

In addition to obtaining data on the axisymmetric configurations, modifications to the aft cone consisting of a windward double slice, a leeward single slice, and the addition of a flap at the second windward slice were made and a full complement of data taken. These data were taken over a 3-4 year span, where the detailed measurements on the $10.5^\circ/7^\circ$ bicone with the slices and flap were performed last and were planned and conducted by SAI under the BMO/MAT program sponsorship.

Data were obtained for both laminar and turbulent boundary layer flows. In order to promote turbulence near the nose for the blunted configurations, boundary layer trips were employed. A considerable effort was directed toward defining the minimum trip size that would promote turbulent flow and yet not materially affect the inviscid shock layer flow. This trip investigation was not only performed at zero angle of attack, but also at the larger angles that maneuvering vehicles fly (i.e., to 20°).

Contained in this section of the report is a summary listing of all of the data obtained on these configurations. Specifically, Table 2 presents an overall summary of the data obtained on the 7° cone, while Table 3 provides a summary of the bicone model data. Sections 3.2 through 3.4 contain details of each of the subset experiments conducted, including detailed AEDC data group numbers for each measurement set.

TABLE 2. SUMMARY OF DATA OBTAINED ON THE SHARP AND BLUNT 7° CONES

CONFIGURATION					FREESTREAM CONDITIONS		DATA ACQUIRED (BY TYPE AND ANGLE OF ATTACK)					TEST DATA SUMMARY
θ_c (deg)	R_N (in)	TRIP	SLICES (deg)	FLAP (deg)	M_∞	$R_{e_\infty} \times 10^{-5}/ft$	FORCE & MOMENT	PRESSURE	HEAT TRANSFER	SHOCK LAYER SURVEY α LOCATION	MACH/FLON ANGLE α LOCATION	TABLE NO.
7	SHARP	NO	NONE	NONE	6	1.0	--	--	0^0	--	--	5
		YES/NO			2.5	2.5	--	--	0^0	FRUSTUM	--	1
		YES/NO			4.7	4.7	--	0^0	0^0	FRUSTUM	--	2
		NO			0.6	0.6	--	--	$0^0, 7^0, 10^0$	--	--	3
		NO			1.0	1.0	--	--	0^0	FRUSTUM	--	4
		NO			2.5	2.5	--	--	$0^0, 2^0, 4^0, 7^0, 10^0$	--	--	5
		YES/NO			3.7	3.7	--	$0^0, 4^0$	$0^0, 4^0, 7^0$	FRUSTUM	$0^0, 4^0$ FRUSTUM	10
		NO			1.0	1.0	-14^0-14^0	--	--	--	--	10
7	0.1	YES/NO	NONE	NONE	6	4.7	--	--	$0^0, -1^0, 10^0$	--	--	5
7	0.5	YES/NO	NONE	NONE	5	1.0	--	--	0^0	--	--	
		YES/NO			6	4.7	--	0^0	$0^0, -1^0, 10^0$	FRUSTUM	--	
		YES/NO			3	1.0	--	--	0^0	FRUSTUM	--	8
		YES			1.5	1.5	--	--	$0^0, 7^0$	--	--	
		YES			2.5	2.5	--	--	$0^0, 7^0$	--	--	
		YES			3.7	3.7	-4^0-20^0	$0^0, 4^0, 10^0$	$0^0, 4^0, 7^0, 10^0$	FRUSTUM	$4^0, 10^0$ FRUSTUM	8, 13
		NO			1.0	1.0	-14^0-14^0	--	--	--	--	10

TABLE 3. SUMMARY OF DATA OBTAINED ON THE SHARP AND BLUNT $10.5^\circ/7^\circ$
AND $14^\circ/7^\circ$ BICONES

CONFIGURATION					FREESTREAM CONDITIONS		DATA ACQUIRED (BY TYPE AND ANGLE OF ATTACK)						TEST DATA SUMMARY
θ_c (deg)	R_N (in)	TRIP	SLICES (deg)	FLAP (deg)	M_∞	$k_u \times 10^{-6}/ft$	FORCE & MOMENT	PRESSURE	HEAT TRANSFER	SHOCK LAYER SURVEY α LOCATION	MACH/ELONG ANGLE α LOCATION	TABLE NO.	
10.5/7	SHARP	YES	NONE	NONE	6	2.5	--	0°	0°	0° FORECONE FRUSTUM (w/o Preston Tube)	--	5	
		YES/NO				4.7	--	0°	0°	--	--	5	
10.5/7	SHARP	NO	$0^\circ/-7^\circ$	NONE	8	3.7	$-4^\circ-20^\circ$	$0^\circ, 20^\circ$	$0^\circ, 20^\circ$	0° FRUSTUM SLICE	--	8	
				10° 20°			$-4^\circ-20^\circ$ $-4^\circ-20^\circ$	-- 0°	$0^\circ-10^\circ, 20^\circ$ --	-- 0° FLAP	-- --		
10.5/7	0.50	YES	NONE	NONE	6	2.5	--	--	0°	0° FRUSTUM	--	5	
						4.7	--	0°	0°	0° FORECONE FRUSTUM	--	5	
					8	3.7	$-4^\circ-20^\circ$	$0^\circ, 4^\circ, 10^\circ$	$0^\circ, 4^\circ, 7^\circ, 10^\circ$	$0^\circ, 4^\circ$ FORECONE FRUSTUM	--	8	
10.5/7	0.50	YES	$0^\circ/-7^\circ$	NONE	8	3.7	$-4^\circ-20^\circ$ $8^\circ-20^\circ$	$0^\circ, 10^\circ, 20^\circ$	$0^\circ-10^\circ, 20^\circ$	$0^\circ, 10^\circ$ FRUSTUM SLICES	$0^\circ, 10^\circ$ SLICE	13	
				10° 20° $20^\circ/10^\circ$			$-4^\circ-20^\circ$ $-4^\circ-20^\circ$ $-4^\circ-20^\circ$	0° 0° 0°	$0^\circ-10^\circ, 20^\circ$ $0^\circ-10^\circ, 20^\circ$ $0^\circ, 4^\circ, 10^\circ, 20^\circ$	$0^\circ, 10^\circ$ FLAP 0° FLAP 0° FLAP	$0^\circ, 10^\circ$ FLAP 0° FLAP 0° FLAP		

TABLE 3. SUMMARY OF DATA OBTAINED ON THE SHARP AND BLUNT $10.5^\circ/7^\circ$
AND $14^\circ/7^\circ$ BICONES (CONT'D)

CONFIGURATION				FREESTREAM CONDITIONS		DATA ACQUIRED (BY TYPE AND ANGLE OF ATTACK)						TEST DATA SUMMARY
θ_c (deg)	R_N (in)	TRIP	SLICES (deg)	FLAP (deg)	M_∞	$R_{eq} \times 10^{-6}/ft$	FORCE & MOMENT	PRESSURE	HEAT TRANSFER	SHOCK LAYER SURVEY LOCATION	MACH/FLOW ANGLE α	TABLE NO.
$14/7$	SHARP	YES	NONE	NONE	6	2.5	--	--	0°	0° FRUSTUM	--	5
		YES/NO	\uparrow	\uparrow	6	4.7	--	--	0°	--	--	5
$14/7$	0.5	YES/NO	NONE	NONE	6	2.5	--	0°	0°	0° FRUSTUM	--	5
		YES/NO	\uparrow	\uparrow	6	4.7	--	0°	$0^\circ, -1^\circ, -14^\circ$	0° FRUSTUM	--	4
		YES	\uparrow	\uparrow	8	3.7	--	--	$0^\circ, 4^\circ, 7^\circ, 10^\circ$	--	--	8
		NO	\uparrow	\uparrow	10	1.0	$-14^\circ, -14^\circ$	--	--	--	--	10
$14/7$	0.5	NO	$0^\circ/0^\circ$	NONE	10	1.0	$-14^\circ, -14^\circ$	--	--	--	--	10
$14/7$	0.5	NO	$0^\circ/-7^\circ$	NONE	10	0.55	--	--	$0^\circ, 2^\circ, 5^\circ, 10^\circ, 14^\circ$	--	--	10
		\uparrow	\uparrow	\uparrow	10	1.0	$-14^\circ, -14^\circ$	$2^\circ, 10^\circ$	$0^\circ, 14^\circ$	$2^\circ, 10^\circ$ FRUSTUM SLICES	$2^\circ, 10^\circ$ FRUSTUM SLICES	10

3.1 Axisymmetric Body - Turbulent Flow;

$$M_{\infty} = 6, \alpha = 0 \text{ (References 4 and 5)}$$

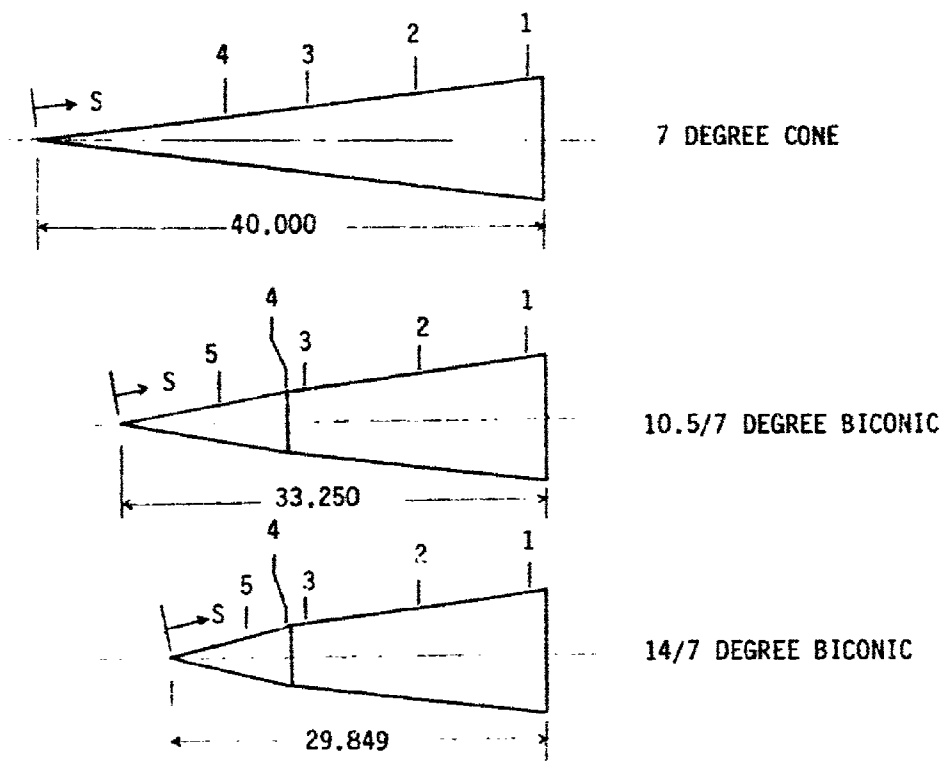
The testing of the axisymmetric 7° cone, and $10.5^\circ/7^\circ$ and $14^\circ/7^\circ$ bicones were conducted in two phases. The objective of the first phase was to determine the smallest boundary layer trip that would bring boundary layer transition near the trip without introducing disturbances in the flow field. A boundary layer trip that brought the end of the transition in the vicinity of the first heat gage ($s = 8.15$ for the 7° cone, and 3.91 for the $14^\circ/7^\circ$ bicone) was considered effective and suitable to be studied in more detail. This initial approach was taken since the ultimate goal was to fix the end of transition on the forebody of the biconic configurations to be studied in detail in later test phases.

The objective of the second test phase was to evaluate the influence of boundary layer trips on boundary layer and flow field characteristics. Flow field surveys were performed at several longitudinal body stations on configurations with different nosetips and trip combinations. Corresponding heat transfer data were obtained to identify transition and verify that turbulent flow existed at the probe survey stations.

Figure 17 lists the survey station for each basic body configuration while Table 4 indicates the location of the surface instrumentation for each of the three configurations.

A summary of the nominal test conditions at each Reynolds number is given below:

M_{∞}	p_o, psia	$T_o, ^\circ\text{R}$	$\rho_o \times 10^5$ slugs/ft^3	q_w, psia	p_w, psia	$Re_w/\text{ft} \times 10^{-6}$
5.91	55	845	2.98	0.919	0.037	1.0
5.94	131	845	7.06	2.180	0.088	2.5
5.95	250	845	13.37	4.131	0.167	4.7

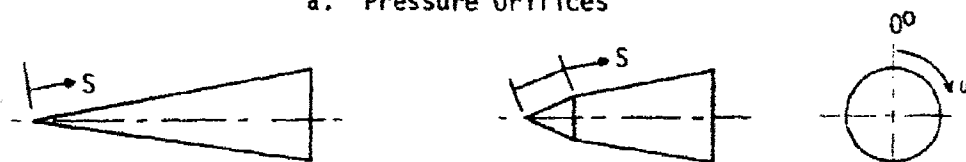


STATION NO.	S, IN.		
	7 DEGREE CONE	10.5/7 DEGREE BICONIC	14/7 DEGREE BICONIC
1	38.800	32.125	28.801
2	30.300	23.625	20.301
3	20.150	14.486	11.162
4	15.150	13.233	9.909
5	-	8.483	6.159

FIGURE 17. PROBE SURVEY LOCATIONS

TABLE 4. SURFACE INSTRUMENTATION LOCATIONS

a. Pressure Orifices



ORIFICE NO.	S, IN.			180°
	7 DEGREE CONE	10.5/7 DEGREE BICONIC	14/7 DEGREE BICONIC	ω DEG.
1	39.800	33.125	29.801	0 ↓ -90 ↓ 90 ↓ 180 ↓ 0 180 0
2	38.300	31.625	28.301	
3	36.300	29.625	26.301	
4	34.300	27.625	24.301	
5	32.300	25.625	22.301	
6	30.300	23.625	20.301	
7	28.300	21.625	18.301	
8	26.300	19.625	16.301	
9	24.300	17.625	14.301	
10	22.300	15.625	12.301	
11	20.150	14.486	11.162	
12	17.150	14.111	10.787	
13	15.150	13.736	10.412	
14	13.150	13.233	9.909	
15	11.150	12.483	9.159	
16	9.150	10.483	7.159	
17	8.150	8.483	6.159	
18	-	7.483	5.159	
19	-	6.483	4.659	
20	-	5.483	4.159	
21	-	4.983	3.659	
22	39.800	33.125	29.801	-90 ↓ 90 ↓ 180 ↓ 0 180 0
23	30.300	23.625	20.301	
24	11.150	5.483	4.659	
25	39.800	33.125	29.801	
26	30.300	23.625	20.301	
27	11.150	5.483	4.659	
28	39.800	33.125	29.801	
29	30.300	23.625	20.301	
30	11.150	5.483	4.659	
31	BASE	BASE	BASE	
32	BASE	BASE	BASE	
33	38.800	32.125	28.801	

TABLE 4. SURFACE INSTRUMENTATION LOCATIONS (CONT'D)

b. Heat Gages

GAGE NO.	S, IN.			ω DEG.
	7 DEGREE CONE	10.5/7 DEGREE BICONIC	14/7 DEGREE BICONIC	
1	38.300	31.625	28.301	180
2	36.300	29.625	26.301	
3	34.300	27.625	24.301	
4	32.340	25.565	22.241	
5	28.240	21.565	18.241	
6	26.240	19.565	16.241	
7	25.240	18.565	15.241	
8	24.240	17.565	14.241	
9	23.240	16.565	13.241	
10	22.240	15.565	12.241	
11	21.150	14.486	11.162	
12	20.150	14.111	10.787	
13	19.150	13.736	10.412	
14	18.150	13.233	9.909	
15	17.150	12.233	9.159	
16	15.150	10.483	7.159	
17	13.150	7.483	6.159	
18	9.150	6.233	5.159	
19	8.150	4.983	3.909	

Transition location was determined from the heat transfer distribution obtained with the Gardon heat-flux gages. Prior to each run the model was cooled to approximately 520°R by flowing air over the model. The model was injected into the tunnel flow for about five seconds while a continuous record of gage output was recorded. Data presented in the Data Package were reduced approximately one second after the model reached the centerline of the wind tunnel. Some runs were obtained with a hot wall to minimize the time required for a full cooling cycle. Since the thermal driving potential ($T_0 - T_w$) was low for these cases, the data uncertainty was significantly greater than the cool wall data. However, these data were qualitatively useful in determining the presence of transition.

Surface pressure distributions were obtained on selected configurations. It should be noted that surface pressure at each probe station was obtained each time a survey point was recorded. This procedure made it possible to confirm that local wall pressure had been obtained in the absence of any local probe disturbance or interference.

Initial probe positioning on the model wall was monitored with the closed circuit television system (CCTV). The television image was used to monitor probe longitudinal location and to verify Preston tube and Pitot probe contact with the model surface. At each survey station, a reference mark was painted on the model surface with black paint to provide an optical target for positioning the probe. The Preston tube and Pitot tube were brought down until they both were in contact with the model surface. It is estimated that the probe was located axially to within ± 0.050 inches of the reference marks.

Initial data were obtained with the Preston tube and Pitot tube in contact with the model surface. The first three probe positions above the model surface were obtained using manual probe drive control to achieve the desired small height increments between points. Remaining points in the survey were obtained using an automatic system which drove the probe to predetermined locations above the model surface. Note that the only point valid for the Preston tube measurements was the initial point at the model wall. Each survey consisted of approximately 50 points.

Table 5a through 5c present the AEDC data group numbers from References 4 and 5 (and the complementary data tabulations) for each configuration tested for the heat transfer, pressure, and shock layer survey tests, respectively.

3.2 Axisymmetric Body-Turbulent Flow: Mach 8, $\alpha=0$ (Reference 6)

The overall test objective was to obtain a turbulent-flow data base with which to validate and develop analytical codes to be used in predicting the hypersonic aerodynamic characteristics of conic and biconic bodies at angles of attack. Data obtained in this series includes surface heat transfer, pressure, and detailed flow field measurements including flow-angle information.

A major portion of the test was devoted to flow-field surveys over two basic configurations, the 7-degree cone (sharp and blunt nose) and the blunt biconic configuration (fore cone/aft cone angles of 10.5 deg/7 deg) at Mach number 8. Windward and leeward surveys were obtained at several model stations, from the model surface to the bow shock using a probing mechanism located on top of the tunnel. In addition, radial surveys were obtained at one model station near the base by using an "onboard" probing mechanism. Roll positions relative to the windward plane of symmetry for these radial surveys were: 50, 75, 100, 120, 140, and 160 degrees. Flow-field probes on the survey mechanisms were: Pitot probes, unshielded thermocouple probes, a Preston tube and a Mach/Flow-Angularity probe.

Surface pressures were measured to provide pressure data for boundary layer calculations, and heat-transfer distributions were obtained to determine the boundary layer state. A machined boundary layer trip was used for the majority of the tests, to provide the desired fully developed turbulent boundary layer. Surface shear stress data were obtained using a flow-angle sensitive Preston tube attached to the model. Data were

TABLE 5A. HEAT TRANSFER DATA SUMMARY - MACH 6, $\alpha = 0$

CONFIGURATION		$Re_{\infty} \times 10^{-6}$ ft ⁻¹	MERIDIAN ANGLE, ω			REMARKS
θ	R_N (IN.)		0°	90°	180°	
7°	0	NONE	4.7	1, 2, 37 93, 97, 109, 110	14 15, 94	
	0.05	NONE	1.0	56	--	
		NONE	2.5	52	--	
		NONE	4.7	22	30	
	.010		4.7	8, 10, 23 ⁺ , 29, 38	9 30, 39	+ Grooves
	.022		2.5	51	--	
	.037		1.0	59	--	
	0.10	NONE	4.7	24	--	
	0.10	.014	4.7	16	--	
	0.50	NONE	1.0	57	--	
		NONE	2.5	48	--	
		NONE	4.7	3, 4, 112	5 --	
	.0065		4.7	11	12 13	
	.010		4.7	17, 18, 19 20, 21, 27, 43	-- 28	
	.014		4.7	7, 113, 124	--	
	.022		2.5	47	--	
	.037		1.0	58	--	
	.093		4.7	114	--	

18: α SWEEP, -1° to 10°
 19: 0-180° ROLL @ $\alpha=0^\circ$
 20: 0-180° ROLL @ $\alpha=5^\circ$
 21: 0-180° ROLL @ $\alpha=10^\circ$

TABLE 5A. HEAT TRANSFER DATA SUMMARY - MACH 6, $\alpha = 0$ (CONT'D)

CONFIGURATION		$Re_x \times 10^{-6}$ ft^{-1}	MERIDIAN ANGLE, ω			REMARKS
r	R_H (IN.)		0°	90°	180°	
10.5°/7°	0.05	4.7	129, 131	--	130	
	0.05	2.5	156	--	157	
	0.50	4.7	132	--	--	
	↑	4.7	153, 154	--	--	
	↑	2.5	171	--	172	HOT WALL H.T.
	↑	2.5	173, 174	--	--	HOT WALL H.T.
14°/7°	0.05	4.7	66	--	67	
	↑	4.7	68	--	69	
	GROOVES	2.5	205	--	--	
	0.10	2.5	206	--	--	
	0.46	2.5	70, 177	--	--	
	0.50	2.5	72	--	--	
	↑	4.7	64, 73, 74*,	91 ⁺	65, 75*	+ ROLL 0 → 180°
	↑	4.7	77, 78*, 80,	76 ⁺	81*	* $\alpha \sim -1$ to $+14^\circ$
	↑	4.7	86	79 ⁺⁺	--	++ $\alpha = 14^\circ$ ROLL 0 → 180°
	↑	2.5	178, 202, 203, 204	--	179	
	0.14	2.5	180, 181	--	--	
	0.093	2.5				

TABLE 5B. SURFACE PRESSURE DATA SUMMARY - MACH 6, $\alpha = 0$

CONFIGURATION		$Re_{\infty} \times 10^{-6}$ ft^{-1}	MERIDIAN ANGLE, ω	
θ	R_N (IN.)		0°	180°
7° ↓	0	4.7	31, 33, 61, 100	32, 99
	0.50		41, 62	--
	.010		125	126
	.014		116	--
10.5°/7° ↓	0.05	4.7	134, 159	135, 160
	0.50		137	--
14°/7° ↓	0.50	4.7	82, 83	--
	.0065	2.5	183, 185	--
	.014	2.5	198	--

TABLE 5c. PROFILE DATA SUMMARY - MACH 6, $\alpha = 0$

CONFIGURATION			$Re_{\infty} \times 10^{-6}$ ft^{-1}	PROBE SYSTEM	
θ	R_N (IN.)	TRIP HT. (IN.)		ON-BOARD	OVERHEAD*
7° ↓	0	NONE	4.7	34, 102, 103	36, 106, 107, 215, 217
	.05	.011	2.5	--	219, 220
	.50	NONE	4.7	26	--
	.50	NONE	1.0	60	--
	.50	.010-.014	4.7	25, 42, 123	119, 120, 218
	.50	.093	4.7	118	117
10.5°/7° ↓	.05	.010	2.5	--	161, 162, 163
	.50	.010	4.7	--	139, 143, 146, 148, 149
	.50	.022	2.5	--	168, 169
	.50	.046	4.7	--	150, 151
	.50	.125	2.5	--	164, 165, 166, 167
14°/7° ↓	.05	.010	2.5	--	213, 214
	.05	.046	2.5	--	207, 208
	.05	.093	2.5	--	209, 210, 211
	.50	.0065	4.7	84	85
	.50	.014	2.5	--	199, 200, 201
	.50	.093	2.5	--	188, 190, 192, 193, 195

* DATA TAKEN AT SEVERAL AXIAL STATIONS

obtained at free-stream Reynolds numbers from 0.5 to 3.7 million per ft, with the majority of the results obtained at 3.7 million per ft. Model angles of attack were from -10 to 10 deg and model roll angles were from 0 to 180 deg.

The locations of the heat transfer gages for the sharp 7° and blunt 7° cones, and the blunt $10.5^\circ/7^\circ$ and $14^\circ/7^\circ$ bicones are listed in Tables 6a to 6d, respectively. Similarly, the locations of the surface pressure crifices, including the identification of the profile measuring stations for the sharp and blunt 7° cone and the blunt $10.5^\circ/7^\circ$ bicone are listed in Tables 7a to 7c, respectively.

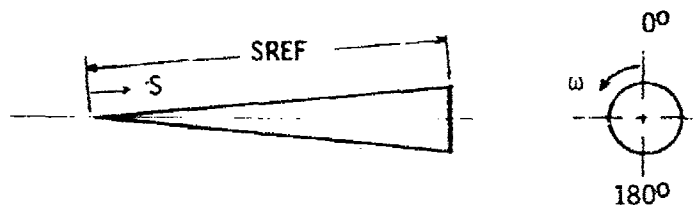
A summary of the nominal test conditions at each Mach number is given below.

M_∞	p_o , psia	T_o , $^\circ R$	q_∞ , psia	p_∞ , psia	$Re_\infty \times 10^{-6}/ft$
7.90	100	1220	0.485	0.011	0.5
7.91	125	1285	0.603	0.014	0.6
7.94	210	1280	0.997	0.023	1.0
7.97	330	1310	1.540	0.035	1.5
7.99	560	1330	2.584	0.058	2.5
8.00	850	1350	3.900	0.087	3.7

Heat-transfer distribution data were obtained with high-sensitivity thermopile heat-flux gages (Gardon type). These data were taken to determine transition locations, and to evaluate trip effectiveness. In most cases the model was injected into the tunnel flow at a fixed model attitude. The data were recorded continuously for a period of about 5 seconds beginning one second after the model reached tunnel centerline. The model was then retracted into the test section tank and cooled with high pressure air. Model wall temperature typically did not exceed $600^\circ R$ during data acquisition. One series of runs was made using the continuous roll sweep mode; with the model pitched at four degrees the model was rolled from 0 to 180 degrees while recording the data continuously.

TABLE 6. HEAT TRANSFER GAGE LOCATIONS

a. 7 Degree Sharp Cone (RN = 0.0015 in.)

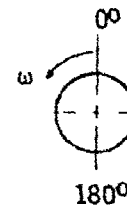
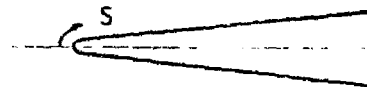


Gage No.	S, In.	S/SREF	ω , DEG.	Gage No.	S, IN.	S/SREF	ω , DEG.
1	38.790	0.963	180	18	22.230	0.552	180
2	38.290	0.950		19	21.140	0.525	
3	37.590	0.933		20	20.140	0.500	
4	36.290	0.901		21	19.140	0.475	
5	35.290	0.876		22	18.140	0.450	
6	34.290	0.851		23	17.140	0.425	
7	33.290	0.826		24	16.140	0.401	
8	32.230	0.800		25	15.140	0.376	
9	31.230	0.772		26	14.140	0.351	
10	29.930	0.743		27	13.140	0.326	
11	29.230	0.726		28	12.140	0.301	
12	28.230	0.701		29	10.840	0.269	
13	27.230	0.676		30	10.140	0.252	
14	26.230	0.651		31	9.140	0.227	
15	25.230	0.626		32	8.140	0.202	
16	24.230	0.601		39	38.791	0.963	5
17	23.230	0.577		40	38.791	0.963	15

SREF = 40.291 IN.

TABLE 6. HEAT TRANSFER GAGE LOCATIONS (CONT.D)

b. 7 Degree Blunt Cone (RN = 0.50 in.)

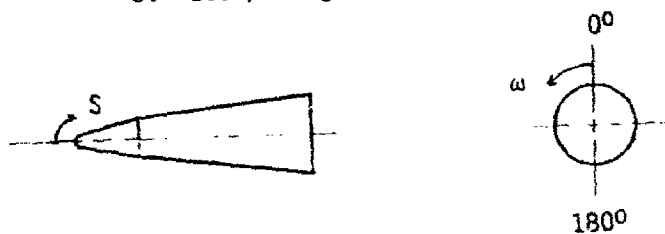


Gage No.	S, In.	S/SREF	ω, DEG.	Gage No.	S, IN.	S/SREF	ω, DEG.
1	35.452	0.959	180	18	18.892	0.511	180
2	34.952	0.946		19	17.802	0.482	
3	34.252	0.927		20	16.802	0.455	
4	32.952	0.892		21	15.802	0.428	
5	31.952	0.865		22	14.802	0.401	
6	30.952	0.837		23	13.802	0.374	
7	29.952	0.811		24	12.802	0.346	
8	28.892	0.782		25	11.802	0.319	
9	27.892	0.755		26	10.802	0.292	
10	26.592	0.720		27	9.802	0.265	
11	25.892	0.701		28	8.802	0.238	
12	24.892	0.674		29	7.502	0.203	
13	23.892	0.647		30	6.802	0.184	
14	22.892	0.620		31	5.802	0.157	
15	21.892	0.592		32	4.802	0.130	
16	20.892	0.565		39	35.453	0.959	
17	19.892	0.538		40	35.453	0.959	

SREF = 36.953 IN.

TABLE 6. HEAT TRANSFER GAGE LOCATIONS (CONT'D)

c. 10.5/7 Degree Biconic (RN = 0.50 in)

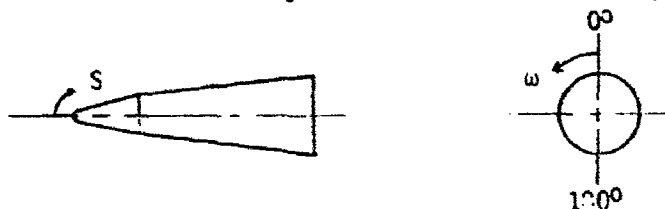


Gage No.	S, In.	S/SREF	ω , DEG.	Gage No.	S, IN.	S/SREF	ω , DEG.
1	30.123	0.953	180	17	14.563	0.461	180
2	29.623	0.937	↓	18	13.563	0.429	↓
3	28.923	0.915		19	12.484	0.395	
4	27.623	0.874		20	12.109	0.383	
5	26.623	0.842		21	11.734	0.371	
6	25.623	0.810		22	11.231	0.355	
7	24.623	0.779		23	10.231	0.324	
8	23.563	0.745		24	9.354	0.296	
9	22.563	0.714		25	8.481	0.268	
10	21.263	0.672		26	7.479	0.237	
11	20.563	0.650		27	6.479	0.205	
12	19.563	0.619		28	5.481	0.173	
13	18.563	0.587		29	4.231	0.134	
14	17.563	0.555		30	2.981	0.094	
15	16.563	0.524		39	30.123	0.953	5
16	15.563	0.492		40	30.123	0.953	15

SREF = 31.623 IN.

TABLE 6. HEAT TRANSFER GAGE LOCATIONS (CONT'D)

d. 14/7 Degree Biconic (RN = 0.50 in)

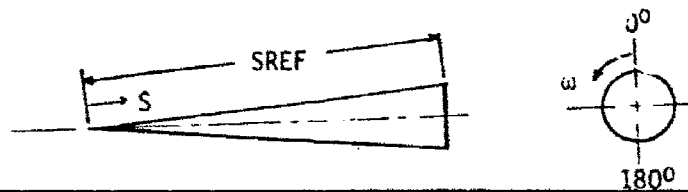


Gage No.	S, In.	S/SREF	ω , DEG.	Gage No.	S, IN.	S/SREF	ω , DEG.
1	27.46	0.948	180	18	10.90	0.376	180
2	26.96	0.931		19	9.82	0.339	
3	26.26	0.907		20	9.45	0.326	
4	24.96	0.862		21	9.07	0.313	
5	23.96	0.827		22	8.56	0.296	
6	22.96	0.793		23	7.81	0.270	
7	21.96	0.758		24	6.81	0.235	
8	20.90	0.722		25	5.81	0.201	
9	19.90	0.687		26	4.81	0.166	
10	18.60	0.642		27	3.81	0.132	
11	17.90	0.618		28	2.56	0.088	
12	16.90	0.584		33	28.46	0.983	40
13	15.90	0.549		34			50
14	14.90	0.515		35			60
15	13.90	0.480		36	18.90	0.653	40
16	12.90	0.445		37			50
17	11.90	0.411		38			60

SREF = 28.96 IN.

TABLE 7. PRESSURE ORIFICE LOCATIONS

a. 7 Degree Sharp Cone (RN = 0.0015 in.)



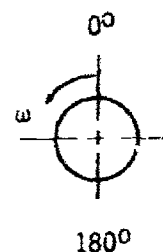
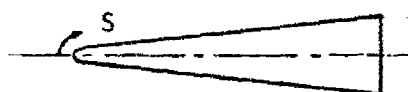
Orifice No.	S, In.	S/SREF	ω , DEG	Orifice No.	S, In.	S/SREF	ω , DEG
1	39.791	0.988	0	15	13.141	0.326	0
2*	38.791	0.963	↓	16	11.141	0.277	↓
3	38.291	0.950		17	9.141	0.227	↓
4	36.291	0.901		18	8.141	0.202	↓
5	34.291	0.851		19	11.141	0.277	90
6	32.231	0.800		20	11.141	0.277	180
7	30.231	0.750		21	11.141	0.277	270
8*	28.231	0.701		26	30.231	0.750	90
9	26.231	0.651		27	30.231	0.750	180
10	24.231	0.601		28	30.231	0.750	270
11	22.231	0.552		29	39.791	0.988	90
12	20.141	0.500		30	39.791	0.988	180
13*	17.141	0.425		31	39.791	0.988	270
14	15.141	0.376					

SREF = 40.291 IN.

* Probe Survey Locations

TABLE 7. PRESSURE ORIFICE LOCATIONS (CONT'D)

b. 7 Degree Blunt Cone (RN = 0.50 in.)



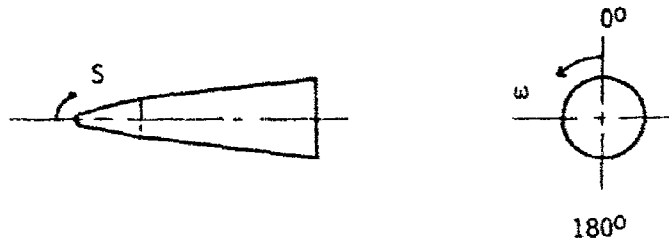
Orifice No.	S, IN.	S/SREF	ω , DEG.	Orifice No.	S, IN.	S/SREF	ω , DEG.
1	36.453	0.986	0	14	11.803	0.319	0
2*	35.453	0.959	↓	15	9.803	0.265	↓
3	34.953	0.946		16	7.803	0.211	
4	32.953	0.892		17	5.803	0.157	
5	30.953	0.838		18	4.803	0.130	
6	28.893	0.782		19	7.803	0.211	90
7	26.893	0.728		20	7.803	0.211	180
8*	24.893	0.674		21	7.803	0.211	270
9	22.893	0.620		26	26.893	0.728	90
10	20.893	0.565		27	26.893	0.728	180
11	18.893	0.511		28	26.893	0.728	270
12	16.803	0.455		29	36.453	0.986	90
13*	13.803	0.374		30	36.453	0.986	180
				31	36.453	0.986	270

SREF = 36.953 IN.

* Probe Survey Locations

TABLE 7. PRESSURE ORIFICE LOCATIONS (CONT'D)

c. 10.5/7 Degree Biconic (RN = 0.50 in.)



Orifice No.	S, IN.	S/SREF	ω , DEG.	Orifice No.	S, IN.	S/SREF	ω , DEG.
1	31.123	0.984	0	17	8.841	0.268	0
2*	30.123	0.953	↓	18*	6.481	0.205	↓
3	29.623	0.937		19	5.481	0.173	
4	27.623	0.874		20	4.481	0.142	
5	25.623	0.810		21	3.481	0.110	
6*	23.563	0.745		22	2.981	0.094	
7	21.563	0.682		23	3.481	0.110	90
8	19.563	0.619		24	3.481	0.110	180
9*	17.563	0.555		25	3.481	0.110	270
10	15.563	0.492		26	21.563	0.682	90
11	13.563	0.429		27	21.563	0.682	180
12	12.484	0.395		28	21.563	0.632	270
13	12.109	0.383		29	31.123	0.984	90
14	11.734	0.371		30	31.123	0.984	180
15	11.231	0.355		31	31.123	0.984	270
16*	10.481	0.331					

SREF = 31.623 IN.

* Probe Survey Locations

Data acquisition procedures can be divided into various data types: (1) heat-transfer data, (2) surface pressure and flow-angle sensitive Preston tube data, (3) overhead probe surveys, (4) onboard probe surveys, (5) Mach/Flow-Angularity probe calibrations and (6) total temperature probe calibrations. The data acquisition procedures for each type are discussed in the subsequent paragraphs.

Heat-transfer distribution data were obtained with coaxial surface thermocouple gages. The model attitude was preset, and the model was then injected into the tunnel flow while recording data continuously. During this time the model wall temperatures were nominally 540 to 580°R. The model was in the tunnel flow (injection to retraction) approximately 6 sec. Model cooling was accomplished in the test section tank between injections by blowing high pressure air over the model.

Surface pressure data, and flow-angle sensitive Preston tube data were obtained at 3 angles of attack and 8 model roll angles. In each case, data acquisition was essentially the same, since the pressures were measured using the AEDC "standard pressure system."

Flow-field surveys with the overhead probes were taken from the model surface to just beyond the bow shock. A survey run typically consisted of 40 to 100 data points obtained at different heights above the model surface. The probe direction of travel (Z' drive direction) was nominally along a "surface normal". The small size of the probe presented a major problem in obtaining high quality pressure measurements, namely, the small tube size causes severe pressure lag or stabilization problems. To alleviate this problem, time-wise data were recorded to provide pressure-time histories which were used to evaluate or define the equilibrium pressures.

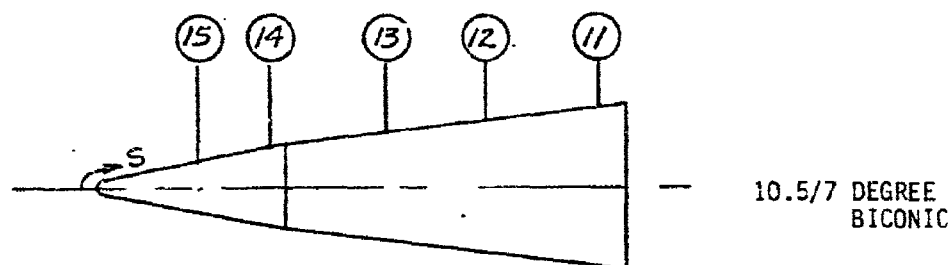
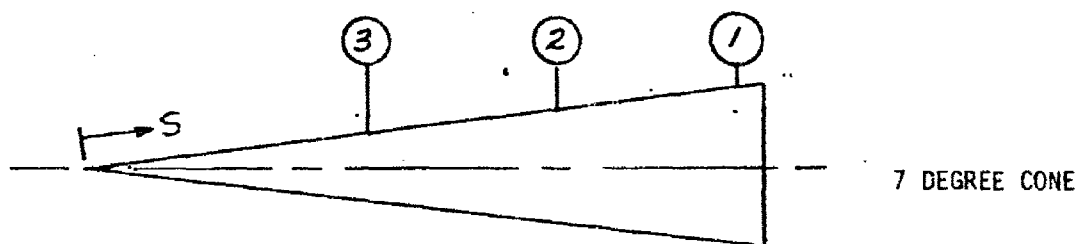
The following data taking sequence was used: (1) the probe was moved to predetermined height and (2) the data acquisition system waited a prescribed delay time (2 to 5 seconds) and then recorded 40 loops of data at a constant time interval (0.1 seconds) which provided pressure-time histories. Positioning the probe on the model surface was monitored optically. An automatic control system was used to drive the probe except at points near the model surface ($ZP \leq 0.09$ in.). Overhead probe survey locations are shown in Figure 18.

Flow-field surveys with the onboard probes were almost identical in data acquisition technique to the overhead surveys. However the onboard probes typically did not get outside the bow shock due to the mechanism limit of travel (2.5 in. maximum). The probes were positioned on the model surface, and then the model was rolled to the desired attitude before starting a survey. Thus most surveys with the onboard probes were conducted without optical monitoring.

Mach/Flow-Angularity probe calibrations were obtained in the freestream at discrete probe pitch attitudes from 3 to 25 degrees. The calibration data were obtained at several freestream Reynolds number conditions in order to evaluate Reynolds number effects.

Total temperature probe calibrations were obtained in the free-stream for each probe used. For these calibration runs, the total pressure (P_0) was varied in 50 psi increments from 150 to 850 psia. Total temperature probe data and tunnel conditions were recorded at each pressure level and used to determine Reynolds number effects on the unshielded total temperature probes.

Tables 8a through 8e present the AEDC data group numbers from Reference 6 (along with the complementary data tabulations) for each configuration tested and data type.



7 DEGREE CONE

10.5/7 BICONIC

STA. NO.	** PRES. ORIF.	RN = 0.0015"		RN = 0.5"	
		S, IN.	S/SREF.	S, IN.	S/SREF.
1*	2	38.791	0.963	35.453	0.959
2	8	28.231	0.701	24.893	0.674
3	13	17.141	0.425	13.803	0.374

STA. NO.	** PRES. ORIF.	RN = 0.5"	
		S, IN.	S/SREF.
11*	2	30.123	0.953
12	6	23.563	0.745
13	9	17.563	0.555
14	16	10.481	0.331
15	18	6.481	0.205

*ON-BOARD SURVEY LOCATION ALSO

**PRESSURE ORIFICES ARE AT AXIAL LOCATION OF SURVEY
STATION BUT ROLLED 180 DEGREES FROM PROBE DURING
SURVEYS

FIGURE 18. OVERHEAD PROBE SURVEY LOCATIONS

TABLE 8. TEST DATA SUMMARY - AXISYMMETRIC MODELS @ MACH 8
a. Gardon Gage Heat Transfer Data

MODEL CONFIGURATION			$Re_{\infty} \times 10^4$ FT ⁻¹	α DEG.	MODEL ROLL ANGLE (ω), DEG.				
CONE ANGLE	RN IN.	TRIP HT., IN.			WIND 0	45	90	135	LEE 180
70	0.0	NONE	0.6	0	-	-	-	-	RUN 1
				7	-	-	-	-	2
				10	-	-	-	-	3
			1.0	0	-	-	-	-	4
				0	-	-	-	-	12,20
				2	16	17	18	19	26
			2.5	4	(0 - 180 ROLL SWEEP)				15
				7	14,21	22	23	24	13,25
				10	27	28	29	30	31
			3.7	0	32	-	-	-	-
				4	33	34	35	36	37
				7	38	39	40	41	42
	0.5	NONE .033	1.0	0	-	-	-	-	5
				0	-	-	-	-	6
				0	-	-	-	-	7
			1.5	7	-	-	-	-	8
				0	-	-	-	-	9
				7	11	-	-	-	10
			2.5	0	43	-	-	-	-
				4	44	45	-	-	46
				7	47	48	49	50	51
			3.7	0	52	53	54	55	56
				10	57	-	-	-	-
				4	58	59	-	-	-
10.50/70		.015 ↓ .033 ↓ .037 ↓		0	60	-	-	-	-
				4	61	62	63	64	65,76*
				7	66	67	68	69	70,77*
				10	71	72	73	74	75,78*
				0	79,85	-	-	-	-
				7	80	81	82	83	84
				0	86	-	-	-	-
				4	87	88	89	90	91
140/70		.021 ↓ .023 ↓		7	92	93	94	95	96
				10	97	98	99	100	101
				0	102,108	-	-	-	-
				7	103	104	105	106	107

*Model Roll = 1570 for Runs 76, 77, 78

TABLE 8. TEST DATA SUMMARY - AXISYMMETRIC MODELS @ MACH 8 (CONT'D)

b. Coax Gage Heat Transfer Data

$$M_{\infty} = 8$$

$$Re_{\infty} = 3.7 \times 10^6 \text{ FT}^{-1}$$

$$\text{B. L. TRIP} = .06 \text{ IN.}$$

MODEL CONFIGURATION		α DEG.	MODEL ROLL ANGLE (ω), DEG.							
CONE ANGLE	RN IN.		WIND 0	-50	-75	-100	-120	-140	-160	LEE -180
7° ↓	0.0015 ↓	0	8	-	-	-	-	-	-	-
		4	204	205	-	206	-	207	-	208
7° ↓	.50 ↓	0	318,5	-	-	-	-	-	-	-
		4	39,6	36	319	35	320	34	321	33,7
		10	63	62	209,212	61	210	60	211	59
10.5°/7° ↓	.50 ↓	0	253	-	-	-	-	-	-	-
		4	254	255	-	256	-	257	-	258
		10	261	262	266	263	267	264	268	265

TABLE 8. TEST DATA SUMMARY - AXISYMMETRIC MODELS @ MACH 8 (CONT'D)

c. Model Surface Pressure Data

$$M_{\infty} = 8$$

$$Re_{\infty} = 3.7 \times 10^6 \text{ FT}^{-1}$$

$$\text{B. L. TRIP} = .06 \text{ IN.}$$

MODEL CONFIGURATION		α DEG.	MODEL ROLL ANGLE (ω), DEG.							
CONE ANGLE	RN IN.		WIND -180	-130	-105	-80	-60	-40	-20	LEE 0
7° ↓	0.0015 ↓	0	-	-	-	-	-	-	-	17
		4	79	78	-	77	-	76	-	75
7° ↓	0.5 ↓	0	-	-	-	-	-	-	-	18
		4	44	43	-	42	-	41	-	40
		10	68	67	107	66	108	65	109	64
10.5°/7° ↓	0.5 ↓	0	-	-	-	-	-	-	-	90
		4	95	94	-	93	-	92	-	91
		10	96	97	-	98	-	99	-	100

TABLE 8. TEST DATA SUMMARY - AXISYMMETRIC MODELS @ MACH 8 (CONT'D)

d. Flow Angle Sensitive Preston Tube Data

$M_{\infty} = 8$

$Re_{\infty} = 3.7 \times 10^6 \text{ FT}^{-1}$

B. L. TRIP - .06 IN.

MODEL CONFIGURATION		α DEG.	MODEL ROLL, DEG.							
CONE ANGLE	RN IN.		WIND							
			-80	-130	-155	0	-20	-40	-60	-80
70 ↓	.0015 ↓	0	401	-	-	-	-	-	-	-
		4	-	-	-	406	405	404	403	402
		-4	400	399	397 398	-	-	-	-	-
70 ↓	.1 ↓	0	232	-	-	-	-	-	-	-
		4	-	-	-	233	234	235	236	237
		-4	238	239	240	-	-	-	-	-
		10	-	-	-	241	242	243	244	245
		-10	246	247	248	-	-	-	-	-
10.50/70 ↓	.50 ↓	0	313 347 370	-	-	-	-	-	-	-
		4	-	-	-	308 342	309 343	310 344	311 345	312 346
		-4	314 348	315 349	316 350	341	-	-	-	-
		10	-	-	-	307	306	305	304	303
		-10	355	356	357	-	-	-	-	-

TABLE 8. TEST DATA SUMMARY - AXISYMMETRIC MODELS @ MACH 8 (CONT'D)
e. Overhead Probe Survey Data

MODEL CONFIGURATION			$Re \times 10^{-4}$ FT ⁻¹	α DEG.	SURVEY STATIONS (MODEL ROLL = 180 DEGREES)										REMARKS
CONE ANGLE	R_N IN.	TRIP HT. (IN.)			1	2	3	11	12	13	14	15			
7° ↓	.0015 ↓	.060 ↓	3.7 ↓	0 -4 +4	24 388* (17)	26 387* (17)	27 386* (17)								WINDWARD LEEWARD
7° ↓	.50 ↓	.060 ↓	3.7 ↓	0 -4 +4 -10 +10	54 226* (18)	51 227* (18)	29 228* (18)								WINDWARD LEEWARD WINDWARD LEEWARD
7° ↓	.50 ↓	NONE ↓	1.0 ↓	0	19	-	-								LAMINAR
10.50/7° ↓	.50 ↓	.060 ↓	3.7 ↓	0 -4 +4 -10 +10			373* (90)	372* (90)	371* (90)	369 (90)	368 (90)				WINDWARD LEEWARD WINDWARD LEEWARD
							363* 351 (95)	364* 352 (95)	365* 353 (95)	366 354 (95)	367 - (95)				
							375 374 (91)	376 - (91)	377* 302 (91)	378* 301 (91)	379* 300 (91)				
							358* 269 (96)	359* 270 (96)	360* 281 (96)	361* 282 (96)	362 (96)				
							384* 293 292 (99)	383* 295 294 (99)	382* 297 296 (99)	381* 298 - (99)	380* 299 - (99)				

NOTES: RUN NUMBER IN PARENTHESES ARE SURFACE PRESSURE RUN NUMBERS ASSOCIATED WITH EACH SURVEY
*PRESTON TUBE DATA ONLY
+ SURVEY OBTAINED 1.06 IN. AFT OF SURVEY STATION

TABLE 8. TEST DATA SUMMARY - AXISYMMETRIC MODELS @ MACH 8 (CONT'D)

f. Onboard Probe Survey Data

$$M_{\infty} = 8$$

$$Re_{\infty} = 3.7 \times 10^6 \text{ ft}^{-1}$$

B.L. TRIP - .06 in.

MODEL CONFIGURATION		α DEG.	MODEL ROLL, DEG.						
CONE ANGLE	R_N IN.		-120	-95	-70	-50	-30	-10	+10 (LEE)
7° ↓	.0015 ↓	0	331(17)						
		4	122 334(78)		121 333(77)		120 332(76)		
7° ↓	.50 ↓	4	110 324 214(43)		111 323(42)		112, 113 322(41)		
		10	114 330(67)	117 329 (107)	115 328(66)	118 327 (108)	116 326(65)	119 325 (109)	
10.5°/7° ↓	.50 ↓	0	284(90)						
		4	101 287(94)		102 286(93)		103 285(92)		
		10	104 291(97)		105 289(98)		106 288 290(99)		

NOTES: RUN NOS. < 200 → PITOT & TOTAL TEMPERATURE PROBE DATA

RUN NOS. > 200 → MACH/FLOW-ANGULARITY PROBE DATA

(RUN NOS. IN PARENTHESES ARE SURFACE PRESSURE RUN
NUMBERS ASSOCIATED WITH EACH SURVEY)

3.3 Sliced Body w/o Flap - Laminar Flow: Mach 10, $\alpha \neq 0$ (References 2, 7)

The objective of this test series was to provide inputs to a laminar flow data base which will be used to validate and develop analytical codes for predicting the hypersonic aerodynamic characteristics of conic and biconic bodies with single and multiple slices (flat surfaces). The data base consists of static force data, which are documented in Reference 2, and heat transfer, surface pressure, and flow field survey data which are documented in Reference 7.

The tests were conducted in Tunnel C at a nominal Mach number of 10 and free-stream unit Reynolds numbers of 0.55 million and 1.0 million per ft. Static-stability, axial-force, and oil flow data were obtained over an angle-of-attack range was -14 to $+14$ deg. The effects of nose radius and single and double flat surfaces were investigated. Oil flow visualization data were acquired on the double flat surface configuration to determine the flow directions in the vicinity of the double flat surface. Static force data were obtained on both the blunted ($R_N = 0.50$) 7° cone and $14^\circ/7^\circ$ bicone, and a sharp 7° cone. The bicone data were obtained for the configuration with an axisymmetric configuration, a single windward slice cut, or a double windward slice cut.

Heat-transfer measurements were obtained over an angle-of-attack range from 0 to 14 degrees with model roll angles varying from 0 to 180 degrees. Model surface pressure and flow-field survey data were obtained at two angles of attack: 2 and 10 degrees. Flow-field instrumentation was: (1) a Mach/Flow-Angularity probe, (2) a pitot probe, and (3) a shielded total temperature probe. Surveys were taken at 17 model stations (wind and leeside) from the model surface to the bow shock. All heat-transfer, pressure and flow-field survey data were obtained on a single model configuration: a $14/7$ degree biconic with a 0.5 inch radius nosetip and flats (or slices) at the model base.

The location of the Gardon-gages, pressure orifices, and the coaxial surface thermocouples on the $14^\circ/7^\circ$ bicone are listed in Tables 9a, 9b, and 9c, respectively. Shown in Figure 19 is the location of the stations where profiles were measured which includes a schematic of the surface instrument locations.

A summary of the nominal test conditions is given below:

M_∞	p_o (psia)	T_o ($^\circ R$)	q_∞ (psia)	p_∞ (psia)	$Re_\infty \times 10^{-6}/ft$
10.0	445	1900	0.70	0.009	0.55
10.0	666	1710	1.07	0.015	1.00
10.0	804	1900	1.27	0.018	1.00

Static force data were recorded in either the point-pause or sweep mode of operation, using the Model Attitude Control System.

The point-pause data were obtained for finite values of angle of attack and model roll angle with a delay before each data point to allow the base pressures to stabilize. The continuous sweep data were obtained for a fixed value of model roll angle with a sweep (α) rate of 1 deg/sec. If applicable, the base pressures were obtained from a curve fit of data obtained during the point-pause mode to calculate the base axial force coefficient.

Heat-transfer distribution data were obtained with high-sensitivity thermopile heat-flux gages. Data were taken over an angle-of-attack range from 0 to 14 degrees in one degree increments and at twenty-six different model roll angles, from 0 to 180 degrees. Prior to each run, the model was cooled to a nominal temperature of $530^\circ R$. The model attitude was preset and was then injected into the tunnel flow for about five seconds while a continuous record of gage output was recorded.

TABLE 9. MODEL INSTRUMENTATION LOCATIONS

a. Gardon Gage Locations

GAGE NO.	XSTAG IN.	Y IN.	GARDON Z, IN.	S IN.	W DEG.	(XAPEX) ¹ ₇₀ IN.
1	2.217	0	.943	2.567	0	13.935
2	3.430		1.246	3.817		15.148
3	4.400		1.488	4.817		16.118
4	5.370		1.729	5.817		17.088
5	7.312		2.214	7.817		19.030
6	8.039		2.395	8.567		19.757
7	8.540		2.488	9.070		20.258
8	8.914		2.533	9.445		20.632
9	9.286		2.579	9.820		21.004
10	10.357		2.711	10.899		22.075
11	11.349		2.832	11.899		23.067
12	12.342		2.954	12.899		24.060
13	13.334		3.076	13.899		25.052
14	14.327		3.198	14.899		26.045
15	16.312		3.442	16.899		28.030
16	20.282		3.929	20.899		32.000
17	20.846		3.960	21.464		32.564
18	20.846	-0.933	3.888	21.464	-13.50	32.564
19	20.690	0	-3.960	21.308	180	32.408
20		1.030	-3.843	21.309	165	
21		1.990	-3.446	21.309	150	
22		2.814	-2.814	21.309	135	
23		3.446	-1.990	21.309	120	
24	20.690	3.979	0	21.309	90	32.408
25	21.783	0	3.960	22.401	0	33.500
26		-1.000	3.960	-	-14.17	
27		-1.495	3.831	22.410	-21.33	
28		-2.255	3.440	22.410	-33.25	
29		-1.000	-3.960	-	-165.83	
30		-0.750	-3.960	-	-169.28	
31		0	-3.960	22.401	160	
32		0.750	-3.960	-	169.28	
33		1.237	-3.923	22.410	162.5	
34	21.783	1.000	3.960	-	14.17	33.500
35	23.533	0	3.960	24.151	0	35.250
36	23.533	-2.131	3.767	24.174	-29.5	35.250
37	25.283	0	3.960	25.901	0	37.000
38		-1.000	3.960	-	-14.17	
39		-2.000	3.960	-	-26.80	
40		-2.606	3.721	25.937	-35	
41		-3.084	3.336	25.937	-42.75	
42	25.283	-3.934	2.272	25.937	-60	37.000
43	25.658	-0.250	3.945	-	-3.63	37.376
44	25.783	0	3.929	26.401	0	37.500
45		-1.000	3.929	-	-14.28	
46		-2.000	3.929	-	-26.98	
47		-2.525	3.851	26.440	-33.25	
48		-3.126	3.382	26.440	-42.75	
49		-3.988	2.303	26.440	-60	
50		-2.250	-3.960	-	-150.40	
51		-1.750	-3.960	-	-156.16	
52		0	-3.960	26.401	180	
53		1.000	-3.960	-	165.83	
54		1.750	-3.960	-	156.16	
55		2.474	-3.884	26.440	147.50	
56		2.250	3.960	-	29.60	
57	25.783	2.000	3.960	-	26.80	37.500
58	26.283	0	3.960	26.901	0	38.000
59	27.783	0	3.960	28.401	0	39.500
60		-1.000	3.960	-	-14.17	
61		-2.000	3.960	-	-26.80	
62		-3.292	3.561	28.455	-42.75	
63		-4.200	2.425	28.455	-60	
64		-2.625	-3.960	-	-146.46	
65		-1.750	-3.960	-	-156.16	
66		0	-3.960	28.401	180	
67		1.000	-3.960	-	165.83	
68		1.750	-3.960	-	156.16	
69		2.919	-4.113	28.455	143	
70		3.429	-3.429	28.455	135	
71		4.200	-2.425	28.455	120	
72		4.85	0	28.455	90	
73		3.000	3.960	-	37.15	
74	27.783	2.000	3.960	-	26.80	39.500
75	21.158	0	-3.960	21.776	180	32.876

TABLE 9. MODEL INSTRUMENTATION LOCATIONS (CONT'D)

b. Pressure Orifice Locations

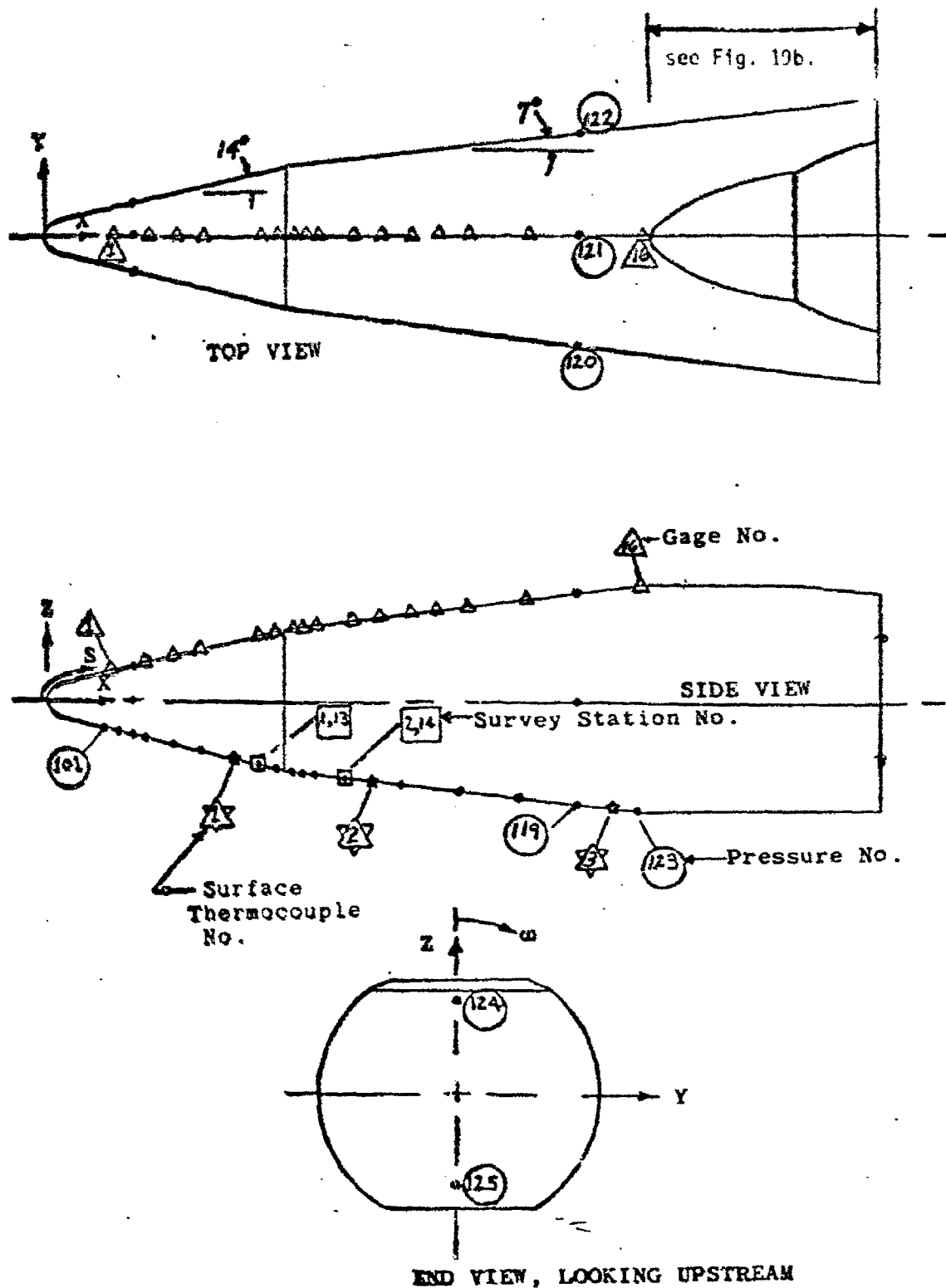
ORIFICE NO.	XSTAG IN.	Y IN.	Z IN.	S IN.	ω DEG.	(XAPEX) ₇₀ IN.
101	2.021	0	-0.894	2.355	180	17.738
102	2.506		-1.015	2.855		14.223
103	2.991		-1.136	3.355		14.708
104		-1.136	0		270	
105		0	1.136		0	
106		1.136	0		90	
107	3.476	0	-1.257	3.855	180	15.193
108	4.446		-1.499	4.855		16.163
109	5.417		-1.741	5.855		17.134
110	7.357		-2.225	7.855		19.074
111	8.085		-2.406	8.605		19.802
112	8.540		-2.488	9.070		20.257
113	8.914		-2.533	9.445		20.631
114	9.286		-2.579	9.820		21.003
115	10.357		-2.711	10.899		22.075
116	12.342		-2.954	12.899		24.059
117	14.327		-3.198	14.899		26.044
118	16.312		-3.442	16.899		28.029
119	18.297		-3.685	18.899		30.014
120		-3.685	0		270	
121		0	3.685		0	
122		3.685	0		90	
123	20.282	0	-3.929	20.899	180	31.999
124	28.283	0	1.62	-	0	40.000
125		0	-1.62	-	180	

c. Coaxial Surface Thermocouple Locations

THERMOCOUPLE NO.	XSTAG IN.	Y IN.	Z IN.	S IN.	ω DEG.	(XAPEX) ₇₀ IN.	SURVEY STATIONS
1	6.583	0	-2.032	7.057	180	18.300	1,13
2	11.283	0	-2.824	11.832	180	23.000	2,14
3	19.533	0	-3.837	20.144	180	31.250	-
4	22.408	0	-3.960	23.026	180	34.125	3,15,16
5	26.783	0	-3.960	27.401	180	38.500	17
6	24.408	0	3.960	25.026	0	36.125	-
7	27.033	0	3.761	27.663	0	38.75	6,9
8	22.658	-1.812	3.813	-	-25.42	34.375	4,5,7,8,10
9	26.783	-3.039	3.621	-	-40.00	38.500	11,12

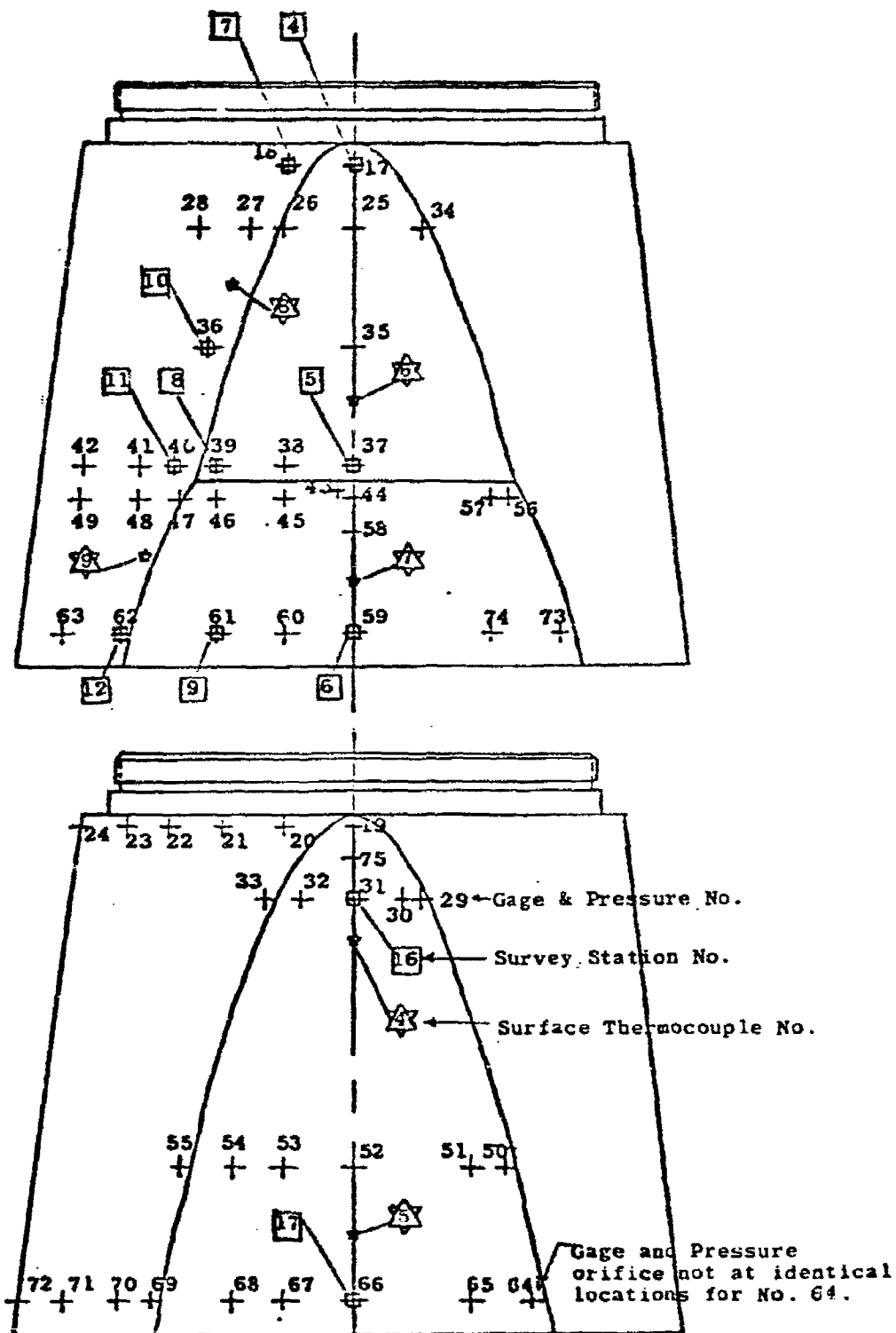
Model surface-pressure data and flow-field survey data were obtained following the heat-transfer test. Both windward and leeward surveys were made at two angles of attack, 2 and 10 degrees at 17 model locations as defined in Figures 19a and 19b. A complementary set of surface-pressure data were obtained at the same model attitudes. For these data (pressure and survey) the model was at a near equilibrium temperature condition; model wall temperatures were typically from 1000 to 1400°R.

Flow-field surveys were taken from the model surface to just beyond the bow shock. A survey typically consisted of 30 to 60 data points obtained at different heights above the model surface. The three instrumentation probes used for this test were mounted in a probe holder as shown in Figure 20. Contrary to the Mach 6 tests defined in Section 3.1, and the Mach 8 tests defined in Sections 3.2 and 3.4 the Mach/Flow-Angularity probe was co-located with the Pitot and total temperature probe in this test series. The probe direction of travel was along a "surface normal" for the majority of the surveys. If it was not possible to obtain "surface normal" surveys then the surveys were made as close to the "surface normal" direction as possible and these data groups are so noted. The time required for taking the survey data was significantly reduced during this test by not waiting for the probe pressures to always reach an equilibrium condition. Rather, timewise data were recorded to provide a pressure-time history whereby the equilibrium pressure was predicted. The sequence of probe data acquisition was: (1) controller moved probe to programmed height and initiated take data, (2) data acquisition system waited a prescribed delay time (usually 3 seconds) and then recorded a specified number of data loops (15 to 30) at constant time intervals (typically 0.6 seconds) which provided time histories for each of the three transducers being scanned, (3) a valve position was changed and the sequence of "step 2) was repeated, which provided the other three pressure-time histories, (4) steps 1 through 3 repeated until all probes and passed the model bow shock.



a.) BICONIC REGION

FIGURE 19. MODEL SURFACE INSTRUMENTATION



b.) SLICED SECTION DETAILS

FIGURE 19. MODEL SURFACE INSTRUMENTATION (CONT'D)

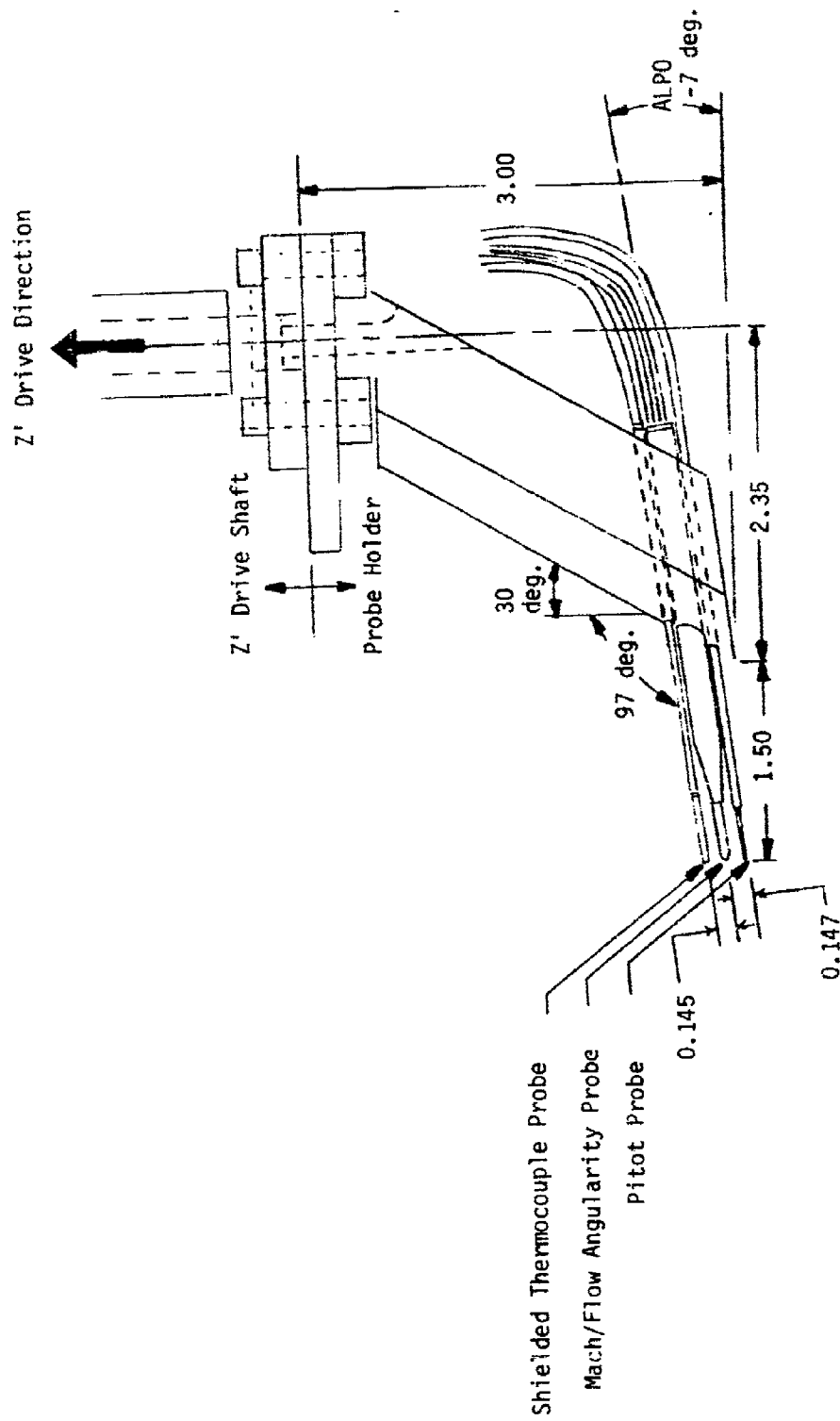


FIGURE 20. SKETCH OF FLOW-FIELD PROBES MOUNTED IN PROBE HOLDER

Probe positioning on the model surface was monitored optically. Survey axial locations (X) were verified by using a scale outline of the model overlayed on the shadowgraph system display. Survey stations (orifice locations) were marked on the outline, making it possible to position the Pitot probe over the desired pressure orifice with an estimated uncertainty of ± 0.05 in. Accurate probe positioning on the model surface was monitored optically with a back lighted high resolution (525 lines/frame) closed-circuit television (CCTV) system. The CCTV camera was fitted with a telscopic lens which gave a total magnification factor of 17. The television image was used to verify contact between the pitot probe and the model surface before obtaining the first data point in a survey. The probe spacing was measured from the photographs and included in the data reduction. Probe positioning for off-centerline stations on the 7-degree cone (SURVEY STATIONS 7, 10, 11, 12) was accomplished using a front-lighted high magnification video system.

Mach/Flow-Angularity probe calibration data were taken in the freestream at the beginning of each test shift and at the conclusion of the last test shift. Calibration data were obtained at different probe pitch attitudes, from 0 to 25 degrees.

Shielded thermocouple calibration data were obtained at the conclusion of this test series. For these data the tunnel stilling chamber pressure (P_0) was decreased in 100 psi increments from 800 to 300 psia while the total temperature was simply maintained above the air liquefaction temperature. Thermocouple probe data were recorded at each pressure level and were used to determine Reynolds number effects on the shielded thermocouple probe.

Tables 10a through 10d present the AEDC data group numbers from References 2 and 7 (and the complementary data tabulations) for each configuration tested and data type.

TABLE 10. TEST DATA SUMMARY - MACH 10

a. Static Force Data - $Re_{\infty} = 1.0 \times 10^6/FT$

MODEL CONFIGURATION		SLICE CONFIGURATION	ANGLE OF ATTACK	$p_0 = 666$ (psia)	$p_0 = 804$ (psia)	REMARKS
CONE ANGLE	RN (in.)					
7°	0	NONE	0	-	26	BASE PRESSURE STABILIZATION STUDY
	0	↓	-140 to +140	-	27	SWEEP MODE
	0.50	↓	0	-	23	POINT-PAUSE MODE
			-140 to +140	-	24	SWEEP MODE
			↓	-	25	POINT-PAUSE MODE
140/70	0.50	NONE	0	20	1	BASE PRESSURE STABILIZATION STUDY
		↓	-140 to +140	21	2,3,4	SWEEP MODE
			↓	22	-	POINT-PAUSE MODE
		SINGLE WIND SLICE	0	16	5	BASE PRESSURE STABILIZATION STUDY
		↓	-140 to +140	17,19	6,7	SWEEP MODE
			↓	18	8,9	POINT-PAUSE MODE
		DOUBLE WIND SLICE	0	14	10	BASE PRESSURE STABILIZATION STUDY
		↓	-140 to +140	15	11,12	SWEEP MODE
			↓		13	POINT-PAUSE MODE - OIL FLOW DATA ALSO TAKEN AT $\alpha = -14, -10, 2, 0, 2, 10, 140$

TABLE 10. TEST DATA SUMMARY - MACH 10 (CONT'D)

b. Heat Transfer Data

Sliced 140/70 Bicone, $R_N = 0.5"$

$Re_x \times 10^{-4}$ FT-1	ROLL ANGLE DEG.	0	1	2	3	4	5	6	7	8	9	10	11	12	13	14
1.0	0	3,28,80,81	89	29,90	93	94	97	98	101	102	105	54,85	106	109	110	1,86
	5	-	-	30	-	-	136	-	112	-	-	55	-	-	-	2
	10	-	-	31	-	-	137	-	113	-	-	56	-	-	-	4
	15	-	-	32	-	-	138	-	114	-	-	57	-	-	-	5
	20	-	-	33	-	-	139	-	115	-	-	58	-	-	-	6
	25	-	-	34	-	-	140	-	116	-	-	59	-	-	-	7
	30	-	-	-	-	-	141	-	117	-	-	60	-	-	-	8
	35	-	-	-	-	-	-	-	-	-	-	61	-	-	-	-
	40	-	-	36	-	-	142	-	118	-	-	62	-	-	-	10
	45	-	-	37	-	-	143	-	119	-	-	63	-	-	-	11
	50	-	-	38	-	-	144	-	120	-	-	64	-	-	-	12
	55	-	-	39	-	-	145	-	121	-	-	65	-	-	-	13
	60	-	-	40	-	-	146	-	122	-	-	66	-	-	-	14
	65	-	-	41	-	-	147	-	123	-	-	67	-	-	-	15
	70	-	-	42	-	-	148	-	124	-	-	68	-	-	-	16
	75	-	-	43	-	-	149	-	125	-	-	69	-	-	-	17
	80	-	-	44	-	-	150	-	126	-	-	70	-	-	-	18
	85	-	-	45	-	-	151	-	127	-	-	71	-	-	-	19
	90	-	-	46	-	-	152	-	128	-	-	72	-	-	-	20
	95	-	-	47	-	-	153	-	129	-	-	73	-	-	-	21
	100	-	-	48	-	-	154	-	130	-	-	74	-	-	-	22
	105	-	-	49	-	-	155	-	131	-	-	75	-	-	-	23
	110	-	-	50	-	-	156	-	132	-	-	76	-	-	-	24
	115	-	-	51	-	-	157	-	133	-	-	77	-	-	-	25
	120	-	-	52	-	-	158	-	134	-	-	78	-	-	-	26
	125	-	-	53,91	-	-	96	99	100	103	104	79,84	107	108	111	27, 87
	130	82,83	88	-	92	95	-	-	-	-	-	-	-	-	-	-
	135	-	-	-	-	-	-	-	-	-	-	-	-	-	-	-
	140	-	-	-	-	-	-	-	-	-	-	-	-	-	-	-
	145	-	-	-	-	-	-	-	-	-	-	-	-	-	-	-
	150	-	-	-	-	-	-	-	-	-	-	-	-	-	-	-
	155	-	-	-	-	-	-	-	-	-	-	-	-	-	-	-
	160	-	-	-	-	-	-	-	-	-	-	-	-	-	-	-
	165	-	-	-	-	-	-	-	-	-	-	-	-	-	-	-
	170	-	-	-	-	-	-	-	-	-	-	-	-	-	-	-
	175	-	-	-	-	-	-	-	-	-	-	-	-	-	-	-
	180	-	-	-	-	-	-	-	-	-	-	-	-	-	-	-
0.55	0	159	-	160	-	-	163	-	164	-	-	167	-	-	-	168
	180	-	-	161	-	-	162	-	165	-	-	166	-	-	-	169

TABLE 10. TEST DATA SUMMARY - MACH 10 (CONT'D)

c. Model Pressure Data

$$Re_{\infty} = 1 \times 10^6 / FT$$

Sliced $14^{\circ}/7^{\circ}$ Bicone, $R_N = 0.5"$

ROLL-MODEL DEG.	ANGLE OF ATTACK, DEGREES		
	-10	-2	10
0	81	80	1609
180	-	100	-

d. Flow Field Survey Data

$$Re_{\infty} = 1.0 \times 10^6 / FT$$

Sliced $14^{\circ}/7^{\circ}$ Bicone, $R_N = 0.5"$

WINDWARD SURVEYS			LEEWARD SURVEYS		
SURVEY STATION	ANGLE OF ATTACK, DEG.		SURVEY STATION	ANGLE OF ATTACK, DEG.	
	-2	-10		2	10
1	13	-	13	14	26
2	12	23	14	15	24
3	11	22	15	16	37
4	19	28	16	17	40*
5	20	31	17	18	39*
6	21	32			
7	44*	45*			
8	35	34			
9	36	33			
10	47*	46*			
11	48*	49*			
12	51*	50*			

- Notes:
- Flow-Angularity/Mach Probe calibrations:
SURVEY: 7, 10, 25, 42, 52, 53
 - *Probe travel was not "surface normal" for these SURVEYS.
 - Shielded thermocouple probe measurements were all outside the model boundary layer for the following SURVEYS: 11-13, 19, 22, 23, 28, 31, 33, 44-50

3.4 Sliced Body w/Flap - Turbulent Flow: $M_{\infty} = 8$, $\alpha \neq 0$ (References 3 and 8)

The objective of this series of tests, conducted under the MAT auspices, was to provide additional data to verify and develop computer codes to predict aerodynamic and aerothermal characteristics of maneuvering vehicles. This specific series concentrated on obtaining data on the sliced configuration with and without flaps for turbulent boundary layer conditions over an angle of attack range from 0 to 20°. The tests were conducted in Tunnel B at a nominal Mach number of 8 and a freestream unit Reynolds number of $3.7 \times 10^6/\text{FT}^{-1}$.

During this series, tests were conducted in three entries: (1) heat transfer and oil flow visualization, (2) shock layer profiles and model surface pressure, and (3) static force and moment measurements. There were two major differences between this test series and those conducted prior to this; specifically (1) the inclusion of the flaps and (2) the acquisition of data at $\alpha = 20^\circ$. Windward and leeward surveys were obtained at several model stations, from the model surface to the bow shock, using a probing mechanism located on top of the tunnel. Flow field probes on the survey mechanism included Pitot probes, an unshielded thermocouple probe, a Preston tube and a Mach/Flow Angularity probe.

Surface pressures were measured to provide pressure data for boundary layer calculations, and heat transfer distributions were obtained to determine the boundary layer state. To provide the desired fully-developed turbulent boundary layer, a machined boundary layer trip was used for the majority of the tests. Surface shear stress data were obtained using a Preston tube attached to the probe mechanism. Model angles of attack were varied from 0 to 20 degrees and model roll angles were varied from 0 to 180 degrees. Static stability and axial force data were obtained over an angle of attack range of -4 to 20 degrees and a sideslip angle range of -2 to 2 degrees. The effects of model nose bluntness (sharp or spherical), body geometry (sliced or unsliced), and body flap angle (0, 10, 20, or split 20/10 degrees) were investigated.

A summary of the nominal test condition for these tests is given below:

M_∞	$p_0(\text{psia})$	$T_0(^{\circ}\text{R})$	$q_\infty(\text{psia})$	$p_\infty(\text{psia})$	$Re_\infty \times 10^{-6}/\text{FT}$
8.0	850	1350	3.900	0.087	3.7

For the heat transfer test entry, the model was instrumented with 82 (Gardon-type) heat flux gages and for the flow field study, the model was instrumented with 88 pressure orifices and 20 coaxial surface thermocouples as shown in Figures 21 and 22. The location of the surface instrumentation is given in Table 11. After the heat transfer test entry and prior to the survey tests the Gardon gages were removed, the holes were plugged or replaced with coaxial gages and the afterbody was replaced with a pressure instrumented afterbody. The pressure orifices in the afterbody were located at the same locations as the Gardon gages, except as noted in Figure 22. The coaxial gages (surface thermocouples) were added for the survey tests to provide model surface temperature.

Three flap assemblies were used: heat transfer, full span pressure, and split pressure as depicted in Figure 23. The heat transfer flap was a full span adjustable deflection flap instrumented with nine Gardon gages. The full span pressure flap was essentially the same as the heat transfer flap except for instrumentation. The split pressure flap had fixed deflection angles of 10 and 20 degrees for its two sides and was instrumented with seven orifices and two coaxial surface thermocouples. Specific gage and orifice locations are presented in Table 12.

The nosetips used in this investigation consisted of a sharp conical nose with a radius of 0.005 inches and spherically blunted noses with radii of 0.500 inches and machined trip heights of 0.013, 0.033, and 0.060 inches (Figure 6).

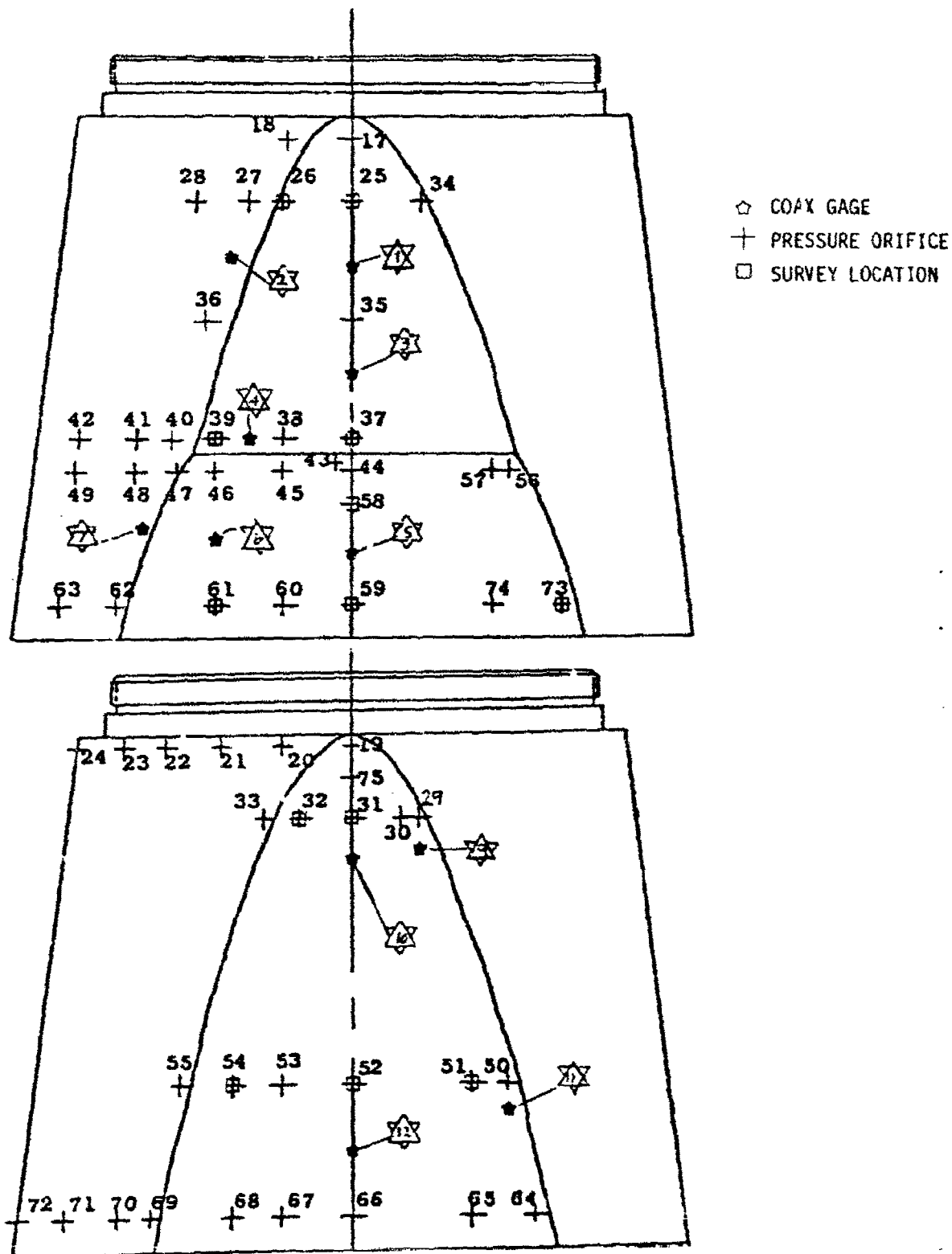


FIGURE 22. MODEL SURFACE INSTRUMENTATION, SLICED REGION DETAIL

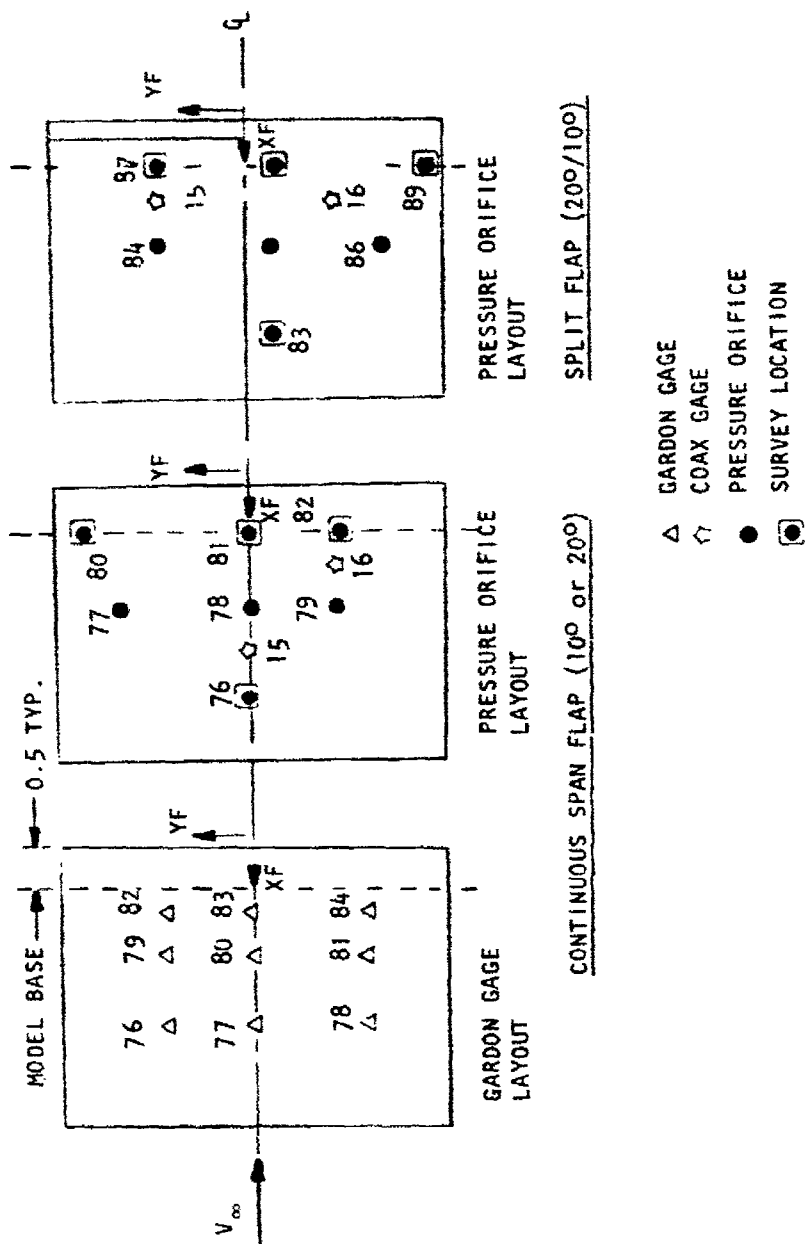


FIGURE 23. FLAP INSTRUMENTATION DETAILS

TABLE 11. MODEL INSTRUMENTATION LOCATIONS

a. Gardon and Coax Gage Locations

<u>GARDON GAGE NO.</u>	<u>X, in.</u>	<u>Y, in.</u>	<u>Z, in.</u>	<u>S, in.</u>	<u>OMEGA, deg</u>
101	2.658	0	.908	2.981	0
102	3.887		1.136	4.231	
103	5.116		1.364	5.481	
104	6.097		1.546	6.479	
105	7.080		1.728	7.479	
106	8.066		1.911	8.481	
107	8.924		2.070	9.354	
108	9.786		2.230	10.231	
109	10.770		2.412	11.231	
110	11.267		2.488	11.734	
111	11.639		2.533	12.109	
112	12.011		2.579	12.484	
113	13.082		2.711	13.563	
114	14.075		2.833	14.563	
115	15.067		2.955	15.563	
116	16.060		3.077	16.563	
117	17.052		3.198	17.563	
118	18.045		3.320	18.563	
119	19.037		3.442	19.563	
120	20.030		3.564	20.563	
121	20.725		3.649	21.263	
122	22.015		3.808	22.563	
123	23.007		3.930	23.563	

<u>COAX GAGE NO.</u>	<u>X, in.</u>	<u>Y, in.</u>	<u>Z, in.</u>	<u>OMEGA, deg</u>
1	25.381	0	3.960	0
2	25.381	-1.812	3.813	-25.42
3	27.131	0	3.960	0
4	28.006	-1.500	3.960	-21.15
5	29.756	0	3.620	0
6	29.506	-2.000	3.807	-28.12
7	29.506	-3.039	3.621	-40.00
9	25.006	-1.000	-3.960	-165.83
10	25.131	0	-3.960	180.00
11	29.006	-2.250	-3.960	-150.40
12	29.506	0	-3.960	180.00
13	22.256	0	-3.838	180.00
14	14.006	0	-2.824	180.00

TABLE 11. MODEL INSTRUMENTATION LOCATIONS (CONT'D)

b. Pressure Orifice Locations

PRESSURE ORIFICE NO.	X, in.	Y, in.	Z, in.	S, in.	OMEGA, deg
101	2.658	0	- .908	2.981	180
102	3.149	↓	- .999	3.481	180
103	3.149	- .999	0	3.481	270
104	3.149	0	.999	3.481	0
105	3.149	.999	0	3.481	90
106	4.133	0	-1.182	4.481	180
107	5.116	↓	-1.364	5.481	↓
108	6.099	↓	-1.546	6.481	↓
109	8.066	↓	-1.911	8.481	↓
110	10.032	↓	-2.275	10.481	↓
111	10.770	↓	-2.412	11.231	↓
112	11.267	↓	-2.488	11.734	↓
113	11.639	↓	-2.533	12.109	↓
114	12.011	↓	-2.579	12.484	↓
115	13.082	↓	-2.711	13.563	↓
116	15.067	↓	-2.955	15.563	↓
117	17.052	↓	-3.198	17.563	↓
118	19.037	↓	-3.442	19.563	↓
119	21.022	↓	-3.686	21.563	↓
120	21.022	-3.686	0	21.563	270
121	21.022	0	3.686	21.563	0
122	21.022	3.686	0	21.563	90
123	23.007	0	-3.930	23.563	180
9103	5.116	↓	1.364	5.481	0
9109	10.770	↓	2.412	11.231	↓
9113	13.082	↓	2.711	13.563	↓
9115	15.067	↓	3.077	16.563	↓
9117	17.052	↓	3.198	17.563	↓
9119	19.037	↓	3.442	19.563	↓

TABLE 11. MODEL INSTRUMENTATION LOCATIONS (CONT'D)

c. Orifice and Gardon Gage Locations

Orifice or Gage Number	X, in.	Y, in.	Z, in.	S, in.	OMEGA_deg
17	23.569	0	3.960	24.124	0
18	23.569	-0.933	3.888	24.124	-13.50
19	23.413	0	-3.960	23.968	180.00
20		1.030	-3.843	23.969	165.00
21		1.990	-3.446		150.00
22		2.814	-2.814		135.00
23		3.446	-1.990		120.00
24	23.413	3.979	0		90.00
25	24.506	0	3.960	25.061	0
26		-1.000	3.960	—	-14.17
27		-1.496	3.831	25.070	-21.33
28		-2.255	3.440	25.070	-33.25
29		-1.000	-3.960	—	-165.83
30		-0.750	-3.960	—	-169.28
31		0	-3.960	25.061	180.00
32		0.750	-3.960	—	169.28
33		1.237	-3.923	25.070	162.50
34	24.506	1.000	3.960	—	14.17
35	26.256	0	3.960	26.811	0
36	26.256	-2.131	3.767	26.834	-29.50
37	28.006	0	3.960	28.561	0
38		-1.000	3.960	—	-14.17
39		-2.000	3.960	—	-26.80
40		-2.606	3.721	28.597	-35.00
41		-3.084	3.336	28.597	-42.75
42	28.006	-3.934	2.272	28.597	-60.00
43	28.381	-0.250	3.945	—	-3.63
44	28.506	0	3.929	29.061	0
45		-1.000	3.929	—	-14.28
46		-2.000	3.929	—	-26.98
47		-2.525	3.851	29.100	-33.25
48		-3.126	3.382	29.100	-42.75
49		-3.988	2.303	29.100	-60.00
50		-2.250	-3.960	—	-150.40

TABLE 11. MODEL INSTRUMENTATION LOCATIONS (CONT'D)

c. Orifice and Gardon Gage Locations (Cont'd)

Orifice or Gage Number	X, in.	Y, in.	Z, in.	S, in.	OMEGA, deg
51	28.506	-1.750	-3.960	—	-156.16
52		0	-3.960	29.061	180.00
53		1.000	-3.960	—	165.83
54		1.750	-3.960	—	156.16
55		2.474	-3.884	29.100	147.50
56		2.250	3.929	—	29.60
57	28.506	2.000	3.929	—	26.80
58	29.006	0	3.568	29.561	0
59	30.506	0	3.684	31.061	0
60		-1.000	3.684	—	-14.17
61		-2.000	3.684	—	-26.80
62		-3.292	3.561	31.115	-42.75
63		-4.200	2.425	31.115	-60.00
64		-2.625 *	-3.960	—	-146.46
65		-1.750	-3.960	—	-156.16
66		0	-3.960	31.061	180.00
67		1.000	-3.960	—	165.83
68		1.750	-3.960	—	156.16
69		2.919	-4.113	31.115	143.00
70		3.429	-3.429	31.115	135.00
71		4.200	-2.425	31.115	120.00
72		4.850	0	31.115	90.00
73		3.000	3.684	—	37.15
74	30.506	2.000	3.684	—	26.80
75	23.881	0	-3.960	24.436	180.00

* Y = -2.625 for Gage 64 and Y = -2.750 for Orifice 64.
All others at same dimensional locations.

TABLE 12. FLAP INSTRUMENTATION LOCATIONS

Pressure Flap

Orifice or Thermocouple(TG) No.	X*, in.	XF	Y; YF, in.	δ^* , deg
76	28.995	2.50	0	10
77	29.979	1.50	1.500	↓
78	29.979	1.50	0	
79	29.979	1.50	-1.000	
80	30.964	0.50	2.000	
81	30.964	0.50	0	
82	30.964	0.50	-1.000	
TG15	29.487	2.00	0	
TG16	30.472	1.00	-1.000	

Heat Flap (Gardon Gage)

76	29.487	2.00	1.000	10
77	29.487	2.00	0	↓
78	29.487	2.00	-1.2500	
79	30.226	1.25	1.000	
80	30.226	1.25	0	
81	30.226	1.25	-1.250	
82	30.718	0.75	1.000	
83	30.718	0.75	0	
84	30.718	0.75	-1.250	

Split Flap (Pressure or TG)

83	29.995	2.50	-0.250	10
84	29.900	1.50	1.000	20
85	29.979	1.50	-0.250	10
86	29.979	1.50	-1.500	10
87	30.840	0.50	1.000	20
88	30.964	0.50	-0.250	10
89	30.964	0.50	-2.000	10
TG15	30.472	1.00	1.000	10
TG16	30.472	1.00	-1.000	20

* X locations for Heat and Pressure Flap quoted for a nominal $\delta_F = 10^\circ$.

The X-Y-Z overhead probe drive referred to earlier in this report was used to survey the flow field. The probe holder assemblies attached to this probe drive are illustrated in Figures 24 and 25. The flattened Pitot, upper Pitot, total temperature and Preston tube probes were mounted in one probe holder, while the Mach/Flow-Angularity probe was mounted separately. The upper Pitot was moved from 2 inches to 3 inches above the pitot, Preston, and total temperature probes, when leeward surveys were performed. It should be pointed out that in this series of tests, the Mach/Flow-Angularity measurements were made using a separate probe for a more efficient use of the tunnel since considerable delay times are required for pressure stabilization relative to the pitot pressures. For this reason, only limited Mach/Flow-Angularity data were obtained.

Probe sizes and geometries similar to those shown earlier were used in this series. The small flattened pitot and unshielded total temperature probes were used to obtain measurements close to the surface within the boundary layers and yet remain parallel to the model surface. Pitot pressure measurements were made using transducers referenced to near vacuum. The unshielded thermocouple probe had a wire junction diameter of approximately 0.007 inches. A reference dimension of 0.005 inches was used for data reduction purposes. The time response and the resolution of the probe location are improved by using such small probes. Total temperature probe uncertainties associated with the heat transfer between the probe and environment were accounted for in the freestream probe calibration (convection and conduction effects). Probe positioning in the vicinity of the model surface, probe deflections and probe spacing were measured and monitored optically with the VKF closed circuit television (CCTV) system described in Section 3.3.

Static force data were recorded in either the point-pause or sweep mode of operation using the MACS. Point-pause data were obtained for finite values of α and β with a delay before each data point to allow the base pressures to stabilize. These data were used to define the base axial force coefficient variation with angle of attack and sideslip angle.

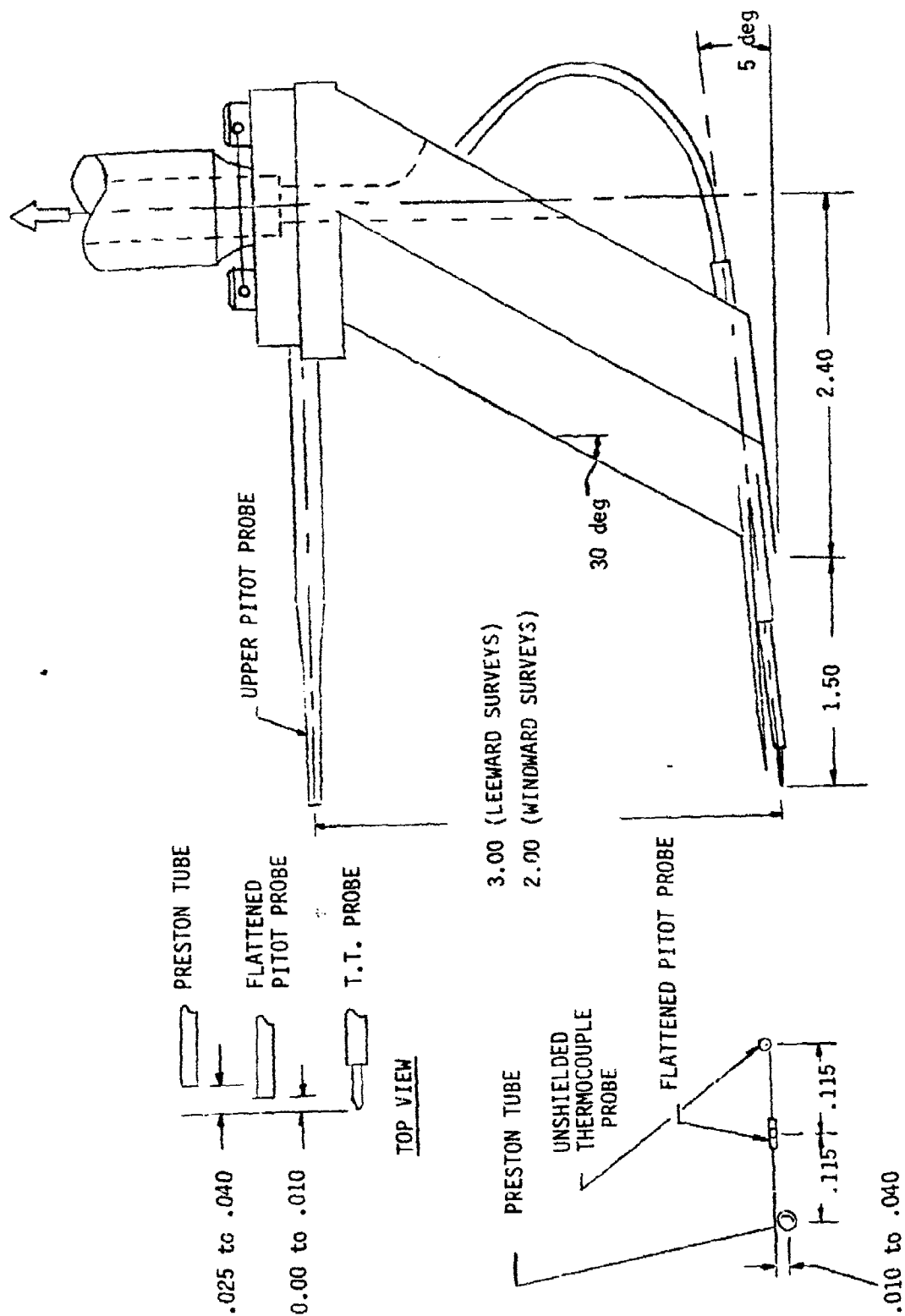


FIGURE 24. PROBE HOLDER ASSEMBLY WITH TOTAL TEMPERATURE, PITOT AND PRESTON PROBES

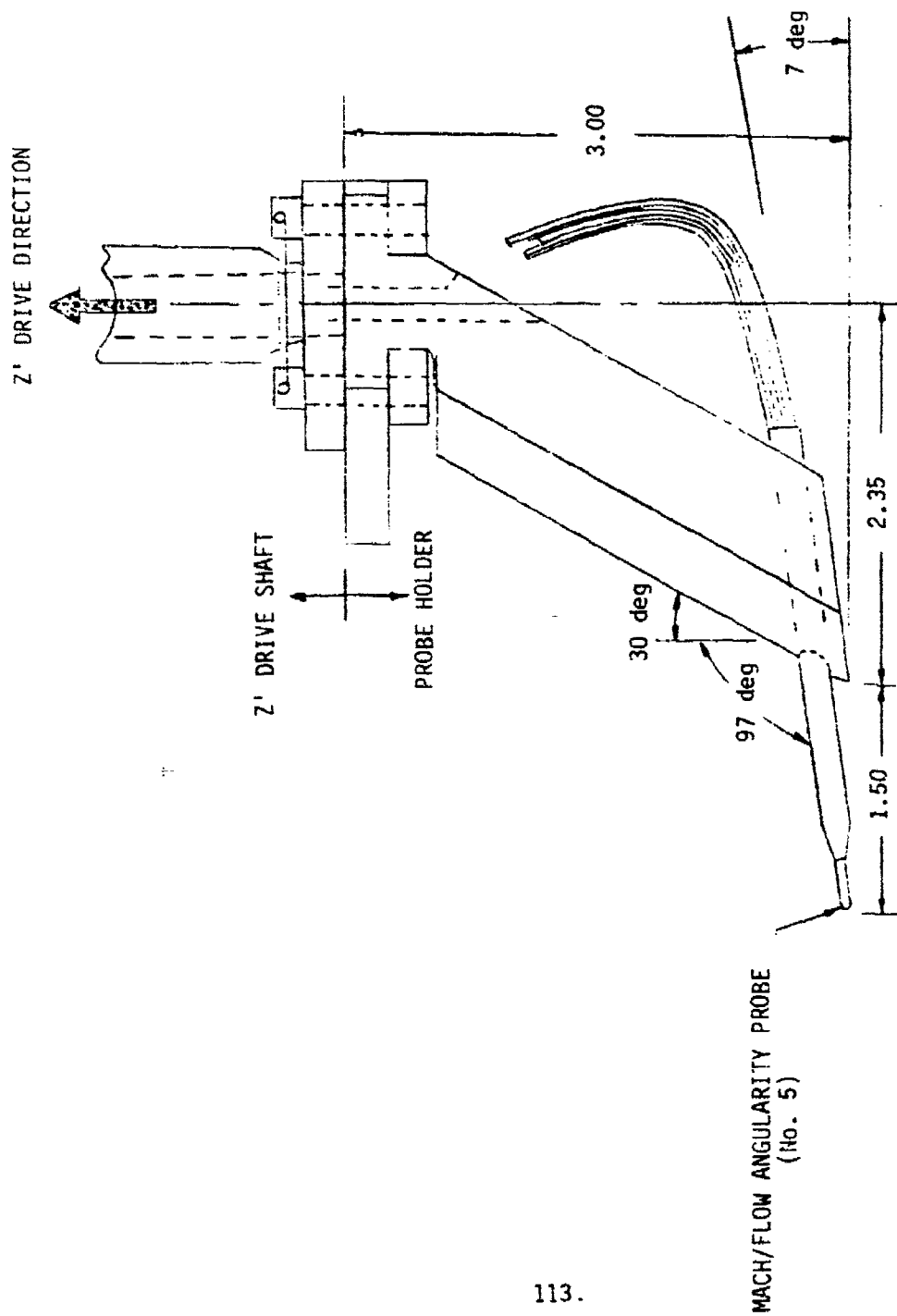


FIGURE 25. PROBE HOLDER ASSEMBLY-MACH/FLOW-ANGULARITY PROBE

These data were obtained over the model attitude range for each primary configuration and were used to provide the base axial force corrections for subsequent variations in flap deflection or for a similar configuration. The base pressure runs are identified in the test summary. The continuous sweep data were obtained for a fixed value of ϕ with a sweep rate of 1.0 deg/sec.

Data acquired during this test series consisted of (a) surface (cold wall) heat transfer, (b) oil flow and heat sensitive paint visualization, (c) surface pressure, (d) overhead probe surveys (i.e., Pitot pressure, total temperature, and Preston tube), (3) Mach/Flow Angularity calibrations, (f) total temperature probe calibrations, and (g) static force data. The procedure utilized to acquire these data were similar to those described in Sections 3.1 to 3.3 with the following two exceptions.

(1) Oil flow runs were made at the end of the heat transfer shift to visualize the flow angularity over the aft section of the model. Oil was applied and the model injected into the flow for approximately 15 seconds. Photographs of the upper and lower cut/slice regions of the model were taken at 1 frame per second.

(2) A small amount (2 RUNS) of qualitative heating data were obtained on the 10 degree flap with the phase-change paint thermal mapping technique (Reference 9). A thin sheet (0.032 inches thick) of synthetic rubber was bonded to the flap to provide an insulated surface. High heating regions were noted by observing the progression of melt (phase change) with time. The results were recorded photographically in the same manner as for oil flow.

Total temperature probe calibrations were conducted in the free-stream for each probe used. For these calibration runs, the total pressure (PT) was changed in nominal 50 psi increments from 190 to 850 psia. Total temperature probe data and tunnel conditions were recorded at each pressure level and used to determine Reynolds number effects on the unshielded total temperature probes. In addition to this Reynolds number calibration which

is built into the final data presented for the T_0 probe, the sensitivity of pitot probe and total temperature readings to flow misalignment were also obtained in the Mach 8 freestream. Data were recorded at discrete probe pitch attitudes from -22° to $+10^\circ$. Contrary to the Reynolds number calibration corrections which are built into the final data T_0 tabulations, the α sensitivity data were not built into the final data since the probe misalignment at each spacial setting is not, in general, known. This will be discussed further in Section 4.

Tables 13a through 13d present the AEDC data group numbers from References 3 and 8 (along with the complementary data tabulations) for each configuration and data type.

TABLE 13. TEST DATA SUMMARY

10.5°/7° SLICED BICONE WITH FLAP

 $M_\infty = 8$ $Re_\infty = 3.7 \times 10^6/\text{ft}$

a. Force and Moment Data

R_N "	TRIP HT. "	WINDWARD SLICES	δ°	α°	β°	RUN NO.
SHARP	NONE	0°/-7°	NONE	-4 to 20	0	10
↓	↓	↓	10	-4 to 20	0	16
			20	-4 to 20	0	14,15
0.5	.060	NONE	NONE	-4 to 20	0	2,4
↓	↓	NONE	NONE	0	-4 to 20	3
0.5	.060	0°/-7°	NONE	-4 to 20	0	5,6
↓	↓	↓	↓	0	-2 to 2	7
			10	-2 to 2	-2 to 2	8
			20	-2 to 2	-2 to 2	9
			10	-4 to 20	0	17
			20	-4 to 20	0	11,12
			20	0	-2 to 2	13
			20/10	-4 to 20	0	18

b. Surface Pressure Data

CONFIGURATION				
R_N "	TRIP HT. "	δ°	α°	RUN NO.
SHARP	NONE	NONE	0	79
↓	NONE	NONE	20	78
	NONE	20	0	22
0.5	.033	NONE	20	63
↓	.060	↓	0	30
	↓	↓	10	31
			20	32
0.5	.033	10	0	1
↓	↓	10	4	2
		10	10	4
	.060	20	0	23
	.060	20/10	0	41

TABLE 13. TEST DATA SUMMARY - (CONT'D)
10.5°/7.0° SLICED BICONE WITH FLAP

$$M_{\infty} = 8 \quad Re_{\infty} = 3.7 \times 10^6 / FT$$

c. Heat Transfer and Oil Flow Data

R _N ^a	TRIP HT. ^b	δ °	α °	FOREBODY GAGE RAY ANGLE FROM WINDWARD, DEGREE				
				0	45	90	135	180
				MODEL ROLL, DEGREES				
				0	45	90	135	180
SHARP ↓	NONE ↓	NONE ↓	0	69*	-	-	-	-
			20	70*	-	-	-	-
			0	36	37	38	39	40
			20	45	44	43	42	41
			SWEEP	47	-	-	-	46
0.5 ↓	0.033 ↓	NONE ↓	0	57,62*	-	-	-	-
			4	58,63*	-	-	-	-
			10	59,64*	-	-	-	-
			20	60,65*	-	-	-	-
0.5 ↓	0.013 ↓	10 ↓	0	-	-	-	-	-
			10	26	27	28	29	30
			20	35	34	33	32	31
			SWEEP	-	-	-	-	25
0.5 ↓	0.033 ↓	10 ↓	0	2,9	-	-	-	1,8
			4	7	6	5	4	3
			10	14	15	16	17	18
			20	23	22	21	20	19
			SWEEP	-	-	-	-	24
0.5 ↓	0.060 ↓	10 ↓	0	-	-	-	-	10
			20	12	-	-	-	11,13
0.5 ↓	0.013 ↓	20 ↓	0	56	-	-	-	-
			4	55	-	-	-	-
			10	54	-	-	-	-
			20	53	-	-	-	-
0.5 ↓	0.033 ↓	20 ↓	0	75,76*	-	-	-	-
			0	51,52,66*	-	-	-	-
			4	50,67*	-	-	-	-
			10	49,68*	-	-	-	-
			20	48	-	-	-	-
0.5 ↓	0.033 ↓	10/20 ↓	0	71*	-	-	-	-
			4	72,73*	-	-	-	-
			10	74*	-	-	-	-

* Indicates Oil Flow Data Run

• Indicates Paint Data Run

SWEEP - 10.5° ≤ α ≤ 0°

TABLE 13. TEST DATA SUMMARY - (CONT'D)

10.5°/70° SLICED BICONE WITH FLAP

$M_\infty = 8$ $Re_\infty = 3.7 \times 10^6/FT$

d. Shock Layer Survey & Surface Shear Data

CONFIGURATION			PROFILE STATIONS																SPLIT FLAP					
			FRUSTUM		SLICE 1 - WIND				SLICE 2 - WIND				LEE SLICE				FLAP							
			WIND	LEE	25	26	37	39	58	59	61	73	31	32	52	54	76	81	80	83	89	88	87	
R_N	TRIP	H.T. (IN) ± 0	118	121	119																			
SHARP	NONE	NONE	-	80	-	81	-	82	83	-	-	-	-	-	-	-	-	-	-	-	-	-	-	-
SHARP	NONE	20	-	-	-	-	-	-	-	-	-	-	-	-	-	-	-	-	-	-	-	-	-	-
0.5	.060	NONE	-	33	-	34	37	35	38	36	49	50	-	-	-	-	-	-	-	-	-	-	-	-
							21*	21*	21*															
0.5	.060	NONE	10	51	97	52	58	53	57	54	55	56	59	91	96	92	93	94	95	-	-	-	-	-
								21*	21*															
0.5	.060	NONE	20	60	98,99	-	-	21*	21*	-	-	-	-	101,	-	103,	105,	-	-	-	-	-	-	-
			74	100	100									102		104	106,	107						
0.5	.033	NONE	20	-	65	-	-	-	-	68	69	70	-	-	-	-	-	-	-	-	-	-	-	-
0.5	.060	10	0	10	-	-	-	-	-	-	-	-	-	-	-	-	-	-	-	-	-	-	-	-
0.5	.033	10	0	6	-	-	-	-	-	-	-	-	-	-	-	-	-	-	-	-	-	-	-	-
0.5	.060	10	10	-	-	-	-	-	-	-	-	-	-	-	-	-	-	-	-	-	-	-	-	-
0.5	.060	20	0	-	-	-	-	-	-	-	-	-	-	-	-	-	-	-	-	-	-	-	-	-
0.5	.060	20/10	0	-	-	-	-	-	-	-	-	-	-	-	-	-	-	-	-	-	-	43	47	46
																					44	-	48	

* SURFACE SHEAR ONLY

* MACH/FLOW ANGULARITY PROBE

4.0 SHOCK LAYER SURVEY DATA REDUCTION AND PROBE CALIBRATION ISSUES

Pitot pressure and total temperature probes are sensitive to flow alignment, and consequently were calibrated for this effect during the course of this investigation. In addition, the unshielded total temperature probes are also Reynolds number dependent and therefore, as mentioned in Section 3, were also calibrated for this effect. In this section, the probe calibrations will be discussed and summary highlights of these results will be presented.

During the course of those experiments which predated the MAT program, data reduction procedures were established to not only provide probe corrections to the data but also to define local state variables in the boundary layer and the entire shock layer. To perform this boundary layer type analysis the assumption was made that the static pressure along a line normal to the wall is constant throughout the shock layer. This assumption is not correct outside the boundary layer and leads to incorrect properties in the shock outside the boundary layer. This will also be discussed in this section.

4.1 Unshielded Total Temperature Probe Reynolds Number Correction

The total temperature measurements in the shock layer were generally made with an unshielded total temperature probe. The probe was constructed from 0.010 inch O.D. sheathed thermocouple housing with 0.0015 inch diameter wires. The junction formed by joining the two wires together was nominally 0.005 inches in diameter. The unshielded total temperature probe was calibrated in the freestream to provide a recovery factor, η , as a function of Reynolds number, as defined by

$$\frac{T_{0c}}{T_{0m}} = \frac{1 + \frac{\gamma-1}{2} M^2}{1 + \frac{\gamma-1}{2} \eta M^2}$$

where $n = a_0 + a_1 Re_0^{1/2}$. Here, M is the local Mach number, γ is the specific heat ratio, a_0 and a_1 are calibration constants, Re_0 is the local Reynolds number with viscosity based on the total temperature, T_{0c} , and T_{0c}/T_{0m} is the ratio of the corrected to measured total temperature. The calibration given in the equation above is discussed by Varner (Reference 17) and is compatible with the correlation for cylinders in incompressible flow as defined in Reference 18.

It should be noted that the calibration n vs. $Re_0^{1/2}$ is probe specific and consequently was performed in each test series and was frequently repeated with a given probe, for verification. Shown in Figure 26 is a representative total temperature probe calibration which was obtained with the probe in the freestream and which was used to define the constants a_0 and a_1 . Although this calibration was obtained at one value of Mach number, earlier results were obtained at several M_∞ 's from 1.5 to 6, and the results could be expressed adequately by a simple T_0 variation, as shown. This correction is built into the final data package and permits the iterative correction of (TTLU) to (TTL), i.e., the uncorrected to corrected total temperature. Throughout each test series one will find data groups defining where these calibrations were performed and the groups which were affected by each calibration. A representative listing from the MAT program test series is shown in Table 14.

4.2 Angle-of-Attack Probe Calibrations

It is well known that flow field survey measurements are sensitive to each probe's alignment with the flow. Consequently the probes used in the current test series were periodically calibrated in the freestream as a function of ALPT or angle of attack. Shown in Figure 27 is a typical α calibration of the Pitot and total temperature probes taken over a 26° range in ALPT. Results from these tests indicate that these α calibrations are peculiar to each probe. Hence α calibrations were periodically performed, especially when the probe tip was changed, for whatever reason. For measurements taken in the shock layer, where the probe tip was nominally aligned parallel to the local model surface, the probe becomes misaligned with

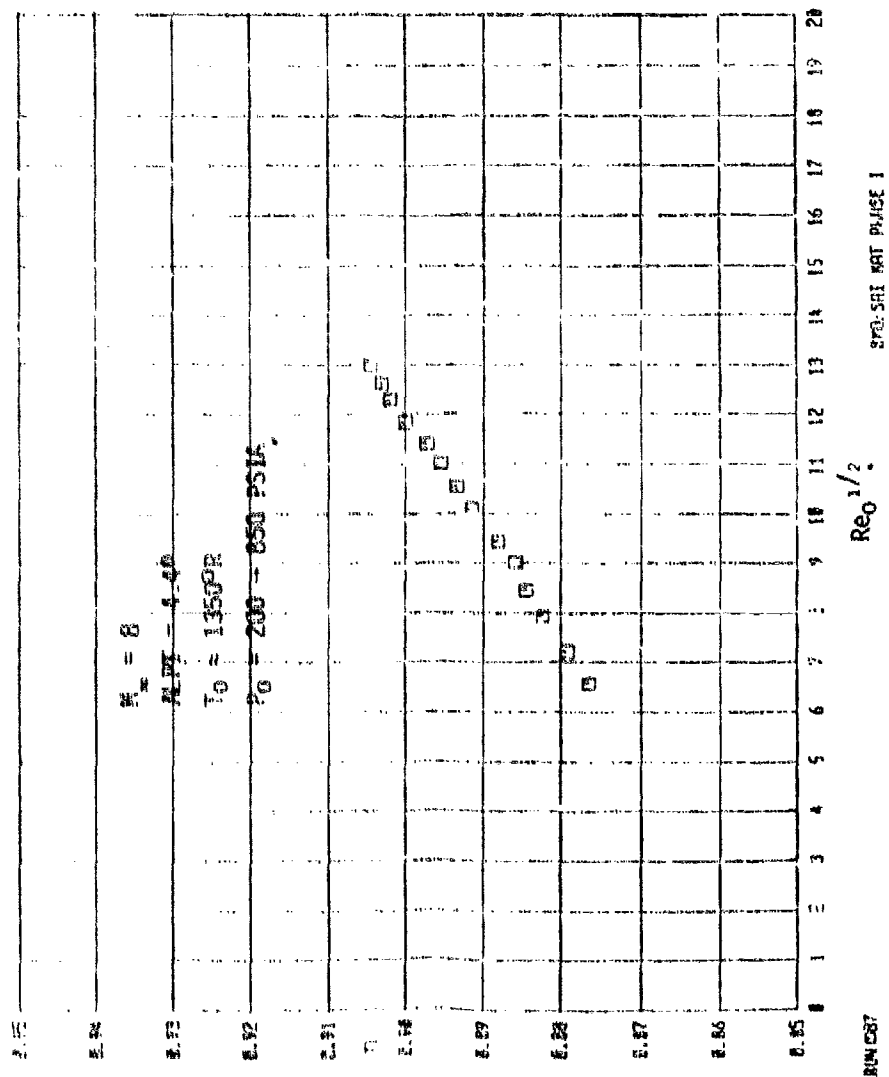


FIGURE 26. REPRESENTATIVE TOTAL TEMPERATURE PROBE CALIBRATION

$$M_{\infty} = 6$$

$$Re_{\infty} = 5 \times 10^6 \text{ FT}^{-1}$$

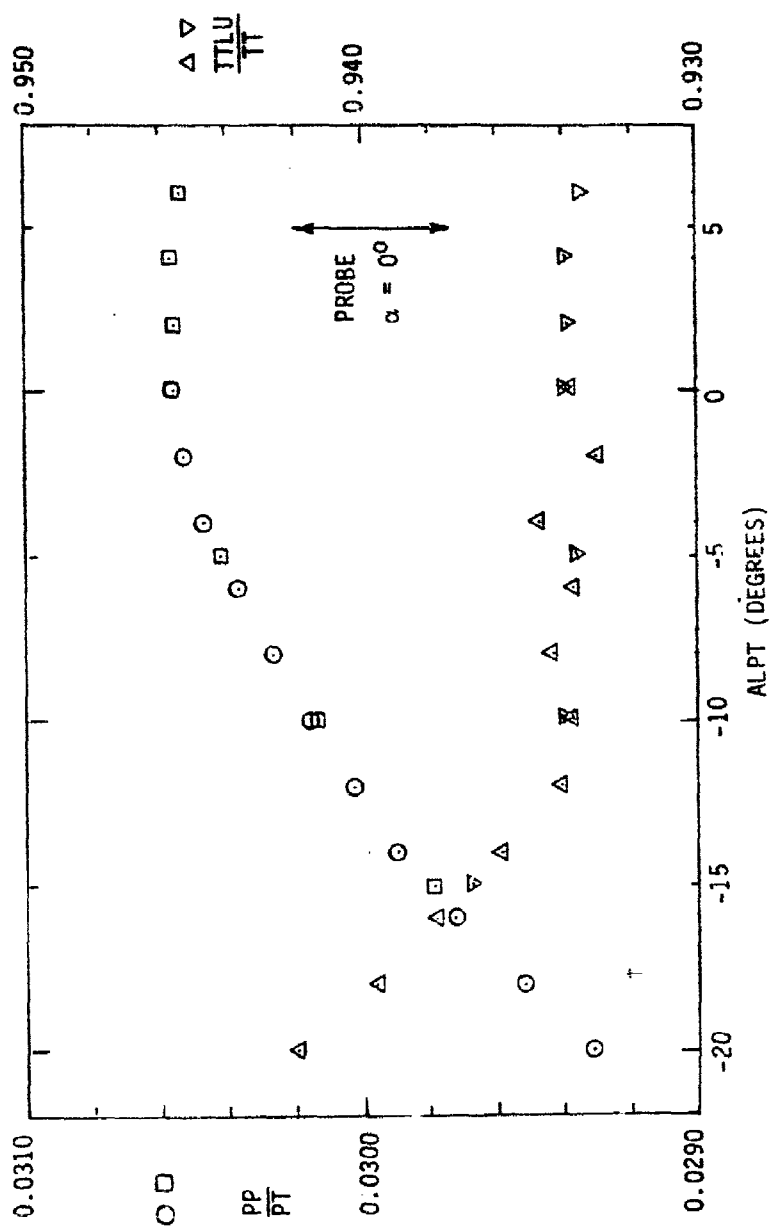


FIGURE 27. REPRESENTATIVE PITOT AND TOTAL TEMPERATURE PROBE CALIBRATION WITH α

TABLE 14. TOTAL TEMPERATURE PROBE CALIBRATION DATA FROM THE
MAT PROGRAM TEST PHASE

RUN	PT,psia	REMARKS
5	500 → 850	ALPT = 0 USED IN OBTAINING CURVE FIT FOR RUNS 5 → 39
14	350 → 850	ALPT = 0 USED IN OBTAINING CURVE FIT FOR RUNS 5 → 39
15	550 → 850	ALPT = 0 USED IN OBTAINING CURVE FIT FOR RUNS 5 → 39
39	187 → 853	ALPT = 0 USED IN OBTAINING CURVE FIT FOR RUNS 5 → 39
40	550 → 850	ALPT = 0 USED IN OBTAINING CURVE FIT FOR RUNS 40 → 44
61	200 → 850	ALPT = 0 DEG USED IN OBTAINING CURVE FIT FOR RUNS 45 → 61
62	570 → 850	ALPT = 0 DEG USED IN OBTAINING CURVE FIT FOR RUNS 62 → 87
73	850	10 > ALPT > -20 DEG USED TO NOTE EFFECT OF ANGLE OF ATTACK ON PROBE OUTPUT
87	200 → 850	ALPT = 4.4 DEG USED IN OBTAINING CURVE FIT FOR RUNS 62 → 87
88	553 → 850	ALPT = 0 DEG USED IN OBTAINING CURVE FIT FOR RUNS 88 → 108
108	300 → 804	ALPT = 0 DEG USED IN OBTAINING CURVE FIT FOR RUNS 88 → 108

the local flow as it is incremented away from the model surface. When the probe penetrates the bow shock the misalignment is greatest.

Since the flow direction in the shock layer is, in general, unknown one cannot readily apply this probe α correction to the data. Consequently the published data from the entire bicone test series does not contain this correction. Scanning the results of the several probe calibrations indicates that the ratio (PP/PT) varies by 3-5% for $\alpha = 0 \rightarrow 20^\circ$ and that the ratio (TTLU/TT) varies by 1-6% in this same α range. These errors can affect the deduced Mach number by $\sim \pm 0.2$ at $M > 7$ and less than ± 0.1 at $M < 4$.

As stated above, since the flow direction at an arbitrary point in the shock layer is unknown, a priori, the following recommendation for the use of this α calibration is suggested. Since one of the primary objectives of acquiring these data is to validate detailed computer codes (i.e., PNS or Inviscid), and since the orientation of the probe is known, a correction can be made on a point by point basis by defining the probe misalignment using the theory to define the "true" flow direction (clearly an assumption). Using this value of $\Delta\alpha$, a correction can be made. The validity of this assumption can be ascertained by utilizing the limited quantity of Mach/Flow-Angularity data. One notes that this correction is not significant, consequently this procedure should be more than adequate.

4.3 Boundary Layer Type-Data Reduction

In general, the preponderance of shock layer profile data consisted of measuring the local Pitot pressure and total temperature at various points from the model surface to the bow shock, and slightly beyond. The authors strongly recommend that comparisons of theory and data be made by directly comparing the experimentally measured Pitot pressure (normalized by P_{T_∞}) and Reynolds number corrected total temperature (also normalized, here with T_{0_∞}) with values deduced numerically. That is, in the numerical simulations, all of the local state variables are known, consequently one can readily define (PP/PT) and (TTL/TT). No assumptions are required. The inverse is

not true however; that is, if one wishes to define the local state variables from the experimental data one must invoke critical assumptions since the local static pressure in the shock layer is unknown, only the wall value is known. Shown in Figure 28 are the static pressure profiles computed for a blunted 7° cone with the parabolized Navier-Stokes (PNS) solution of Reference 19. This figure presents the normalized static pressure profile versus a normalized shock layer thickness. One will note that the classical assumption that $\partial p / \partial y$ in the boundary layer is zero is quite valid here. However gradients exist outside of the boundary layer and consequently the constant P_w assumption in the shock layer is poor. To further illustrate that large static pressure gradients exist in the shock layer, PNS calculations were also made in the flap region for the $10.5^\circ/7^\circ$ bicone, for $M_\infty = 8$, $\alpha = 0^\circ$, and $\delta = 10^\circ$ (Figure 29). Rather dramatic departures from the wall static pressure are seen through the shock layer.

Nevertheless the final data reduction performed at AEDC used the local values of PP and TTL in concert with the local wall static pressure (assumed to be constant in the shock layer) to deduce the state variables. That is, from P_w and PP one can deduce M ; then with M and TTL known one can deduce the local T , etc. Although this analysis was performed throughout the shock layer, it is clearly valid only in the boundary layer, and the final results therein can be used with confidence. Shown in Figure 30 is a sample of the final reduced data made using this constant P_w assumption. Values of M_L and u_L defined at $ZP < 0.18$ are clearly valid, however values beyond this point are incorrect. One notes, for example, that beyond the bow shock in the freestream $M_L/M_e = 0.6$ and $u_L/u_e \approx 0.83$.

In this post test analysis procedure, the viscous layer thicknesses were also deduced from the measured data. This analysis was based on the experimental definition of the boundary layer thickness. For these tests it must be based on the character of the total temperature profile rather than the velocity profile. That is, for blunted bodies, in regions of entropy layer swallowing, velocity gradients exist at the boundary layer edge rendering this method of defining δ intractable. The total temperature can be used to define the boundary layer thickness, albeit the thermal thickness and not the classical velocity thickness as illustrated below.

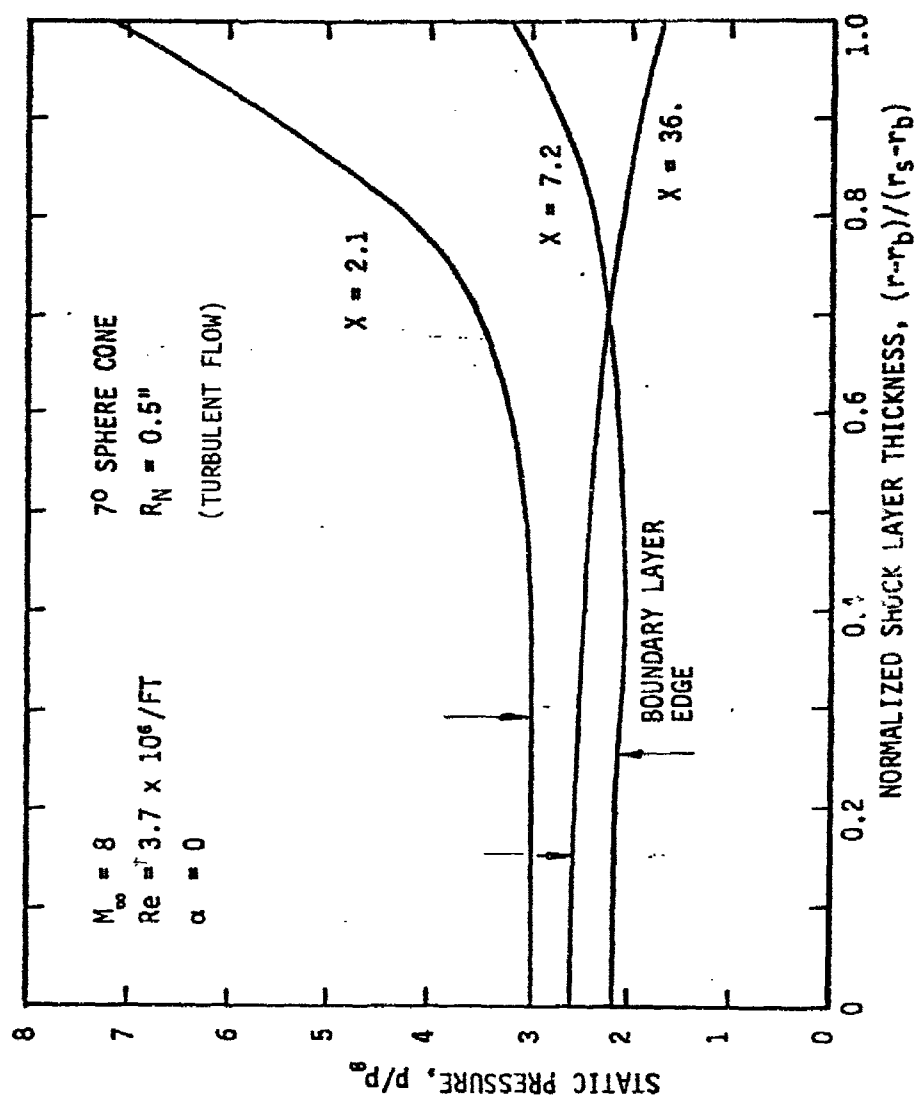


FIGURE 28. STATIC PRESSURE DISTRIBUTIONS THROUGH THE SHOCK LAYER

$M_\infty = 8$
 $\alpha = 0^\circ$

10.5°/7° BICONE
 $\delta = 10^\circ$

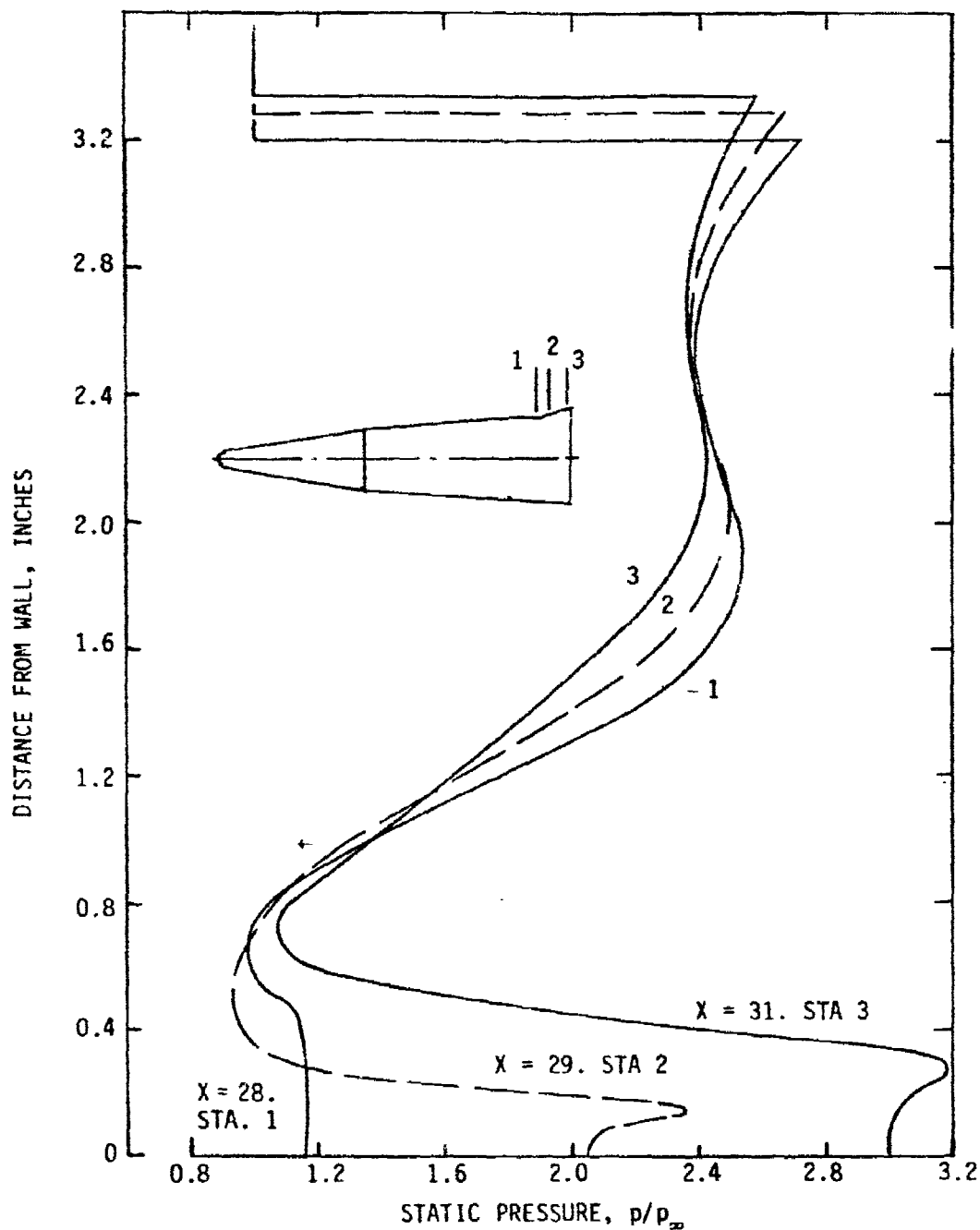


FIGURE 29. PNS PREDICTED FLAP REGION STATIC PRESSURE PROFILES THROUGH THE SHOCK LAYER

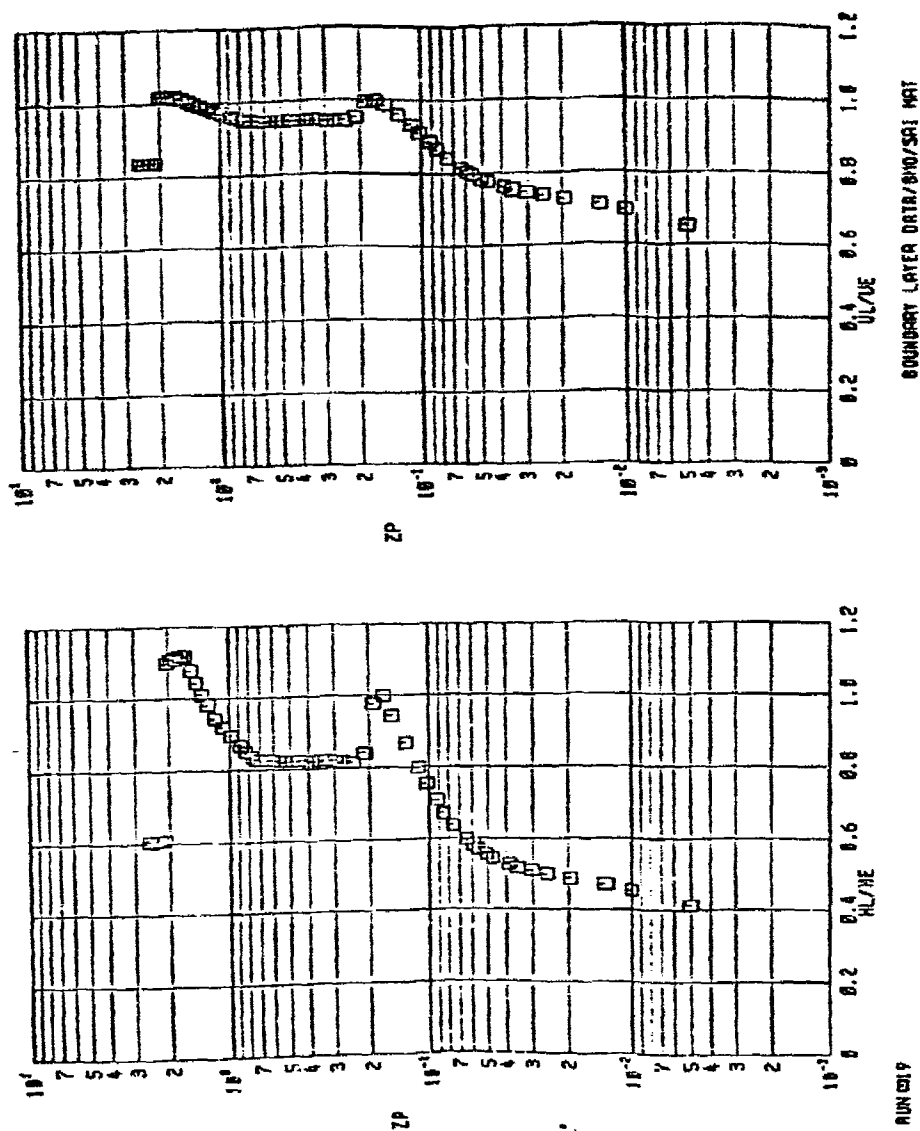
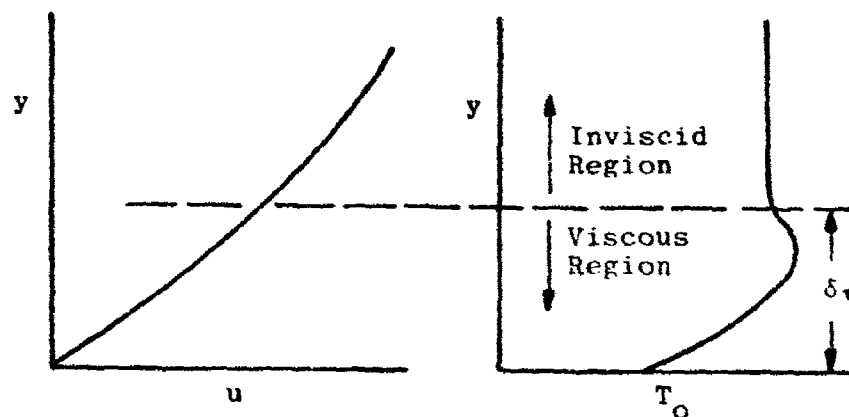


FIGURE 30. ILLUSTRATIVE EXAMPLE OF REDUCED 'HYTAC' DATA - 10.50/70 BICONE

$\alpha = -100^\circ$, $\delta_f = 100^\circ$, STATION 76



In the data analysis at AEDC, the boundary layer thickness is defined as that distance above the model surface where the total temperature attains a value of either $0.9975 T_{o\infty}$ for profiles with no overshoot or $1.0025 T_{o\infty}$ for profiles with a significant overshoot. Based on the boundary layer thickness defined in this manner, the displacement, momentum, kinetic energy, and total enthalpy thicknesses (δ^* , θ , δ_3 , and δ_4 , respectively) are also presented. These thickness parameters have a well-defined physical interpretation only for flows in which the velocity asymptotes to a constant edge value (i.e., sharp cone flow). Based on a well-defined boundary layer edge condition, they are, however, mathematically unique and can provide additional insight into interpretation of local flow field behavior especially if one is comparing results to boundary layer formulations. The thicknesses are defined as follows:

$$\delta^* + \frac{\cos \theta_c}{2 r_w} \delta^{*2} = \int_0^{\delta_\tau} \left(1 - \frac{\rho u}{\rho_e u_e} \right) \left(1 + \frac{y}{r_w} \cos \theta_c \right) dy$$

$$\theta + \frac{\cos \theta_c}{2 r_w} \theta^2 = \int_0^{\delta_\tau} \frac{\rho u}{\rho_e u_e} \left(1 - \frac{u}{u_e} \right) \left(1 + \frac{y}{r_w} \cos \theta_c \right) dy$$

$$\delta_3 + \frac{\cos \theta_c}{2 r_w} \delta_3^2 = \int_0^{\delta_\tau} \frac{\rho u}{\rho_e u_e} \left[1 - \left(\frac{u}{u_e} \right)^2 \right] \left(1 + \frac{y}{r_w} \cos \theta_c \right) dy$$

$$\delta_4 + \frac{\cos \theta_c}{2 r_w} \delta_4^2 = \int_0^{\delta_\tau} \frac{\rho u}{\rho_e u_e} \left(1 - \frac{T_o}{T_{o_e}} \right) \left(1 + \frac{y}{r_w} \cos \theta_c \right) dy$$

where θ_c is the local cone angle and r_w is the body radius measured normal to the model centerline. Shown in the Appendix is an example of the complete results of this boundary layer analysis. For each of the tests performed in this test series, that is both those conducted prior to the MAT program and in the MAT program tests, this post test analysis was performed and the results were tabulated and plotted.

5.0 TEST DATA HIGHLIGHTS

During the course of this experimental investigation, a considerable body of data were obtained on the sharp and blunt 7° cone and two bicone configurations (i.e., $10.5^\circ/7^\circ$ and $14^\circ/7^\circ$). The latter test series focused on the acquisition of data in the slice and flap regions. Body surface and shock layer profile data were obtained for laminar and turbulent flow conditions. To promote turbulence on the model for the Mach 8 conditions with the $R_N = 0.5$ " nose, boundary layer trips were used. Some highlights of the trip investigation results will be presented here. In addition, two of the primary contributions provided in the last test series sponsored by the MAT program were the $\alpha = 20^\circ$ sliced bicone data and the flap data. Consequently, highlights of these results also will be presented here.

5.1 Boundary Layer Trip Effectiveness

Boundary layer trips were required in order to promote a turbulent boundary layer for the configuration with a nose radius of 0.50 inches. Shown in Figure 31 is the axial distribution of surface heat transfer obtained at Mach 8 and $\alpha = 0^\circ$ on the blunted $10.5^\circ/7^\circ$ bicone for three trip geometries. Also shown is a turbulent boundary layer prediction obtained with the finite difference boundary layer code of Reference 20. It is evident from this figure that the flow remains laminar with the 13 mil trip, is transitional on the 10.5° forecone for the 33 mil trip and is turbulent at the roughness site with the 60 mil trip. It should be noted that the data shown here were obtained at a model wall temperature of 560°R . It was found (although not shown here) that the boundary layer profile obtained at the reference survey station at $\alpha = 0^\circ$ and at an equilibrium wall temperature of nominally 1100°R was laminar-transitional when the 33 mil trip was used and turbulent for the 60 mil trip. Consequently, these data indicate that boundary layer trip effectiveness is dependent on the wall

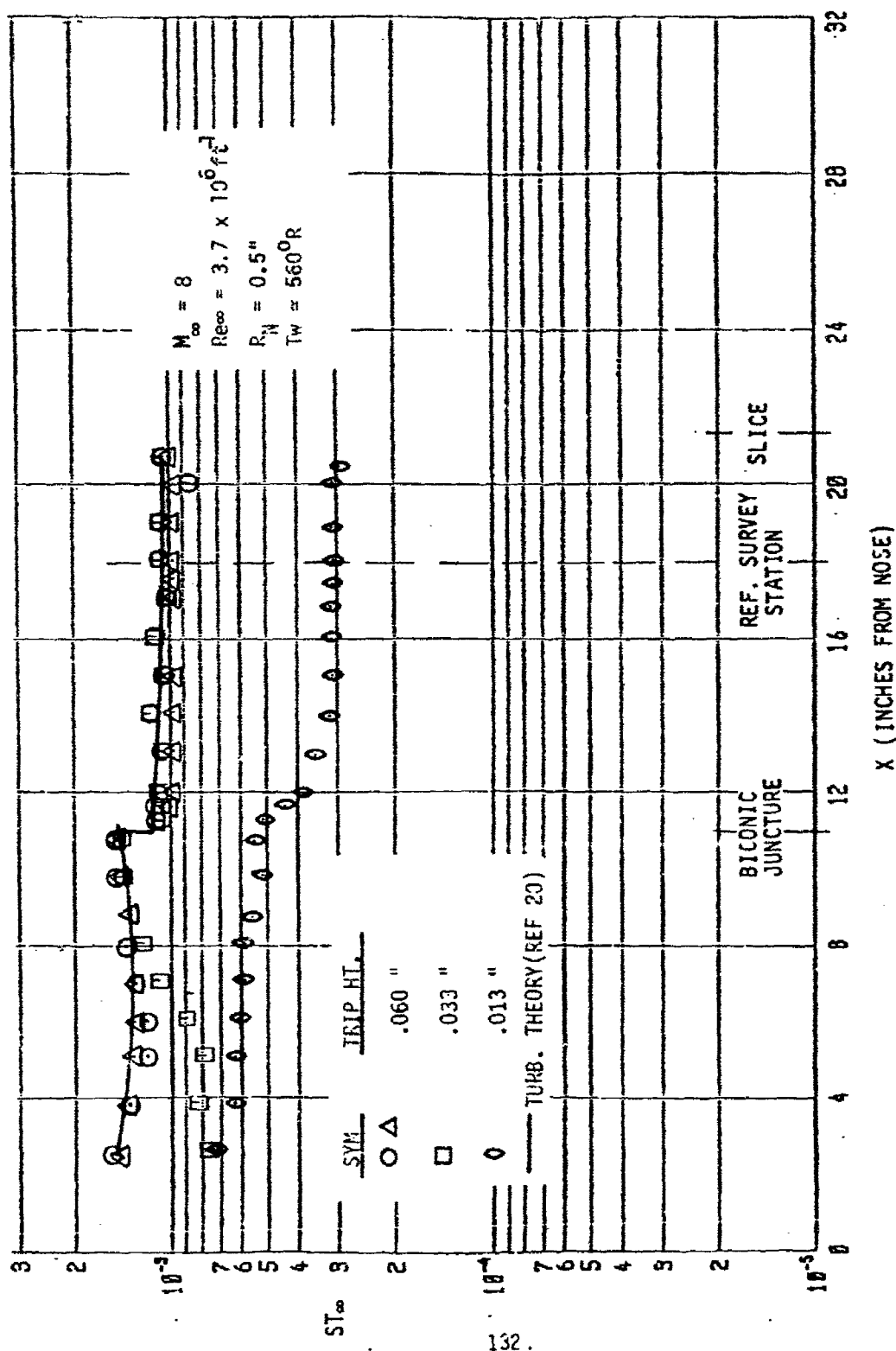


FIGURE 31. BOUNDARY LAYER TRIP EFFECT ON $10.5^{\circ}/7^{\circ}$ BICONE SURFACE HEAT
 TRANSFER AT $\alpha = 0^{\circ}$

temperature. Boundary layer trip effectiveness at angle of attack was also investigated. Shown in Figure 32 is the distribution of surface heating on the 0° and 180° meridional ray at $\alpha = 0, 4^\circ, 10^\circ$, and 20° for an axial model station 22 inches downstream of the stagnation point (i.e., just upstream of the slice). One will note that at this station the flow on the wind and leeward sides at $\alpha = 20^\circ$ is turbulent with the 13 mil trip, and is transitional for the smaller values of α .

Complete axial heating distributions obtained at roll angles from 0 to 100° at $\alpha = 10^\circ$ for the 13 mil and 33 mil trip are shown in Figures 33 and 34, respectively. The comparable set obtained at $\alpha = 20^\circ$ is shown in Figures 35 and 36. These data corroborate the results shown in Figure 32; namely, that the 13 mil trip is ineffective at $\alpha = 10^\circ$ and is quite effective in promoting turbulent cold wall heating at $\alpha = 20^\circ$.

From these data, and the associated shock (boundary) layer profile data it was decided that the 33 mil trip would be used for the heat transfer tests, the 60 mil trip for the shock layer survey tests at $\alpha \leq 10^\circ$ and also the leeside at $\alpha = 20^\circ$, and the 33 mil trip for the $\alpha = 20^\circ$ windward side profile test. The concern at $\alpha = 20^\circ$ (windward) was that with the thinned boundary layer the larger trip would affect the outer inviscid flow; consequently, the smallest trip required to promote turbulence was used.

5.2 Limited Data Trends and Highlights

As indicated earlier, the most significant contribution of the MAT program sponsored tests to the earlier series conducted at AEDC on these cones and bicones was to obtain data on the $10.5^\circ/7^\circ$ bicone at $\alpha = 20^\circ$ and to obtain data with the inclusion of the flap system. In addition to the surface heating, pressure, and shear

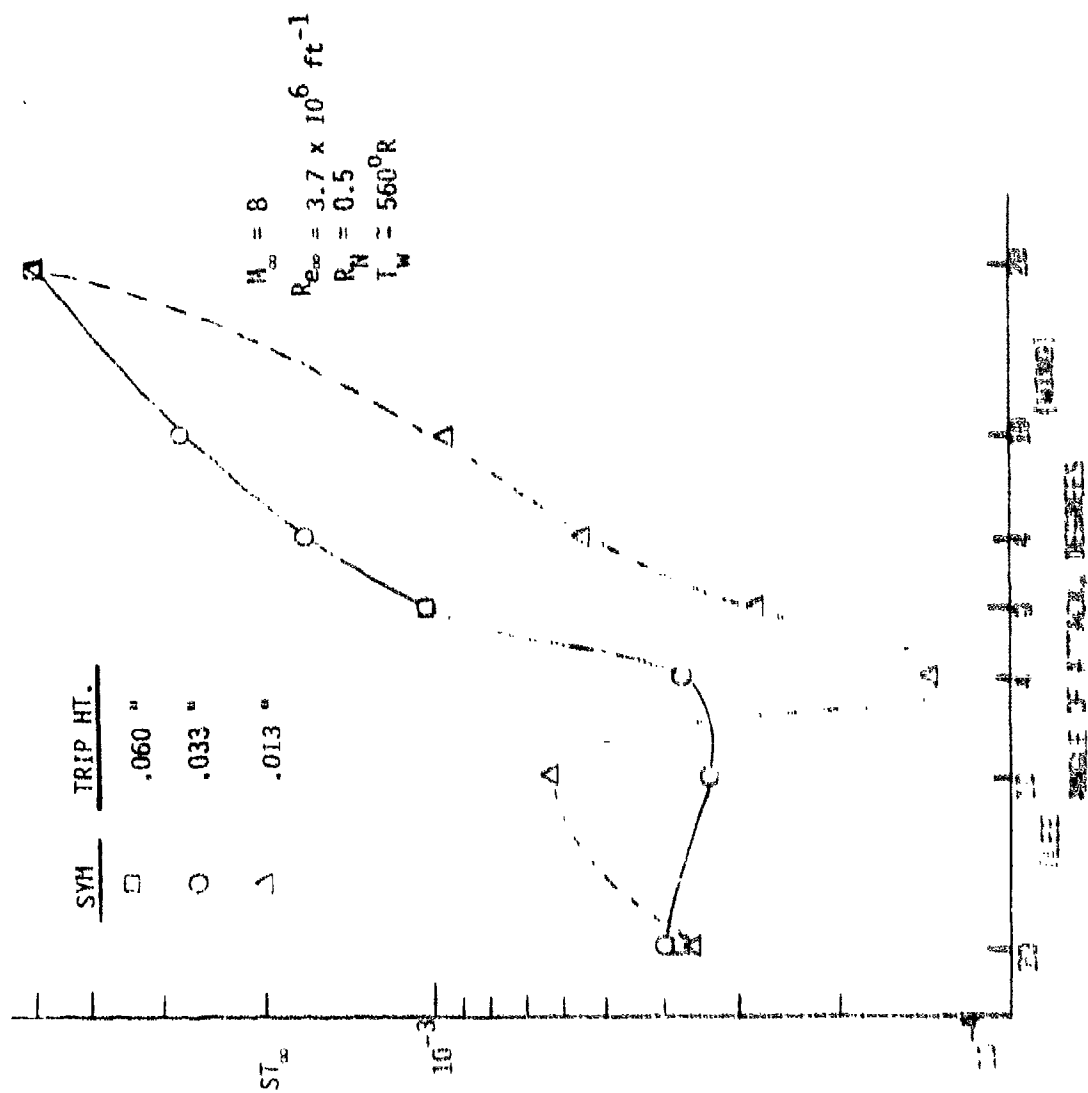


FIGURE 52. VARIATION OF HEAT TRANSFER COEFFICIENT WITH ANGLE OF ATTACK AT $Re_{\infty} = 3.7 \times 10^6 \text{ ft}^{-1}$
 FOR VARIOUS TRIP HEIGHTS

$M = 8$
 $Re_L = 3.7 \times 10^6 ft^{-1}$
 $\beta = 0.5$
 $T_w = 560^\circ R$
 $\epsilon = 10^{-6}$

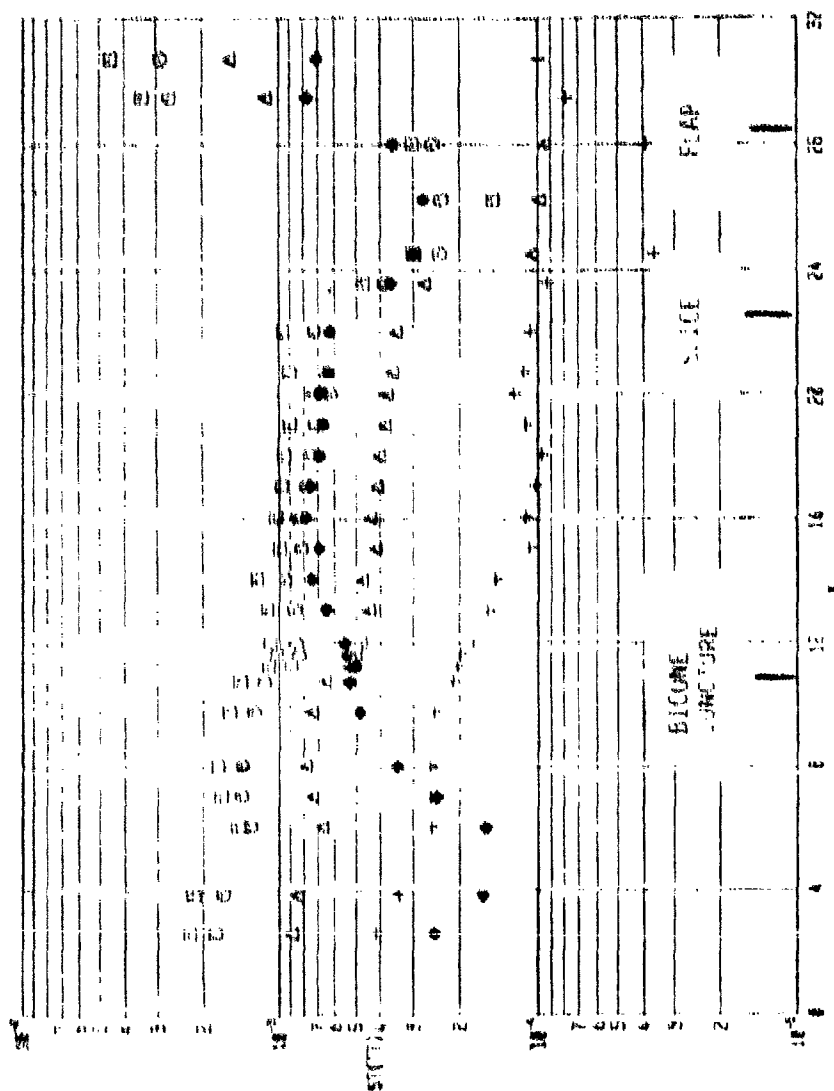


FIGURE 33. AXIAL HEATING DISTRIBUTION FOR SEVERAL MERIDIONAL RAYS
 10.5°/7° BICONE WITH 13 MIL TRIP AT $\alpha = 10^\circ$

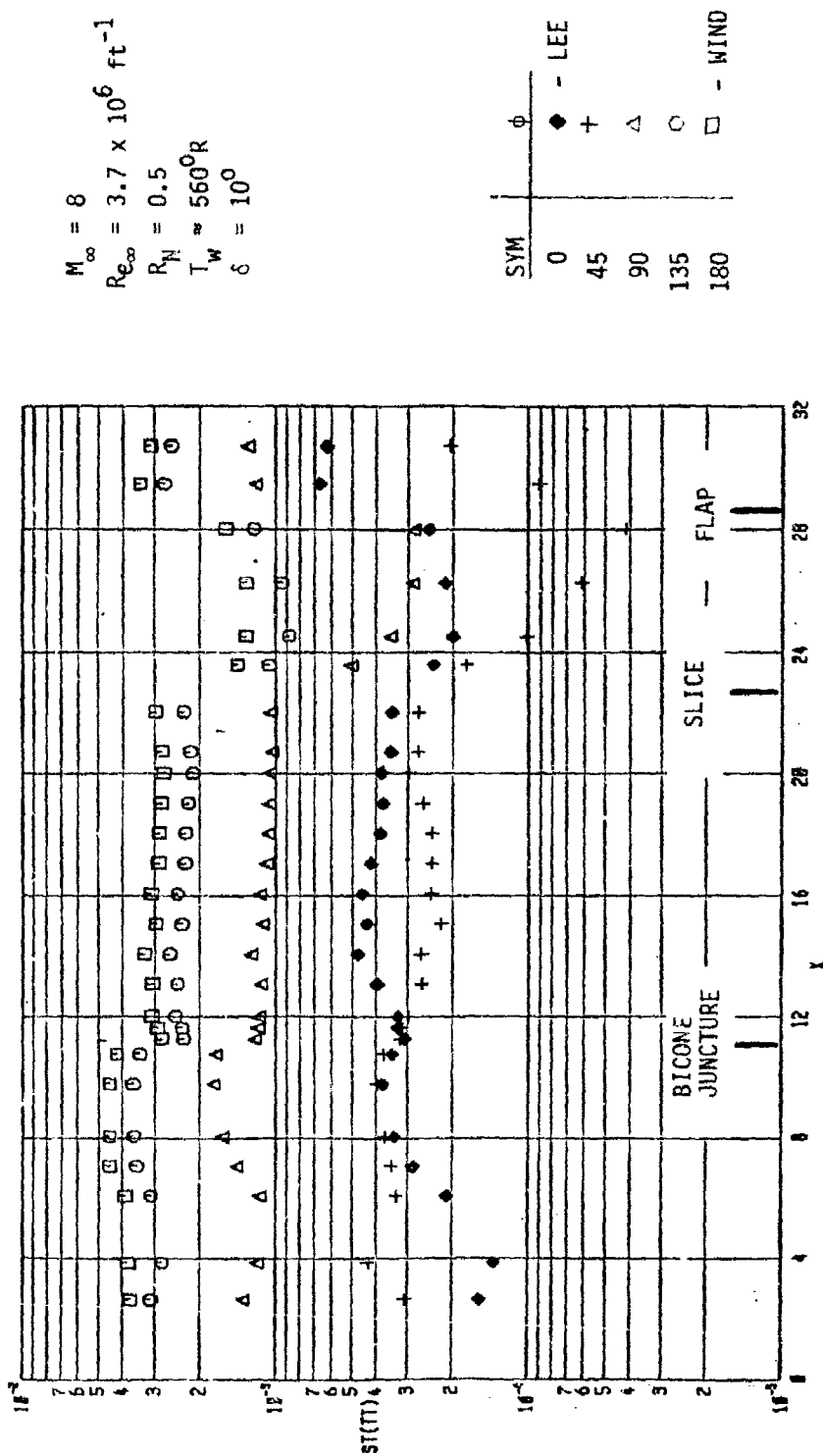
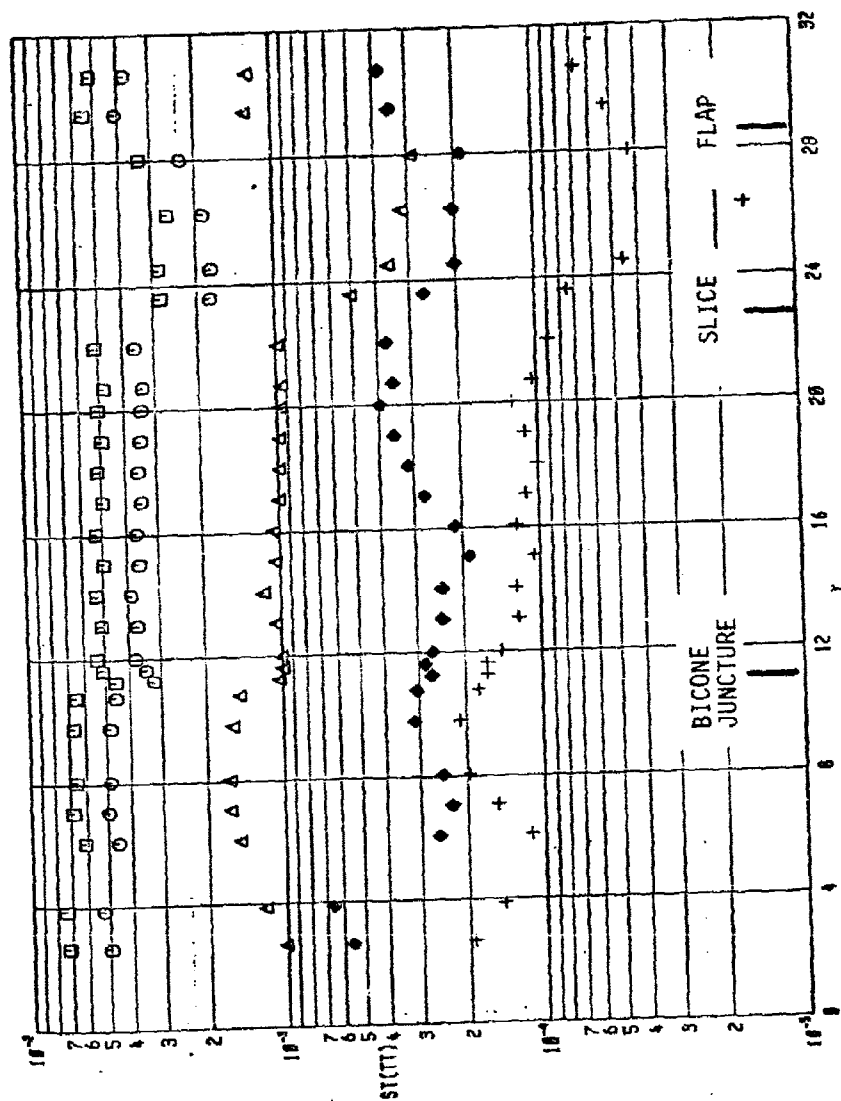


FIGURE 34. AXIAL HEATING DISTRIBUTION FOR SEVERAL MERIDIONAL RAYS
 10.5°/7° BICONE WITH 33 MIL TRIP AT $\alpha = 10^\circ$



$M_\infty = 8$
 $Re_\infty = 3.7 \times 10^6 \text{ ft}^{-1}$
 $R_N = 0.5$
 $T_w = 560^\circ R$
 $\delta = 10^\circ$

SYM	ϕ
0	◆ - LEE
45	+
90	△
135	○
180	□ - WIND

FIGURE 35. AXIAL HEATING DISTRIBUTION FOR SEVERAL MERIDIONAL RAYS
 10.5°/7° BICONE WITH 13 MIL TRIP AT $\alpha = 20^\circ$

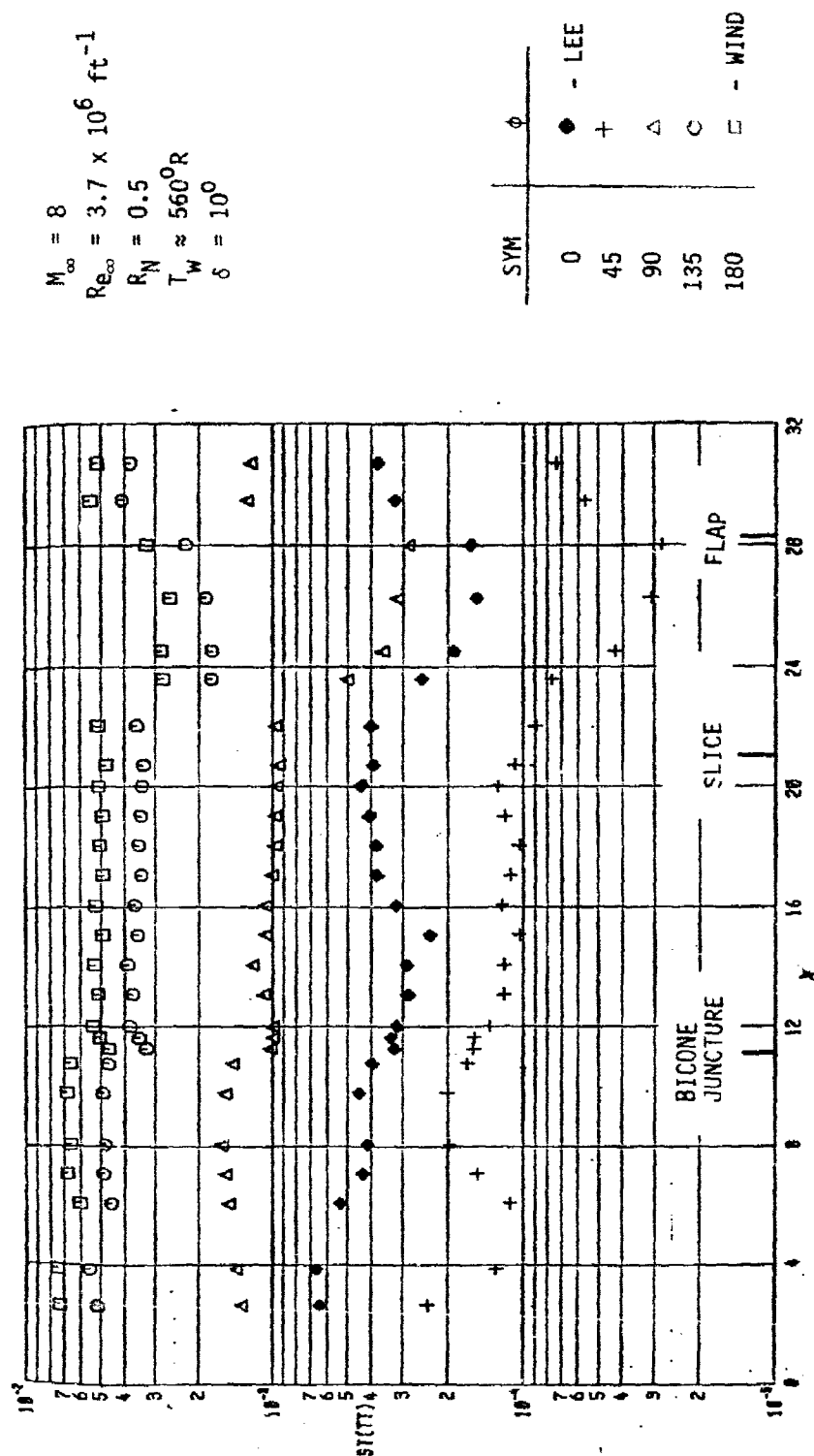


FIGURE 36. AXIAL HEATING DISTRIBUTION FOR SEVERAL MERIDIONAL RAYS
 $10.5^\circ/7^\circ$ BICONE WITH 33 MIL TRIP AT $\alpha = 20^\circ$

(Preston tube) measurements, shock layer survey tests were obtained for turbulent boundary layer flow conditions primarily in the slice/flap region. Shown in the schematic of Figure 37 are the nominal locations where shock layer surveys were obtained. The exact locations may be found in the tables presented in Section 3. From this array one can obtain a representative measure of the flow field properties in this slice/flap region along with a reference profile, wind and 1e_∞ , on the 7° cone surface. Shown in Figure 38 is a representative shock layer survey data set on the cone/ 0° slice/ -7° slice that would be available for comparison with the detailed computer codes. This particular set is for Mach 8, $\alpha = 0^\circ$. A representative set of flap shock layer profiles (at station 17, Figure 37) is shown in Figure 39, also for $\alpha = 0^\circ$. The reader is referred to Section 3.4 for a complete summary listing of the data obtained.

The angle of attack variation of the slice centerline pressure distribution for the blunted $10.5^\circ/7^\circ$ bicone is shown in Figure 40. The complementary flap centerline pressure distribution is shown in Figure 41. Also shown in Figure 41 is the pressure distribution on the flap for the sharp ($R_N = 0$) $10.5^\circ/7^\circ$ bicone. It is evident from this figure that the flap effectiveness for the blunt configuration is reduced due to vortical (entropy swallowing) flow effects. In addition, the pressure distribution (near C_L) for the split flap ($\delta = 20^\circ/10^\circ$) is also shown in Figure 41 as the filled symbols. The 20° split flap pressure is nominally the same as for the 20° continuous flap. However, due to spill-over effects, the pressure on the adjacent 10° split flap section is higher than that for the 10° continuous flap. Thus the rolling moment produced by the split flap configuration would be smaller than that determined from the continuous 20° and 10° flap data. It should be noted that since the flap is split on the model centerline the split flap pressures shown are at the offset stations noted in Figure 41. The chord and spanwise pressure distribution for the 10° continuous flap at $\alpha = 0, 4^\circ$, and 10° , for the

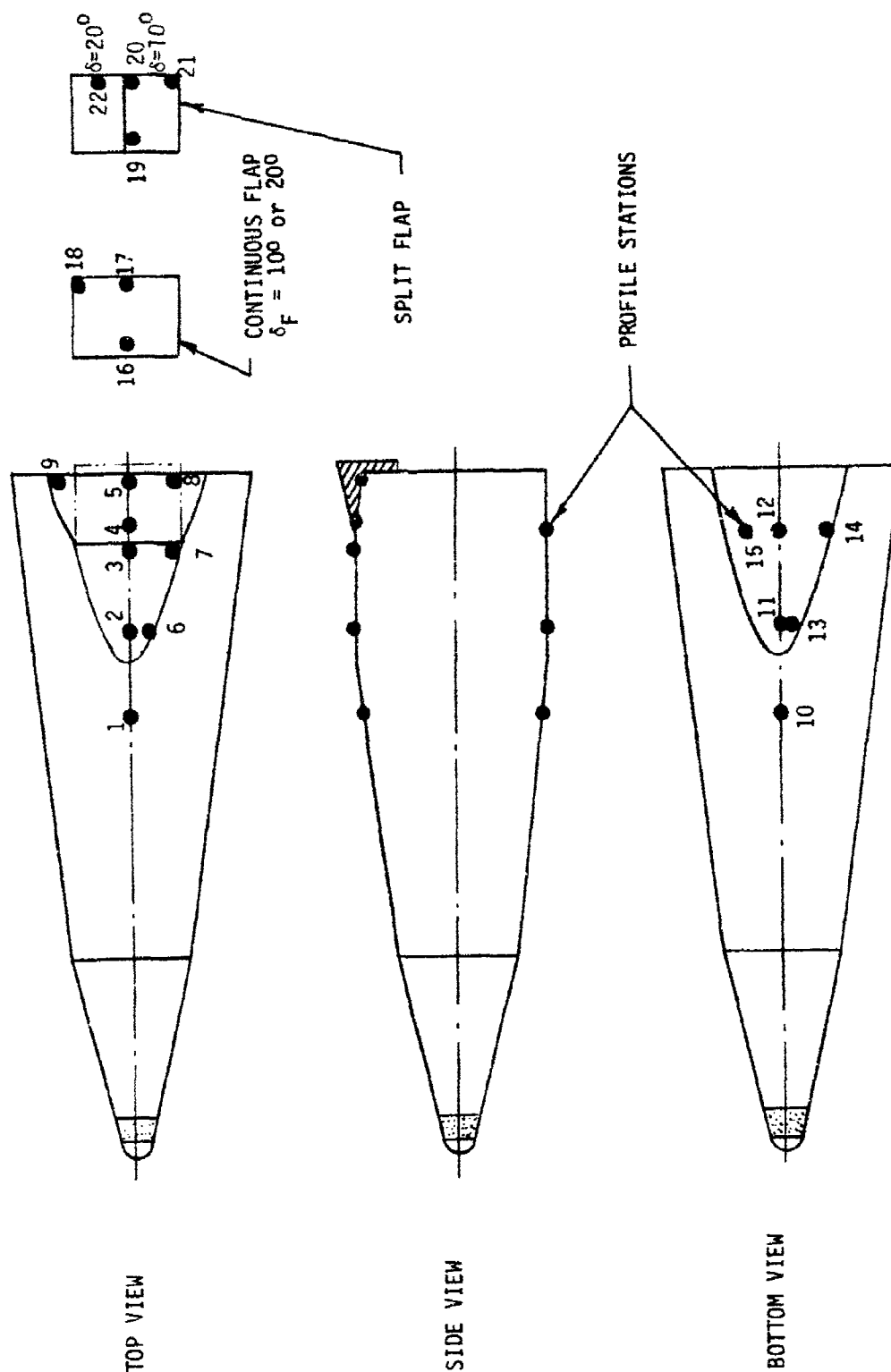


FIGURE 37. SCHEMATIC LOCATION OF THE PROFILE STATIONS ON THE 10.5°/7° BICONE

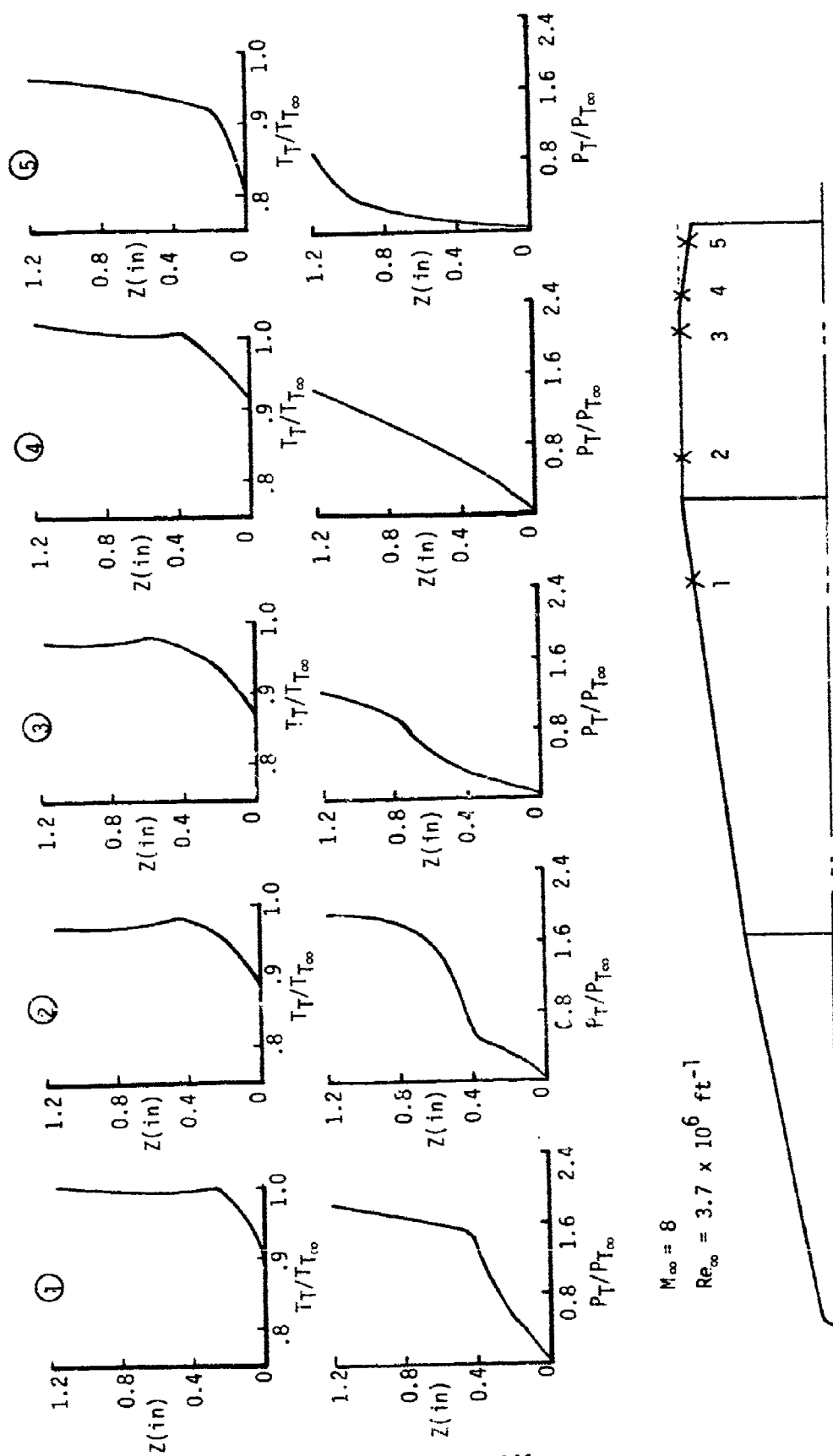
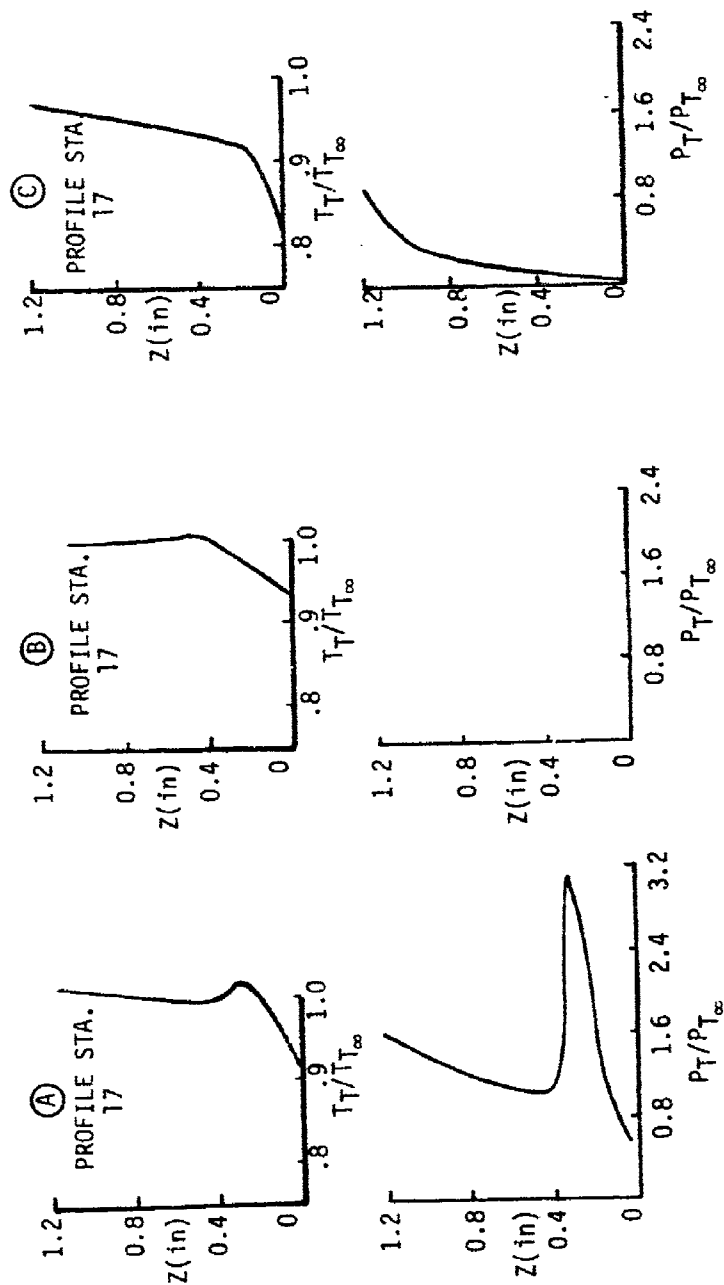


FIGURE 38. REPRESENTATIVE SHOCK LAYER PROFILES ON THE 10.5°/7° BICONE AT $\alpha = 0^\circ$



$M_\infty = 8$
 $Re_\infty = 3.7 \times 10^6 \text{ ft}^{-1}$

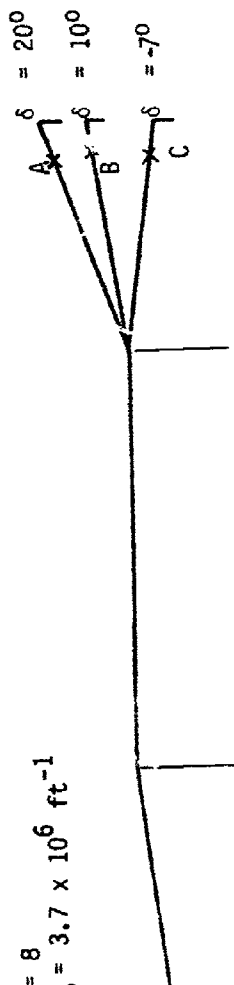


FIGURE 39. REPRESENTATIVE FLAP SHOCK LAYER PROFILES ON THE 10.5°/7° BICONE
 AT $\alpha = 0^\circ$

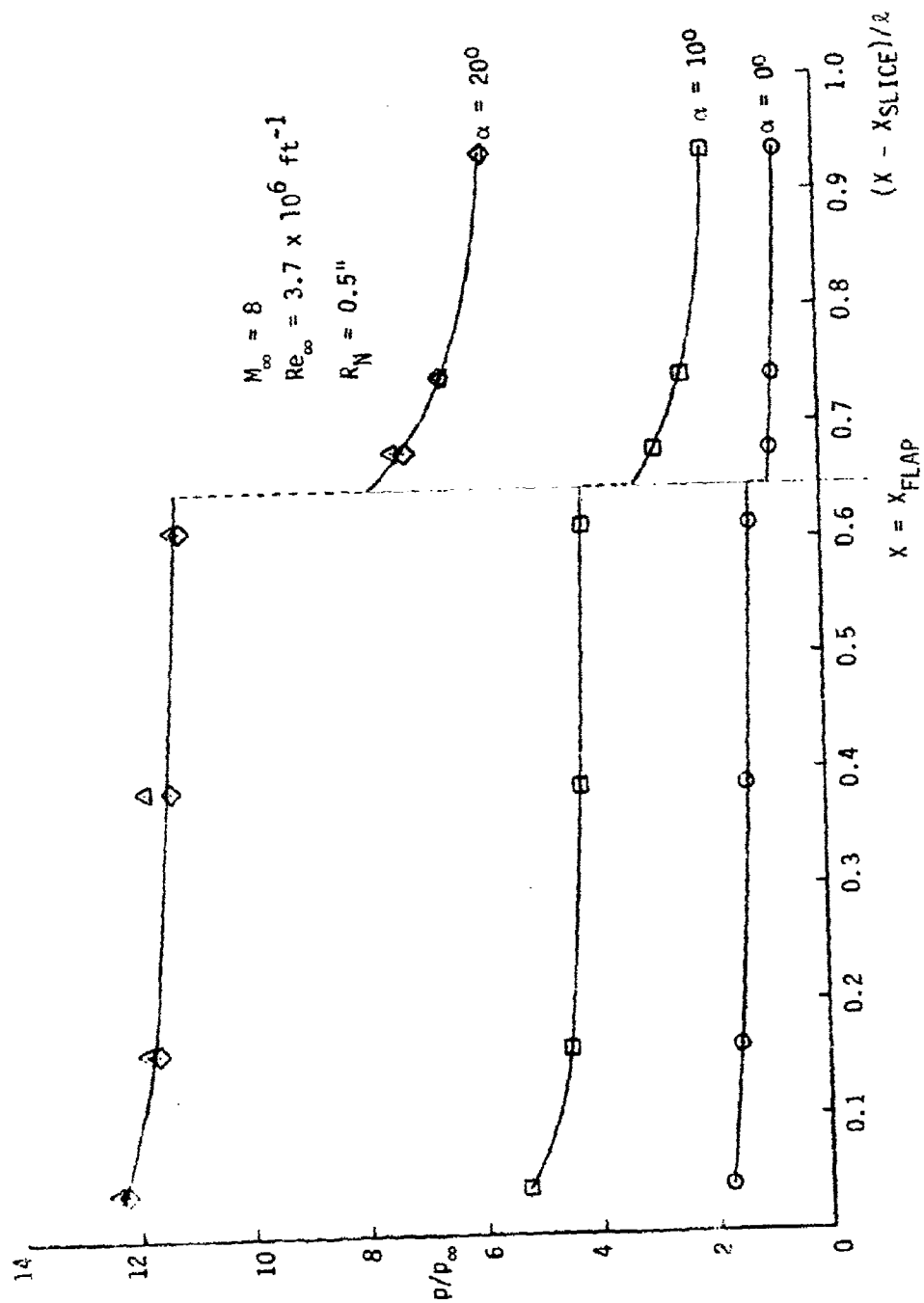


FIGURE 40. ANGLE OF ATTACK VARIATION OF THE 10.5:77° BICONE SLICE
CENTERLINE PRESSURE DISTRIBUTION

$$M_o = 8 \quad Re_\infty = 3.7 \times 10^6 \text{ ft}^{-1}$$

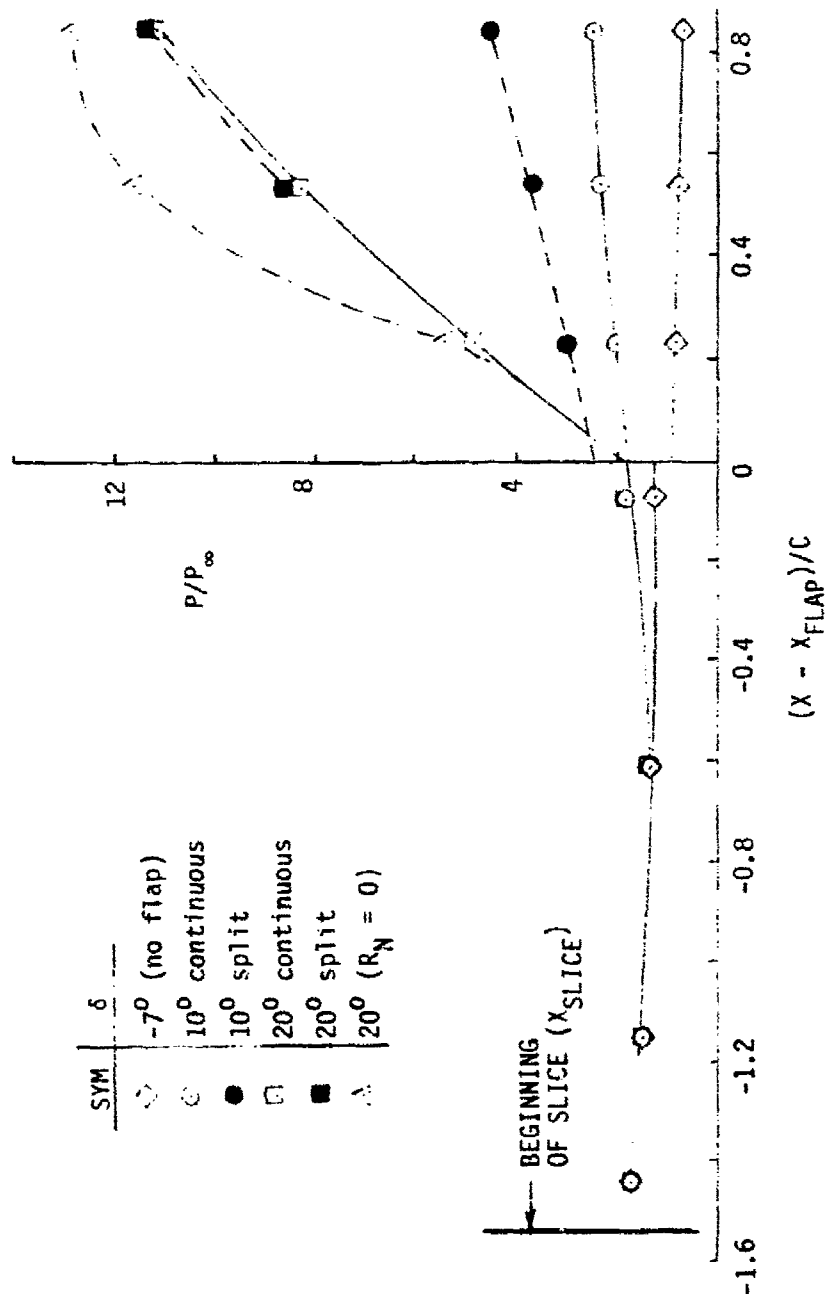


FIGURE 41. SLICE/FLAP CENTERLINE PRESSURE DISTRIBUTION FOR THE 0.50" BLUNTED 10.5°/7° BICONE AT $\alpha = 0^\circ$

blunted $10.5^\circ/7^\circ$ bicone is shown in Figure 42. It is evident from this figure that at $\alpha = 10^\circ$ one observes a drop-off in pressure near the flap edge which is not present for $\alpha \leq 4^\circ$.

In addition to the pressure distributions recorded, the slice region centerline heating distribution for the blunted $10.5^\circ/7^\circ$ configuration is shown in Figure 43, while Figure 44 depicts the slice/flap heating. Again, also shown in Figure 44 is the heating on the flap for the sharp bicone. One notes that the flap heating, like the pressure, is higher for the sharp bicone due to the absence of vortical flow effects. The variation of the chord and spanwise heating distribution on the 10° flap with angle of attack is shown in Figure 45. The heating is slightly higher near the flap edges $|y|/S \rightarrow 1$ due to the boundary layer thinning.

A sample of the surface shear data, in terms of the skin friction coefficient, $C_F = \tau_w/q_\infty$ as deduced from the Preston tube measurements is shown in Figure 46 for the slice region centerline (vs. α) and for the flap centerline (vs. δ). The variation with α at the frustum and forward slice station is shown in Figure 47. These data should be useful in evaluating the 3D PNS codes ability to handle local three dimensionality associated with the slice and flap.

The limited data presentation shown here does not do justice to the rather extensive data base acquired; rather it serves to demonstrate the type of data acquired. In the following section some few examples of computer code comparisons with select sets of these data will be presented as illustrations of the utility of the data to validate computer code prediction ability.

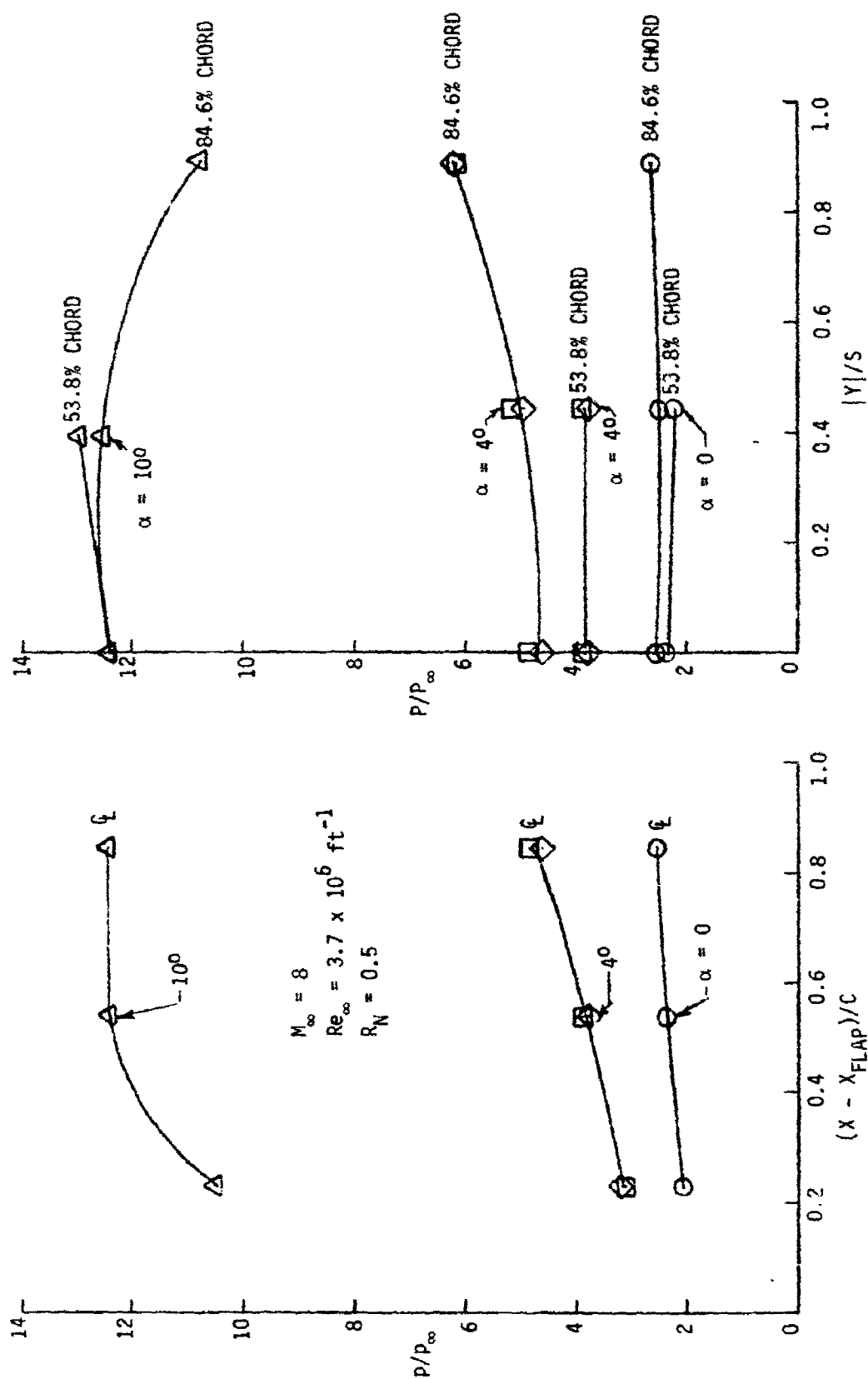


FIGURE 42. CHORD AND SPANWISE DISTRIBUTION OF FLAP PRESSURES FOR $\delta = 10^\circ$

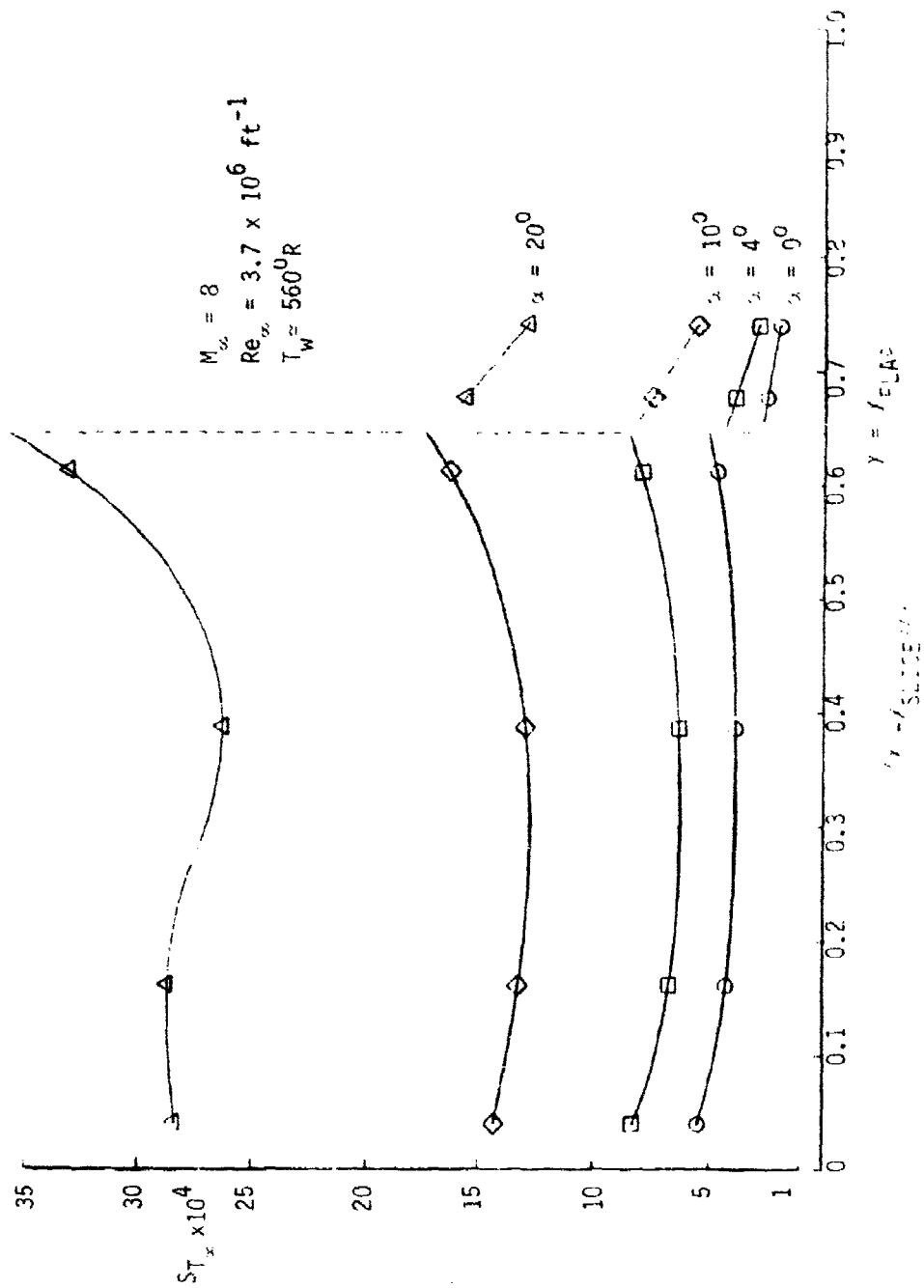


FIGURE 43. ANGLE OF ATTACK VARIATION OF THE $10.5^\circ/7^\circ$ BLUNTED BICONE CENTERLINE SLICE HEATING DISTRIBUTION

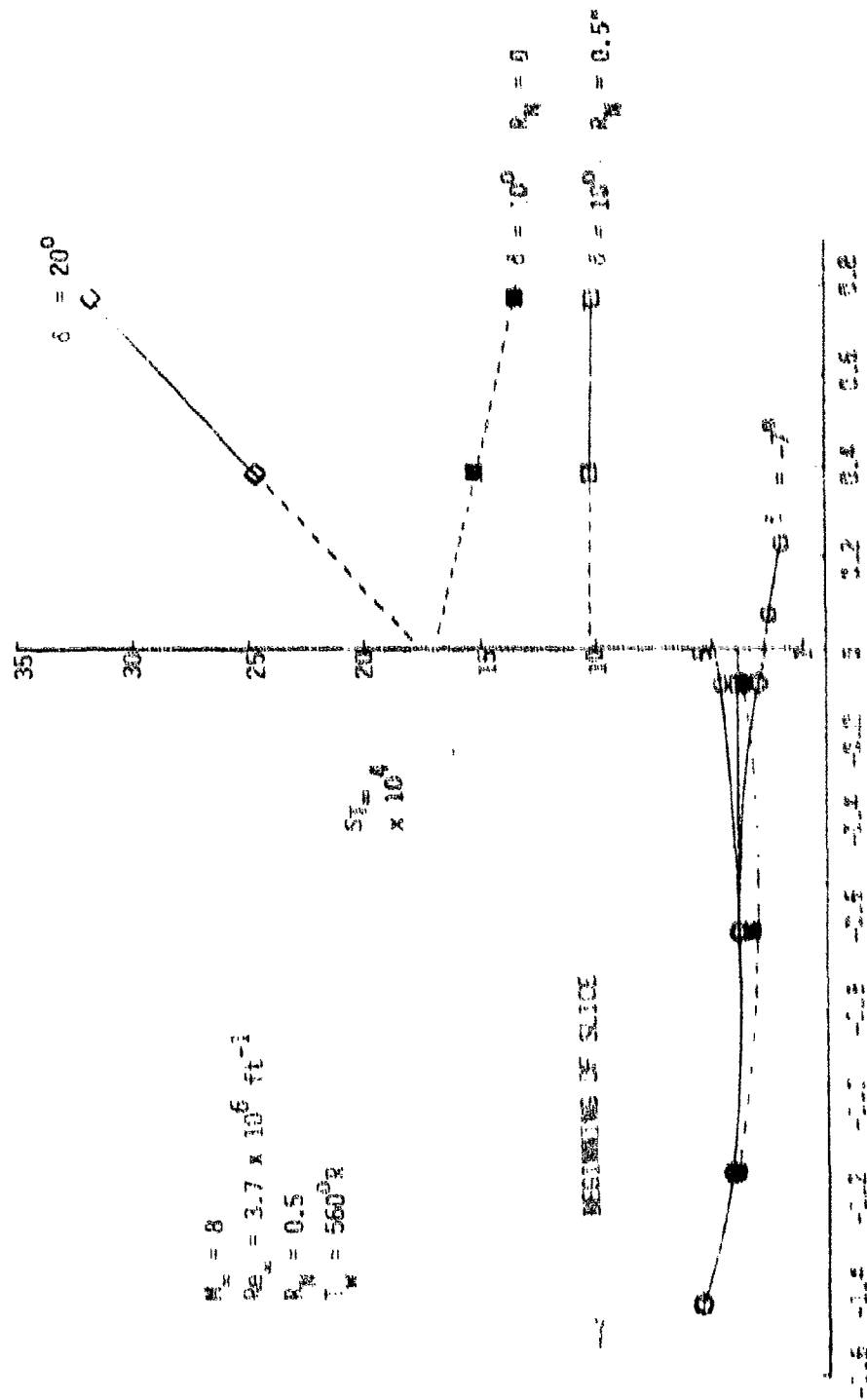


FIGURE 11. CENTERLINE HEATING INTERACTION ON THE 10.577° BICONIC
 SLICE 1-12

$$\begin{aligned} \alpha &= 10^\circ \\ Re_{\infty} &= 1.7 \times 10^6 \\ \beta_{\infty} &= 0.5 \\ T_{\infty} &= 560^\circ R \end{aligned}$$

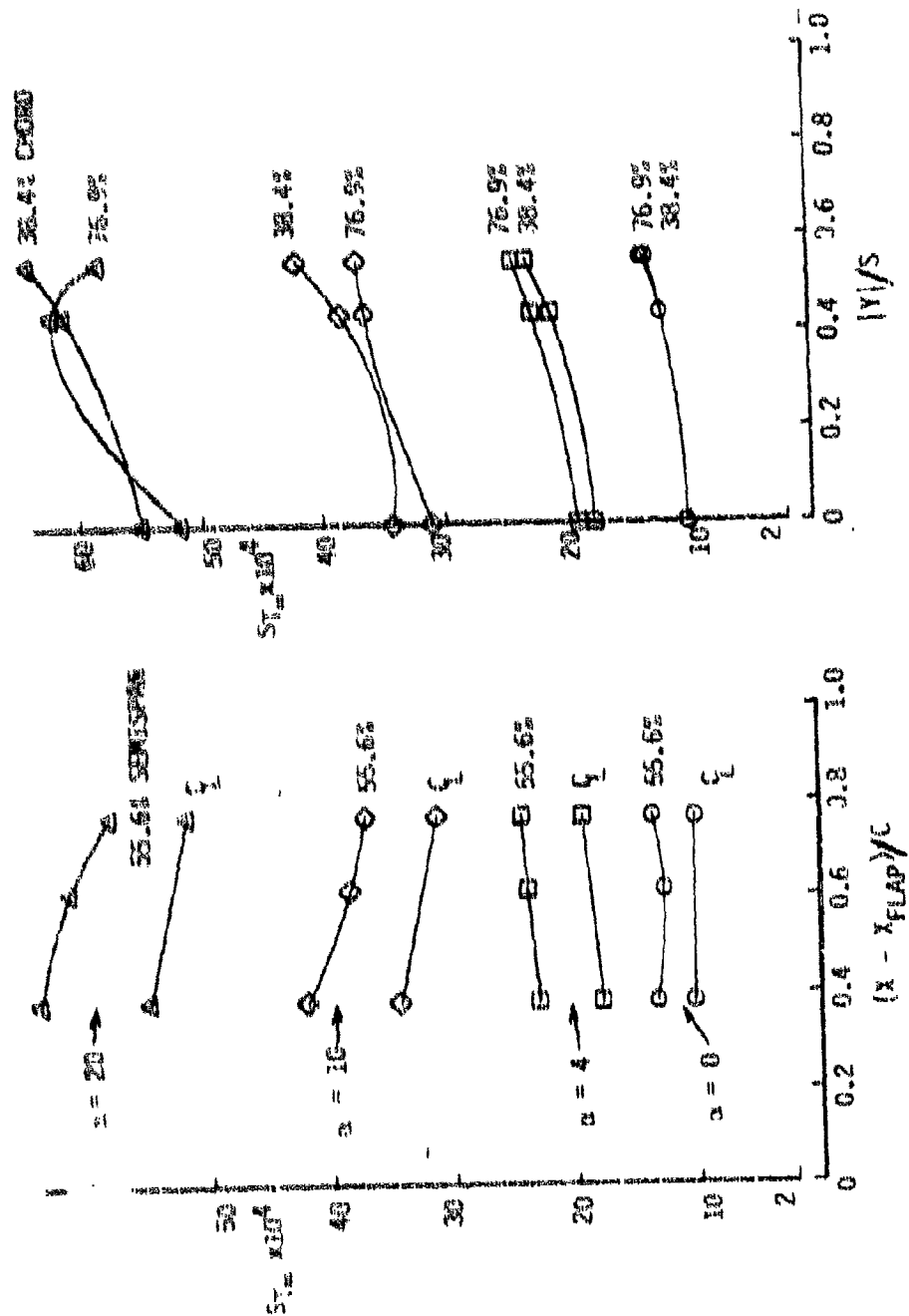


FIGURE 45. CHORD AND SPANWISE DISTRIBUTION OF FLAP HEATING ON THE 10.5°/7° BICONE FOR $\delta = 10^\circ$

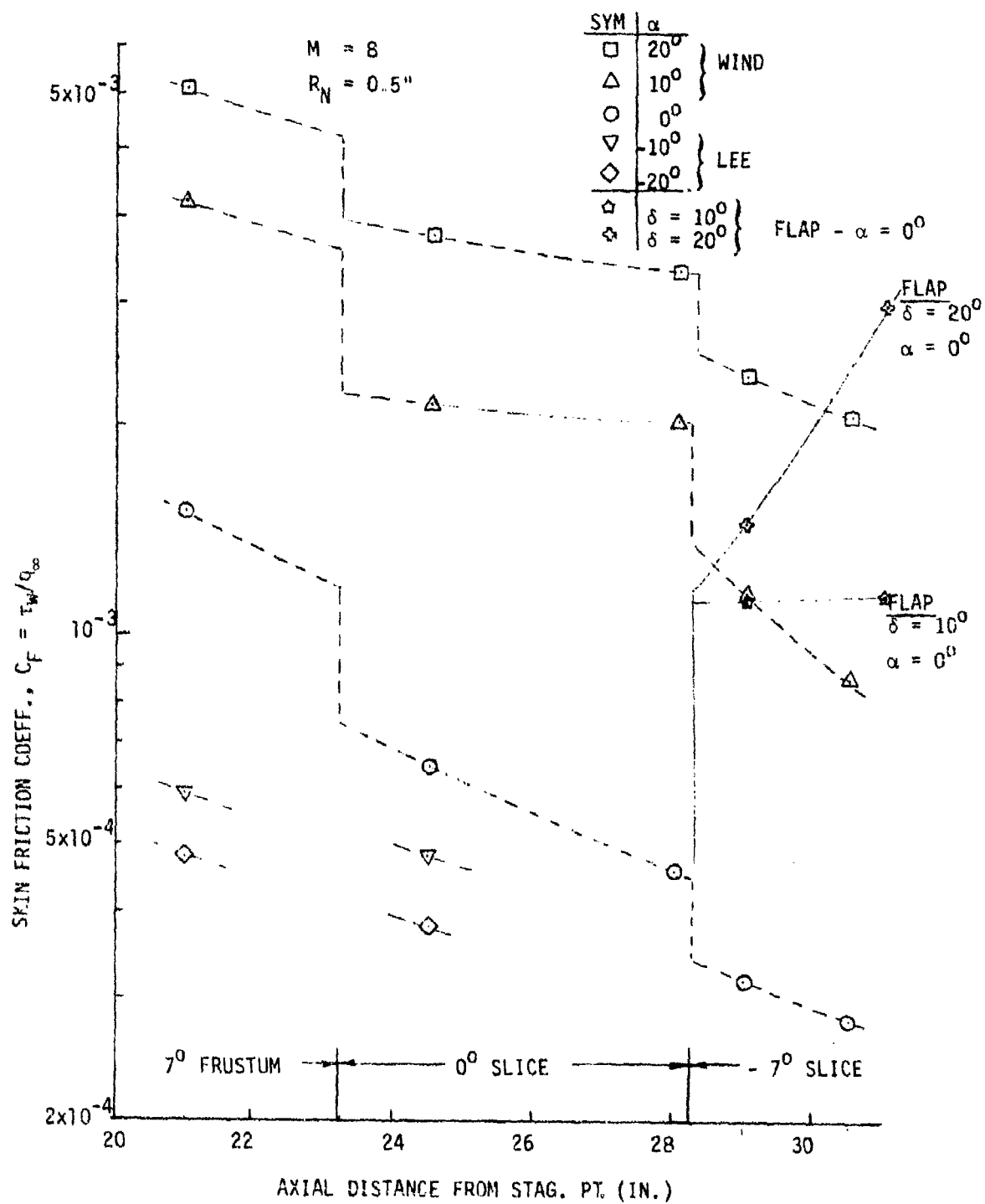


FIGURE 46. SURFACE SHEAR DISTRIBUTION IN THE SLICE REGION OF THE BLUNTED 10.5°/7° BICONE

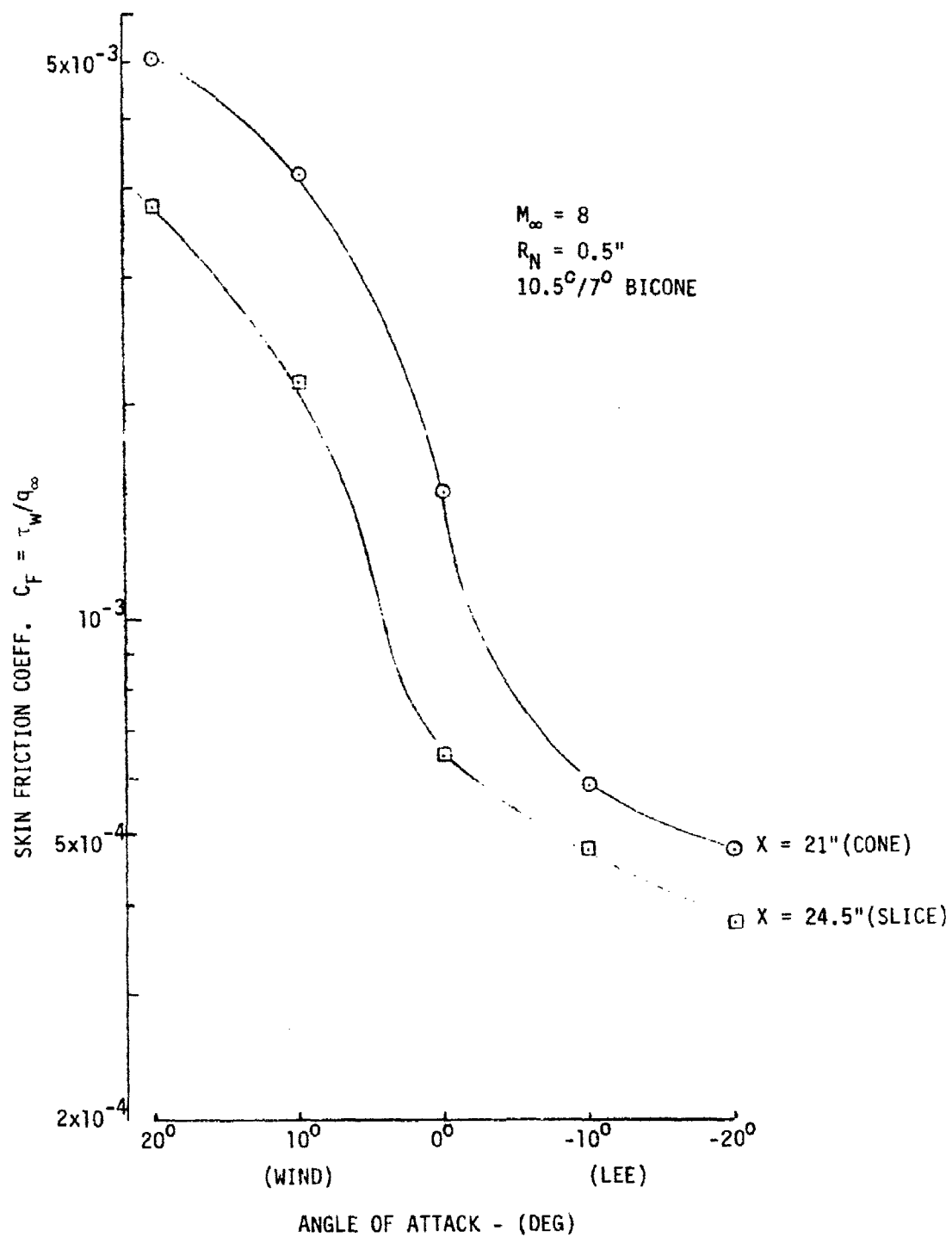


FIGURE 47. SURFACE SHEAR VARIATION WITH ANGLE OF ATTACK
 CONE AND SLICE REGION

6.0 DATA USAGE FOR TECHNIQUE VALIDATION

As mentioned earlier, one (if not the) primary reason for acquiring this rather large body of data on a current MaRV type configuration is for the validation of complex computer codes. Comparisons of prediction capability with discrete sets of experimental data are generally performed and judgments made relative to code prediction accuracy. Quite often, for example, one is able to adequately predict surface pressure distributions but not static forces and moments. Or, one can predict the laminar heating rate quite well but not the turbulent heating levels. The current set of data provides one consistent base for comparing static loads, surface pressure, laminar and turbulent heating, viscous shear forces, and detailed properties in the shock layer. Sufficient diagnostic data are available to establish the potential cause(s) of an apparent prediction discrepancy if total agreement is not achieved. In this section, several discrete comparisons of code prediction with data will be shown as illustrative examples of the data usage.

6.1 Wall Temperature Considerations

Due to the manner in which the data are obtained in the AEDC Tunnels B and C, the model wall temperature will vary for the different data types. This has been discussed in detail in Section 3. In general, the model wall temperature is initially at ambient room temperature ($\sim 540^{\circ}\text{R}$). Due to aerodynamic heating the wall temperature varies (increases) with the length of time in the tunnel flow. Thus the Gardon gage heat transfer data, which are obtained in 1-6 seconds after exposure to the flow, will have a wall temperature close to ambient. At the other extreme, the shock layer survey data are obtained after the model has achieved an equilibrium wall temperature; that is, a temperature close to the adiabatic wall value where the convective heating to the model is balanced by the radiative losses to the tunnel.

walls. The static force and moment data are generally obtained after several seconds of exposure to tunnel flow - long enough to run through an angle of attack sweep. Thus the model is close to the ambient value. However, one finds that the static forces are not very sensitive to the specific wall temperature value. That is, the normal force and static moment coefficient are primarily dominated by the inviscid pressure field and therefore wall temperature effects are not pertinent. The axial force - specifically the viscous component (which comprises approximately 10% of the total forebody axial force at $\alpha = 0^\circ$ and diminishes with increasing α) is only weakly dependent on the wall temperature. Consequently, the total axial force, to all intents and purposes, is independent of wall temperature.

Model surface pressure measurements are a combination of the inviscid and viscous induced pressure. The latter is weakly dependent on wall temperature. Since the viscous induced increment accounts for less than 5% of the local static pressure, the wall pressure is also independent of wall temperature.

Thus if one wishes to generate computer code predictions and comparisons to a set of data for a prescribed configuration, two runs must be made; one at the cold wall ambient temperature condition ostensibly for heat transfer comparison, and one at the hot wall equilibrium wall temperature condition for comparisons with the profile (including the Preston tube-wall shear) data. Force and moment and wall pressure comparisons can be established from either run.

6.2 Representative Comparisons of Theories with Data

6.2.1 Static Force and Moment

Comparisons of computer code predictions with the data from the current test series have been made with the inviscid codes of

References 21, 22, and 23 and with the PNS code of Reference 24. Shown in Figures 48 and 49 are comparisons of the normal force coefficient, C_N , and pitching moment coefficient, C_m for the blunted 7° cone and $14^\circ/7^\circ$ bicone predicted with the inviscid codes of References 21-23 and the data from the current test series. One will note that the 3D inviscid code predictions of References 21, 22 are in excellent agreement with the data for α as high as 14° . It should be noted that although the flow is separated on the leeside for $\alpha \geq 7^\circ$, the predicted coefficients agree well with the data. It will be shown later that the leeside pressures are poorly predicted with the inviscid code when separation is present (as they should be); however, since the static loads are dominated in hypersonic flow by the windward surface pressures, the good agreement will be shown to be a consequence of good windward surface pressure predictions.

Helliwell, et al⁽²⁴⁾ have generated several comparisons of their version of a parabolized Navier Stokes (PNS) code (called HYTAC) with the data from the current tests. Shown in Figure 50 are comparisons of HYTAC with $14^\circ/7^\circ$ sliced bicone (without a flap) laminar flow data taken at Mach 10 (see Section 3.3). One notes that up to $\alpha = 10^\circ$ agreement is excellent. To generate these comparisons one need only set up the geometry, free stream conditions and vary α .

6.2.2 Surface Static Pressure

Comparisons of data from the current test series were made with the PNS codes of References 24 and 25 and with the inviscid code of References 21 & 22. Shown in Figures 51 and 52 are comparisons made with the PNS codes of References 24 and 25, with the surface pressure data obtained at the Mach 8 condition on the $10.5^\circ/7^\circ$ bicone with a double windward slice and single leeward slice at $\alpha = 0^\circ$ and 10° , respectively. At $\alpha = 0^\circ$, the agreement between theory and data on the conic surfaces is quite good; however, code improvements are needed in the slice region to affect better agreement. It is in this context

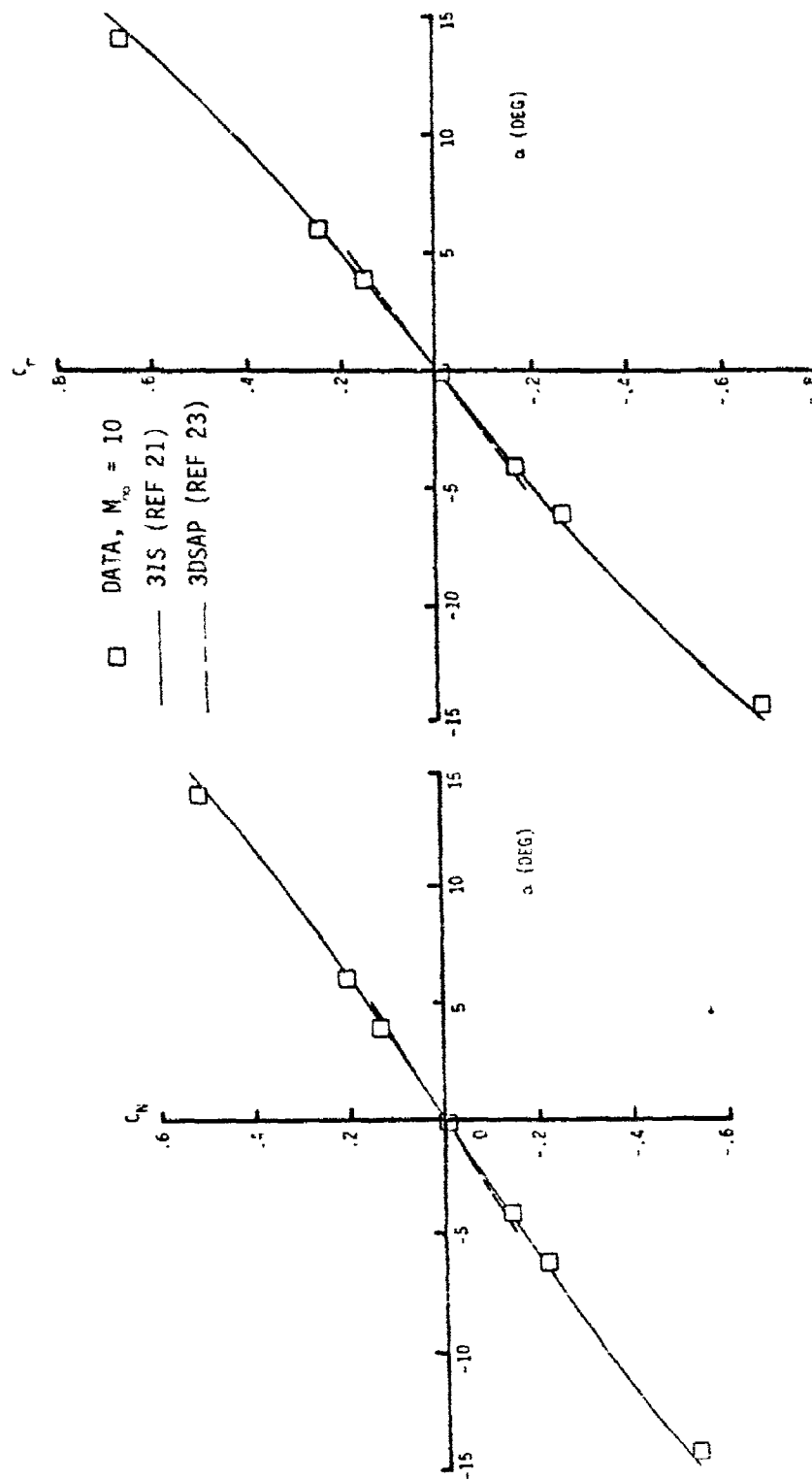


FIGURE 48. FORCE AND MOMENT COEFFICIENTS FOR THE 0.5"R BLUNTED 7° CONE

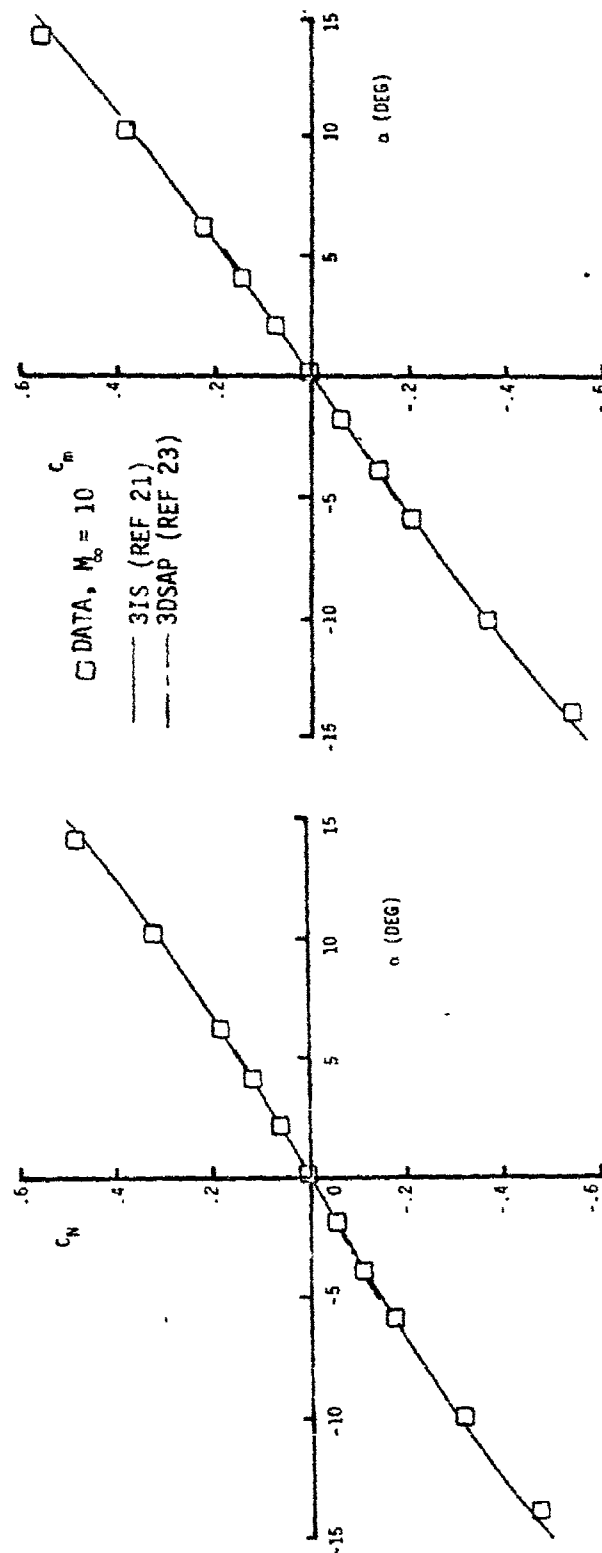


FIGURE 49. FORCE AND MOMENT COEFFICIENTS FOR THE 0.5"R BLUNTED 14°/7° BICONE

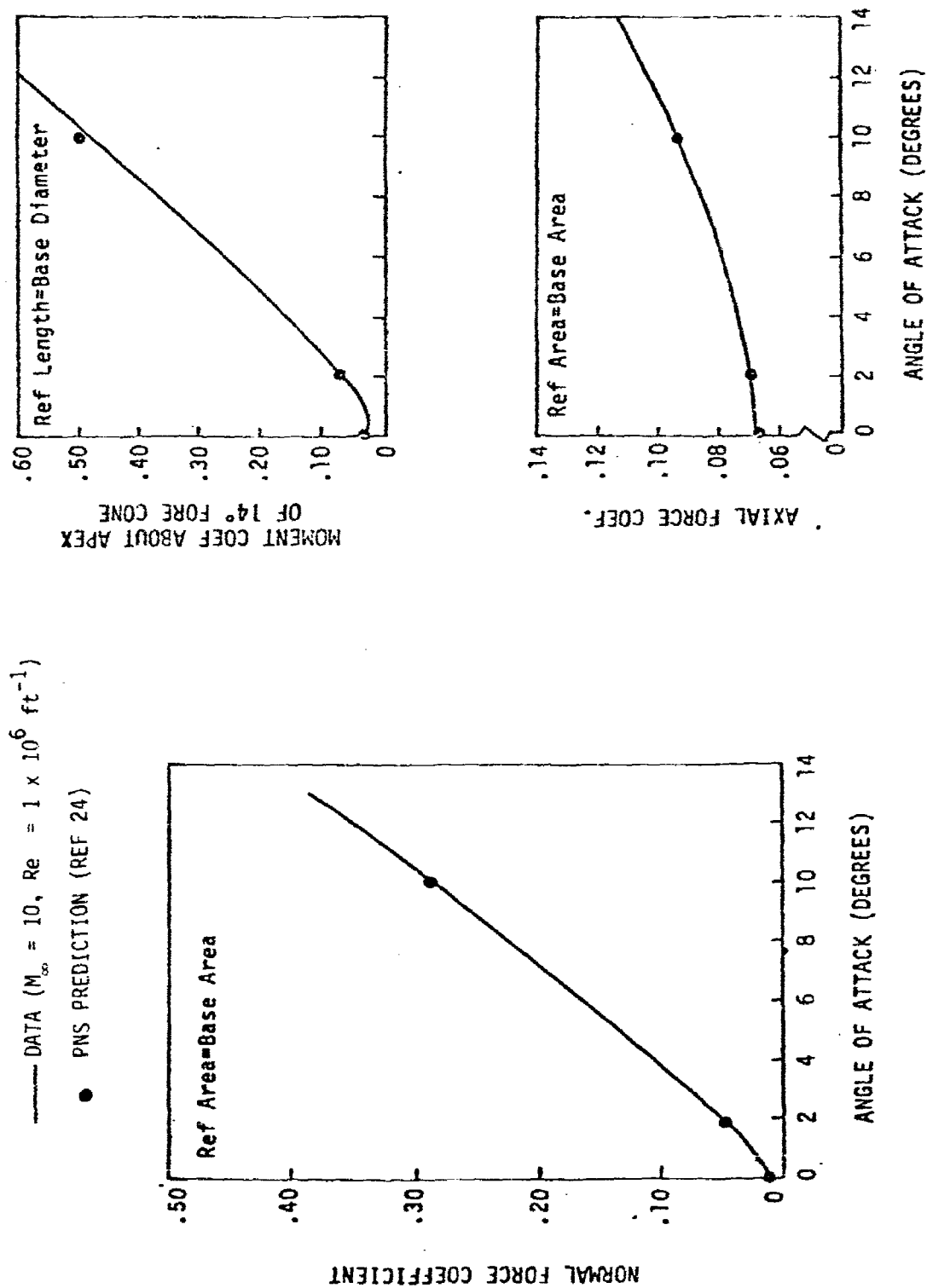


FIGURE 50. FORCE AND MOMENT COEFFICIENT COMPARISONS FOR THE BLUNTED $14^\circ/7^\circ$ BICONE WITH WINDWARD CUT

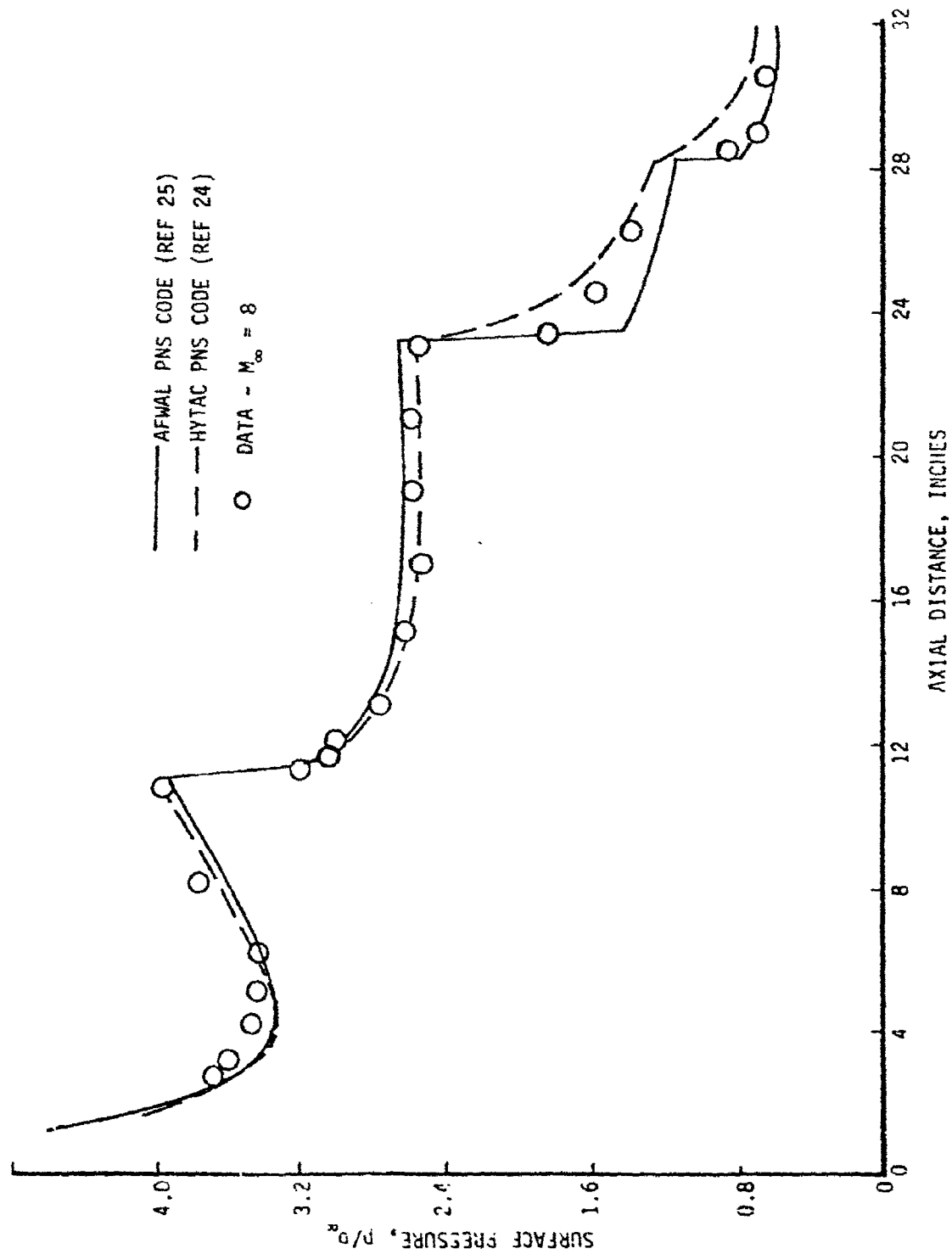


FIGURE 51. LONGITUDINAL PRESSURE DISTRIBUTION ON THE BLUNTED $10.5^\circ/7^\circ$ BICONE AT $\alpha = 0^\circ$

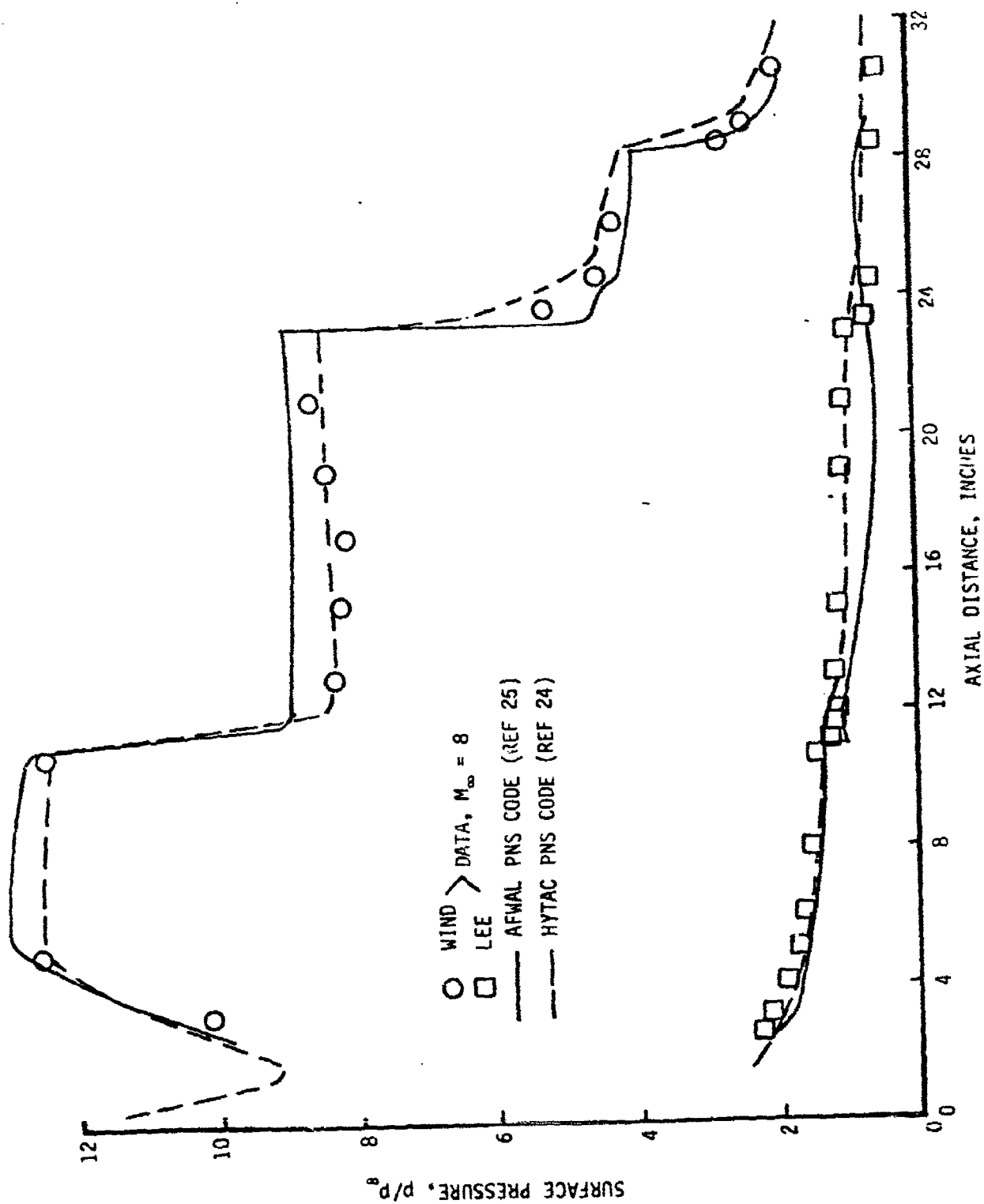


FIGURE 52. LONGITUDINAL PRESSURE DISTRIBUTION ON THE BLUNTED $10.5^\circ/7^\circ$ BICONE AT $\alpha = 10^\circ$

that the complementary profile data are useful in providing another diagnostic for establishing the time cause of the numerical difficulty. At $\alpha = 10^\circ$ (Figure 52), one notes that the HYTAC code agrees well with the data on the conic surface where as the AFWAL code tends to overpredict the aft cone pressure on the windward side and underpredict on the leeward side. Fair agreement in the slice region is evident. Subsequent to these comparisons being made, improvements to the AFWAL code were made (in terms step size determination and numerical damping) and although not shown here, better agreement was achieved at $\alpha = 10^\circ$.

In the test series defined in Section 3.4, data were obtained on the $10.5^\circ/7^\circ$ bicone with the flap system installed. Data were taken at Mach 8 (turbulent flow) at $\alpha = 0^\circ$ with flap deflection angle, $\delta = -7^\circ$ (no flap) and for $\delta = 10^\circ$ and 20° , and at $\alpha = 10^\circ$ for $\delta = -7^\circ$ and $\delta = 10^\circ$. Shown in Figures 53 and 54 are comparisons of the AFWAL PNS code prediction (Reference 25) with the measured surface pressure data. At the time these predictions were made, difficulties were being encountered with the PNS code predictions associated with the marching step size. Shown in Figure 53 are predictions for two values of step size, DX . One notes that although better agreement is shown for $DX = 0.10$ than 0.05 , numerical instabilities are encountered for $\delta = 20^\circ$ case. Again the associated flow field survey data (shown in Section 6.2.4) are extremely useful in resolving this difficulty. At $\alpha = 10^\circ$, the numerical solutions did not have this sensitivity and one notes that relatively good agreement was achieved.

In addition to the surface pressure comparisons made with the PNS codes, data comparisons were also made with the 3D inviscid code of References 21, 22. Shown in Figures 55 and 56 are axial and peripheral surface pressure distribution comparisons of the inviscid code prediction with the Mach 8 data for the blunted ($0.5'' R_N$) $10.5^\circ/7^\circ$ bicone at $\alpha = 10^\circ$. The agreement of theory with data is excellent on the windward surface, however, agreement for $\phi > 90^\circ$ is rather poor (as one would expect from an inviscid technique). Since the pressure on the windward surface is more than an order of magnitude greater

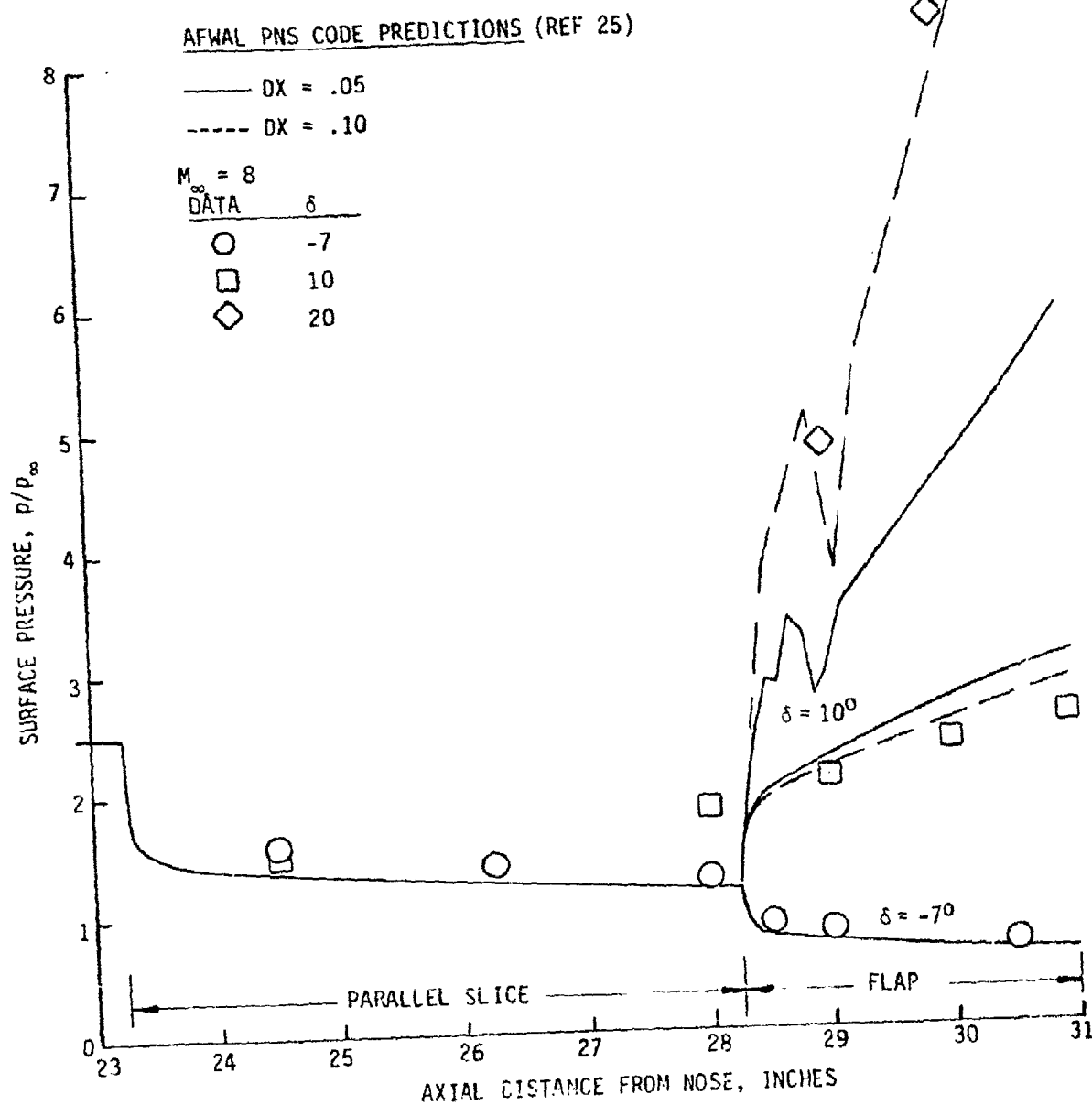


FIGURE 53. SURFACE PRESSURE DISTRIBUTION IN THE $10.5^\circ/7^\circ$
 BLUNTED BICONE CONTROL REGION - $\alpha = 0^\circ$

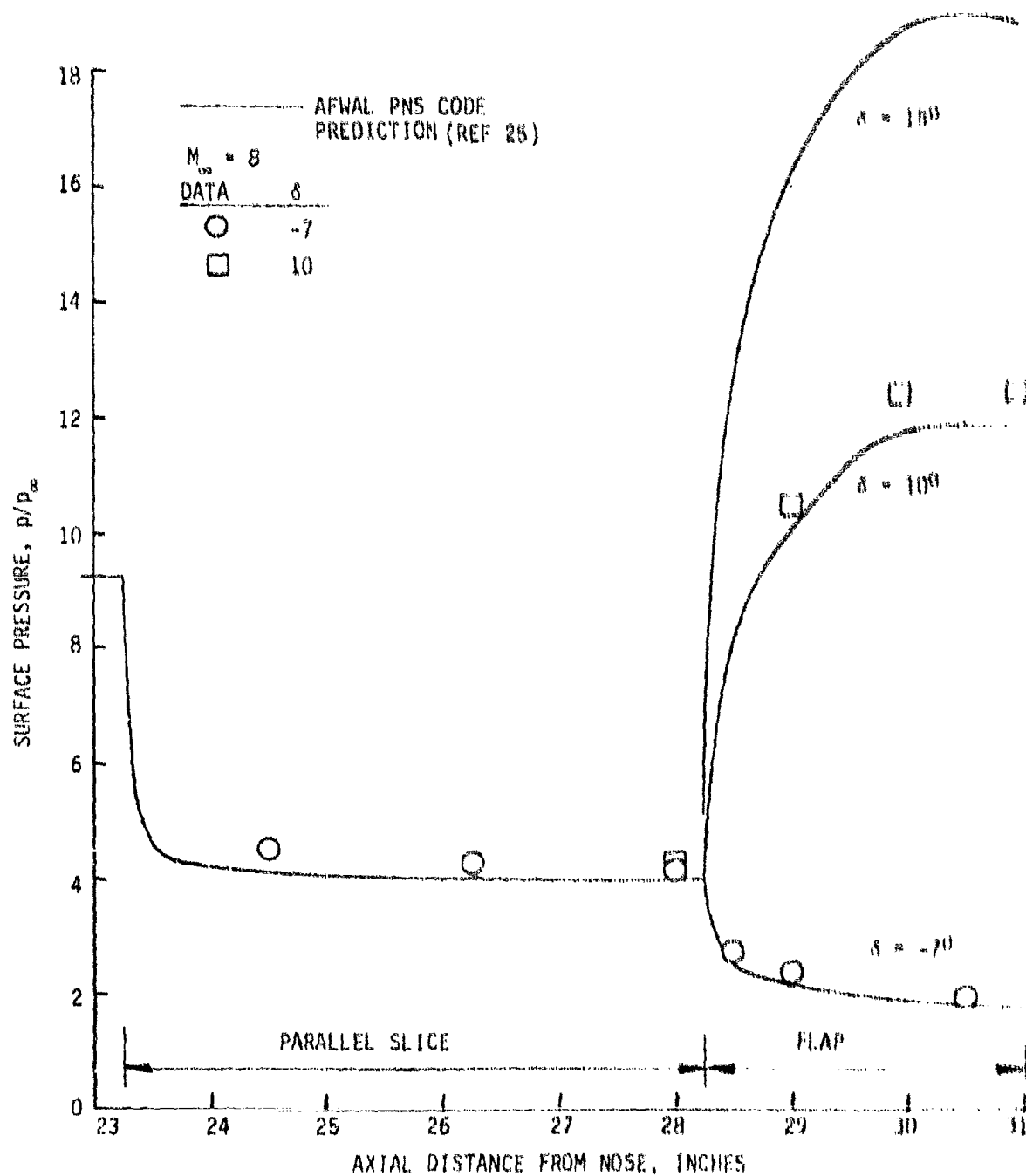


FIGURE 54. SURFACE PRESSURE DISTRIBUTION IN THE 10.5°/7°
BLUNTED BICONE CONTROL REGION - $\alpha = 10^\circ$

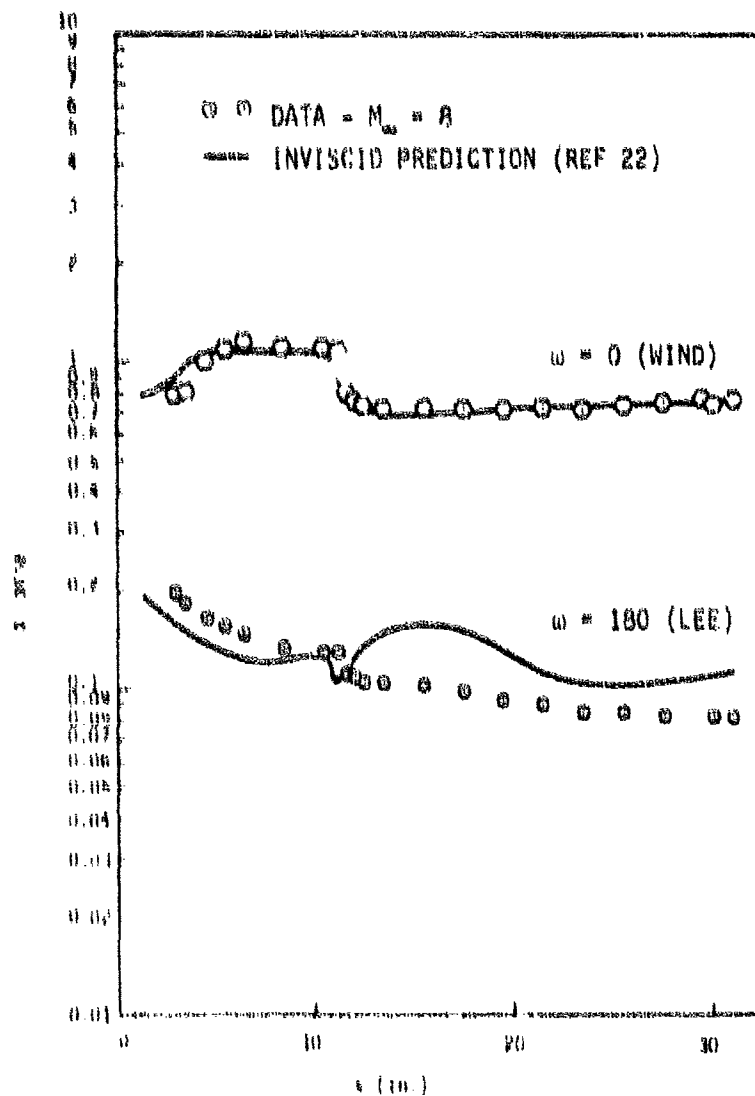


FIGURE 55. AXIAL PRESSURE DISTRIBUTION FOR THE BLUNTED 10.5°/7° BICONE AT $\alpha = 10^\circ$

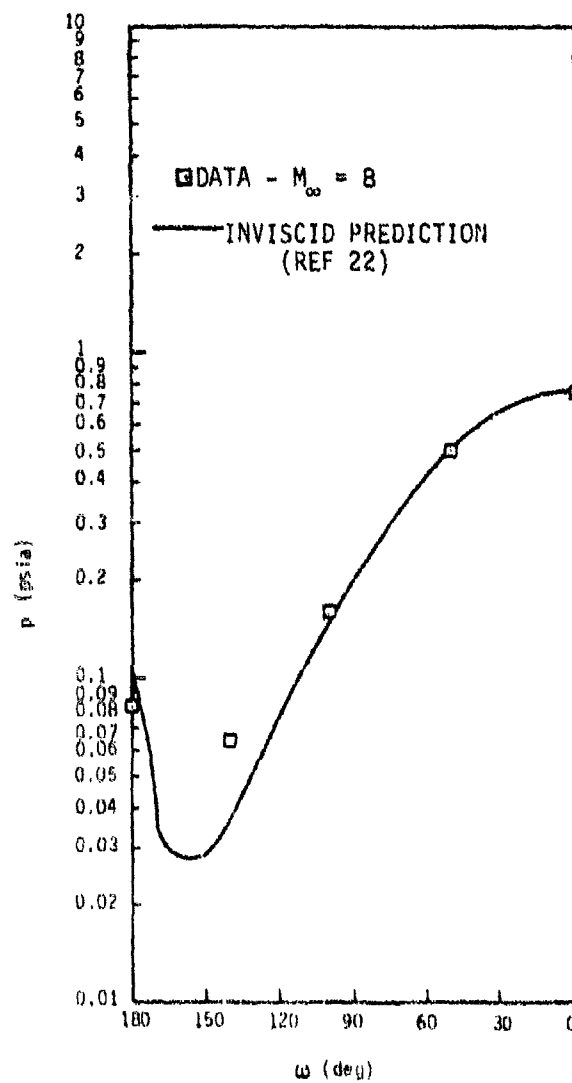


FIGURE 56. PERIPHERAL PRESSURE DISTRIBUTION FOR THE BLUNTED $10.5^\circ/7^\circ$ BICONE AT $\alpha = 10^\circ$

than the leeside pressure, one finds that the static loads are unaffected by this poor leeside match. A word of caution here is that as M_∞ decreases, the stability at α is more sensitive to the leeside pressure because it is of the same magnitude as the windward pressure. Consequently one must model the separated flow on the leeside for good stability agreement. In this flow domain, prediction techniques such as the aforementioned PNS codes would be required.

6.2.3 Surface Heat Transfer

Heat transfer data were obtained for each of the configurations considered in this investigation. Data were obtained for laminar and turbulent flow conditions where boundary layer trips were required to promote turbulence on the blunted configurations. As mentioned earlier (see Section 2.2.4), considerable effort was expended to evaluate the minimum trip size required to promote turbulence in the forecone region. The objective was to affect the flow in the boundary layer yet have minimal effect on the shock layer flow.

Many comparisons have been made of theory with the current data, a limited quantity of which will be presented here. The objective of the few comparisons that will be shown is to demonstrate the quality of the data and to demonstrate that the trips did indeed promote turbulence. These data in concert with shock layer survey comparisons will demonstrate that the trips have minimal effects on the shock layer flow.

A comparison of the measured axial distribution of laminar surface heat transfer for the 0.5" R blunted $14^\circ/7^\circ$ bicone at $\alpha = 10^\circ$ with the PNS prediction of Reference 24 is shown in Figure 57. An equivalent comparison for turbulent flow on the 0.5" R blunted $10.5^\circ/7^\circ$ bicone is shown in Figure 58. It was shown (e.g., Reference 24 and Figure 52) that the surface pressure predicted by the code is in excellent agreement with the data, and it is evident from Figure 57 that

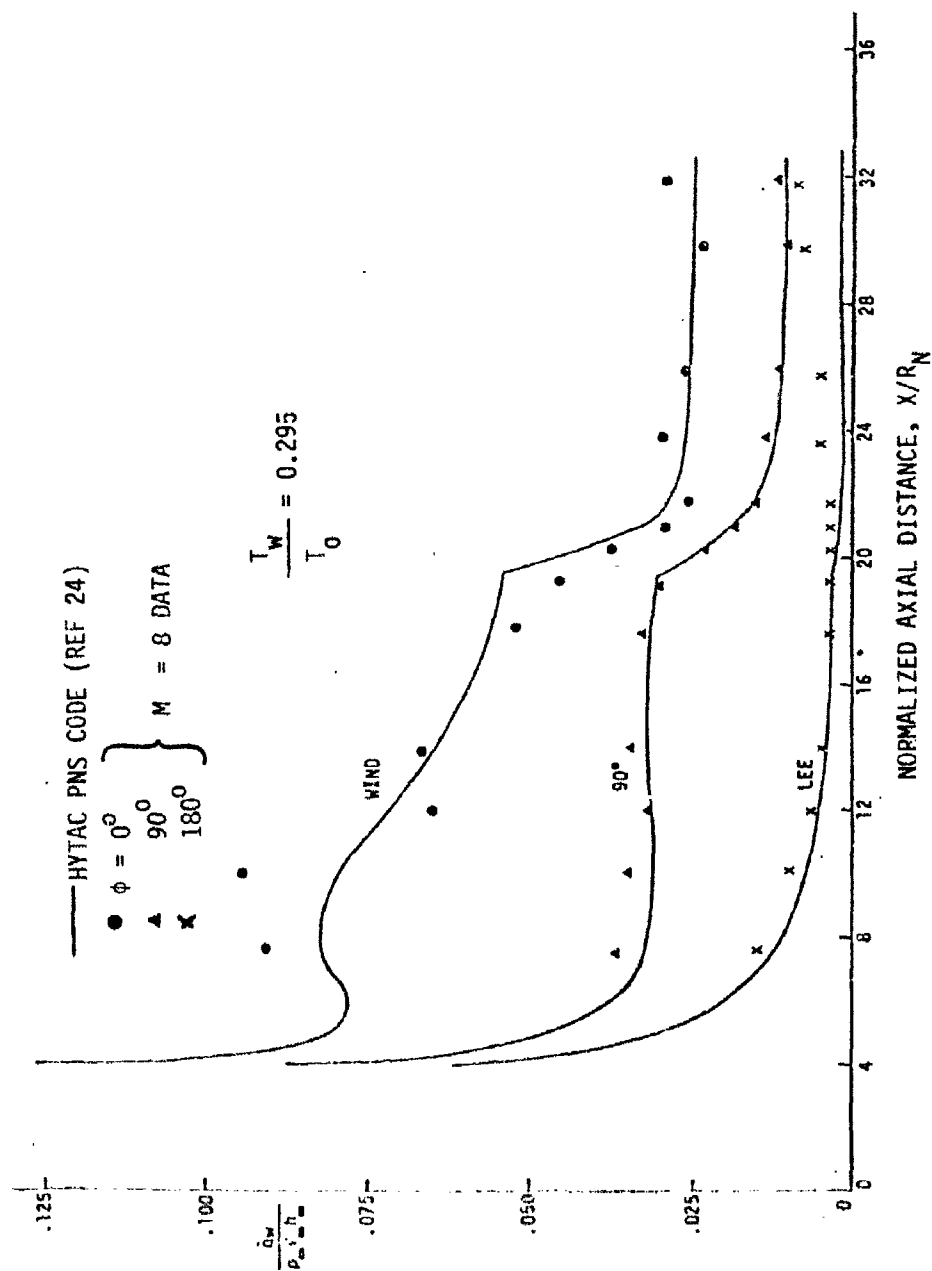


FIGURE 57. AXIAL DISTRIBUTION OF THE LAMINAR HEAT TRANSFER RESULTS
FOR THE BLUNTED $14^\circ/7^\circ$ BICONE AT $\alpha = 10^\circ$

$M_\infty = 8$ HYTAC PNS CODE (REF 24)

$\phi = 0^\circ$ --- Eddy Model

$\phi = 180^\circ$ — 1-Equation Model

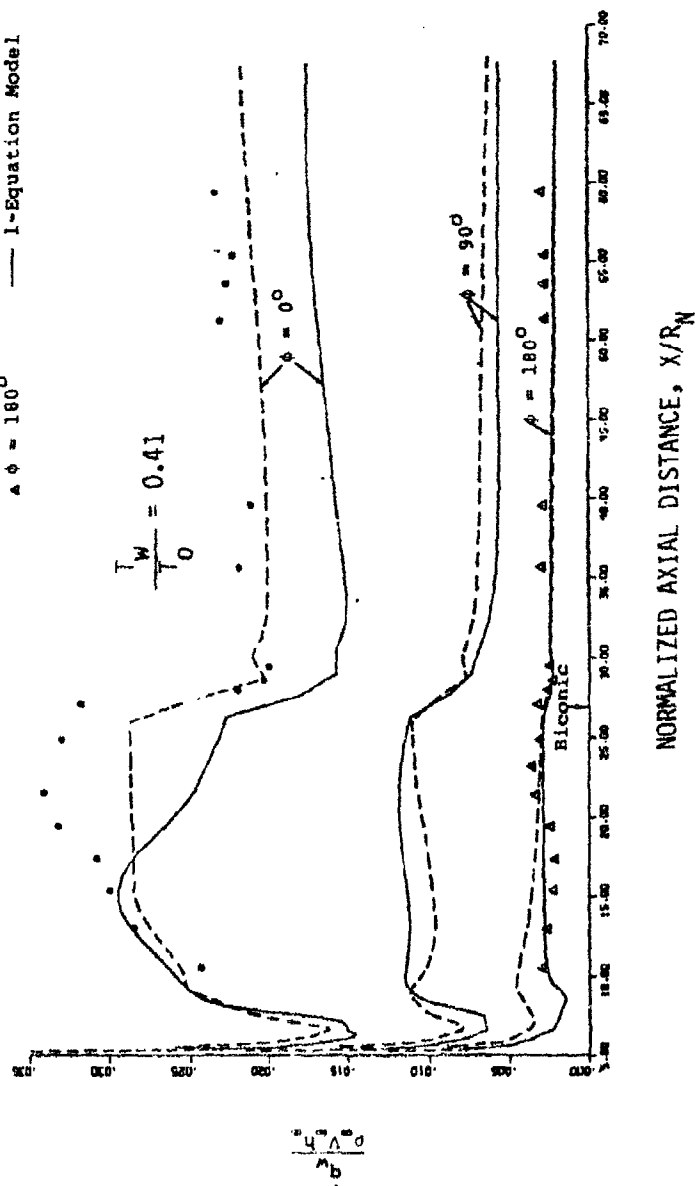


FIGURE 58. AXIAL DISTRIBUTION OF THE TURBULENT HEAT TRANSFER ON THE BLUNTED $10.5^\circ/7^\circ$ BICONE AT $\alpha = 10^\circ$

the laminar heating is in excellent agreement with the data. In the turbulent flow case, the agreement is considered poor. Shown in Figure 58 are turbulent flow predictions for two turbulence models; one which is a mean eddy viscosity model and the second which is a one equation turbulent energy model. The reader is referred to Reference 24 for the definitions of these models. It is clear that neither of these formulations provides good agreement with the data.

Under MAT program auspices the coupling of a 3D momentum integral boundary layer code (3DMEIT - Reference 26) was coupled to the inviscid code of Reference 21 and 22. Shown in Figure 59 is a comparison of the surface heat transfer predicted by 3DMEIT with the same data shown in Figure 58 (i.e., the 0.5" R blunted $10.5^\circ/7^\circ$ bicone). One notes that the agreement between theory and data is excellent, even on the leeside where the flow is separated. It is important to note that the heating prediction on the leeside follows on a one-to-one basis the variation of the surface pressures predicted by the inviscid code (see Figure 55). A comparison of the peripheral distribution of turbulent heating predicted by 3DMEIT with the Mach 8 turbulent data is shown in Figure 60. Agreement is considered quite good.

6.2.4 Shock Layer Surveys

Considerable wind tunnel test time was expended in acquiring the shock layer survey data on the conic and biconic configurations, including the slice and flap regions. Comparisons of theory with data were made with the inviscid codes of References 21, 22, and 23, and with the PNS codes of References 24 and 25. Shown in Figure 61 are comparisons of the predicted Pitot pressure profile with the Mach 6 data for the blunted $14^\circ/7^\circ$ bicone at $\alpha = 0^\circ$. One will note that the more exact flow field code (References 21, 22) agrees well with the data in the inviscid part of the shock layer (i.e., $Z_p > .2$ ") at both

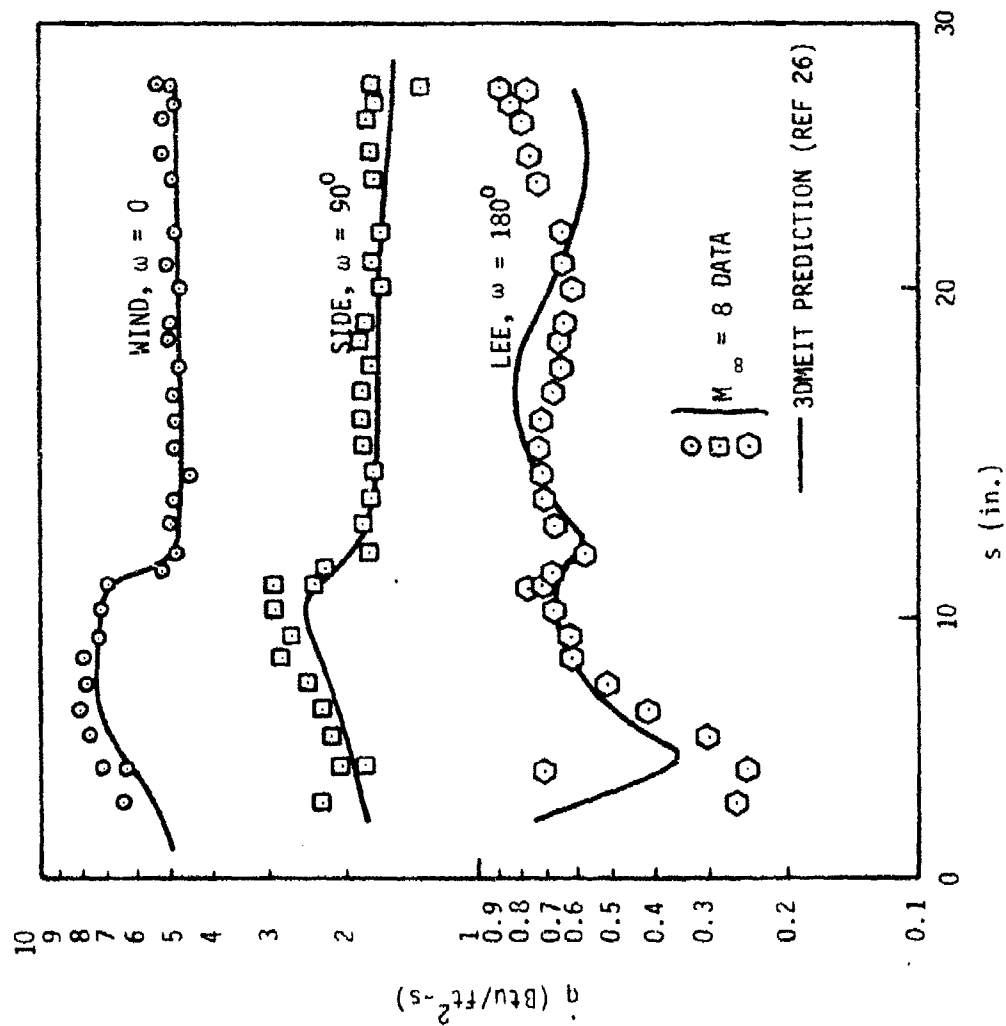


FIGURE 59. AXIAL DISTRIBUTION OF THE 3DMEIT PREDICTED TURBULENT HEAT TRANSFER FOR THE 10.5°/7° BLUNTED BICONE AT $\alpha = 10^\circ$.

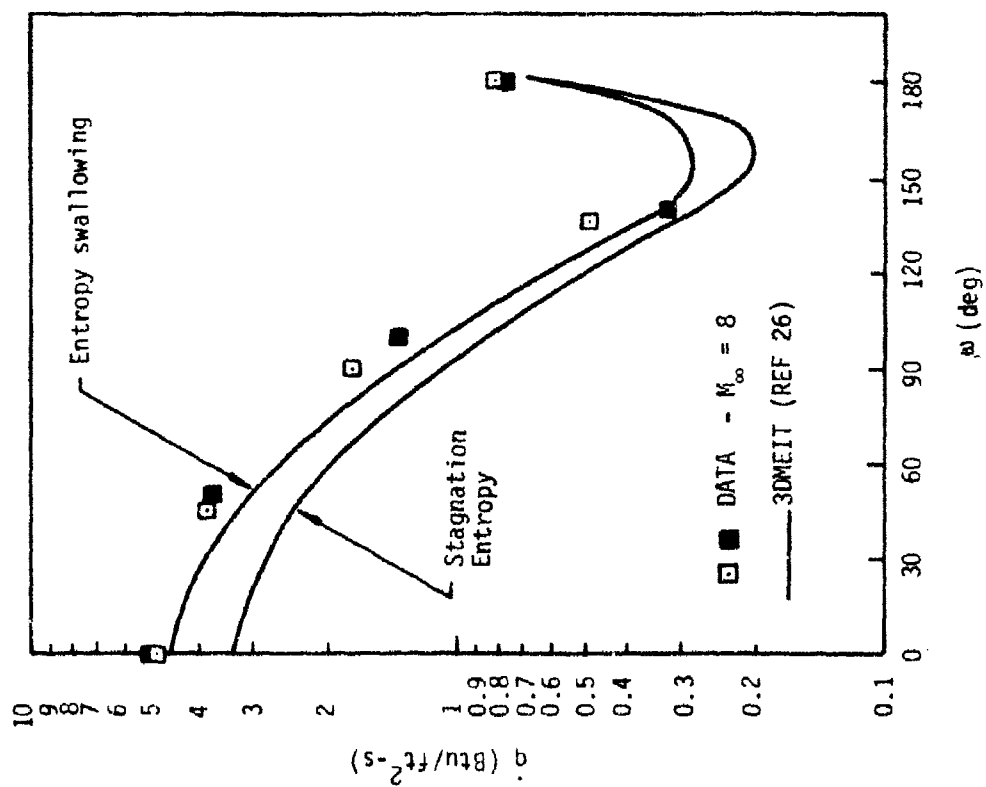


FIGURE 50. PERIPHERAL DISTRIBUTION OF THE 3DMEIT PREDICTED TURBULENT HEAT TRANSFER FOR THE 10.5°/7° BLUNTED BICONE AT $\alpha = 10^\circ$ ($s=30''$)

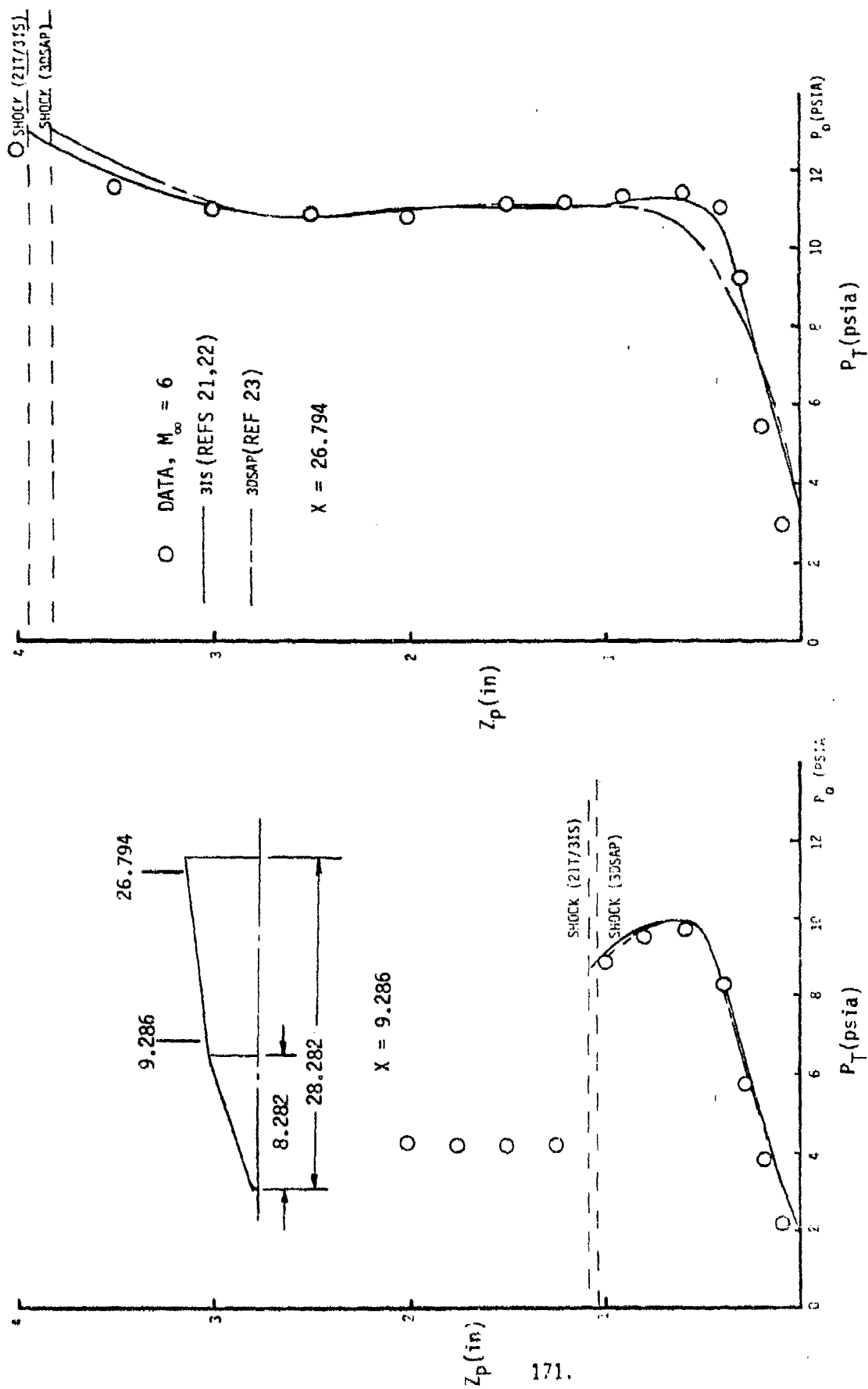


FIGURE 61. COMPARISON OF THE PITOT PRESSURE INVISCID PREDICTIONS WITH DATA FOR THE 14°/7° BLUNTED BICONE AT $\alpha = 0^\circ$

stations. The approximate method of Reference 23 provides good agreement at the forward station ($x = 9.286''$), which is nominally one inch downstream of the bicone juncture, however, underpredicts the pressure for $0.2 < Z_p < 1$. This was attributed to a grid resolution problem associated with the thick shock layer at this station.

Shown in Figures 62 through 64 are comparisons of the PNS code of Reference 25 with data for the blunted 7° cone obtained at Mach 8 at $\alpha = 10^\circ$. The agreement between theory and data is fair on the windward side, more so in the outer parts of the shock layer than near the wall. The thermal boundary layer thickness is approximately 20 percent of the total shock layer thickness at both stations. The leeside prediction shown in Figure 64 is not in good agreement with the data. The predictions indicate a thick viscous layer with a gradient structure markedly different from that in the windward plane. However, the gradients predicted are not nearly as large as those exhibited by the data. The utility of the data here is not only to point out the prediction deficiency but also to provide sufficient quantitative information to deduce why the prediction deficiency exists.

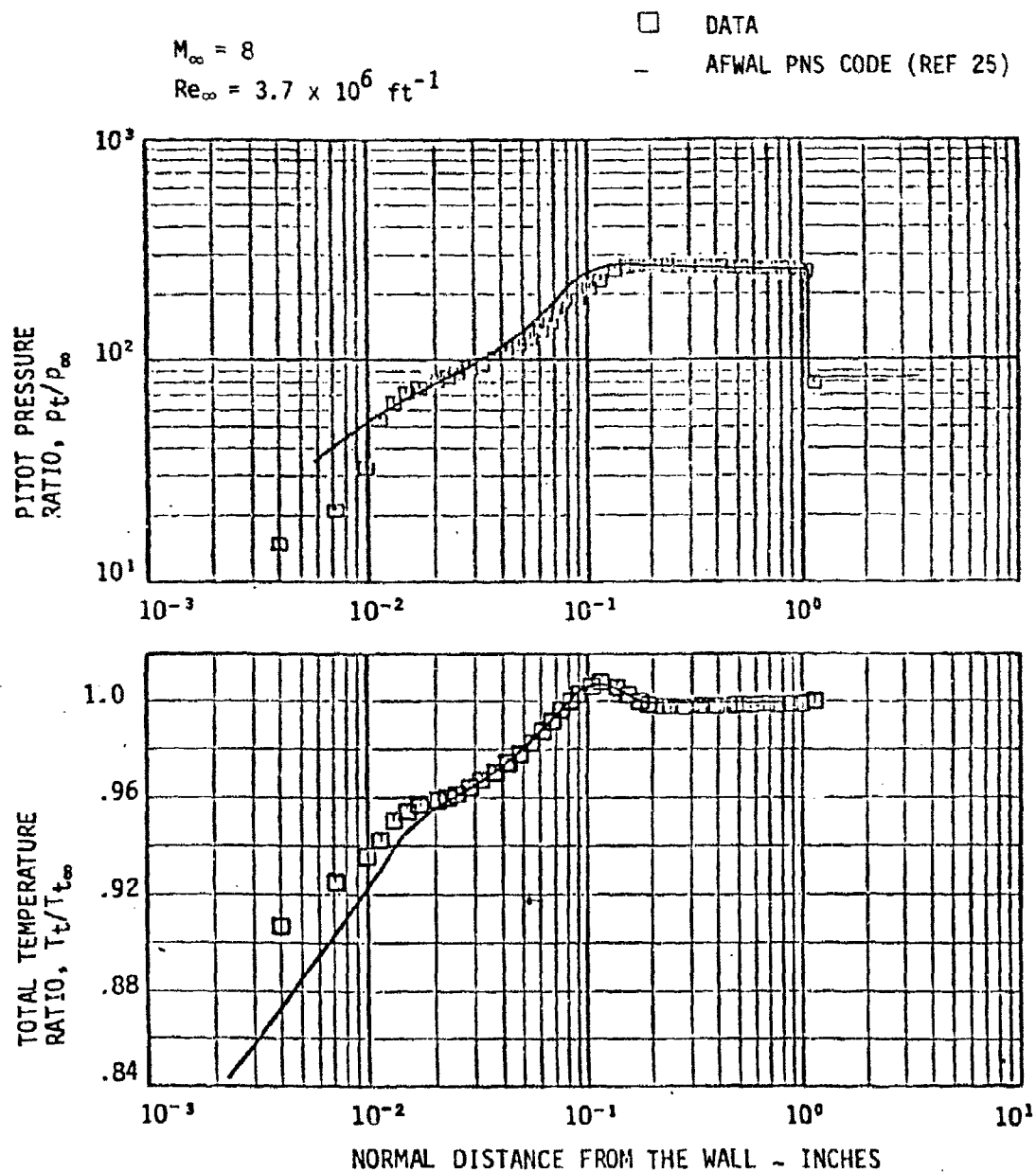


FIGURE 62, COMPARISON OF PREDICTED SHOCK LAYER PROFILES WITH WINDWARD RAY DATA FOR THE BLUNTED 7° CONE AT $\alpha = 10^\circ$ ($x = 24.4''$)

$M_\infty = 8$
 $Re_\infty = 3.7 \times 10^6 \text{ ft}^{-1}$

□ DATA
 — AFWAL PNS CODE (REF 25)

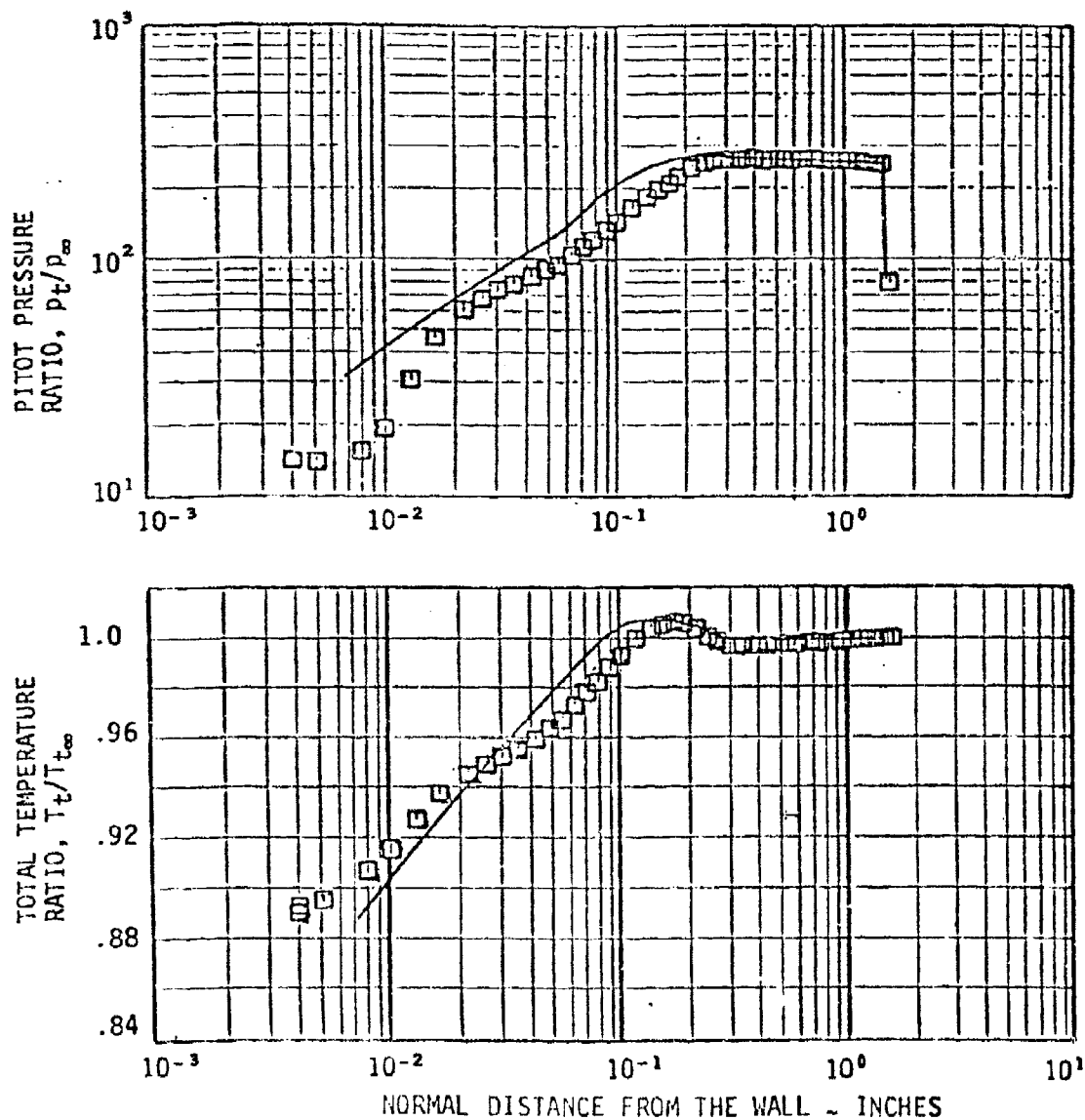


FIGURE 63. COMPARISON OF PREDICTED SHOCK LAYER PROFILES WITH
 WINDWARD RAY DATA FOR THE BLUNTED 7° CONE AT
 AT $\alpha = 10^\circ$ ($x = 34.4''$)

$M_\infty = 8$
 $Re_\infty = 3.7 \times 10^6 \text{ ft}^{-1}$

□ DATA
 — AFWAL PNS CODE (REF 25)

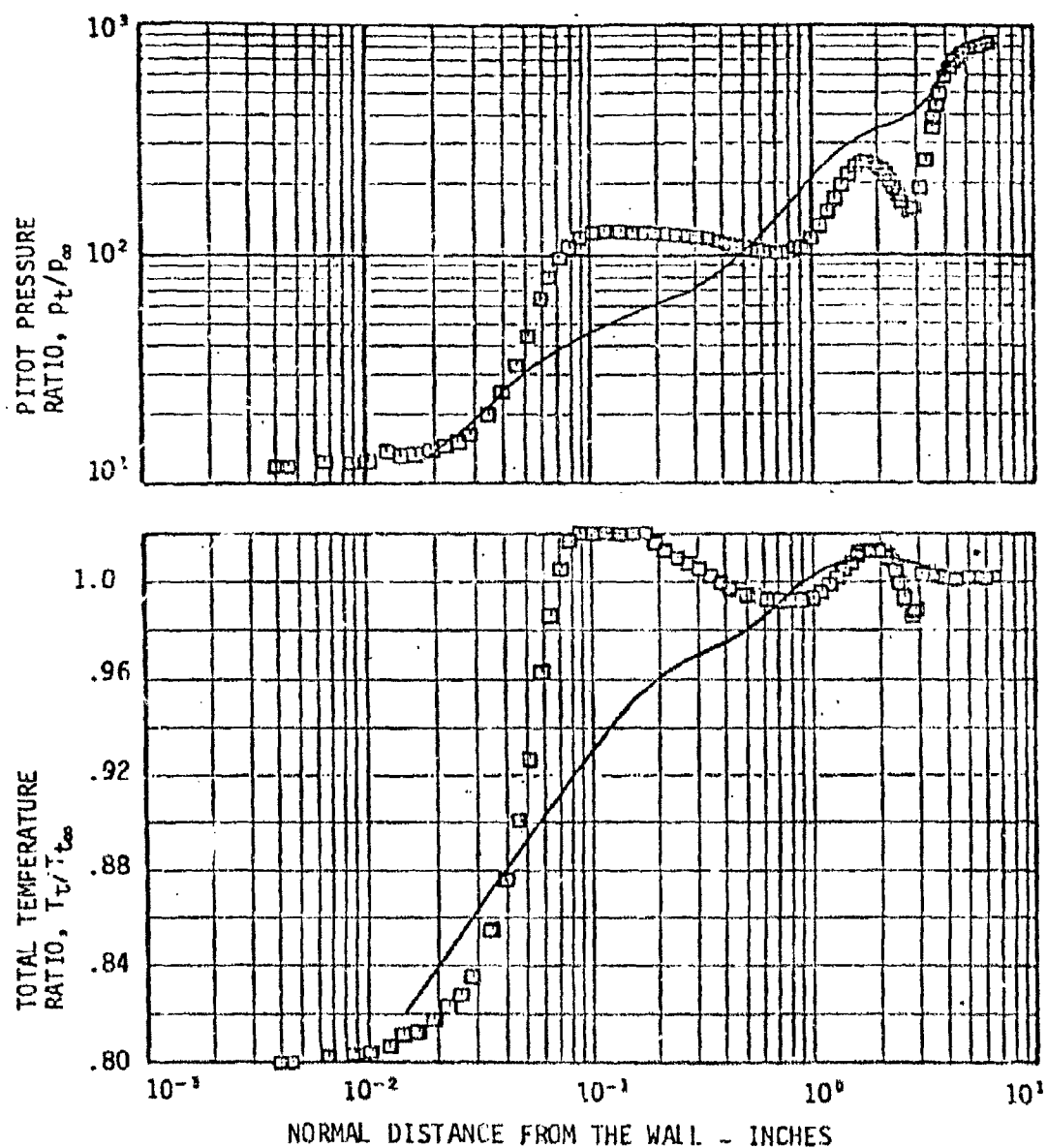


FIGURE 64. COMPARISON OF PREDICTED SHOCK LAYER PROFILES WITH
 LEeward RAY DATA FOR THE BLUNTED 7° CONE AT
 $\alpha = 10^\circ$ ($x = 34.4''$)

REFERENCES

1. Test Facilities Handbook (Eleventh Edition), Arnold Engineering Development Center, June 1979.
2. Hahn, J. S., "Static Force Tests of Conic and Biconic Bodies at Mach Number 10, Phase V," AEDC-TSR-78-V40, November 1978.
3. Lanhan, D. L., "Static Force Test of the Maneuvering Aerothermal Technology (MAT) Configurations at Mach Number 8," AEDC-TSR-81-V26, August 1981.
4. Hube, F. K., "Heat-Transfer, Surface-Pressure, and Boundary-Layer Surveys on Conic and Biconic Bodies with Boundary-Layer Trips at Mach Number 6 - Phase I," AEDC-TSR-78-V24, August 1978.
5. Hube, F. K., "Heat-Transfer, Surface-Pressure, and Boundary-Layer Surveys on Conic and Biconic Bodies with Boundary-Layer Trips at Mach Number 6 - Phase II," AEDC-TSR-78-V25, August 1978.
6. Carver, D. B., "Heat-Transfer, Surface Pressure and Flow-Field Surveys on Conic and Biconic Models with Boundary Layer Trips at Mach Number 8 - Phases IV & VI," AEDC-TSR-80-V14, March 1980.
7. Carver, D. B., "Heat-Transfer, Surface Pressure, and Flow-Field Survey Tests on a Blunt Biconic Model at Mach Number 10 - Phase V," AEDC-TSR-79-V36, June 1979.
8. Coulter, S. M. and Carver, D. B., "Heat Transfer, Surface Pressure and Flow-Field Surveys on the AEDC Biconic with Slits and Flaps at Mach 8 - MAT Phase I," AEDC-TSR-81-V24, July 1981.
9. Trimmer, L. L., Matthews, R. K., and Buchanan, T. D., "Measurement of Aerodynamic Heat Rates at the AEDC von Karman Facility," International Congress on Instrumentation in Aerospace Simulation Facilities IEEE Publication CHO 784-9 AES, September 1973.
10. Allen, J. M., "Reevaluation of Compressible-Flow Preston Tube Calibrations," NASA TM X-3488, February 1977.
11. Allen, J. M., "Evaluation of Compressible Preston Tube Calibrations," National Aeronautics and Space Administration Report NASA TN D-7190, May 1973.
12. Brown, D. L., "Predicting Equilibrium Pressures from Transient Pressure Data," Aerospace Research Laboratories, ARL 65-7, January 1965.

13. Preston, J. H., "The Determination of Turbulent Skin Friction by Means of Pitot Tubes," Journal of the Royal Aeronautical Society, Vol. 58, No. 518, February 1954, pp. 109-121.
14. Bertelrud, A., "Pipe Flow Calibration of Preston Tubes of Different Diameters and Relative Lengths Including Recommendations on Data Presentation for Best Accuracy," The Aeronautical Research Institute of Sweden, IFA Report 125, 1974.
15. Hopkins, E. J. and Keener, E. R., "Study of Surface Pitots for Measuring Turbulent Skin Friction at Supersonic Mach Numbers-Adiabatic wall," National Aeronautics and Space Administration Report NASA TN-D-1478, July 1966.
16. Varner, M. O., "Corrections to Single-Shielded Total Temperature Probes in Subsonic, Supersonic, and Hypersonic Flow," AEDC-TR-76-140, November 1976.
17. Varner, M. O., "A Compilation and Analysis of Hypersonic Turbulent Flow-Field Data for Sharp and Blunt Conic or Biconic Bodies at Zero Angle of Attack," AEDC-TR-80-14, August 1980.
18. Hirschberg, A. and Van Marrewinkel, J. E., "A Correlation of Recovery Temperature Data for Cylinders in Compressible Flow at High Reynolds Number," International Journal of Heat and Mass Transfer, Vol. 20, No. 6, June 1977, pp. 689-694.
19. Harris, L. B., "A Two-Layer Solution of the Hypersonic Viscous Flow on a Cone at Angle-of-Attack," Ph.D. dissertation - University of Pennsylvania, 1981.
20. Levine, J. N., "Finite-Difference Solution of the Laminar Boundary Layer Equations Including the Effects of Transverse Curvature, Vorticity, and Displacement Thickness," AIJ 605D149, December 1966.
21. Byrles, C. and Harris, L. B., "A Three-Dimensional Flow Field Computer Program for Maneuvering and Ballistic Reentry Vehicles," Presented at the Tenth Navy Symposium on Aeroballistics, July 1974.
22. Haywell, J., Grant, D., Roseworth, L., "Computational technique for three dimensional inviscid flow fields about Reentry Vehicles," NAMD-TR-78-4, April 1978.
23. Hall, P. W., "The Three Dimensional Shock and Pressure (3DAP) Approximate Flow Field technique," Vol. 1, Engineering Analysis, Vol. 11, User's Manual, NAMD-TR-77-146, May 1977.
24. Halliwell, W. S., et al., "HYIAL Phase II Report: Turbulent Flow over Arbitrary Geometries at High Angle of Attack," Aerob Assoc Rep 78-20-19-10, July, 1980.

- 25 Schiff, L.B. and Stager, J.L., "Numerical Simulation of Steady Supersonic Viscous Flow," AIAA Journal, Vol. 18, No. 12, December 1980, pp. 1421-1430.
26. Harris, T., Hall, D., Wolf, C., Murray, A., "A Method for Coupled Three Dimensional Inviscid (3IS) and Integral Boundary Layer (3DMEIT) Calculations," BMD-TR- (to be published), February 1982.

APPENDIX A

DATA REDUCTION AND REPRESENTATIVE TABULAR AND GRAPHICAL PRESENTATIONS

The material contained in this appendix was excerpted from several AEDC TSRs and is included here for completeness.

A.1 Test Conditions

Freestream test conditions were evaluated using the assumption of a real gas isentropic expansion from the stilling chamber to the test section. The test conditions printed at the top of each page of tabulated data are mean values and were computed using the average stilling chamber pressure and temperature. However, the values of freestream test conditions used to normalize the data were computed from stilling chamber conditions which were recorded at the same time as the data.

A.2 Surface Heat Transfer Measurements

The high sensitivity Gardon gages used to obtain the heat transfer data are direct reading heat flux transducers whose voltage outputs may be converted to heating rate by means of a laboratory-obtained scale factor. The heat transfer coefficients were calculated using the measured heat flux (q_{wall}), the measured gage surface temperature (T_{gauge}), and the tunnel stilling chamber temperature (T_0). The heat transfer coefficients were computed using:

$$h(T_0) = \frac{q_{wall}}{T_{gauge} - T_0} \quad \text{BTU/SEC.SQ.FT.} \quad (A.1)$$

The data were reduced from the recorded readings obtained at approximately 1/6 seconds after the model reached the tunnel centerline.

Stanton number values were computed as follows:

$$ST(INF) = \frac{H(TO)}{(RHOTNF)(VTNF)} \cdot \frac{TO-TGAGE}{ITO-TGAGE} \quad (A-2)$$

where ITO and TGAGE are air enthalpy values based on TO and TGAGE, respectively.

An example of a heat transfer data tabulation is shown in Table A-1 (3 pages). The complementary graphical display of the axial heat transfer distribution for this same case is shown in Figure A-1. This corresponds to a leeside distribution at $\alpha = 100^\circ$. A definition of the nomenclature used in the Tables is defined in the Tabulated Data Key in the front of this report.

A.1 Model Surface Pressure

The pressure transducers were all calibrated with a known pressure differential and their readings are recorded. A zero pressure differential is applied across each transducer and the zero readings are recorded. From these data linear scale factors for each transducer (or each range) are calculated. Model surface pressures are calculated from differential pressure readings using the calibrated scale factors, plus a reference pressure (near vacuum) which is measured with an absolute pressure transducer.

An example of a surface pressure tabulation is shown in Table A-2 (4 pages). The corresponding graphical displays of data are shown in Figures A-2, A-3, and A-4. Although not labeled in the A111 data book, Figures A-2 (Page 1) and A-3 (Page 2) correspond to the axial displays of P_{ws}/P for the windward ($\alpha = 0^\circ$) and leeward ($\alpha = 180^\circ$) sides, respectively. Figure A-4 presents meridional distributions of P_{ws}/P at four axial stations. The stations which are displayed are indicated in the A111 data book but can be reconstructed from the data tabulation. These stations are as indicated in Figure A-1.

SECRET

REF ID: A66541

THE

100

THE

[illegible]

1	2	3	4	5	6	7	8	9	10	11	12	13	14	15	16	17	18	19	20	21	22	23	24	25	26	27	28	29	30	31	32	33	34	35	36	37	38	39	40	41	42	43	44	45	46	47	48	49	50	51	52	53	54	55	56	57	58	59	60	61	62	63	64	65	66	67	68	69	70	71	72	73	74	75	76	77	78	79	80	81	82	83	84	85	86	87	88	89	90	91	92	93	94	95	96	97	98	99	100
1	2	3	4	5	6	7	8	9	10	11	12	13	14	15	16	17	18	19	20	21	22	23	24	25	26	27	28	29	30	31	32	33	34	35	36	37	38	39	40	41	42	43	44	45	46	47	48	49	50	51	52	53	54	55	56	57	58	59	60	61	62	63	64	65	66	67	68	69	70	71	72	73	74	75	76	77	78	79	80	81	82	83	84	85	86	87	88	89	90	91	92	93	94	95	96	97	98	99	100

[illegible]

1. The first step in the process is to identify the problem or issue that needs to be addressed. This involves gathering information and understanding the context of the problem.

THE
2.44
SEC.

[illegible]

[illegible][illegible]

100

THE

[illegible]

FLAP
LINE

THE UNIVERSITY OF CHICAGO

THE UNIVERSITY OF CHICAGO

[illegible]

PT/SEC	2-26-83
PZIA	2-26-83
DESP	9-26-83
PZIA	9-26-83
LEAD/PF13	2-26-83
Y	2-26-83

ALL INFORMATION CONTAINED
HEREIN IS UNCLASSIFIED
DATE 06-13-2001 BY 60322
UC, 1363

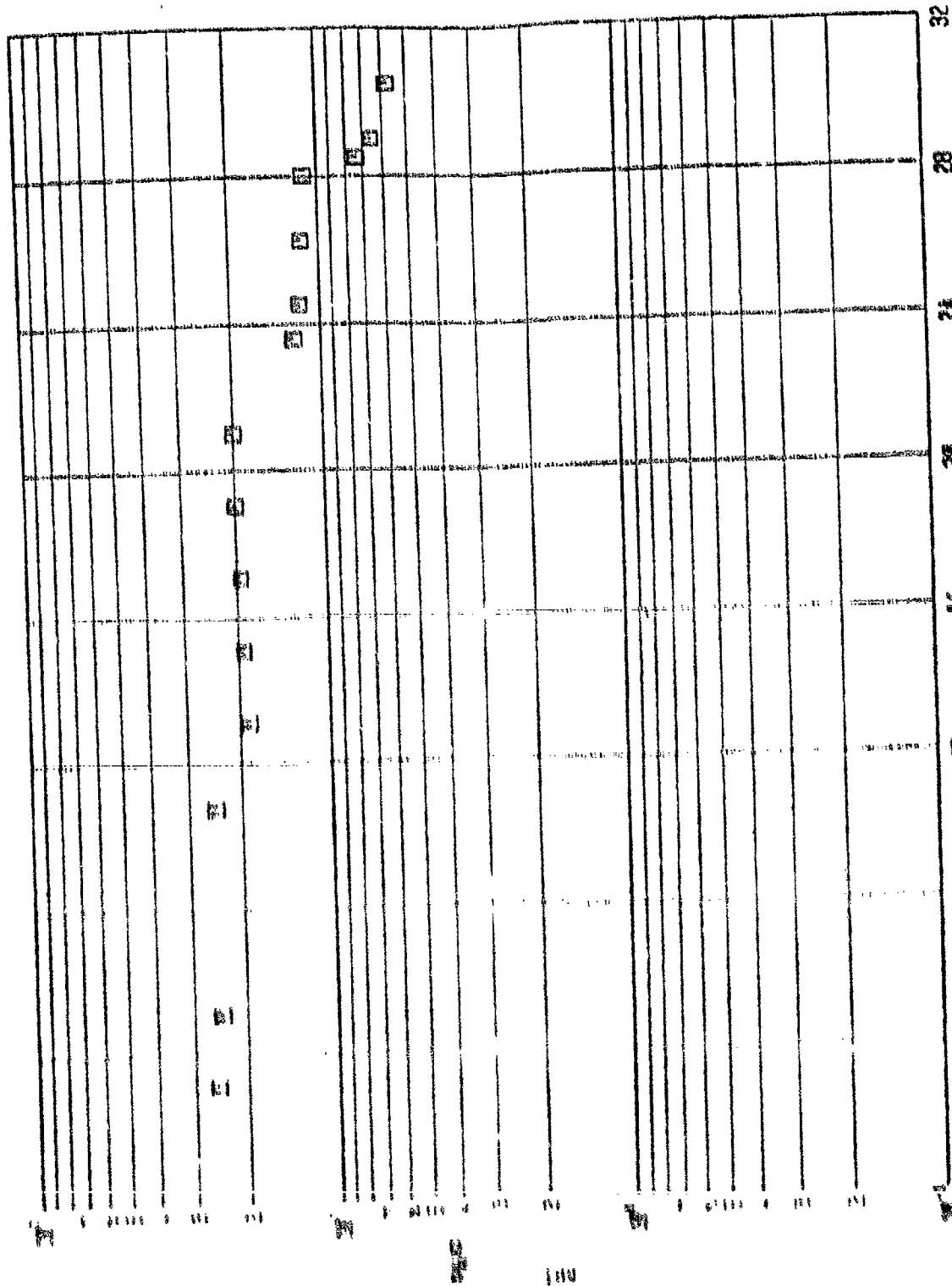
SECRET

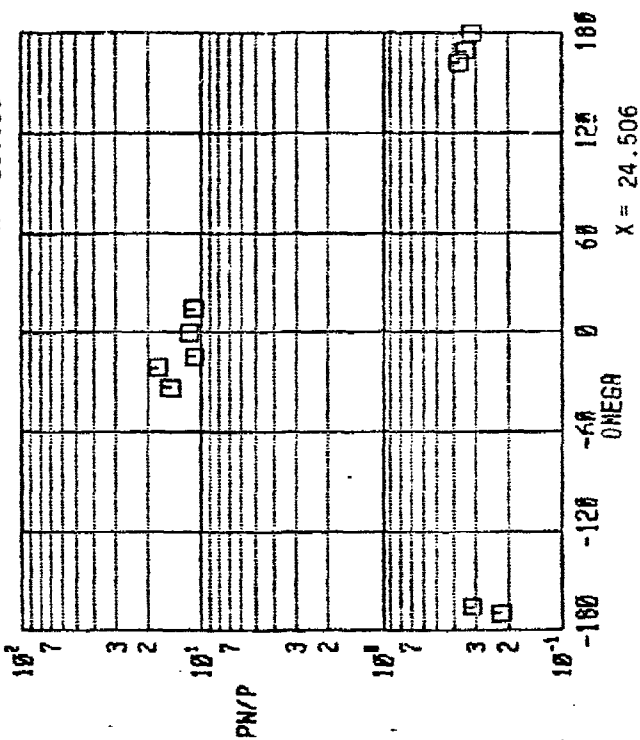
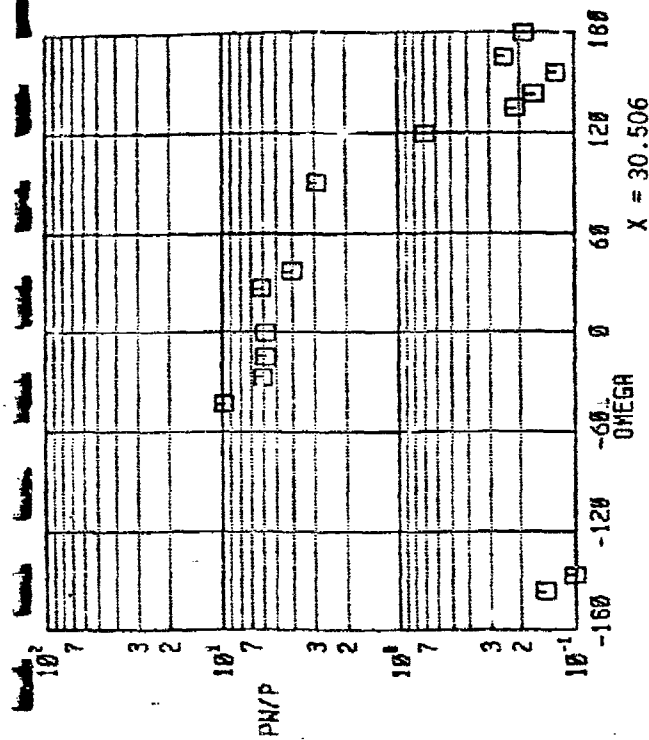
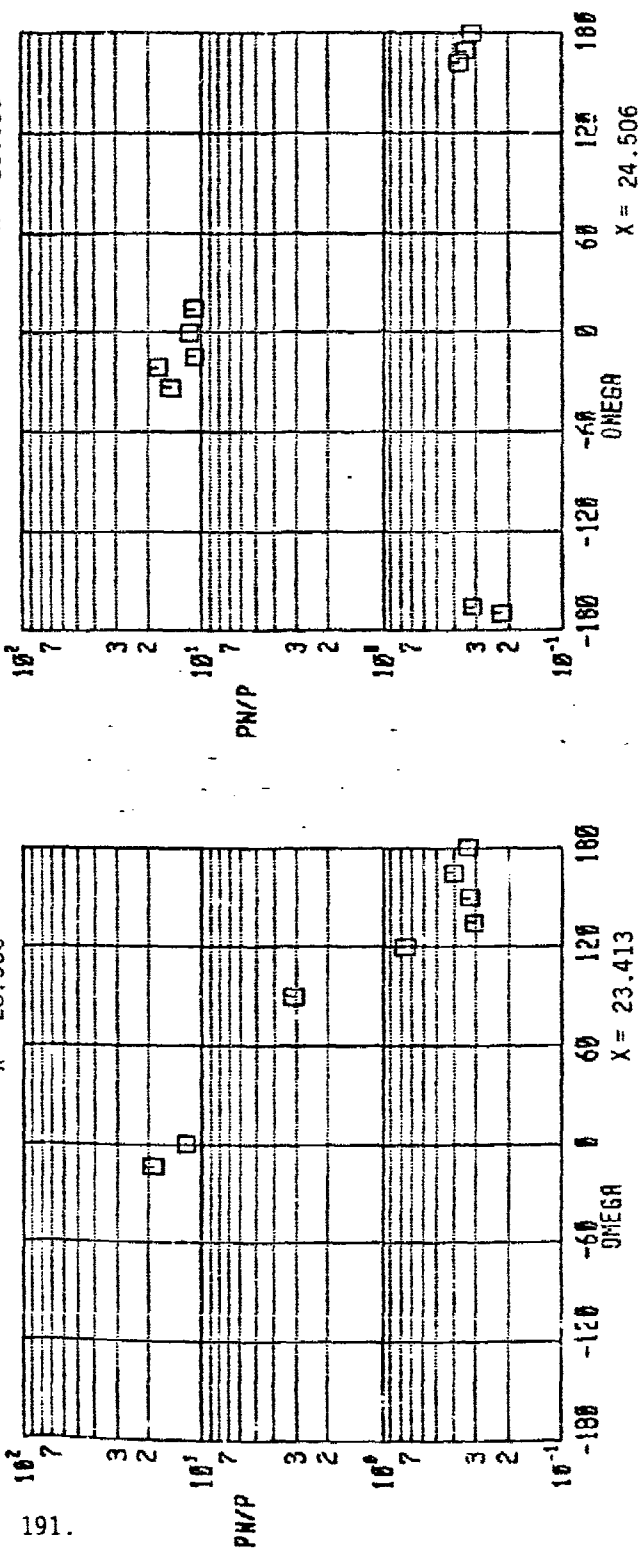
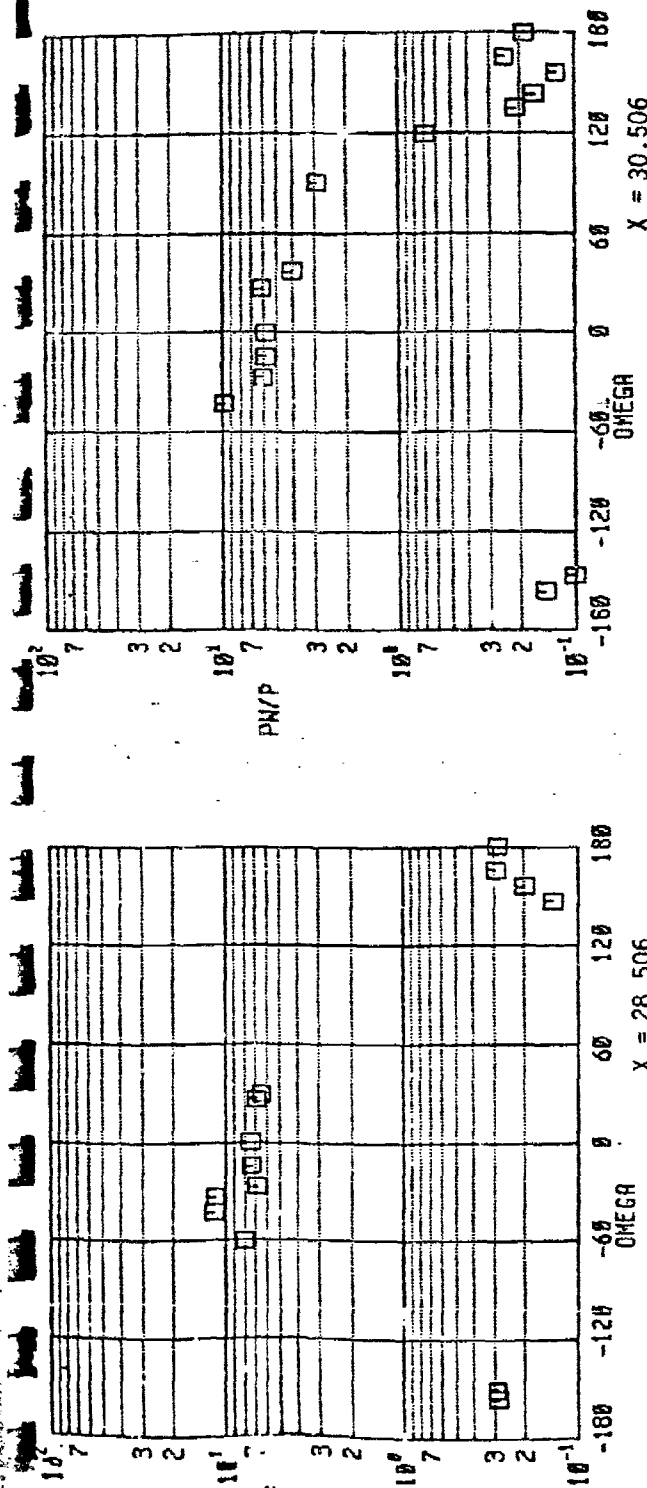
100

[illegible]

[Illegible text]

1927	1928	1929	1930	1931	1932	1933	1934	1935	1936	1937	1938	1939	1940	1941	1942	1943	1944	1945	1946	1947	1948	1949	1950	1951	1952	1953	1954	1955	1956	1957	1958	1959	1960	1961	1962	1963	1964	1965	1966	1967	1968	1969	1970	1971	1972	1973	1974	1975	1976	1977	1978	1979	1980	1981	1982	1983	1984	1985	1986	1987	1988	1989	1990	1991	1992	1993	1994	1995	1996	1997	1998	1999	2000	2001	2002	2003	2004	2005	2006	2007	2008	2009	2010	2011	2012	2013	2014	2015	2016	2017	2018	2019	2020	2021	2022	2023	2024	2025	2026	2027	2028	2029	2030	2031	2032	2033	2034	2035	2036	2037	2038	2039	2040	2041	2042	2043	2044	2045	2046	2047	2048	2049	2050	2051	2052	2053	2054	2055	2056	2057	2058	2059	2060	2061	2062	2063	2064	2065	2066	2067	2068	2069	2070	2071	2072	2073	2074	2075	2076	2077	2078	2079	2080	2081	2082	2083	2084	2085	2086	2087	2088	2089	2090	2091	2092	2093	2094	2095	2096	2097	2098	2099	2100	2101	2102	2103	2104	2105	2106	2107	2108	2109	2110	2111	2112	2113	2114	2115	2116	2117	2118	2119	2120	2121	2122	2123	2124	2125	2126	2127	2128	2129	2130	2131	2132	2133	2134	2135	2136	2137	2138	2139	2140	2141	2142	2143	2144	2145	2146	2147	2148	2149	2150	2151	2152	2153	2154	2155	2156	2157	2158	2159	2160	2161	2162	2163	2164	2165	2166	2167	2168	2169	2170	2171	2172	2173	2174	2175	2176	2177	2178	2179	2180	2181	2182	2183	2184	2185	2186	2187	2188	2189	2190	2191	2192	2193	2194	2195	2196	2197	2198	2199	2200	2201	2202	2203	2204	2205	2206	2207	2208	2209	2210	2211	2212	2213	2214	2215	2216	2217	2218	2219	2220	2221	2222	2223	2224	2225	2226	2227	2228	2229	2230	2231	2232	2233	2234	2235	2236	2237	2238	2239	2240	2241	2242	2243	2244	2245	2246	2247	2248	2249	2250	2251	2252	2253	2254	2255	2256	2257	2258	2259	2260	2261	2262	2263	2264	2265	2266	2267	2268	2269	2270	2271	2272	2273	2274	2275	2276	2277	2278	2279	2280	2281	2282	2283	2284	2285	2286	2287	2288	2289	2290	2291	2292	2293	2294	2295	2296	2297	2298	2299	2300	2301	2302	2303	2304	2305	2306	2307	2308	2309	2310	2311	2312	2313	2314	2315	2316	2317	2318	2319	2320	2321	2322	2323	2324	2325	2326	2327	2328	2329	2330	2331	2332	2333	2334	2335</
------	------	------	------	------	------	------	------	------	------	------	------	------	------	------	------	------	------	------	------	------	------	------	------	------	------	------	------	------	------	------	------	------	------	------	------	------	------	------	------	------	------	------	------	------	------	------	------	------	------	------	------	------	------	------	------	------	------	------	------	------	------	------	------	------	------	------	------	------	------	------	------	------	------	------	------	------	------	------	------	------	------	------	------	------	------	------	------	------	------	------	------	------	------	------	------	------	------	------	------	------	------	------	------	------	------	------	------	------	------	------	------	------	------	------	------	------	------	------	------	------	------	------	------	------	------	------	------	------	------	------	------	------	------	------	------	------	------	------	------	------	------	------	------	------	------	------	------	------	------	------	------	------	------	------	------	------	------	------	------	------	------	------	------	------	------	------	------	------	------	------	------	------	------	------	------	------	------	------	------	------	------	------	------	------	------	------	------	------	------	------	------	------	------	------	------	------	------	------	------	------	------	------	------	------	------	------	------	------	------	------	------	------	------	------	------	------	------	------	------	------	------	------	------	------	------	------	------	------	------	------	------	------	------	------	------	------	------	------	------	------	------	------	------	------	------	------	------	------	------	------	------	------	------	------	------	------	------	------	------	------	------	------	------	------	------	------	------	------	------	------	------	------	------	------	------	------	------	------	------	------	------	------	------	------	------	------	------	------	------	------	------	------	------	------	------	------	------	------	------	------	------	------	------	------	------	------	------	------	------	------	------	------	------	------	------	------	------	------	------	------	------	------	------	------	------	------	------	------	------	------	------	------	------	------	------	------	------	------	------	------	------	------	------	------	------	------	------	------	------	------	------	------	------	------	------	------	------	------	------	------	------	------	------	------	------	------	------	------	------	------	------	------	------	------	------	------	------	------	------	------	------	------	------	------	------	------	------	------	------	------	------	------	------	------	------	------	------	------	------	------	------	------	------	------	------	------	------	--------





RUN 032 FIGURE A-4. SURFACE PRESSURE DATA (MERIDIONAL, $\alpha = 20^\circ$) BMQ/SAT MAT PHASE I

A.4 Shock Layer Surveys

Surveys of the boundary layer and shock layer were made at several stations on the body, generally in a body normal mode. Where it was not possible to probe in a local surface normal mode, due to hardware restrictions, it is so noted in the AEDC data tabulations. For the majority of the surveys, the Pitot, total temperature, and Preston tube were located on one probe head and the Mach/Flow Angularity probe on a separate holder. Thus for the multi-probe head, the first step in the data sequence was to obtain the surface shear + i.e., the Preston tube data. Once these data were obtained, the probe holder was moved incrementally upward off of the model surface and flow field survey data were obtained.

A.4.1. Preston Tube Data

Model wall shear stress and the corresponding skin friction coefficient were calculated using the Preston tube pressure relationships first described by Preston (Reference 13). The shear stress was calculated by an iterative process, using calibration curve fits and boundary layer equations. A flow chart defining the data reduction procedure is shown in Figure A-5.

The calibration coefficients presented in this figure are based on previously published results (References 11, 14, and 15) and data obtained at AEDC that are yet to be published. The calibrations are considered valid over an RT and MT range of 5 to 1000 and 0 to 0.15, respectively. As indicated earlier, the shear stress and skin friction coefficient were calculated for the first point in a survey only, when the Preston tube was flush against the model surface.

MAJOR EQUATIONS

$$MT = \sqrt{TAUX / RHOX / AW}$$

$$RT = (D) \sqrt{(TAUX / RHOX) / MUW}$$

$$PTAU = (PPRESS - PWX) / TAUX$$

$$FRA = 1 - ES(RT)^{E6}$$

$$G = e^{[E1(2RT) + E2 + (E3(2RT) + E4) / (1 - (ES(RT)^{E6}))]}$$

$$\dot{G} = e^{[(E1(2RT) + E2 - E3 / (ES(E6)))]}$$

$$FUN = -RT + CC1(PTP) +$$

$$CC2 \left[e^F - 1 - F - \frac{F^2}{2} - \frac{F^3}{6} \right]$$

$$\text{where } F = (CC3)(PTP)$$

$$PTP = PTAU - MT^2(G)$$

COEFFICIENTS

$$CC1 = 0.93973$$

$$CC2 = 11.285$$

$$CC3 = 0.02354$$

$$E1 \rightarrow E6 = 0.343, 8.243, 2.657, -8.193, 0.00346, 1.94$$

NOTE: FOR A DEFINITION OF THE NOMENCLATURE SEE THE "TABULATED DATA KEY" IN THE FRONT OF THIS REPORT.

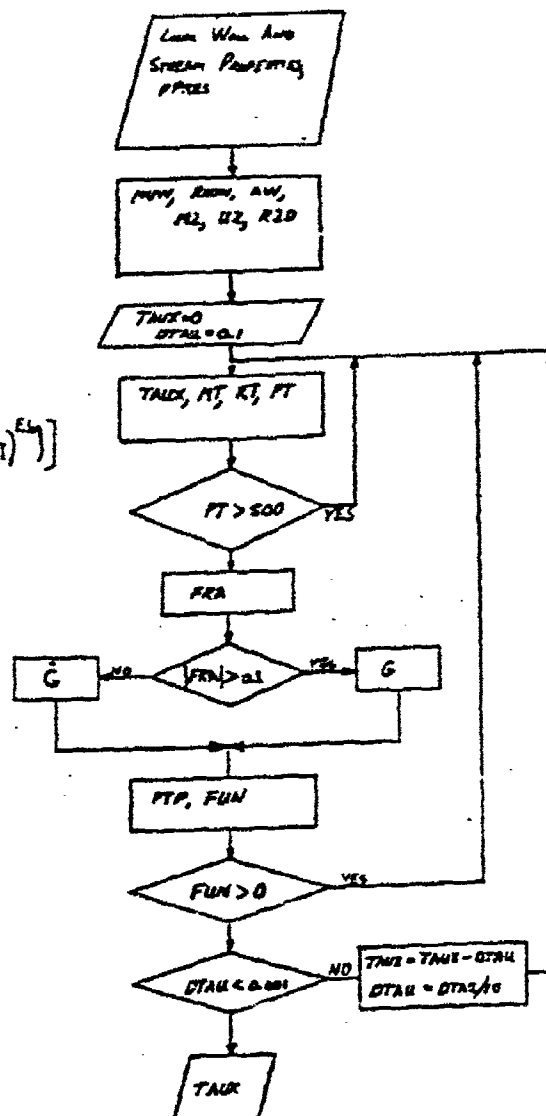


FIGURE A-5. PRESTON TUBE DATA REDUCTION FLOW CHART

A.4.2. Shock Layer Survey Data

Probe locations within a survey are presented as heights above the model surface measured along the direction of the traverse, and coordinate values are given in terms of the model axis system. Corrections have been included for the fact that the Pitot probe was sometimes slightly deflected at the model surface.

Mach/Flow-Angularity probe pressures (P1, P2, P3, P4, P5) and the Pitot pressure (PP) were computed using the equilibrium pressure prediction technique presented in Reference 12. The technique uses a mathematical model of the pressure lag/time history and fits the pressure history with a least squares curve fit to predict equilibrium pressure. The basic assumption is that the pressure measured at the transducer exponentially approaches the equilibrium pressure at the orifice. It is also assumed that the orifice pressure is a constant, during the time when the transient data were recorded. Inputs to the curve fit routine are: (1) slip flow coefficient and (2) pressure-time data. The data reduction equations for predicting equilibrium pressure from transient data as follows (from Reference 12).

Slip Flow Coefficient:

$$A = 1.776 (10^{-6}) \left(\frac{\text{Mean tube temperature}}{\text{Tube I.D.}} \right)$$

Mean tube temperature = 1200°R, assumed
Tube ID = 0.012 in., smallest diameter } For these tests
A = 0.18 psi, (only rough estimate required)

Pressure-Time Data:

Pi ~ Transducer pressure of data point, i, psia (computed in same manner as model surface pressures)

ti ~ Time of data point i, sec.

n ~ Total number of data points

Slope of Pressure-Time Data:

$$\frac{dP_i}{dt} \sim \text{Local slope} = \frac{P_{(i+m)} - P_{(i-m)}}{2m\Delta t}, \text{ psi/sec}$$

where Δt = time between successive data points, sec

m = integer smoothing function = 1 for this test.

With the above inputs (A , P_i , dP_i/dt) the following computations are made to evaluate (or predict) the equilibrium pressure (P_e).

$$C_i = (P_i)^2 + AP_i \quad (A-3)$$

$$K = n \frac{\left\{ \sum_{i=1}^n \frac{dP_i}{dt} \cdot C_i \right\} - \left\{ \sum_{i=1}^n \frac{dP_i}{dt} \right\} \left\{ \sum_{i=1}^n C_i \right\}}{\left\{ \sum_{i=1}^n C_i \right\}^2 - n \left\{ \sum_{i=1}^n (C_i)^2 \right\}} \quad (A-4)$$

$$D = \left\{ K \sum_{i=1}^n C_i + \sum_{i=1}^n \frac{dP_i}{dt} \right\} / n \quad (A-5)$$

$$P_e = \frac{-A}{2} + \sqrt{\left(\frac{A}{2}\right)^2 + \frac{D}{K}}, \text{ psia} \quad (A-6)$$

The prediction technique fails whenever there is an insufficient sample of transient data with which to evaluate the constant K . In fact K is undefined for the case where the pressure, P_i , is constant. To alleviate this problem a check was made, based on the value of K for this test.

If $0.05 < K < 3$, the predicted pressure was used, otherwise the final measured value was used.

There were a few instances wherein the transient data were changing so rapidly for this test that the calculated value of dP_i/dt was inaccurate for the first points of the pressure-time history. Whenever this happened the initial transient data adversely affected the prediction, giving inaccurate results. To alleviate the problem initial data points were dropped from the curve fit; one point was dropped at a time and P_e was recomputed and compared to the last computed value. The iteration ended whenever the change in the predicted pressure was less than two percent, or more than four data points were dropped. It should be noted that the inaccuracy in dP_i/dt can be eliminated by taking data at a faster rate or by delaying the beginning of the data record. For early tests the data acquisition rate was limited to 0.6 sec per point, for the majority of the test program. Improvements in the data acquisition system permitted taking the same type of data at a significantly faster rate (up to 10 points per sec) in later tests.

Figures A-6 and A-7 contain typical results from the equilibrium pressure prediction program.

Local Mach number and flow angle are computed from pressure P_1 through P_5 using curve-fitted calibration data. Extensive calibration data have been obtained on similar probes and these data have been correlated against the parameters $DPSQP$ and $PAVG P_5$ which are defined as:

$$DPSQP = \sqrt{(P_1 - P_3)^2 + (P_2 - P_4)^2} / (2 \cdot P_5) \quad (A-7)$$

and

$$PAVG P_5 = PAVG / P_5 = (P_1 + P_2 + P_3 + P_4) / (4 \cdot P_5) \quad (A-8)$$

For the present tests, calibration data were obtained with the Mach/Flow-Angularity probe (identified as Probe #4) in the tunnel freestream and these data were combined with previous calibrations obtained on a similar probe at Mach number 1.5 through 5.0. The combined data set was curve fitted and the curve fits were used in the data reduction. The calibration data and

the curve fits are shown in Figures A-8a and A-8b where the actual data reduction equations are as follows:

Local Mach Number:

$$MLC = e^{[AK + BK(DPSQP)^2 + CK(DPSQP)^4]}$$

$$\text{where } AK = \sum_{i=0}^5 [AM_i (\ln PAVGP5)^i]$$

$$BK = \sum_{i=0}^4 [BM_i (\ln PAVGP5)^i]$$

$$CK = \sum_{i=0}^4 [CM_i (\ln PAVGP5)^i]$$

Total Angle of Attack:

$$AATCA = (DPSQP) [D1 + D2 \ln(MLC) + D3 (\ln(MLC))^2] + [D4 + D5 (\ln(MLC))^2] (DPSQP)^{D6}, \text{ deg}$$

Curve Fit Coefficients:

$$AM0-5 = 3.6474, 10.8249, 12.5254, 5.90988, 1.03548, 0$$

$$BM0-4 = 7.64593, 0, -16.5279, 0, 8.66794$$

$$CM0-4 = -108.870, 0, 182.245, 0, -37.4971$$

$$D1-D6 = 121.044, 18.6043, -74.2038, -37.4837, 58.2593, 0.872233$$

Radial Angle: (Not a Curve Fit)

$$PHI = \tan^{-1} \left(\frac{DP24}{DP13} \right) + 90 \left(\frac{1+DP13}{|DP13|} \right), \text{ deg}$$

$$\text{If } PHI < 0 \text{ then } PHI = PHI + 360.$$

PROBE PRESSURE DATA, P3

Inputs: $A = 0.16$ psi, P_i values as shown

$\frac{dP_i}{dt}$ computed using M-1, $\Delta t = 0.6$ sec

Outputs: $K = 0.339$

$D = 0.00673$

$P_o = 0.094$ psi

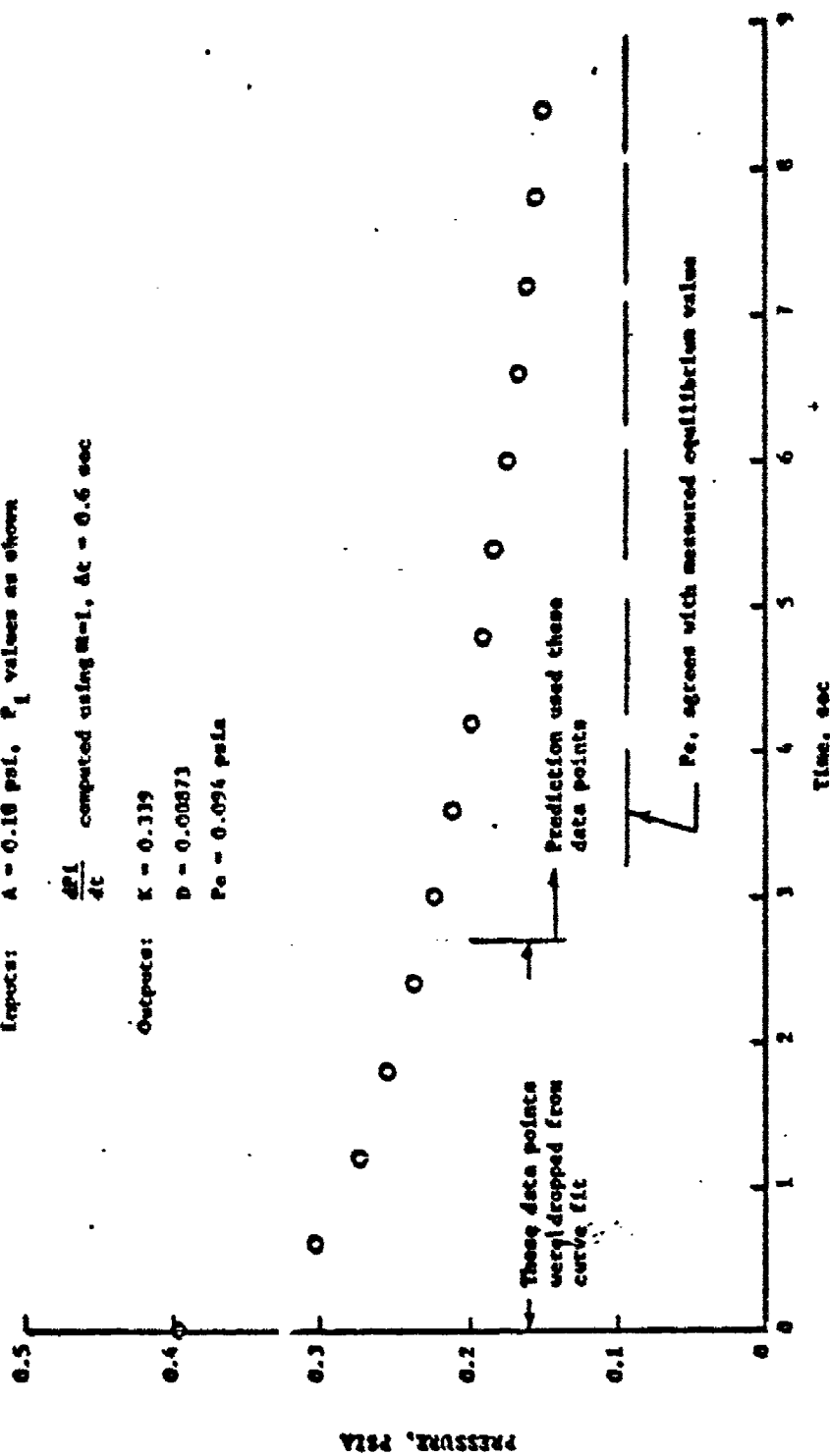


FIGURE A-6. TYPICAL PREDICTION PROGRAM RESULTS (PROBE PRESSURE)

***NOTE: Prediction gives mean value of the equilibrium pressure, these data were chosen to illustrate the program's ability to use "noisy" data.

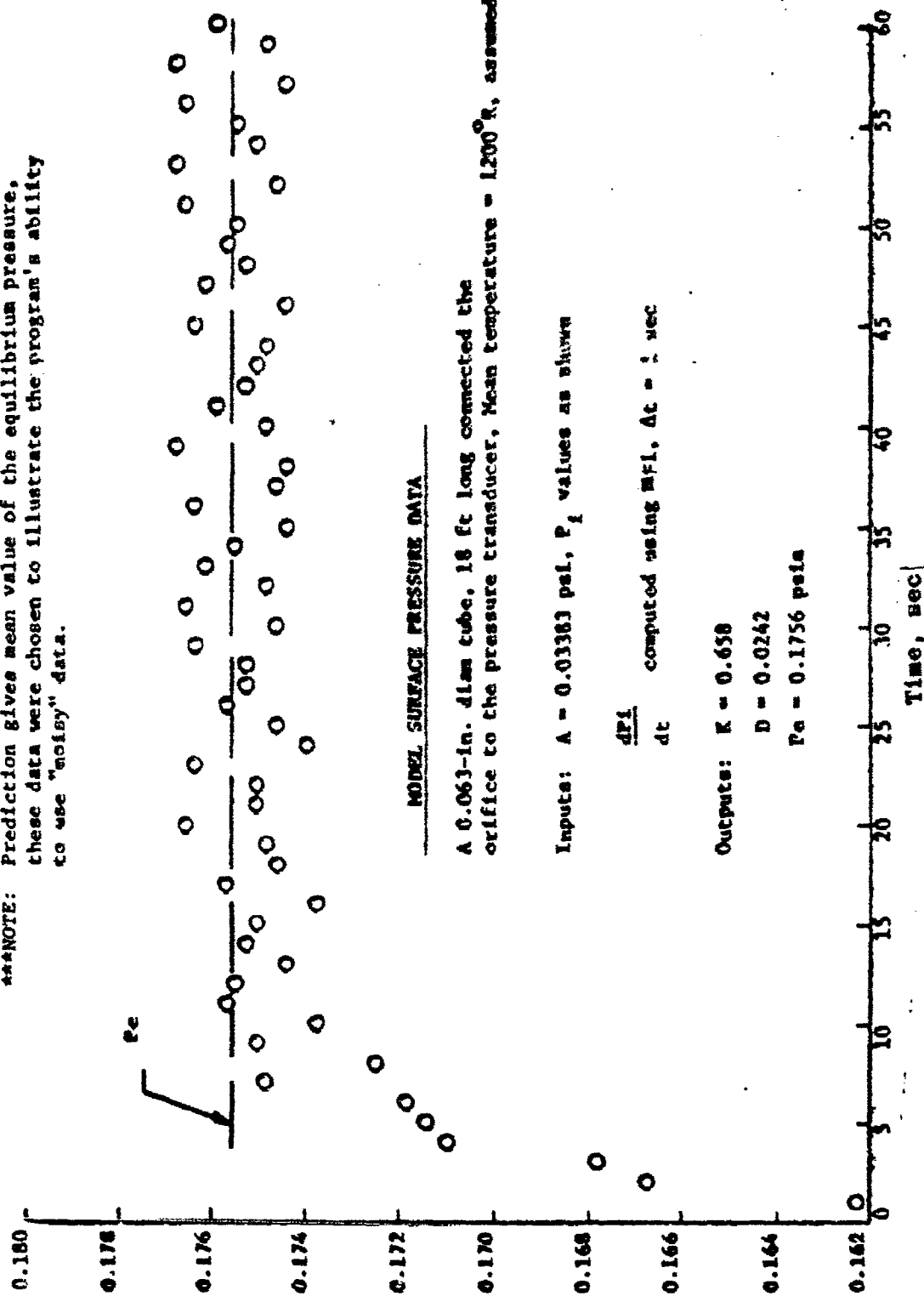
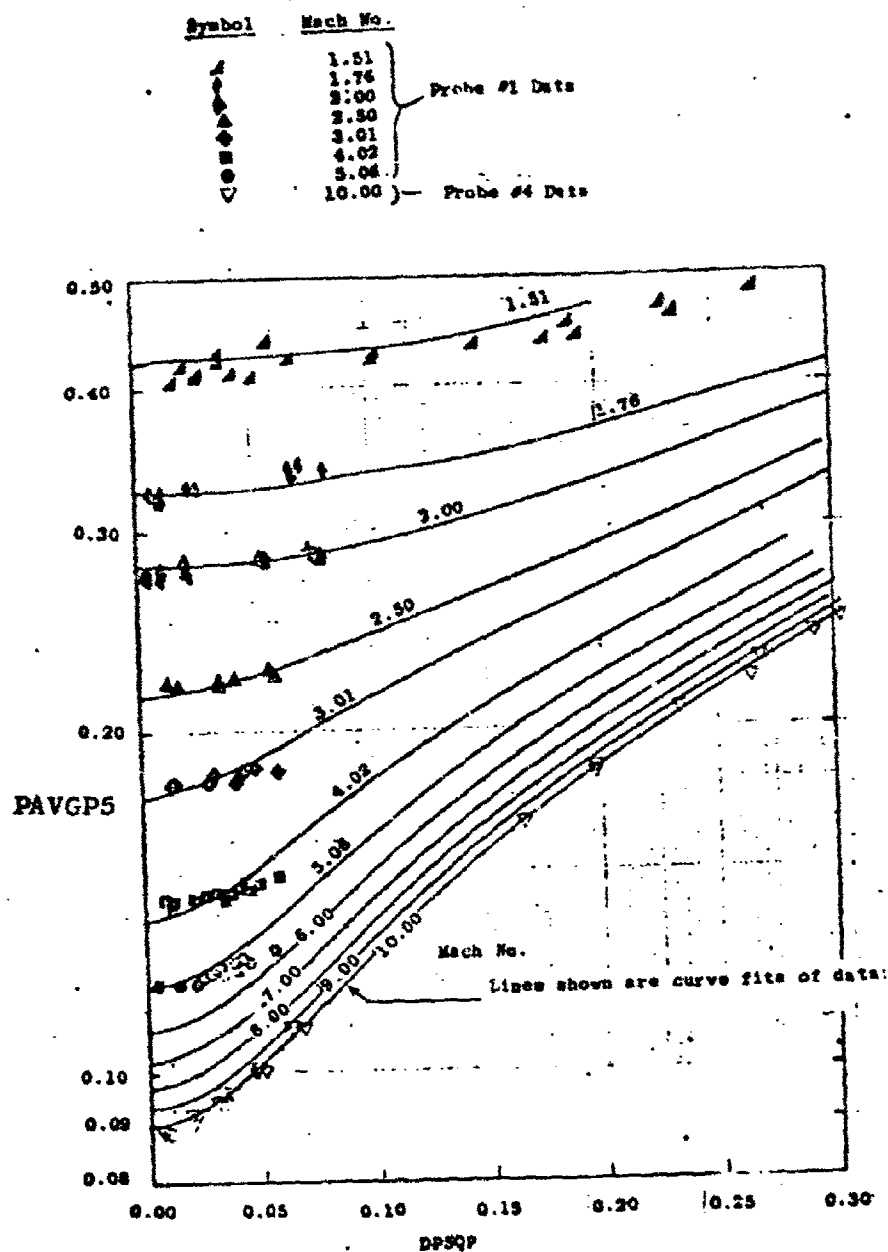


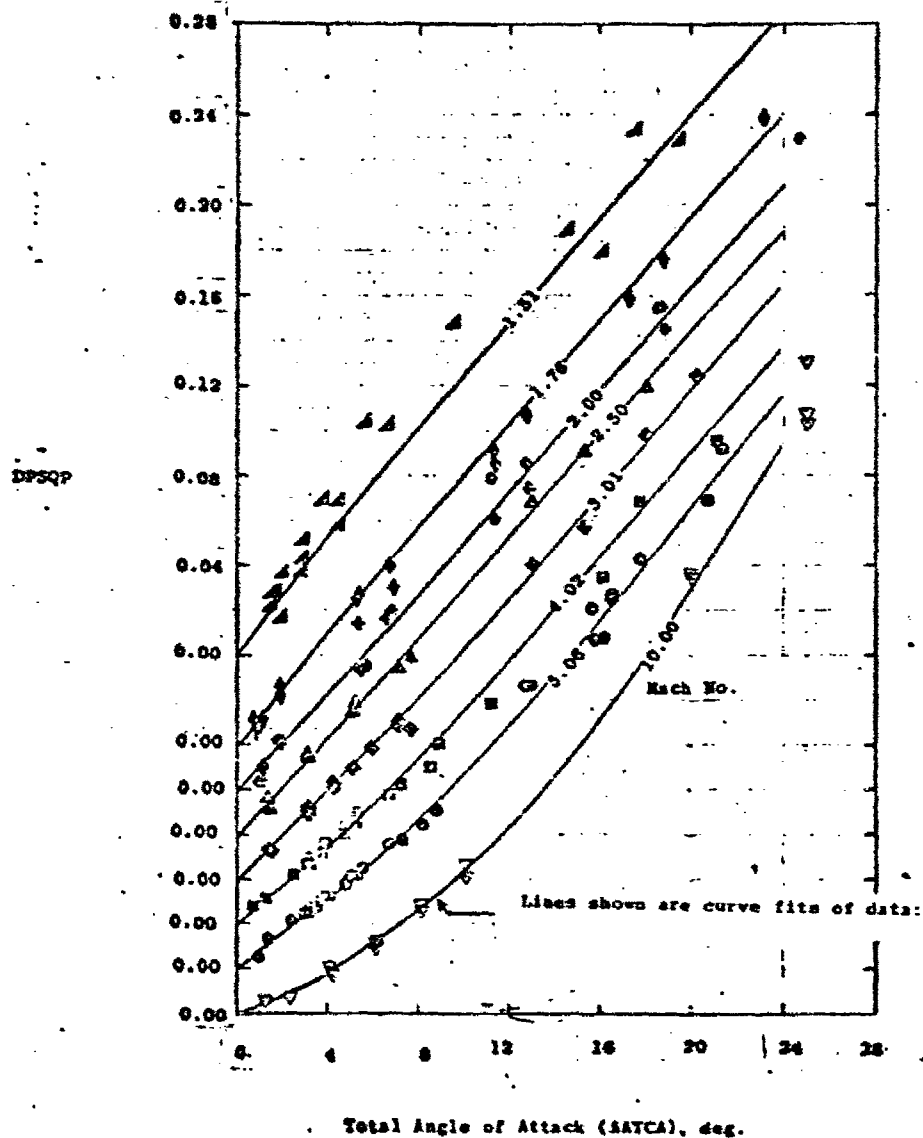
FIGURE A-7. TYPICAL PREDICTION PROGRAM RESULTS (MODEL PRESSURE)



a. MACH NUMBER

FIGURE A-8. MACH/FLOW ANGULARITY PROBE CALIBRATION DATA AND CURVE FITS

Symbol	Mach No.	
▲	1.31	Probe #1 Data
●	1.76	
○	2.00	
△	2.50	
◆	3.01	
■	4.02	Probe #4 Data
●	5.06	
▽	10.00	



B. TOTAL ANGLE OF ATTACK

FIGURE A-8. MACH/FLOW ANGULARITY PROBE CALIBRATION DATA AND CURVE FITS (CONT'D)

Not all existing calibration data for Probe #1 are included on Figure A-8a. A distinct difference in the shape of the PAVGP5 vs. DPSQP curves was noted between the two probes, therefore all data for total angle of attack greater than 7 degrees (corresponds to DPSQP ≥ 0.7) was omitted for Probe No. 1, with the exception of data at Mach No. 1.5. This omission forced the curve fit to agree with Probe No. 4 calibration data. The resulting curve fits used to reduce the data are considered to be the best possible based on the available calibration data, but these could be significantly improved with additional calibration data for the same probe (No. 4).

Local total temperature was computed from the shielded thermocouple measured value (TOSM) using the method of Varner, Reference 16. In this method, the analysis is based on the total temperature variation in a laminar developing flow within a tube whose walls are at the adiabatic recovery temperature of the local flow field. This approach results in the ability to theoretically correct probe data for all local flow field conditions (a wide range of Reynolds numbers) using a limited amount of calibration data acquired in the tunnel freestream. To correct the measured temperature, the following parameters must be defined experimentally: local Mach number and Pitot pressure in front of the probe, the effective vent area ratio (AV/AE) and the local Mach number of the flow entering the probe (ME). For this test, the local corrected total temperatures were evaluated at the Mach/Flow-Angularity probe positions (TOSC values) and at the Pitot tube positions (TOSCP values) by an interpolation scheme. The approach used was to define, by linear interpolation, the local measured total temperature at the probe height and then to correct the interpolated value using the probe defined Mach number (MLC or MP) and the measured Pitot pressure (either P5 or PP). The nearest wall temperature measurement (TWJ) was included in the interpolation to define a value of uncorrected temperature at zero height. The effective vent area ratio, AV/AE was determined from freestream calibration data to be time dependent, decreasing in value as the test progressed, indicating that the tube vent holes were decreasing in size. The value used in the data reduction was:

$$AV/AE = 0.153 - 0.0005 (\text{SURVEY}) \quad (\text{A-9})$$

The entrance Mach number was defined in terms of the vent area ratio by an approximate equation:

$$ME = 0.578(AV/AE) \quad (\text{A-10})$$

which assumes that the flow is sonic at the vent area and AV/AE is less than 0.5. Shielded thermocouple data reduction equations are given in detail in Reference 4.

Ideal compressible gas relationships were used in the calculation of local static temperature and pressure values and in evaluating the local Mach number at the Pitot tube. The equations for air (ratio of specific heats = 1.4), are listed below:

$$\frac{T}{T_t} = (1 + \frac{M^2}{5})^{-1} \quad (\text{A-11})$$

$$\frac{P}{P_t} = (1 + \frac{M^2}{5})^{-7/2}, \text{ for } M \leq 1 \quad (\text{A-12})$$

$$\frac{P_{t2}}{P_1} = \left\{ \frac{6M_1^2}{5} \right\}^{7/2} \left\{ \frac{6}{7M_1^2 - 1} \right\}^{5/2}, \text{ for } M_1 > 1 \quad (\text{A-13})$$

The first step in using the above equations was to compute the static pressure at the Mach/Flow-Angularity probe heights. To make these calculations, the following substitutions were made in Equations (A-12) and (A-13):

$P_t \sim P_5$, $P_{t2} \sim P_5$, $M \sim \text{MLC}$, $M_1 \sim \text{MLC}$. Static pressure at the Pitot probe (PSP) was defined by linear interpolation of the inferred static pressure based on the Mach/Flow-Angularity probe results and the model wall orifice pressure used to define the static pressure at zero height. The Mach number determined from the Pitot tube (MP) was then defined from Equations (A-12) and (A-13) with the substitutions: $p \sim \text{PSP}$, $P_1 \sim \text{PSP}$, $P_{t2} \sim \text{PP}$.

The local static temperatures were computed using the appropriate local Mach number for Equation (A-11).

Local velocities were calculated from

$$V_L = 49.0223 M \sqrt{T}, \text{ ft/sec} \quad (\text{A-14})$$

where M and T ($^{\circ}\text{R}$) are the appropriate local values of Mach number and static temperature.

Velocity vectors with respect to the Mach/Flow-Angularity probe axis system were computed according to the definitions given in Figure A-9. These values were transformed to the tunnel axis system (Figure A-10) by rotation of the axes through pitch, yaw and roll angle sequence corresponding to the probe misalignment angles defined as THETA0, PSIO and PHIO. Misalignment values in yaw and roll were determined from the freestream calibration that was obtained at the beginning of each test shift. The pitch misalignment was evaluated for each survey by determining what value of THETA0 would best null the pressure differential DP13 on the probe, i.e., THETA0 value for DP13 = 0.0.

The freestream velocity vectors were transformed to the model axis system by rotation of the axes through pitch and roll respectively, corresponding to the model pitch angle (ALPHA-MODEL) and the model roll angle (ROLL-MODEL). Velocity vector definitions in the model axis system are noted in Figure A-11.

The quantity of tabular and graphical data involved in the shock layer surveys is rather lengthy, involving several volumes of reports for this test series. An example of the Pitot and total temperature data tabulations is shown in Table A-3 (11 pages). Included in this table (on Page 3) are the Preston tube data results defining the wall shear and skin friction coefficient. A representative set of graphs for these data are shown in Figures A-12 through A-15. Figures A-12 and A-13 depict the uncorrected and

Notes:

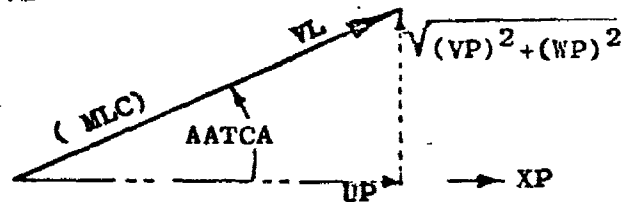
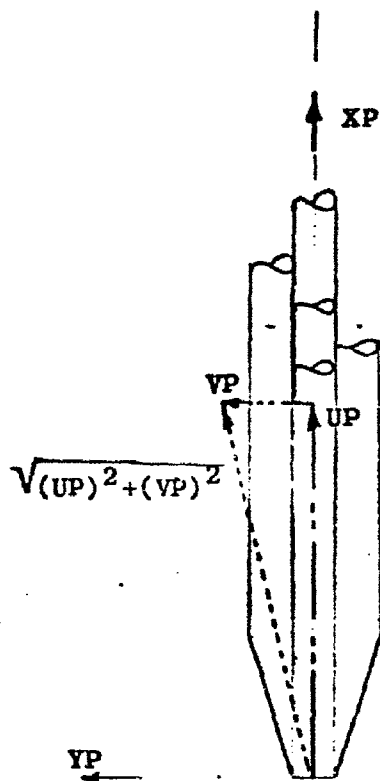
1. All vectors are shown in positive directions.
2. PHI is computed directly from the pressures
3. Local Mach number (MLC) and the total angle of attack (AATCA) are computed from curve fits

4. Velocity vector components:

$$\frac{UP}{VL} = \cos(AATCA)$$

$$\frac{VP}{VL} = \sin(AATCA) \cdot \sin(PHI)$$

$$\frac{WP}{VL} = \sin(AATCA) \cdot \cos(PHI)$$



View A-A
(Probe not shown)

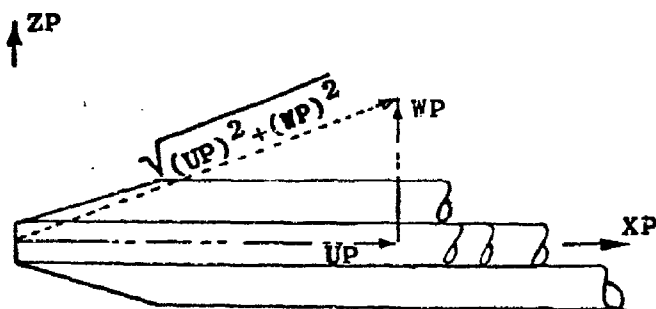
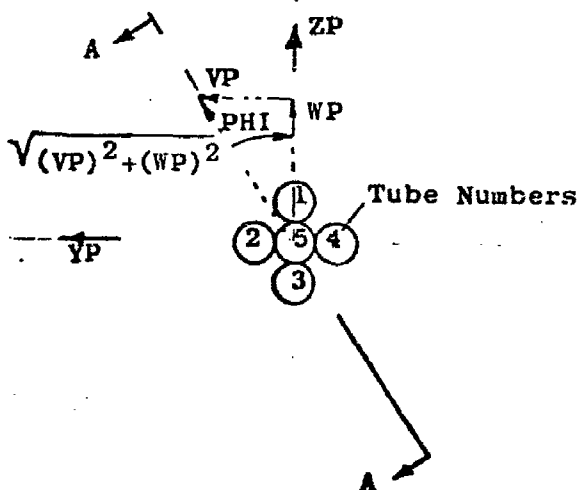


FIGURE A-9. VELOCITY VECTOR DEFINITION WITH RESPECT TO THE PROBE AXIS SYSTEM

NOTES:

1. Positive directions of velocity vectors and probe misalignments are shown.
2. See Fig. A-9 for definition of velocity vector components in the probe axis system (i.e., U_P/V_L , V_P/V_L , W_P/V_L).
3. Velocity vector components:

$$\frac{U_P}{V_L} = \frac{U_P}{V_L} (A1) + \frac{V_P}{V_L} (A2) + \frac{W_P}{V_L}$$

$$\frac{V_P}{V_L} = \frac{U_P}{V_L} (B1) + \frac{V_P}{V_L} (B2) + \frac{W_P}{V_L} (B3)$$

$$\frac{W_P}{V_L} = \frac{U_P}{V_L} (C1) + \frac{V_P}{V_L} (C2) + \frac{W_P}{V_L} (C3)$$

Where $\begin{Bmatrix} A1, A2, A3 \\ B1, B2, B3 \\ C1, C2, C3 \end{Bmatrix}$ are axis rotation coefficients:

$$A1 = \cos(\text{THETAO}) \cdot \cos(\text{PSIO})$$

$$A2 = -\cos(\text{THETAO}) \cdot \sin(\text{PSIO}) \cdot \cos(\text{PHIO}) + \sin(\text{THETAO}) \cdot \sin(\text{PHIO})$$

$$A3 = \cos(\text{THETAO}) \cdot \sin(\text{PSIO}) \cdot \sin(\text{PHIO}) + \sin(\text{THETAO}) \cdot \cos(\text{PHIO})$$

$$B1 = \sin(\text{PSIO})$$

$$B2 = \cos(\text{PSIO}) \cdot \cos(\text{PHIO})$$

$$B3 = -\cos(\text{PSIO}) \cdot \sin(\text{PHIO})$$

$$C1 = -\sin(\text{THETAO}) \cdot \cos(\text{PSIO})$$

$$C2 = \sin(\text{THETAO}) \cdot \sin(\text{PSIO}) \cdot \cos(\text{PHIO}) + \cos(\text{THETAO}) \cdot \sin(\text{PHIO})$$

$$C3 = -\sin(\text{THETAO}) \cdot \sin(\text{PSIO}) \cdot \sin(\text{PHIO}) + \cos(\text{THETAO}) \cdot \cos(\text{PHIO})$$

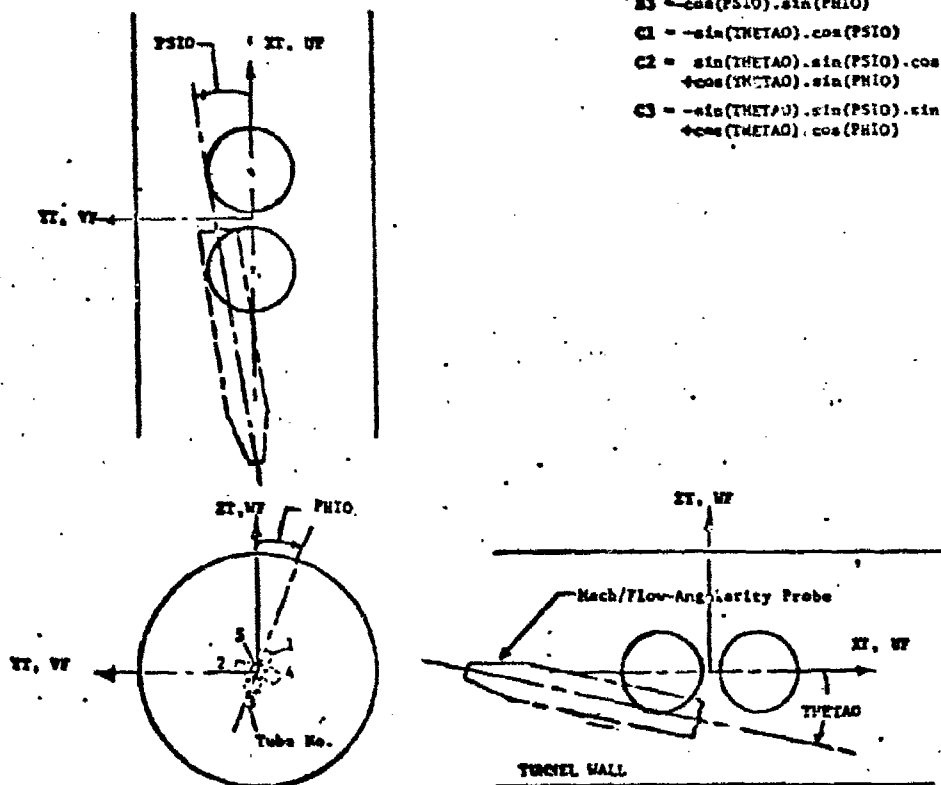


FIGURE A-10. VELOCITY VECTOR DEFINITION WITH RESPECT TO THE TUNNEL AXIS SYSTEM

NOTES:

1. Positive direction of velocity vectors are shown.
2. See Fig. A-10 for definitions of velocity vector components in the tunnel axis system. (i.e. U_F/V_L , V_F/V_L , W_F/V_L)
3. Velocity vector components:

$$\frac{U}{V_L} = \left(\frac{U_F}{V_L} \right) \cdot \cos(\text{ALPHA-MODEL}) - \left(\frac{W_F}{V_L} \right) \cdot \sin(\text{ALPHA-MODEL})$$

$$\begin{aligned} \frac{V}{V_L} = & \left(\frac{U_F}{V_L} \right) \left(-\sin(\text{ROLL-MODEL}) \cdot \sin(\text{ALPHA-MODEL}) \right) \\ & + \left(\frac{V_F}{V_L} \right) \cdot \cos(\text{ROLL-MODEL}) + \left(\frac{W_F}{V_L} \right) \left(-\sin(\text{ROLL-MODEL}) \right) \\ & \cdot \cos(\text{ALPHA-MODEL}) \end{aligned}$$

$$\begin{aligned} \frac{W}{V_L} = & \left(\frac{U_F}{V_L} \right) \left(\cos(\text{ROLL-MODEL}) \cdot \sin(\text{ALPHA-MODEL}) \right) \\ & + \left(\frac{V_F}{V_L} \right) \cdot \sin(\text{ROLL-MODEL}) \\ & + \left(\frac{W_F}{V_L} \right) \left(\cos(\text{ROLL-MODEL}) \cdot \cos(\text{ALPHA-MODEL}) \right) \end{aligned}$$

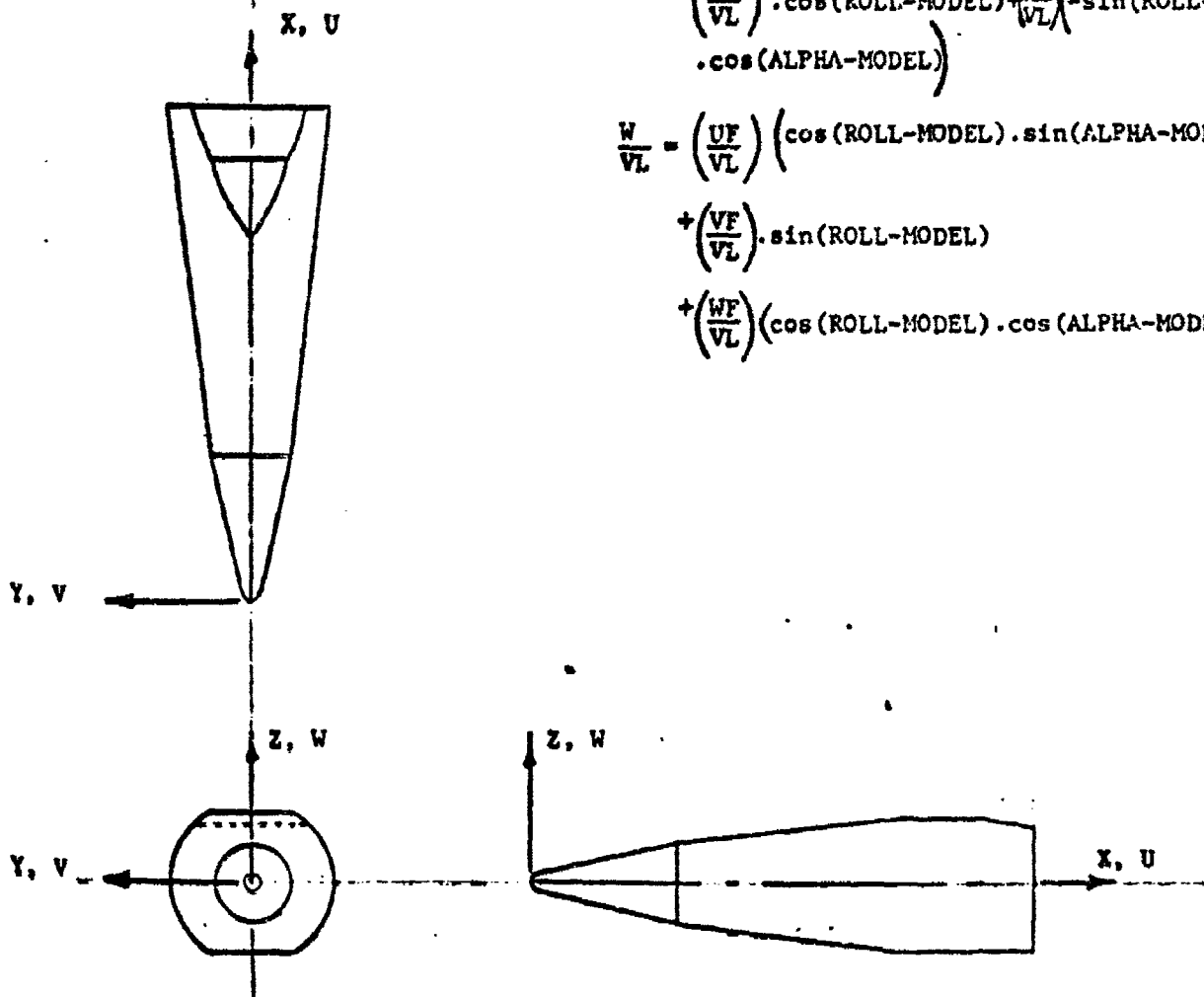


FIGURE A-11. VELOCITY VECTOR DEFINITION WITH RESPECT TO THE MODEL AXIS SYSTEM

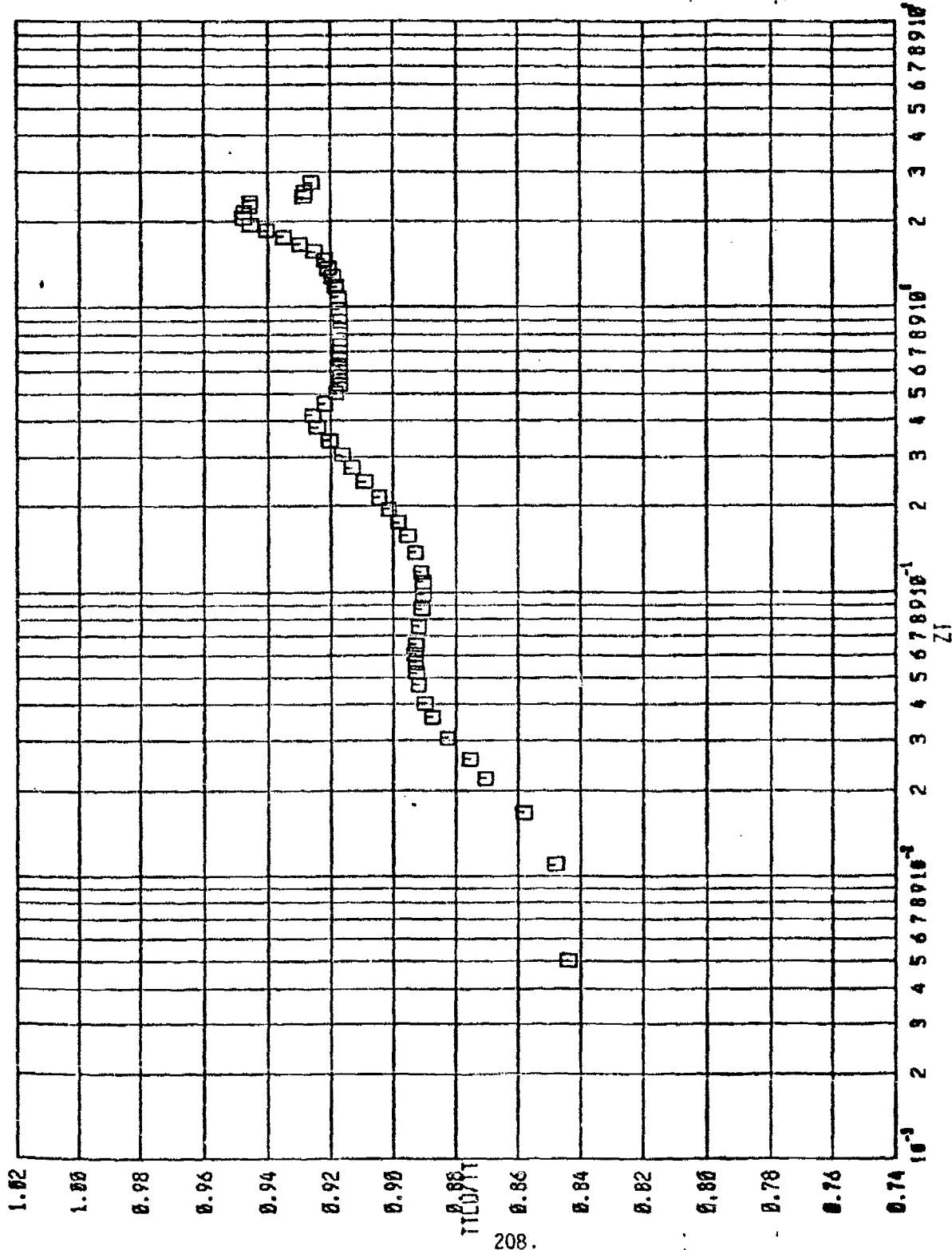
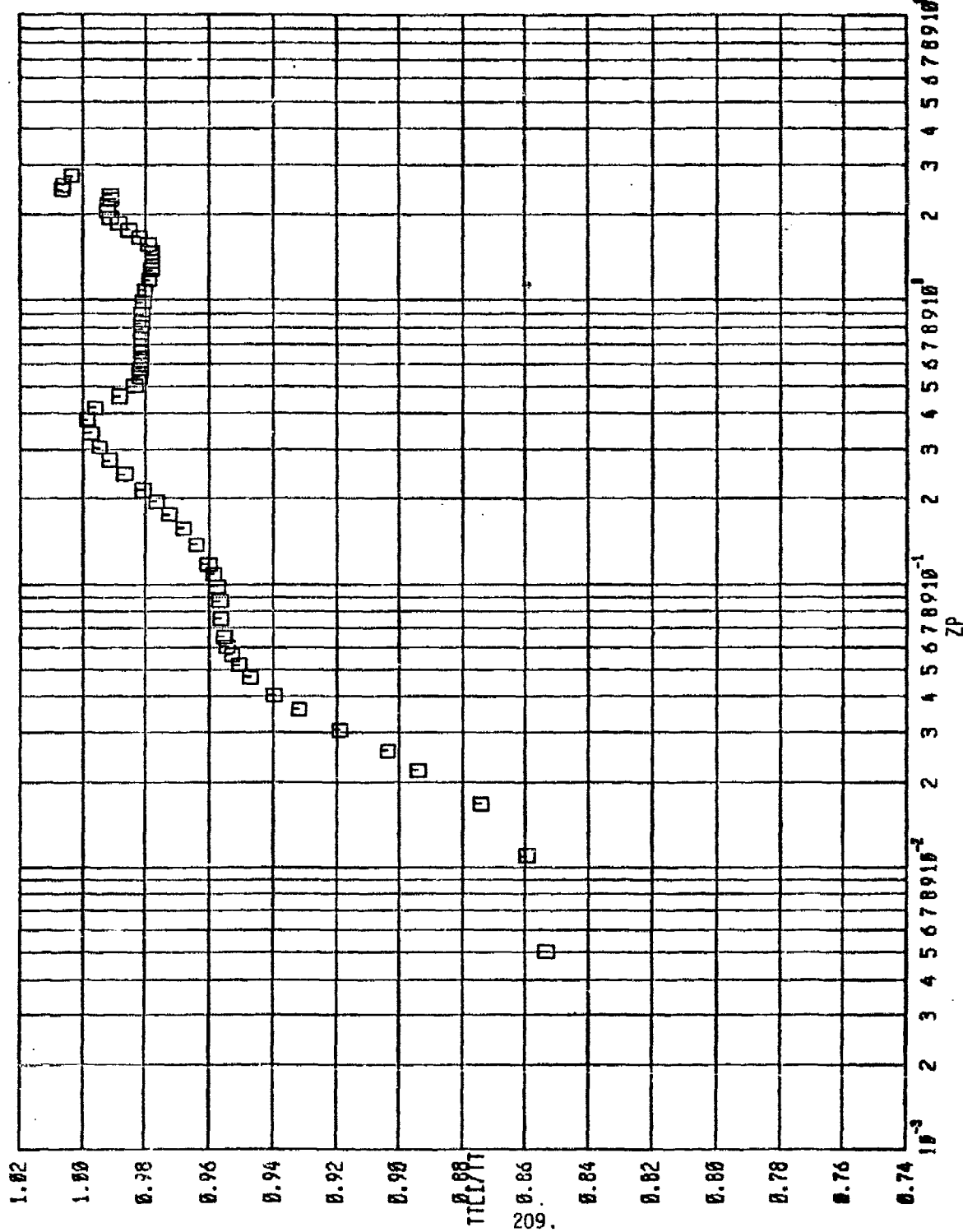


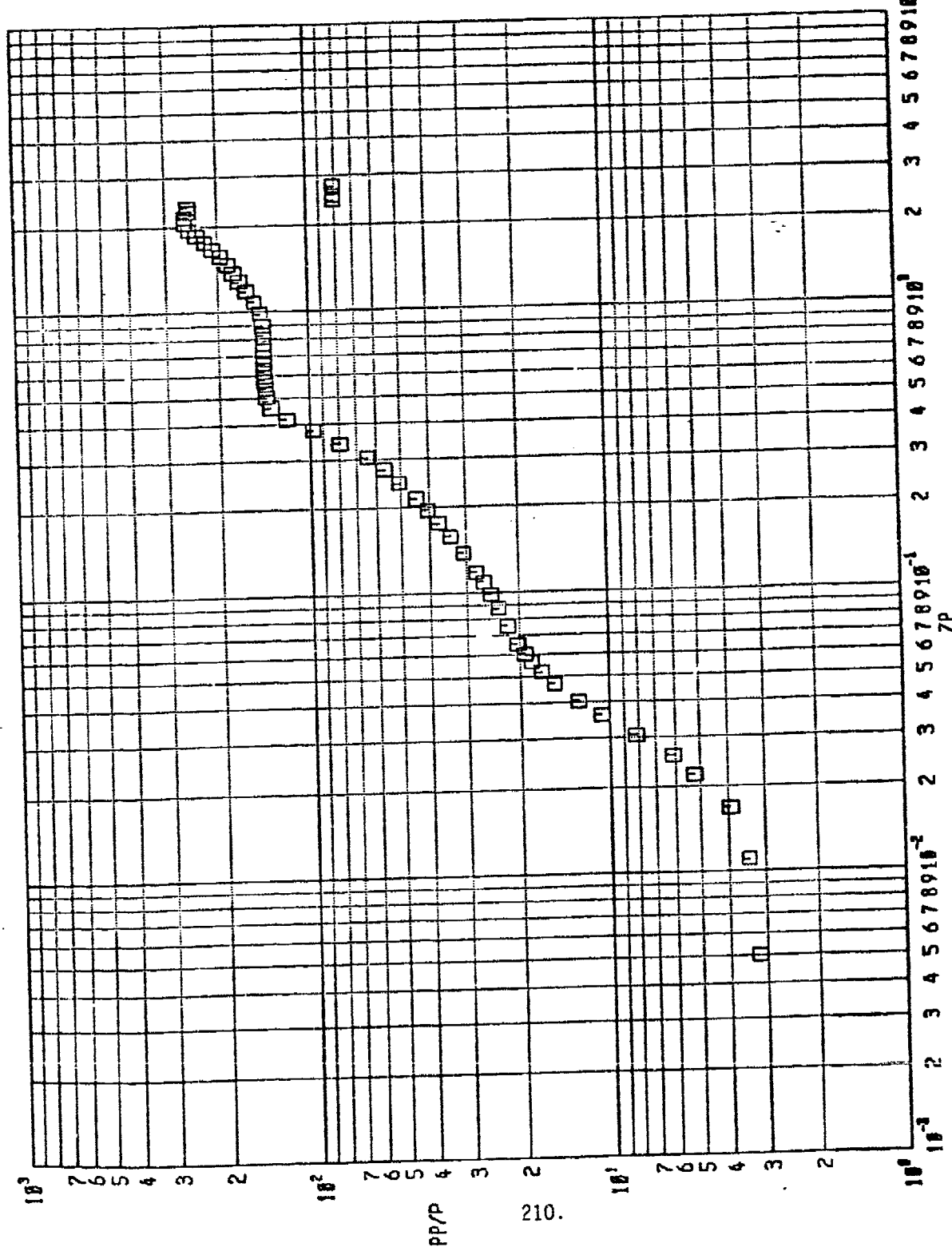
FIG. 1
23-JUL-61
1428

BMD/SRI MAT PHASE I

SHOCK LAYER UNCORRECTED TOTAL
TEMPERATURE DATA

RUN 054



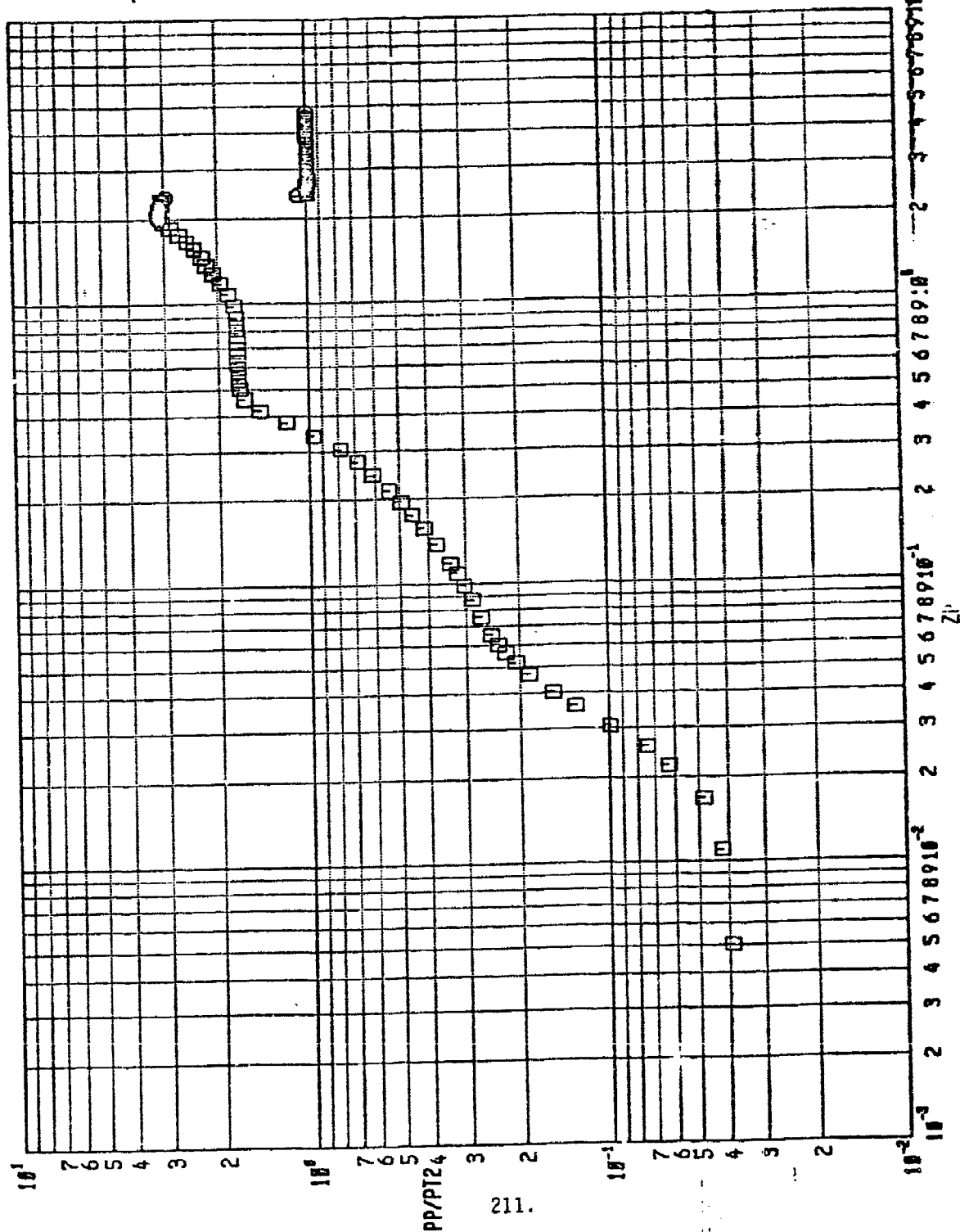


RUN 154

FIGURE A-14. SHOCK LAYER PITOT PRESSURE DATA

BMQ/SRI MAT PHASE I

PAGE 5
23-JUL-81
11155



RUN 054 054 FIGURE A-15. SHOCK LAYER PITOT PRESSURE DATA BND/SRI MAT PHASE I

Proc 1
23-Jul-61
15:11

ARVIN/CALSPAN FIELD SERVICES, INC.
AEC DIVISION
VON KARMAN GAS DYNAMICS FACILITY
ARNOLD AIR FORCE STATION, TENNESSEE
BHO/SAI MAT PHASE I

TABLE A-3. SHOCK LAYER DATA

DATE COMPUTED 22-JUL-81
TIME COMPUTED 06:23:18
DATE RECORDED 24-APR-81
TIME RECORDED 5:51:22
PROJECT NUMBER C145VB

PAGE 1
RUN 54 ALPHA SECTOR= 1.99 DEG
M = 7.97 ALPHAP = -10.01 DEG
RE = 1.623E+06 MUREL-ROLL = 180.00 DEG

CONFIGURATION NOSE RADIUS, IN .06 MACHINED
FLAP NONE

DATA TYPE 1 3.SURVEY - PP AND TT SURVEY STATION NO = 58 PMX/PT= 0.250E-03 ALPT= -2.99 DEG

TEST CONDITIONS AND LOCAL CONDITIONS AT THE PITOT PROBE

POINT	PT (PSIA)	TT (UFGF)	P (PSIA)	PT2 (PSIA)	ZP (IN)	PP (PSIA)	PP/PT2	PP/P	PP/PMX	TTLI/TT	ML	ZPU (IN)	PPU (PSIA)	PPU/PT2
1	934.52	1355.4	0.087	7.190	0.0050	0.280	0.0390	3.21	1.34	0.85	0.66	2.0050	22.3360	3.1067
2	934.62	1355.4	0.087	7.191	0.0110	0.301	0.0418	3.44	1.44	0.86	0.74	2.0110	22.3606	3.1097
3	934.72	1355.4	0.087	7.191	0.0168	0.346	0.0481	3.96	1.66	0.87	0.88	2.0168	22.3860	3.1132
4	934.56	1355.3	0.087	7.190	0.0220	0.454	0.0632	5.20	2.18	0.89	1.12	2.0220	22.4099	3.1168
5	934.47	1355.3	0.087	7.189	0.0258	0.535	0.0745	6.13	2.57	0.90	1.25	2.0258	22.4214	3.1189
6	934.47	1355.2	0.087	7.189	0.0306	0.712	0.0990	8.15	3.42	0.92	1.50	2.0306	22.4427	3.1217
7	934.56	1355.1	0.087	7.190	0.0362	0.930	0.1294	10.65	4.46	0.93	1.75	2.0362	22.4828	3.1269
8	934.49	1355.2	0.087	7.189	0.0406	1.111	0.1545	12.72	5.33	0.94	1.94	2.0406	22.5082	3.1307
9	934.51	1355.2	0.087	7.190	0.0470	1.339	0.1863	15.33	6.43	0.95	2.15	2.0470	22.5502	3.1365
10	934.56	1355.0	0.087	7.190	0.0518	1.483	0.2063	16.98	7.12	0.95	2.27	2.0518	22.5862	3.1413
11	934.41	1354.9	0.087	7.189	0.0565	1.599	0.2225	18.31	7.68	0.95	2.36	2.0565	22.6126	3.1455
12	934.45	1355.0	0.087	7.189	0.0602	1.686	0.2346	19.31	8.09	0.95	2.43	2.0602	22.6402	3.1492
13	934.34	1354.9	0.087	7.188	0.0654	1.781	0.2478	20.40	8.55	0.96	2.50	2.0654	22.6708	3.1519
14	934.58	1354.8	0.087	7.190	0.0654	1.785	0.2482	20.44	8.57	0.96	2.50	2.0654	22.6821	3.1546
15	934.56	1354.7	0.087	7.190	0.0754	1.924	0.2675	22.02	9.21	0.96	2.60	2.0754	22.7212	3.1601
16	934.67	1354.7	0.087	7.191	0.0871	2.058	0.2861	23.55	9.87	0.96	2.70	2.0871	22.7168	3.1592
17	934.62	1354.7	0.087	7.191	0.0871	2.057	0.2861	23.55	9.87	0.96	2.70	2.0871	22.7168	3.1592
18	934.62	1354.6	0.087	7.191	0.0980	2.182	0.3034	24.98	10.47	0.96	2.78	2.0980	22.6550	3.1506
19	934.51	1354.6	0.087	7.190	0.1088	2.302	0.3202	26.35	11.05	0.96	2.86	2.1088	22.5767	3.1401
20	934.45	1354.5	0.087	7.189	0.1180	2.427	0.3376	27.79	11.65	0.96	2.94	2.1180	22.5182	3.1322
21	934.54	1354.4	0.087	7.189	0.1377	2.689	0.3740	30.79	12.91	0.96	3.11	2.1377	22.4940	3.1285
22	934.48	1354.4	0.087	7.189	0.1578	2.968	0.4128	33.98	14.24	0.97	3.27	2.1578	22.5484	3.1264
23	934.45	1354.5	0.087	7.189	0.1764	3.251	0.4522	37.23	15.60	0.97	3.43	2.1764	22.5713	3.1296
24	934.65	1354.4	0.087	7.191	0.1958	3.536	0.4917	40.48	16.97	0.98	3.58	2.1958	22.4886	3.1274
25	934.61	1354.4	0.087	7.191	0.2153	3.873	0.5386	44.34	18.58	0.98	3.75	2.2153	22.2562	3.0952
26	934.67	1354.3	0.087	7.191	0.2449	4.398	0.6117	50.35	21.10	0.99	4.00	2.2449	21.9860	3.0374
27	934.67	1354.4	0.087	7.191	0.2746	4.947	0.6880	56.63	23.74	0.99	4.25	2.2746	22.0327	3.0039
28	934.85	1354.4	0.087	7.192	0.3032	5.635	0.7834	64.49	27.03	0.99	4.54	2.3032	22.0943	3.0719
29	934.87	1354.3	0.087	7.193	0.3422	5.963	0.9681	79.70	33.40	1.00	5.06	2.3422	22.0659	3.0678

ARVIN/CALSPAN FIELD SERVICES, INC.
AEDC DIVISION
VON KARMAN GAS DYNAMICS FACILITY
ARNOLD AIR FORCE STATION, TENNESSEE
BNO/SAI MAT PHASE I

TABLE A-3. SHOCK LAYER DATA (CONT.D)

DATE COMPUTED 22-JUL-81
TIME COMPUTED 06:23:16
DATE RECORDED 24-APR-81
TIME RECORDED 5:51:22
PROJECT NUMBER C145VA

PAGE 2
HUN = 54
M = 7.97
RE = 1.623E+06
ALPHA SECTOR = 1.99 DEG
ALPHAP = -10.01 DEG
MODEL-ROLL = 180.00 DEG

CONFIGURATION
10.5/7-DEG BICONIC/SS+DS
NOSE RADIUS, IN
0.5000
TRIP
.06 MACHINED
FLAP
NONE

DATA TYPE 1 3, SURVEY - PP AND TT SURVEY STATION NO = 58 PPX/PT = 0.250E-03 ALPT = -2.99 DEG

TEST CONDITIONS AND LOCAL CONDITIONS AT THE PITOT PROBE

POINT	PT (PSIA)	TT (DEGR)	P (PSIA)	PT2 (PSIA)	ZP (IN)	PP (PSIA)	PP/PT2	PP/P	PP/PWX	TTLI/TT	MU	ZPU (IN)	PPU (PSIA)	PPU/PT2
30	834.83	1354.2	0.087	7.192	0.3814	8.554	1.1893	97.90	41.03	1.00	5.61	2.3814	21.3340	2.9652
31	834.76	1354.3	0.087	7.192	0.4197	10.484	1.4578	120.01	50.30	1.00	6.22	2.4197	7.6203	1.0596
32	834.85	1354.3	0.087	7.192	0.4601	11.815	1.6427	135.23	56.68	0.99	6.61	2.4601	7.1471	0.9937
33	834.68	1354.2	0.087	7.191	0.4985	12.204	1.6971	139.71	58.55	0.98	6.71	2.4985	7.1418	0.9932
34	834.80	1354.1	0.087	7.192	0.5381	12.297	1.7098	140.75	58.99	0.98	6.74	2.5381	7.1402	0.9928
35	834.87	1354.2	0.087	7.193	0.5755	12.346	1.7165	141.30	59.22	0.98	6.75	2.5755	7.1389	0.9925
36	834.89	1354.2	0.087	7.193	0.6151	12.393	1.7229	141.83	59.44	0.98	6.77	2.6151	7.1361	0.9921
37	834.85	1354.1	0.087	7.192	0.6546	12.415	1.7261	142.09	59.55	0.98	6.77	2.6546	7.1337	0.9918
38	834.78	1354.2	0.087	7.192	0.6942	12.402	1.7244	141.96	59.50	0.98	6.77	2.6942	7.1287	0.9912
39	834.80	1354.3	0.087	7.192	0.7329	12.387	1.7223	141.78	59.42	0.98	6.76	2.7329	7.1272	0.9910
40	834.87	1354.3	0.087	7.193	0.7716	12.391	1.7228	141.82	59.44	0.98	6.77	2.7716	7.1246	0.9905
41	834.75	1354.1	0.087	7.192	0.8306	12.433	1.7289	142.32	59.65	0.98	6.78	2.8306	7.1205	0.9901
42	834.92	1354.2	0.087	7.193	0.8896	12.482	1.7353	142.85	59.87	0.98	6.79	2.8896	7.1231	0.9903
43	834.92	1354.2	0.087	7.193	0.9861	12.670	1.7615	145.01	60.77	0.98	6.84	2.9861	7.1189	0.9897
44	834.89	1354.1	0.087	7.193	1.0855	13.247	1.8416	151.61	63.54	0.98	7.00	3.0855	7.1182	0.9896
45	834.77	1354.2	0.087	7.192	1.1817	14.091	1.9593	161.30	67.60	0.98	7.22	3.1817	7.1170	0.9896
46	834.79	1354.2	0.087	7.192	1.2787	14.884	2.0701	170.41	71.42	0.98	7.42	3.2787	7.1157	0.9894
47	834.65	1354.2	0.087	7.191	1.3756	15.584	2.1671	178.40	74.77	0.98	7.60	3.3756	7.1127	0.9891
48	834.54	1354.2	0.087	7.190	1.4740	16.164	2.2482	185.07	77.57	0.98	7.74	3.4740	7.1115	0.9891
49	834.67	1354.2	0.087	7.191	1.5706	17.100	2.3780	193.76	82.05	0.98	7.96	3.5706	7.1117	0.9890
50	834.71	1354.3	0.087	7.191	1.6698	18.164	2.5259	207.94	87.15	0.98	8.20	3.6698	7.1174	0.9897
51	834.76	1354.3	0.087	7.192	1.7667	19.227	2.6735	220.08	92.24	0.99	8.44	3.7667	7.1211	0.9902
52	834.81	1354.1	0.087	7.192	1.8635	20.529	2.8543	234.97	98.48	0.99	8.72	3.8635	7.1285	0.9911
53	834.84	1354.2	0.087	7.192	1.9616	21.805	3.0317	249.57	104.60	0.99	8.99	3.9616	7.1359	0.9921
54	834.69	1354.2	0.087	7.191	2.0602	22.530	3.1330	257.91	108.10	0.99	9.14	4.0602	7.1388	0.9927
55	834.81	1354.1	0.087	7.192	2.1559	22.463	3.1233	257.11	107.76	0.99	9.13	4.1559	7.1428	0.9931
56	834.77	1354.2	0.087	7.192	2.2551	21.904	3.0457	250.72	105.08	0.99	9.01	4.2551	7.1426	0.9932
57	834.83	1354.2	0.087	7.192	2.3503	21.934	3.0496	251.05	105.22	0.99	9.02	4.3503	7.1426	0.9931
58	834.79	1354.2	0.087	7.192	2.4491	7.094	0.9864	81.20	34.03	1.01	5.10	4.4491	7.1427	0.9931

ARVN/CALSPAN FIELD SERVICES, INC.
AERC DIVISION
VUH KEMAN GAS DYNAMICS FACILITY
ARNOLD AIR FORCE STATION, TENNESSEE
BHO/SAI MAT PHASE I

TABLE A-3. SHOCK LAYER DATA (CONT'D)

DATE COMPUTED 22-JUL-81
TIME COMPUTED 06:23:23
DATE RECORDED 24-SEP-81
TIME RECORDED 5:51:22
PROJECT NUMBER C145VB

FLAP
NONE

TRIP
.06 MACHINED

NOSE RADIUS, IN
0.5000

CONFIGURATION
10.5/7-DEG BICONIC/SS+DS

1.99 DEG

ALPHA SECTION
ALPHAP = -10.01 DEG

3.523E+06

MUNEL-ROLL = 180.00 DEG

ALPTE -2.99 DEG

PHX/PT = 0.250E-03

SURVEY STATION NO = 58

DATA TYPE : 3, SURVEY - PP AND TT

LOCAL CONDITIONS AT THE TOTAL TEMPERATURE PROBE

POINT	ZT (TN)	PPI (PSIA)	PPI/PMX	TTIU (DEGR)	TTLN/TT	ML	RETD	ETA	TTL (DEGR)	TTL/TT	TX (OFCR)	TIME HR:MIN:SEC
1	0.005	0.280	1.34	1143.8	0.844	0.66	1.164E+01	0.8634	1156.6	0.853	1082.	51 51:22
2	0.011	0.301	1.44	1149.3	0.848	0.74	1.239E+01	0.8643	1165.0	0.860	1082.	51 51:36
3	0.017	0.346	1.66	1163.1	0.858	0.88	1.471E+01	0.8657	1184.6	0.874	1082.	51 51:52
4	0.022	0.454	2.18	1179.5	0.870	1.12	1.887E+01	0.8681	1211.4	0.894	1082.	51 52:08
5	0.026	0.535	2.57	1186.4	0.875	1.25	2.140E+01	0.8694	1224.5	0.904	1082.	51 52:20
6	0.031	0.712	3.42	1195.8	0.882	1.50	2.642E+01	0.8718	1245.3	0.919	1082.	51 52:36
7	0.036	0.930	4.46	1202.5	0.887	1.75	3.208E+01	0.8742	1262.9	0.932	1082.	51 52:50
8	0.041	1.111	5.33	1205.9	0.890	1.94	3.657E+01	0.8759	1273.6	0.940	1081.	51 53:04
9	0.047	1.339	6.43	1208.4	0.892	2.15	4.209E+01	0.8780	1283.5	0.947	1081.	51 53:17
10	0.052	1.483	7.12	1209.3	0.893	2.27	4.552E+01	0.8792	1288.3	0.951	1081.	51 53:30
11	0.056	1.599	7.68	1209.7	0.893	2.36	4.829E+01	0.8801	1291.4	0.953	1081.	51 53:43
12	0.060	1.686	8.09	1209.8	0.893	2.43	5.034E+01	0.8808	1293.3	0.954	1081.	51 53:58
13	0.065	1.781	8.55	1209.3	0.893	2.50	5.260E+01	0.8815	1294.6	0.956	1081.	51 54:15
14	0.065	1.780	8.54	1209.3	0.893	2.50	5.257E+01	0.8815	1294.6	0.956	1081.	51 54:35
15	0.075	1.924	9.23	1208.1	0.892	2.60	5.599E+01	0.8825	1295.8	0.956	1081.	51 54:54
16	0.087	2.058	9.87	1206.7	0.891	2.70	5.923E+01	0.8835	1296.2	0.957	1081.	51 55:11
17	0.087	2.055	9.86	1206.7	0.891	2.70	5.917E+01	0.8835	1296.2	0.957	1081.	51 55:41
18	0.098	2.182	10.47	1206.0	0.890	2.78	6.217E+01	0.8844	1297.1	0.958	1080.	51 55:49
19	0.109	2.302	11.05	1206.0	0.890	2.86	6.498E+01	0.8852	1298.6	0.959	1080.	51 55:57
20	0.118	2.427	11.65	1206.7	0.891	2.94	6.783E+01	0.8860	1300.7	0.960	1080.	51 56:12
21	0.138	2.689	12.91	1209.2	0.893	3.11	7.377E+01	0.8876	1305.8	0.964	1080.	51 56:14
22	0.158	2.968	14.24	1212.5	0.895	3.27	7.998E+01	0.8893	1311.4	0.968	1080.	51 56:20
23	0.176	3.251	15.60	1216.4	0.898	3.43	8.615E+01	0.8908	1317.2	0.972	1080.	51 56:28
24	0.196	3.536	16.97	1220.4	0.901	3.58	9.238E+01	0.8923	1322.9	0.977	1080.	51 56:54
25	0.215	3.873	18.58	1224.7	0.904	3.75	9.961E+01	0.8940	1328.5	0.981	1080.	51 57:02
26	0.245	4.398	21.10	1231.0	0.909	4.00	1.109E+02	0.8966	1336.3	0.987	1080.	51 57:10
27	0.275	4.947	23.74	1236.6	0.913	4.25	1.227E+02	0.8991	1342.7	0.991	1080.	51 57:19
28	0.303	5.635	27.03	1240.9	0.916	4.54	1.377E+02	0.9021	1347.0	0.995	1080.	51 57:25
29	0.342	6.963	33.40	1246.7	0.920	5.06	1.670E+02	0.9076	1350.6	0.997	1080.	51 57:32
30	0.381	8.554	41.03	1251.4	0.924	5.61	2.022E+02	0.9136	1352.3	0.999	1079.	51 57:38

ARVIN/CALSPAN FIELD SERVICES, INC.
AEDC DIVISION
VON KARMAN GAS DYNAMICS FACILITY
ARNOLD AIR FORCE STATION, TENNESSEE
BMO/SAI MAT PHASE I

TABLE A-3. SHOCK LAYER DATA (CONT'D)

PAGE 5
RUN 54
ALPHA SECTOR = 1.99 DEG
M = 7.97
ALPHAP = -10.01 DEG
RE = 3.623E+06
MODEL-ROLL = 180.00 DEG

DATA TYPE 1 3 SURVEY - PP AND TT

SURVEY STATION NO = 58

PHX/PT = 0.250E-03

ALPT = -2.59 DEG

TRIP .06 MACHINED
FLAP NONE

CONFIGURATION
10.5/7-DEG RICONIC/SS+DS
NOSE RADIUS, IN 0.5000

LOCAL CONDITIONS AT THE TOTAL TEMPERATURE PROBE

POINT	Z ² (IN)	PRI (PSIA)	PPI/PMX	TTIU (DEGR)	TTIU/TT	ML	RETD	ETA	TTL (DEGR)	TTL/TT	TX (DEGR)	TIME HR:MIN:SEC
31	0.420	10.484	50.30	1253.5	0.926	6.22	2.460E+02	0.9203	1348.7	0.996	1079.	5: 57:45
32	0.400	11.815	56.68	1248.3	0.922	6.61	2.781E+02	0.9249	1338.5	0.988	1079.	5: 57:52
33	0.458	12.204	58.55	1243.4	0.918	6.71	2.858E+02	0.9263	1331.8	0.983	1079.	5: 57:59
34	0.538	12.297	58.99	1241.9	0.917	6.74	2.911E+02	0.9266	1329.4	0.982	1079.	5: 58: 5
35	0.516	12.346	59.22	1241.7	0.917	6.75	2.923E+02	0.9268	1329.4	0.982	1079.	5: 58:12
36	0.415	12.393	59.44	1241.7	0.917	6.77	2.933E+02	0.9270	1329.3	0.982	1078.	5: 58:19
37	0.455	12.415	59.55	1241.7	0.917	6.77	2.935E+02	0.9270	1329.2	0.982	1078.	5: 58:26
38	0.604	12.402	59.50	1241.7	0.917	6.77	2.935E+02	0.9270	1329.2	0.982	1078.	5: 58:32
39	0.733	12.387	59.42	1241.7	0.917	6.76	2.935E+02	0.9269	1329.2	0.981	1078.	5: 58:39
40	0.772	12.391	59.44	1241.6	0.917	6.77	2.935E+02	0.9270	1329.1	0.981	1078.	5: 58:46
41	0.831	12.433	59.65	1241.5	0.917	6.78	2.944E+02	0.9271	1328.9	0.981	1078.	5: 58:53
42	0.890	12.482	59.87	1241.5	0.917	6.79	2.953E+02	0.9272	1328.7	0.981	1078.	5: 59: 0
43	0.986	12.570	60.77	1241.8	0.917	6.84	2.988E+02	0.9278	1328.4	0.981	1078.	5: 59: 9
44	1.086	13.247	63.54	1242.4	0.917	7.00	3.132E+02	0.9296	1327.2	0.980	1078.	5: 59:17
45	1.182	14.091	67.60	1243.6	0.918	7.22	3.330E+02	0.9321	1325.7	0.979	1078.	5: 59:25
46	1.279	14.888	71.42	1244.8	0.919	7.42	3.514E+02	0.9346	1324.5	0.978	1078.	5: 59:34
47	1.376	15.584	74.77	1246.8	0.921	7.60	3.674E+02	0.9364	1323.3	0.978	1077.	5: 59:42
48	1.474	16.164	77.57	1248.3	0.922	7.74	3.807E+02	0.9379	1324.1	0.978	1077.	5: 59:51
49	1.571	17.100	82.05	1252.6	0.925	7.96	4.014E+02	0.9403	1325.9	0.979	1077.	5: 59:59
50	1.670	18.164	87.15	1259.1	0.930	8.20	4.242E+02	0.9429	1329.7	0.982	1077.	6: 0: 6
51	1.767	19.227	92.24	1266.2	0.935	8.44	4.465E+02	0.9454	1334.3	0.985	1077.	6: 0:16
52	1.863	20.579	98.48	1273.6	0.941	8.72	4.742E+02	0.9488	1338.4	0.988	1077.	6: 0:25
53	1.962	21.805	104.60	1280.6	0.946	8.99	5.013E+02	0.9512	1342.3	0.991	1077.	6: 0:33
54	2.060	22.530	108.10	1283.2	0.948	9.14	5.171E+02	0.9528	1343.4	0.992	1077.	6: 0:42
55	2.156	22.463	107.76	1283.2	0.948	9.13	5.157E+02	0.9527	1343.2	0.992	1077.	6: 0:50
56	2.255	21.904	105.08	1280.8	0.946	9.01	5.036E+02	0.9514	1342.2	0.991	1077.	6: 0:59
57	2.350	21.934	105.22	1280.8	0.946	9.02	5.042E+02	0.9515	1342.2	0.991	1077.	6: 1: 7
58	2.449	7.094	34.03	1257.6	0.929	5.10	1.682E+02	0.9078	1363.0	1.007	1077.	6: 1:16
59	2.548	7.088	34.00	1257.0	0.928	5.10	1.682E+02	0.9078	1362.4	1.006	1077.	6: 1:24
60	2.742	7.073	33.93	1253.9	0.926	5.10	1.683E+02	0.9078	1359.0	1.003	1077.	6: 1:35

RUN 54
PT = 834.52 PSIA
TT = 1355.4 DEGR
P = 0.0873 PSIA
RE = 3.623E+06 PER FT
MU = 7.952E-08 LBF-SEC/FT²
DENS = -52. DEG F
V = 3685.7
O = 3.887 PSIA
T = 98.8
PT2 = 7.19 PSIA
RHO = 2.385E-03 LBM/FT³
C.R. = 24.06 IN

DATE COMPUTED 22-JUL-81
TIME COMPUTED 061231Z
DATE RECORDED 24-APR-81
TIME RECORDED 5:51:22
PROJECT NUMBER C145VN

Page 1

FLAP
NONE

ARVIN/CULSPAN FIELD SERVICES, INC.
AEDC DIVISION
VON KARMAN GAS DYNAMICS FACILITY
ARKHOLD AIR FORCE STATION, TENNESSEE
RHO/SCL MAT PHASE I

TABLE A-3. SHOCK LAYER DATA (CONT'D)

PAGE 7		ALPHA SECTOR = 1.99 DEG		CONFIGURATION		NOSE RADIUS, IN		TRIP		FLAP	
RUN 54		M = 7.97		10.5/7-DEG BICONIC/SS+05		0.5000		.06		MACHINED	
RE = 3.623E+06		ALPHAP = -10.01 DEG		KNPP = 0.100		KNPPU = 1.000		APP = 0.100		APPU = 0.030	
RE = 180.00 DEG		MODEL-ROLL = 180.00 DEG		KNPP = 0.100		KNPPU = 1.000		APP = 0.100		APPU = 0.030	
DATA TYPE 1 3, SURVEY-PP AND TT		PRESSURE STABILIZATION STATISTICS		PP1/PPF		PP/PPF		KPP		THPP (SEC)	
POINT		TIME		PP (PSIA)		PP1/PPF		PP/PPF		KPP	
HR:MIN:SEC		PP (PSIA)		PP1/PPF		PP/PPF		KPP		THPP (SEC)	
31	57:45	10.484	0.9795	0.9989	0.094	0.47	7.620	1.0539	1.0063	0.150	0.07
32	57:52	11.815	0.9914	0.9997	0.083	0.42	7.147	1.0004	0.9992	-0.012	0.07
33	57:59	12.297	0.9993	0.9999	0.028	0.41	7.142	1.0013	1.0006	0.012	0.07
34	58:05	12.346	0.9993	0.9999	-0.008	0.40	7.140	1.0000	1.0003	0.011	0.07
35	58:12	12.393	1.0002	1.0003	-0.001	0.40	7.139	1.0000	1.0010	0.000	0.07
36	58:19	12.393	0.9990	1.0001	0.068	0.40	7.136	0.9992	1.0002	0.053	0.07
37	58:26	12.415	0.9995	0.9998	-0.003	0.40	7.134	1.0000	1.0003	0.004	0.07
38	58:32	12.402	1.0007	1.0004	-0.003	0.40	7.129	1.0000	0.9996	0.033	0.07
39	58:39	12.387	0.9995	0.9999	0.007	0.40	7.127	0.9992	0.9998	-0.006	0.07
40	58:46	12.391	0.9990	0.9998	-0.005	0.40	7.125	1.0013	1.0011	0.018	0.07
41	58:53	12.433	1.0002	1.0001	0.004	0.40	7.121	1.0000	1.0005	0.019	0.07
42	59:00	12.482	0.9943	0.9996	0.003	0.40	7.123	0.9996	1.0005	-0.000	0.07
43	59:07	12.670	0.9993	1.0001	0.016	0.39	7.119	1.0008	1.0011	0.021	0.07
44	59:14	13.247	0.9989	1.0002	0.029	0.38	7.118	0.9996	0.9998	0.012	0.07
45	59:21	14.091	0.9987	0.9998	0.027	0.35	7.117	1.0008	1.0004	-0.019	0.07
46	59:28	14.888	0.9986	0.9992	0.009	0.33	7.116	1.0000	1.0003	0.004	0.07
47	59:35	15.584	0.9994	1.0001	0.018	0.32	7.113	0.9983	0.9994	0.017	0.07
48	59:42	16.164	1.0002	1.0003	-0.000	0.31	7.111	1.0000	0.9992	-0.000	0.07
49	59:49	17.100	0.9990	0.9995	-0.004	0.29	7.112	1.0000	0.9997	-0.005	0.07
50	59:56	18.164	1.0007	1.0004	-0.007	0.27	7.117	0.9996	1.0001	0.010	0.07
51	60:03	19.227	0.9994	0.9999	0.010	0.26	7.121	1.0004	0.9998	0.004	0.07
52	60:10	20.529	0.9990	0.9998	0.020	0.24	7.128	1.0000	1.0000	-0.003	0.07
53	60:17	21.805	0.9997	0.9998	0.000	0.23	7.136	1.0000	1.0002	-0.007	0.07
54	60:24	22.530	0.9999	0.9998	-0.002	0.22	7.139	1.0000	1.0001	-0.000	0.07
55	60:31	22.463	0.9991	0.9997	0.004	0.22	7.143	0.9987	0.9994	-0.013	0.07
56	60:38	21.904	0.9999	0.9998	0.001	0.23	7.143	1.0004	1.0007	0.016	0.07
57	60:45	21.934	1.0003	1.0002	0.002	0.23	7.143	1.0008	1.0007	0.006	0.07
58	60:52	7.094	1.0506	0.9999	0.105	0.70	7.143	1.0000	1.0003	-0.000	0.07
59	60:59	7.088	0.9996	0.9995	0.001	0.70	7.142	0.9996	1.0005	0.009	0.07
60	61:06	7.073	1.0004	0.9998	0.005	0.70	7.134	0.9992	0.9994	0.007	0.07

PT = 834.52 PSIA
TT = 1355.4 DEGR
P = 0.0873 PSIA
RE = 3.623E+06 PER FT
MU = 7.952E-08 LBF-SEC/FT2
DEN = -52. DEG F

V = 3885.7 FT/SEC
Q = 3.887 PSIA
T = 98.8 DEGR
PT2 = 7.19 PSIA
RHO = 2.385E-03 LBM/FT3
C.R. = 24.06 IN

DATE COMPUTED 22-JUL-81
TIME COMPUTED 06:23:25
DATE RECORDED 24-APR-81
TIME RECORDED 5:51:22
PROJECT NUMBER C145VB

TABLE A-3. SHOCK LAYER DATA (CONT'D)

ARVIN/CALSPAN FIELD SERVICES, INC.
AEDC DIVISION
YUN FARMAN GAS DYNAMICS FACILITY
ARNOLD AIR FORCE STATION, TENNESSEE
RMO/SAI MAT PHASE I

PAGE 9
RUN 54 ALPHA SECTOR = 1.99 DEG
M = 7.97 ALPHAP = -10.01 DEG
RE = 3.623E+06 MODEL-ROLL = 180.00 DEG

DATA TYPE 1 3, SURVEY- PP AND TT
MODEL SURFACE TEMPERATURES

POINT	TG 1		TG 2		TG 3		TG 4		TG 5		TG 6		TG 7		TG 8		TG 9		TG 10		TG 11		TG 12		TG 13		TG 14		TG 15		TG 16		TG 17		TG 18		TG 19		TG 20		TG 21		TG 22																																																																																																																																																																																																																																																																																																																																																																																																																																																																																																																																																																																																																																																																																																																																																																																																																																																																																																																																													
	DEGR	DEGR	DEGR	DEGR	DEGR	DEGR	DEGR	DEGR	DEGR	DEGR	DEGR	DEGR	DEGR	DEGR	DEGR	DEGR	DEGR	DEGR	DEGR	DEGR	DEGR	DEGR	DEGR	DEGR	DEGR	DEGR	DEGR	DEGR	DEGR	DEGR	DEGR	DEGR	DEGR	DEGR	DEGR	DEGR	DEGR	DEGR	DEGR	DEGR	DEGR	DEGR	DEGR	DEGR	DEGR	DEGR	DEGR	DEGR	DEGR	DEGR	DEGR	DEGR	DEGR	DEGR	DEGR	DEGR	DEGR	DEGR	DEGR	DEGR	DEGR	DEGR	DEGR	DEGR	DEGR	DEGR	DEGR	DEGR	DEGR	DEGR	DEGR	DEGR	DEGR	DEGR	DEGR	DEGR	DEGR	DEGR	DEGR	DEGR	DEGR	DEGR	DEGR	DEGR	DEGR	DEGR	DEGR	DEGR	DEGR	DEGR	DEGR	DEGR	DEGR	DEGR	DEGR	DEGR	DEGR	DEGR	DEGR	DEGR	DEGR	DEGR	DEGR	DEGR	DEGR	DEGR	DEGR	DEGR	DEGR	DEGR	DEGR	DEGR	DEGR	DEGR	DEGR	DEGR	DEGR	DEGR	DEGR	DEGR	DEGR	DEGR	DEGR	DEGR	DEGR	DEGR	DEGR	DEGR	DEGR	DEGR	DEGR	DEGR	DEGR	DEGR	DEGR	DEGR	DEGR	DEGR	DEGR	DEGR	DEGR	DEGR	DEGR	DEGR	DEGR	DEGR	DEGR	DEGR	DEGR	DEGR	DEGR	DEGR	DEGR	DEGR	DEGR	DEGR	DEGR	DEGR	DEGR	DEGR	DEGR	DEGR	DEGR	DEGR	DEGR	DEGR	DEGR	DEGR	DEGR	DEGR	DEGR	DEGR	DEGR	DEGR	DEGR	DEGR	DEGR	DEGR	DEGR	DEGR	DEGR	DEGR	DEGR	DEGR	DEGR	DEGR	DEGR	DEGR	DEGR	DEGR	DEGR	DEGR	DEGR	DEGR	DEGR	DEGR	DEGR	DEGR	DEGR	DEGR	DEGR	DEGR	DEGR	DEGR	DEGR	DEGR	DEGR	DEGR	DEGR	DEGR	DEGR	DEGR	DEGR	DEGR	DEGR	DEGR	DEGR	DEGR	DEGR	DEGR	DEGR	DEGR	DEGR	DEGR	DEGR	DEGR	DEGR	DEGR	DEGR	DEGR	DEGR	DEGR	DEGR	DEGR	DEGR	DEGR	DEGR	DEGR	DEGR	DEGR	DEGR	DEGR	DEGR	DEGR	DEGR	DEGR	DEGR	DEGR	DEGR	DEGR	DEGR	DEGR	DEGR	DEGR	DEGR	DEGR	DEGR	DEGR	DEGR	DEGR	DEGR	DEGR	DEGR	DEGR	DEGR	DEGR	DEGR	DEGR	DEGR	DEGR	DEGR	DEGR	DEGR	DEGR	DEGR	DEGR	DEGR	DEGR	DEGR	DEGR	DEGR	DEGR	DEGR	DEGR	DEGR	DEGR	DEGR	DEGR	DEGR	DEGR	DEGR	DEGR	DEGR	DEGR	DEGR	DEGR	DEGR	DEGR	DEGR	DEGR	DEGR	DEGR	DEGR	DEGR	DEGR	DEGR	DEGR	DEGR	DEGR	DEGR	DEGR	DEGR	DEGR	DEGR	DEGR	DEGR	DEGR	DEGR	DEGR	DEGR	DEGR	DEGR	DEGR	DEGR	DEGR	DEGR	DEGR	DEGR	DEGR	DEGR	DEGR	DEGR	DEGR	DEGR	DEGR	DEGR	DEGR	DEGR	DEGR	DEGR	DEGR	DEGR	DEGR	DEGR	DEGR	DEGR	DEGR	DEGR	DEGR	DEGR	DEGR	DEGR	DEGR	DEGR	DEGR	DEGR	DEGR	DEGR	DEGR	DEGR	DEGR	DEGR	DEGR	DEGR	DEGR	DEGR	DEGR	DEGR	DEGR	DEGR	DEGR	DEGR	DEGR	DEGR	DEGR	DEGR	DEGR	DEGR	DEGR	DEGR	DEGR	DEGR	DEGR	DEGR	DEGR	DEGR	DEGR	DEGR	DEGR	DEGR	DEGR	DEGR	DEGR	DEGR	DEGR	DEGR	DEGR	DEGR	DEGR	DEGR	DEGR	DEGR	DEGR	DEGR	DEGR	DEGR	DEGR	DEGR	DEGR	DEGR	DEGR	DEGR	DEGR	DEGR	DEGR	DEGR	DEGR	DEGR	DEGR	DEGR	DEGR	DEGR	DEGR	DEGR	DEGR	DEGR	DEGR	DEGR	DEGR	DEGR	DEGR	DEGR	DEGR	DEGR	DEGR	DEGR	DEGR	DEGR	DEGR	DEGR	DEGR	DEGR	DEGR	DEGR	DEGR	DEGR	DEGR	DEGR	DEGR	DEGR	DEGR	DEGR	DEGR	DEGR	DEGR	DEGR	DEGR	DEGR	DEGR	DEGR	DEGR	DEGR	DEGR	DEGR	DEGR	DEGR	DEGR	DEGR	DEGR	DEGR	DEGR	DEGR	DEGR	DEGR	DEGR	DEGR	DEGR	DEGR	DEGR	DEGR	DEGR	DEGR	DEGR	DEGR	DEGR	DEGR	DEGR	DEGR	DEGR	DEGR	DEGR	DEGR	DEGR	DEGR	DEGR	DEGR	DEGR	DEGR	DEGR	DEGR	DEGR	DEGR	DEGR	DEGR	DEGR	DEGR	DEGR	DEGR	DEGR	DEGR	DEGR	DEGR	DEGR	DEGR	DEGR	DEGR	DEGR	DEGR	DEGR	DEGR	DEGR	DEGR	DEGR	DEGR	DEGR	DEGR	DEGR	DEGR	DEGR	DEGR	DEGR	DEGR	DEGR	DEGR	DEGR	DEGR	DEGR	DEGR	DEGR	DEGR	DEGR	DEGR	DEGR	DEGR	DEGR	DEGR	DEGR	DEGR	DEGR	DEGR	DEGR	DEGR	DEGR	DEGR	DEGR	DEGR	DEGR	DEGR	DEGR	DEGR	DEGR	DEGR	DEGR	DEGR	DEGR	DEGR	DEGR	DEGR	DEGR	DEGR	DEGR	DEGR	DEGR	DEGR	DEGR	DEGR	DEGR	DEGR	DEGR	DEGR	DEGR	DEGR	DEGR	DEGR	DEGR	DEGR	DEGR	DEGR	DEGR	DEGR	DEGR	DEGR	DEGR	DEGR	DEGR	DEGR	DEGR	DEGR	DEGR	DEGR	DEGR	DEGR	DEGR	DEGR	DEGR	DEGR	DEGR	DEGR	DEGR	DEGR	DEGR	DEGR	DEGR	DEGR	DEGR	DEGR	DEGR	DEGR	DEGR	DEGR	DEGR	DEGR	DEGR	DEGR	DEGR	DEGR	DEGR	DEGR	DEGR	DEGR	DEGR	DEGR	DEGR	DEGR	DEGR	DEGR	DEGR	DEGR	DEGR	DEGR	DEGR	DEGR	DEGR	DEGR	DEGR	DEGR	DEGR	DEGR	DEGR	DEGR	DEGR	DEGR	DEGR	DEGR	DEGR	DEGR	DEGR	DEGR	DEGR	DEGR	DEGR	DEGR	DEGR	DEGR	DEGR	DEGR	DEGR	DEGR	DEGR	DEGR	DEGR	DEGR	DEGR	DEGR	DEGR	DEGR	DEGR	DEGR	DEGR	DEGR	DEGR	DEGR	DEGR	DEGR	DEGR	DEGR	DEGR	DEGR	DEGR	DEGR	DEGR	DEGR	DEGR	DEGR	DEGR	DEGR	DEGR	DEGR	DEGR	DEGR	DEGR	DEGR	DEGR	DEGR	DEGR	DEGR	DEGR	DEGR	DEGR	DEGR	DEGR	DEGR	DEGR	DEGR	DEGR	DEGR	DEGR	DEGR	DEGR	DEGR	DEGR	DEGR	DEGR	DEGR	DEGR	DEGR	DEGR	DEGR	DEGR	DEGR	DEGR	DEGR	DEGR	DEGR	DEGR	DEGR	DEGR	DEGR	DEGR	DEGR	DEGR	DEGR	DEGR	DEGR	DEGR	DEGR	DEGR	DEGR	DEGR	DEGR	DEGR	DEGR	DEGR	DEGR	DEGR	DEGR	DEGR	DEGR	DEGR	DEGR	DEGR	DEGR	DEGR	DEGR	DEGR	DEGR	DEGR	DEGR	DEGR	DEGR	DEGR	DEGR	DEGR	DEGR	DEGR	DEGR	DEGR	DEGR	DEGR	DEGR	DEGR	DEGR	DEGR	DEGR	DEGR	DEGR	DEGR	DEGR	DEGR	DEGR	DEGR	DEGR	DEGR	DEGR	DEGR	DEGR	DEGR	DEGR	DEGR	DEGR	DEGR	DEGR	DEGR	DEGR	DEGR	DEGR	DEGR	DEGR	DEGR	DEGR	DEGR	DEGR	DEGR	DEGR	DEGR	DEGR	DEGR	DEGR	DEGR	DEGR	DEGR	DEGR	DEGR	DEGR	DEGR	DEGR	DEGR	DEGR	DEGR	DEGR	DEGR	DEGR	DEGR	DEGR	DEGR	DEGR	DEGR	DEGR	DEGR	DEGR	DEGR	DEGR	DEGR	DEGR	DEGR	DEGR	DEGR	DEGR	DEGR	DEGR	DEGR	DEGR	DEGR	DEGR	DEGR	DEGR	DEGR	DEGR	DEGR	DEGR	DEGR	DEGR	DEGR	DEGR	DEGR	DEGR	DEGR	DEGR	DEGR	DEGR	DEGR	DEGR	DEGR	DEGR	DEGR	DEGR	DEGR	DEGR	DEGR	DEGR	DEGR	DEGR	DEGR	DEGR	DEGR	DEGR	DEGR	DEGR	DEGR	DEGR	DEGR	DEGR	DEGR	DEGR	DEGR	DEGR	DEGR	DEGR	DEGR	DEGR	DEGR	DEGR	DEGR	DEGR	DEGR	DEGR	DEGR	DEGR	DEGR	DEGR	DEGR	DEGR	DEGR	DEGR	DEGR	DEGR	DEGR	DEGR	DEGR	DEGR	DEGR	DEGR	DEGR	DEGR	DEGR	DEGR	DEGR	DEGR	DEGR	DEGR	DEGR	DEGR	DEGR	DEGR	DEGR	DEGR	DEGR	DEGR	DEGR	DEGR	DEGR	DEGR	DEGR	DEGR	DEGR	DEGR	DEGR	DEGR	DEGR	DEGR	DEGR	DEGR

DATE COMPUTED 22-JUL-81
TIME COMPUTED 06:23:25
DATE RECORDED 24-APR-81
TIME RECORDED 5151:22
PROJECT NUMBER C145VB

TABLE A-3. SHOCK LAYER DATA (CONT'D)

ARVIN/CALSPAN FIELD SERVICES, INC.
AEDC DIVISION
VON KARMAN GAS DYNAMICS FACILITY
ARNOLD AIR FORCE STATION, TENNESSEE
BMD/SAT MAT PHASE I

PAGE 9
R/N 54
M 7.97
RE 3.623E+06
ALPHA SECTOR = 1.99 DEG
ALPHAP = -10.01 DEG
MODEL-ROLL = 180.00 DEG
CONFIGURATION 10.5/7-DEG BICONIC/SS+DS
MOSE RADIUS, IN 0.5000
TRIP .06 MACHINED
FLAP NONE

DATA TYPE 1 3, SURVEY- PP AND TT
MODEL SURFACE TEMPERATURES

POINT	TG 1	TG 2	TG 3	TG 4	TG 5	TG 6	TG 7	TG 8	TG 9	TG 10	TG 11	TG 12	TG 13	TG 14	TG 15	TG 16	TG 17	TG 18	TG 19	TG 20	TG 21	TG 22	TG 23	TG 24	TG 25	TG 26	TG 27	TG 28	TG 29	TG 30	TG 31	TG 32	TG 33	TG 34
	DEGR	DEGR	DEGR	DEGR	DEGR	DEGR	DEGR	DEGR	DEGR	DEGR	DEGR	DEGR	DEGR	DEGR	DEGR	DEGR	DEGR	DEGR	DEGR	DEGR	DEGR	DEGR	DEGR	DEGR	DEGR	DEGR	DEGR	DEGR	DEGR	DEGR	DEGR	DEGR	DEGR	DEGR
18	1163.	1163.	1141.	1131.	1080.	1099.	1081.	1081.	1012.	1012.	1012.	1012.	1012.	1012.	1012.	1012.	1012.	1012.	1012.	1012.	1012.	1012.	1012.	1012.	1012.	1012.	1012.	1012.	1012.	1012.	1012.	1012.	1012.	1012.
19	1163.	1163.	1141.	1131.	1080.	1099.	1081.	1081.	1012.	1012.	1012.	1012.	1012.	1012.	1012.	1012.	1012.	1012.	1012.	1012.	1012.	1012.	1012.	1012.	1012.	1012.	1012.	1012.	1012.	1012.	1012.	1012.	1012.	1012.
20	1163.	1163.	1139.	1131.	1080.	1099.	1081.	1081.	1012.	1012.	1012.	1012.	1012.	1012.	1012.	1012.	1012.	1012.	1012.	1012.	1012.	1012.	1012.	1012.	1012.	1012.	1012.	1012.	1012.	1012.	1012.	1012.	1012.	1012.
21	1163.	1163.	1139.	1131.	1080.	1099.	1081.	1081.	1012.	1012.	1012.	1012.	1012.	1012.	1012.	1012.	1012.	1012.	1012.	1012.	1012.	1012.	1012.	1012.	1012.	1012.	1012.	1012.	1012.	1012.	1012.	1012.	1012.	1012.
22	1163.	1163.	1139.	1131.	1080.	1099.	1081.	1081.	1012.	1012.	1012.	1012.	1012.	1012.	1012.	1012.	1012.	1012.	1012.	1012.	1012.	1012.	1012.	1012.	1012.	1012.	1012.	1012.	1012.	1012.	1012.	1012.	1012.	1012.
23	1163.	1163.	1140.	1131.	1080.	1099.	1081.	1081.	1012.	1012.	1012.	1012.	1012.	1012.	1012.	1012.	1012.	1012.	1012.	1012.	1012.	1012.	1012.	1012.	1012.	1012.	1012.	1012.	1012.	1012.	1012.	1012.	1012.	1012.
24	1163.	1163.	1140.	1131.	1080.	1099.	1081.	1081.	1012.	1012.	1012.	1012.	1012.	1012.	1012.	1012.	1012.	1012.	1012.	1012.	1012.	1012.	1012.	1012.	1012.	1012.	1012.	1012.	1012.	1012.	1012.	1012.	1012.	1012.
25	1163.	1163.	1140.	1131.	1080.	1099.	1081.	1081.	1012.	1012.	1012.	1012.	1012.	1012.	1012.	1012.	1012.	1012.	1012.	1012.	1012.	1012.	1012.	1012.	1012.	1012.	1012.	1012.	1012.	1012.	1012.	1012.	1012.	1012.
26	1163.	1163.	1139.	1131.	1080.	1099.	1081.	1081.	1012.	1012.	1012.	1012.	1012.	1012.	1012.	1012.	1012.	1012.	1012.	1012.	1012.	1012.	1012.	1012.	1012.	1012.	1012.	1012.	1012.	1012.	1012.	1012.	1012.	1012.
27	1163.	1163.	1131.	1131.	1080.	1099.	1081.	1081.	1012.	1012.	1012.	1012.	1012.	1012.	1012.	1012.	1012.	1012.	1012.	1012.	1012.	1012.	1012.	1012.	1012.	1012.	1012.	1012.	1012.	1012.	1012.	1012.	1012.	1012.
28	1163.	1163.	1142.	1131.	1080.	1099.	1081.	1081.	1012.	1012.	1012.	1012.	1012.	1012.	1012.	1012.	1012.	1012.	1012.	1012.	1012.	1012.	1012.	1012.	1012.	1012.	1012.	1012.	1012.	1012.	1012.	1012.	1012.	1012.
29	1163.	1163.	1131.	1131.	1080.	1099.	1081.	1081.	1012.	1012.	1012.	1012.	1012.	1012.	1012.	1012.	1012.	1012.	1012.	1012.	1012.	1012.	1012.	1012.	1012.	1012.	1012.	1012.	1012.	1012.	1012.	1012.	1012.	1012.
30	1163.	1163.	1137.	1131.	1079.	1099.	1081.	1081.	1012.	1012.	1012.	1012.	1012.	1012.	1012.	1012.	1012.	1012.	1012.	1012.	1012.	1012.	1012.	1012.	1012.	1012.	1012.	1012.	1012.	1012.	1012.	1012.	1012.	1012.
31	1163.	1163.	1140.	1131.	1079.	1099.	1081.	1081.	1012.	1012.	1012.	1012.	1012.	1012.	1012.	1012.	1012.	1012.	1012.	1012.	1012.	1012.	1012.	1012.	1012.	1012.	1012.	1012.	1012.	1012.	1012.	1012.	1012.	1012.
32	1163.	1163.	1142.	1131.	1079.	1099.	1081.	1081.	1012.	1012.	1012.	1012.	1012.	1012.	1012.	1012.	1012.	1012.	1012.	1012.	1012.	1012.	1012.	1012.	1012.	1012.	1012.	1012.	1012.	1012.	1012.	1012.	1012.	1012.
33	1163.	1163.	1140.	1131.	1079.	1099.	1081.	1081.	1012.	1012.	1012.	1012.	1012.	1012.	1012.	1012.	1012.	1012.	1012.	1012.	1012.	1012.	1012.	1012.	1012.	1012.	1012.	1012.	1012.	1012.	1012.	1012.	1012.	1012.
34	1163.	1163.	1136.	1131.	1079.	1099.	1081.	1081.	1012.	1012.	1012.	1012.	1012.	1012.	1012.	1012.	1012.	1012.	1012.	1012.	1012.	1012.	1012.	1012.	1012.	1012.	1012.	1012.	1012.	1012.	1012.	1012.	1012.	1012.

ARVIN/CALSPAN FIELD SERVICES, INC.
AEDC DIVISION
VON KARMAN GAS DYNAMICS FACILITY
ARNOLD AIR FORCE STATION, TENNESSEE
BMD/SAI MAT PHASE I

TABLE A-3. SHOCK LAYER DATA (CONT'D)

DATE COMPUTED 22-JUL-81
TIME COMPUTED 06:23:26
DATE RECORDED 24-APR-81
TIME RECORDED 5:51:22
PROJECT NUMBER C145VB

PAGE 10
RUN 54
ALPHA SECTOR = 1.99 DEG
M = 7.97
ALPHAP = -10.01 DEG
RE = 3.623E+06
MODEL-ROLL = 180.00 DEG

DATA TYPE 1 3, SURVEY- PP AND TT
MODEL SURFACE TEMPERATURES

POINT	TC 1	TC 2	TC 3	TC 4	TC 5	TC 6	TC 7	TC 8	TC 9	TC 10	TC 11	TC 12	TC 13	TC 14	TC 15	TC 16	TC 102	TC 104	TC 106	TC 108	TC 110	TC 112	TC 114	TC 116	TC 118	TC 120	TC 122
35	1163.	1163.	1131.	1131.	1078.	1078.	1109.	1109.	1081.	1081.	1012.	1012.	1012.	1012.	1012.	1012.	1214.	1214.	1214.	1214.	1214.	1214.	1199.	1199.	1196.	1196.	1191.
36	1163.	1163.	1131.	1131.	1078.	1078.	1109.	1109.	1081.	1081.	1012.	1012.	1012.	1012.	1012.	1012.	1215.	1215.	1215.	1215.	1215.	1215.	1199.	1199.	1196.	1196.	1193.
37	1163.	1163.	1131.	1131.	1078.	1078.	1109.	1109.	1081.	1081.	1012.	1012.	1012.	1012.	1012.	1012.	1213.	1213.	1213.	1213.	1213.	1213.	1200.	1200.	1196.	1196.	1191.
38	1163.	1163.	1131.	1131.	1078.	1078.	1109.	1109.	1081.	1081.	1012.	1012.	1012.	1012.	1012.	1012.	1216.	1216.	1216.	1216.	1216.	1216.	1200.	1200.	1196.	1196.	1193.
39	1163.	1163.	1131.	1131.	1078.	1078.	1109.	1109.	1081.	1081.	1012.	1012.	1012.	1012.	1012.	1012.	1215.	1215.	1215.	1215.	1215.	1215.	1198.	1198.	1196.	1196.	1192.
40	1163.	1163.	1131.	1131.	1078.	1078.	1109.	1109.	1081.	1081.	1012.	1012.	1012.	1012.	1012.	1012.	1212.	1212.	1212.	1212.	1212.	1212.	1199.	1199.	1196.	1196.	1189.
41	1163.	1163.	1131.	1131.	1078.	1078.	1109.	1109.	1081.	1081.	1012.	1012.	1012.	1012.	1012.	1012.	1214.	1214.	1214.	1214.	1214.	1214.	1199.	1199.	1196.	1196.	1190.
42	1163.	1163.	1131.	1131.	1078.	1078.	1109.	1109.	1081.	1081.	1012.	1012.	1012.	1012.	1012.	1012.	1214.	1214.	1214.	1214.	1214.	1214.	1199.	1199.	1196.	1196.	1190.
43	1163.	1163.	1131.	1131.	1078.	1078.	1109.	1109.	1081.	1081.	1012.	1012.	1012.	1012.	1012.	1012.	1215.	1215.	1215.	1215.	1215.	1215.	1198.	1198.	1196.	1196.	1191.
44	1163.	1163.	1131.	1131.	1078.	1078.	1109.	1109.	1081.	1081.	1012.	1012.	1012.	1012.	1012.	1012.	1212.	1212.	1212.	1212.	1212.	1212.	1198.	1198.	1195.	1195.	1189.
45	1163.	1163.	1131.	1131.	1078.	1078.	1109.	1109.	1081.	1081.	1012.	1012.	1012.	1012.	1012.	1012.	1215.	1215.	1215.	1215.	1215.	1215.	1199.	1199.	1196.	1196.	1190.
46	1163.	1163.	1131.	1131.	1078.	1078.	1109.	1109.	1081.	1081.	1012.	1012.	1012.	1012.	1012.	1012.	1214.	1214.	1214.	1214.	1214.	1214.	1199.	1199.	1196.	1196.	1192.
47	1163.	1163.	1131.	1131.	1077.	1077.	1109.	1109.	1081.	1081.	1012.	1012.	1012.	1012.	1012.	1012.	1212.	1212.	1212.	1212.	1212.	1212.	1198.	1198.	1195.	1195.	1190.
48	1163.	1163.	1131.	1131.	1077.	1077.	1109.	1109.	1081.	1081.	1012.	1012.	1012.	1012.	1012.	1012.	1216.	1216.	1216.	1216.	1216.	1216.	1199.	1199.	1196.	1196.	1191.
49	1163.	1163.	1131.	1131.	1077.	1077.	1109.	1109.	1081.	1081.	1012.	1012.	1012.	1012.	1012.	1012.	1213.	1213.	1213.	1213.	1213.	1213.	1199.	1199.	1195.	1195.	1191.
50	1163.	1163.	1131.	1131.	1077.	1077.	1109.	1109.	1081.	1081.	1012.	1012.	1012.	1012.	1012.	1012.	1214.	1214.	1214.	1214.	1214.	1214.	1199.	1199.	1196.	1196.	1191.
51	1163.	1163.	1131.	1131.	1077.	1077.	1109.	1109.	1081.	1081.	1012.	1012.	1012.	1012.	1012.	1012.	1215.	1215.	1215.	1215.	1215.	1215.	1199.	1199.	1196.	1196.	1191.

ARVIN/CALSPAN FIELD SERVICES, INC.
AEDC DIVISION
VON KARMAN GAS DYNAMICS FACILITY
ARNOLD AIR FORCE STATION, TENNESSEE
BMD/SAI MAT PHASE I

TABLE A-3. SHOCK LAYER DATA (CONT'D)

DATE COMPUTED 22-JUL-81
TIME COMPUTED 06:23:27
DATE RECORDED 24-APR-81
TIME RECORDED 5:51:22
PROJECT NUMBER C145VR

PAGE 11
RUN 54 ALPHA SECTOR = 1.99 DEG
M = 7.97 ALPHA = -10.01 DEG
RE = 1.623E+06 MODEL-ROLL = 180.00 DEG

NOSE RADIUS, IN 0.5000
TRIP .06 MACHINED
FLAP NONE

DATA TYPE : 3, SURVEY- PP AND TT
MODEL SURFACE TEMPERATURES

POINT	TC 1	TC 2	TC 3	TC 4	TC 5	TC 6	TC 7	TC 8	TC 9	TC 10	TC 11	TC 12	TC 13	TC 14	TC 15	TC 16	TC 102	TC 106	TC 110	TC 114	TC 118	TC 122
52	1163.	1138.	1130.	1140.	1077.	1109.	1080.	1012.	1012.	1012.	1012.	1012.	1012.	1012.	1012.	1012.	1214.	1195.	1199.	1199.	1196.	1190.
53	1163.	1130.	1140.	1077.	1109.	1080.	1012.	1012.	1012.	1012.	1012.	1012.	1012.	1012.	1012.	1012.	1215.	1191.	1200.	1196.	1196.	1191.
54	1163.	1131.	1142.	1077.	1109.	1080.	1012.	1012.	1012.	1012.	1012.	1012.	1012.	1012.	1012.	1012.	1216.	1193.	1199.	1196.	1196.	1192.
55	1163.	1131.	1139.	1077.	1109.	1080.	1012.	1012.	1012.	1012.	1012.	1012.	1012.	1012.	1012.	1012.	1213.	1177.	1199.	1196.	1196.	1190.
56	1163.	1139.	1130.	1077.	1108.	1080.	1012.	1012.	1012.	1012.	1012.	1012.	1012.	1012.	1012.	1012.	1214.	1189.	1199.	1196.	1196.	1190.
57	1163.	1130.	1139.	1077.	1108.	1080.	1012.	1012.	1012.	1012.	1012.	1012.	1012.	1012.	1012.	1012.	1215.	1188.	1199.	1196.	1196.	1191.
58	1163.	1138.	1130.	1077.	1108.	1080.	1012.	1012.	1012.	1012.	1012.	1012.	1012.	1012.	1012.	1012.	1214.	1189.	1199.	1196.	1196.	1190.
59	1162.	1130.	1140.	1077.	1109.	1080.	1012.	1012.	1012.	1012.	1012.	1012.	1012.	1012.	1012.	1012.	1215.	1190.	1199.	1196.	1196.	1191.
60	1163.	1140.	1130.	1077.	1109.	1080.	1012.	1012.	1012.	1012.	1012.	1012.	1012.	1012.	1012.	1012.	1214.	1190.	1199.	1196.	1196.	1191.

RUN 54
PT = 834.52 PSIA
TT = 1355.4 DEGR
P = 0.0873 PSIA
RE = 3.623E+06 PER FT
MU = 7.952E-08 LBF-SEC/FT2
DEW = -52. DEG F
V = 3885.7 FT/SEC
Q = 3.887 PSIA
T = 98.8 DEGR
PT2 = 7.19 PSIA
RHO = 2.385E-03 LBM/FT3
C.P. = 24.06 IN

(Reynolds number) corrected total temperature profiles, respectively. Figures A-14 and A-15 are the Pitot pressure profiles normalized by the local wall static pressure, P , (Figure A-14) and by the freestream Pitot pressure, PT_2 (Figure A-15).

Boundary layer type analyses were performed using these data and the assumption that the static pressure in the shock layer was constant and equal to the local wall static pressure. Thus with the static pressure assumed and the local values of PT_2 and TT , local state variables in the shock layer were defined including local values of the viscous layer thicknesses. Note, the assumption of constant static pressure is incorrect outside of the boundary layer and consequently the local derived properties in the "inviscid" flow are not valid. The reader is referred to Section 4 of the report for a discussion of this. Nevertheless, Table A-4 (4 pages) defines the derived local properties for the same data group defined in Table A-3. Figures A-16 through A-18 graphically define the derived local properties. One notes from Figure A-16 that the freestream Mach number (noted by the several data points at $ZP > 2.3$) is ~ 0.75 of the boundary layer edge Mach number, clearly incorrect.

The Mach/Flow-Angularity data tabulations for a given data group are contained in two tables sets, Table A-5 (9 pages) and Table A-6 (2 pages). Table A-5 defines the measured data while Table A-6 presents the computed flow direction results. The corresponding graphical presentation of these data are shown in Figure A-19 for the raw data and Figure A-20 for the derived properties.

A.5 Static Force Data

The force and moment measurements were reduced to coefficient form using digitally filtered data points and correcting for first and second order balance interaction effects. The coefficients were also corrected for model tare weight and balance-sting deflections. Model attitude and tunnel stilling chamber pressure were calculated from digitally filtered values.

AMERICAN AIR FORCE RESEARCH LABORATORY
AFCO DIVISION
VON KARMAN GAS DYNAMICS FACILITY
ARMED AIR FORCE STATION, TENNESSEE
RND/SAI MAT PHASE I

TABLE A-4. BOUNDARY LAYER AND SHOCK LAYER DERIVED DATA

PROJECT NUMBER C14SV8

PAGE 1
RUN 54
M = 7.97
PE = 3.623E+06

ALPHA SCOTON = 1.99 DEG
ALPHAP = -10.01 DEG
MODEL-POUL = 180.00 DEG

CONFIGURATION
10.5/7-DEG RICONIC/SS+DS

NOISE RADIUS, IN
0.5000

FLAP
NONE

DATA TYPE: 3. SURVEY-PP AND TT SURVEY STATION 58 PHX/PT = 2.497E-04

POINT	ZP (IN)	PP (PSIA)	TX (DEGR)	PP/PHX	PP/P	ML	TL (DEGR)	W (FT/SEC)	RETO	PT (PSIA)	TT (DEGR)
1	0.0050	0.280	1156.6	1.344	3.207	0.66	1062.8	1061.4	1.104E+01	834.516	1355.4
2	0.0110	0.301	1165.0	1.444	3.445	0.74	1049.0	1180.8	1.239E+01	834.625	1355.4
3	0.0168	0.346	1184.6	1.659	3.959	0.88	1025.0	1384.6	1.471E+01	834.719	1355.4
4	0.0220	0.454	1211.4	2.180	5.200	1.12	969.5	1705.0	1.887E+01	834.559	1355.3
5	0.0258	0.535	1221.5	2.569	6.129	1.25	932.6	1872.7	2.140E+01	834.422	1355.3
6	0.0306	0.712	1245.3	3.417	8.153	1.50	859.4	2153.3	2.642E+01	834.465	1355.2
7	0.0362	0.930	1262.9	4.405	10.653	1.75	782.6	2402.4	3.208E+01	834.559	1355.1
8	0.0406	1.111	1273.6	5.330	12.717	1.94	727.9	2560.6	3.658E+01	834.489	1355.2
9	0.0470	1.339	1283.5	6.427	15.334	2.15	668.2	2719.1	4.209E+01	834.512	1355.2
10	0.0518	1.483	1284.3	7.118	16.984	2.27	635.1	2801.4	4.551E+01	834.565	1355.0
11	0.0565	1.599	1291.4	7.676	18.314	2.36	610.4	2860.4	4.827E+01	834.411	1354.9
12	0.0602	1.686	1293.3	8.094	19.312	2.43	593.1	2900.5	5.033E+01	834.447	1355.0
13	0.0654	1.781	1294.6	8.550	20.399	2.50	575.3	2940.4	5.259E+01	834.344	1354.9
14	0.0654	1.781	1294.6	8.550	20.430	2.50	575.3	2939.8	5.257E+01	834.578	1354.8
15	0.0753	1.924	1295.8	9.731	22.024	2.60	549.8	2994.0	5.590E+01	834.563	1354.7
16	0.0873	2.058	1296.2	9.873	23.556	2.70	527.9	3039.2	5.923E+01	834.570	1354.7
17	0.0871	2.057	1296.2	9.872	23.554	2.70	527.9	3038.4	5.917E+01	834.622	1354.7
18	0.0980	2.182	1297.1	10.469	24.978	2.78	508.7	3077.9	6.217E+01	834.625	1354.6
19	0.1086	2.302	1298.6	11.049	26.363	2.86	491.9	3113.4	6.498E+01	834.512	1354.6
20	0.1160	2.427	1300.7	11.647	27.780	2.94	476.0	3148.0	6.782E+01	834.455	1354.5
21	0.1377	2.669	1305.8	12.405	30.791	3.11	445.9	3214.5	7.376E+01	834.544	1354.4
22	0.1578	2.968	1311.4	14.244	33.985	3.27	418.1	3276.2	7.944E+01	834.476	1354.4
23	0.1764	3.251	1317.2	15.603	37.227	3.43	393.5	3331.5	8.613E+01	834.453	1354.5
24	0.1958	3.536	1322.9	16.866	40.460	3.58	371.6	3380.8	9.233E+01	834.646	1354.4
25	0.2153	3.873	1328.5	18.582	44.337	3.75	348.7	3431.4	9.961E+01	834.613	1354.4
26	0.2449	4.398	1336.3	21.104	50.353	4.00	318.0	3497.9	1.109E+02	834.674	1354.3
27	0.2746	4.947	1342.7	23.736	56.634	4.25	291.2	3554.6	1.227E+02	834.667	1354.4
28	0.3032	5.635	1347.0	27.030	64.492	4.54	263.0	3609.0	1.377E+02	831.845	1354.4
29	0.3422	6.863	1350.6	33.403	79.698	5.06	220.9	3684.2	1.671E+02	834.868	1354.3
30	0.3914	8.554	1352.3	50.297	120.005	5.61	185.3	3744.6	2.023E+02	834.835	1354.2
31	0.4197	10.484	1348.7	56.679	135.212	6.22	154.4	3788.2	2.461E+02	834.755	1354.3
32	0.4601	11.815	1338.5	58.553	150.705	6.71	132.9	3795.4	2.781E+02	834.867	1354.3
33	0.4985	12.204	1331.8	58.993	160.754	6.74	131.8	3794.0	2.845E+02	834.676	1354.2
34	0.5381	12.297	1329.8	59.224	141.304	6.75	131.3	3784.1	2.923E+02	834.796	1354.1
35	0.5755	12.346	1329.4	59.444	141.831	6.77	130.9	3794.7	2.934E+02	834.894	1354.2
36	0.6151	12.393	1329.3	59.555	142.094	6.77	130.7	3794.9	2.930E+02	834.851	1354.1
37	0.6546	12.415	1329.2	59.555	142.094	6.77	130.7	3794.8	2.930E+02	834.776	1354.2
38	0.6942	12.402	1329.2	59.497	141.957	6.77	130.8	3794.8	2.933E+02	834.799	1354.3
39	0.7329	12.387	1329.2	59.425	141.784	6.76	130.9	3794.6	2.933E+02	834.874	1354.3
40	0.7716	12.391	1329.1	59.440	141.821	6.77	130.9	3794.4	2.933E+02	834.874	1354.3

TABLE A-4. BOUNDARY LAYER AND SHOCK LAYER DERIVED DATA (CONT'D)

AVIATION SPAN FILLED SERVICES, INC.
AEROC DEVELOPMENT
VON KARMAN GAS DYNAMICS FACILITY
ARMED AIR FORCE STATION, TENNESSEE
PRO/SAT MAT PHASE I

PROJECT NUMBER C14SV8

PAGE 2
PUN = 54
M = 7.97
PE = 3.623E+06
ALPHA SECTOR = 1.99 DEG
ALPHAF = -10.01 DEG
MODEL-PULL = 180.00 DEG

NOSE RADIUS, IN 0.5000

TRIP MACHINED
FLAP NONE

DATA TYPE 3, SURVEY-PP AND TT
SURVEY STATION 58
PWX/PT = 2.497E-04

LOCAL CONDITIONS AT THE PITOT PROBE

POINT	ZN	PP	TTLI	PP/PWX	PP/P	ML	TL (DEGR)	UL (FT/SEC)	RETD	PT (PSIA)	TT (DEGR)
41	0.8300	12.433	1328.9	59.651	142.324	6.78	130.4	3794.8	2.944E+02	834.751	1354.1
42	0.8896	12.482	1328.7	59.872	142.852	6.79	130.0	3795.3	2.956E+02	834.916	1354.2
43	0.9361	12.670	1328.4	60.775	143.005	6.84	128.2	3787.6	2.994E+02	834.919	1354.2
44	1.0955	13.247	1327.2	63.541	151.605	7.00	123.0	3803.9	3.133E+02	834.892	1354.1
45	1.1817	14.091	1325.7	67.603	161.296	7.22	116.0	3812.4	3.330E+02	834.775	1354.2
46	1.2787	14.888	1324.5	71.424	170.414	7.42	110.2	3819.7	3.515E+02	834.794	1354.2
47	1.3756	15.584	1324.3	73.773	178.404	7.60	105.6	3826.7	3.674E+02	834.655	1354.2
48	1.4740	16.164	1324.1	77.569	185.074	7.74	102.1	3832.0	3.807E+02	834.544	1354.2
49	1.5706	17.100	1325.9	82.047	195.760	7.96	97.0	3847.6	4.014E+02	834.668	1354.2
50	1.6698	18.164	1329.7	87.150	207.935	8.20	92.0	3856.5	4.247E+02	834.712	1354.3
51	1.7667	19.227	1344.3	92.242	220.045	8.44	87.5	3870.5	4.466E+02	834.763	1354.3
52	1.8635	20.529	1338.4	98.482	234.973	8.72	82.5	3884.7	4.743E+02	834.809	1354.1
53	1.9616	21.805	1342.3	104.600	249.570	8.99	78.2	3897.4	5.014E+02	834.842	1354.2
54	2.0602	22.530	1343.4	108.097	257.914	9.14	75.8	3902.7	5.172E+02	834.692	1354.2
55	2.1559	22.463	1343.2	107.762	257.113	9.13	76.1	3902.0	5.158E+02	834.811	1354.1
56	2.2551	21.904	1342.2	105.084	250.725	9.01	77.0	3897.8	5.037E+02	834.775	1354.2
57	2.3503	21.934	1342.2	105.219	251.046	9.02	77.7	3897.8	5.044E+02	834.829	1354.2
58	2.4491	7.094	1363.0	34.033	81.202	5.10	219.5	3706.9	1.682E+02	834.743	1354.2
59	2.5475	7.048	1362.4	34.004	81.132	5.10	219.5	3705.7	1.682E+02	834.787	1354.3
60	2.7416	7.073	1349.0	31.930	80.956	5.10	219.4	3700.4	1.683E+02	834.703	1354.3

TUNNEL CONDITIONS (MEAN VALUES)

PT = 834.68 PSIA
TT = 1354.5 DEGR
P = 0.0874 PSIA
PE = 3.627E+06 PER FT
MU = 7.947E-08 LMF-SEC/FT2
V = 3884.4 FT/SEC
Q = 3.888 PSIA
T = 98.8 DEGR
PT2 = 7.19 PSIA
RHU = 2.387E-03 LHM/FT3

PUN 54

INVENT/CAUSPAN PFILO SERVICES, INC.
 AEC DIVISION
 VON KARMAN GAS DYNAMICS FACILITY
 ARNOLD AIR FORCE STATION, TENNESSEE
 RAO/SAI "AT PHASE 1"

TABLE A-4. BOUNDARY LAYER AND SHOCK LAYER DERIVED DATA (CONT'D)

PROJECT NUMBER C145VR

FLAP
 NONE

TRIP
 .06 MACHINED

NOSE RADIUS, IN
 0.5000

CONFIGURATION
 10.5/7-DEG BICONIC/SS+DS

PAGE 3
 RUN 54 ALPHA SECTOR = 1.99 DEG
 M = 7.97 ALPHA = -10.01 DEG
 PC = 3.673F+06 MODEL-ROLL = 180.00 DEG

SURVEY STATION NO = 58

DATA TYPE 3, SURVEY-PP AND TT

POINT	2P/DEL	NP/PP	MI/WE	TTL/TTE	TI/TE	PHOL/RHOP	UL/UE	MUTL/MUTE	REL/REE	RETL/RETTE	DITTL/DOITTE
1	1.097E-02	2.371E-02	1.005E-01	8.641E-01	7.723E+00	1.294E-01	2.794E-01	5.636E+00	6.417E-03	3.969E-02	2.844E-01
2	2.380E-02	2.547E-02	1.126E-01	8.704E-01	7.623E+00	1.312E-01	3.109E-01	5.581E+00	7.297E-03	4.454E-02	3.165E-01
3	3.647E-02	2.927E-02	1.336E-01	8.850E-01	7.448E+00	1.342E-01	3.545E-01	5.502E+00	8.892E-03	5.288E-02	3.912E-01
4	4.781E-02	3.844E-02	1.691E-01	9.051E-01	7.045E+00	1.419E-01	4.488E-01	5.302E+00	1.201E-02	6.785E-02	4.946E-01
5	5.690E-02	4.502E-02	1.894E-01	9.148E-01	6.777E+00	1.475E-01	4.930E-01	5.166E+00	1.407E-02	7.693E-02	5.452E-01
6	6.642E-02	6.024E-02	2.268E-01	9.304E-01	6.245E+00	1.601E-01	5.669E-01	4.886E+00	1.857E-02	9.497E-02	6.257E-01
7	7.672E-02	7.875E-02	2.652E-01	9.435E-01	5.687E+00	1.758E-01	6.374E-01	4.578E+00	2.479E-02	1.153E-01	6.940E-01
8	8.817E-02	9.400E-02	2.911E-01	9.515E-01	5.248E+00	1.890E-01	6.741E-01	4.340E+00	2.929E-02	1.313E-01	7.364E-01
9	1.021E-01	1.135E-01	3.244E-01	9.549E-01	4.856E+00	2.050E-01	7.158E-01	4.088E+00	3.605E-02	1.513E-01	7.752E-01
10	1.175E-01	1.255E-01	3.443E-01	9.628E-01	4.461E+00	2.166E-01	7.375E-01	3.939E+00	4.055E-02	1.636E-01	7.935E-01
11	1.223E-01	1.354E-01	3.575E-01	9.648E-01	4.043E+00	2.253E-01	7.530E-01	3.825E+00	4.416E-02	1.734E-01	8.059E-01
12	1.308E-01	1.427E-01	3.678E-01	9.662E-01	4.310E+00	2.319E-01	7.616E-01	3.741E+00	4.711E-02	1.810E-01	8.134E-01
13	1.427E-01	1.508E-01	3.747E-01	9.672E-01	4.179E+00	2.342E-01	7.741E-01	3.657E+00	5.062E-02	1.891E-01	8.184E-01
14	1.421E-01	1.511E-01	3.785E-01	9.672E-01	4.180E+00	2.341E-01	7.739E-01	3.658E+00	5.054E-02	1.890E-01	8.184E-01
15	1.604E-01	1.624E-01	3.943E-01	9.681E-01	3.955E+00	2.507E-01	7.882E-01	3.534E+00	5.581E-02	2.013E-01	8.242E-01
16	1.898E-01	1.742E-01	4.064E-01	9.685E-01	3.833E+00	2.608E-01	8.001E-01	3.425E+00	6.086E-02	2.130E-01	8.264E-01
17	1.892E-01	1.741E-01	4.064E-01	9.685E-01	3.833E+00	2.608E-01	8.001E-01	3.425E+00	6.086E-02	2.127E-01	8.272E-01
18	2.131E-01	1.872E-01	4.214E-01	9.691E-01	3.697E+00	2.704E-01	8.103E-01	3.328E+00	6.584E-02	2.235E-01	8.312E-01
19	2.364E-01	1.949E-01	4.334E-01	9.707E-01	3.575E+00	2.796E-01	8.146E-01	3.242E+00	7.070E-02	2.336E-01	8.381E-01
20	2.564E-01	2.054E-01	4.456E-01	9.718E-01	3.450E+00	2.898E-01	8.247E-01	3.158E+00	7.582E-02	2.438E-01	8.460E-01
21	2.943E-01	2.276E-01	4.701E-01	9.756E-01	3.240E+00	3.085E-01	8.462E-01	2.947E+00	8.711E-02	2.552E-01	8.559E-01
22	3.410E-01	2.517E-01	4.968E-01	9.798E-01	3.038E+00	3.290E-01	8.625E-01	2.844E+00	9.976E-02	2.674E-01	8.681E-01
23	3.813E-01	2.752E-01	5.196E-01	9.841E-01	2.860E+00	3.492E-01	8.770E-01	2.705E+00	1.133E-01	3.097E-01	9.109E-01
24	4.255E-01	2.993E-01	5.414E-01	9.883E-01	2.700E+00	3.702E-01	8.900E-01	2.578E+00	1.278E-01	3.319E-01	9.336E-01
25	4.678E-01	3.278E-01	5.675E-01	9.926E-01	2.534E+00	3.948E-01	9.033E-01	2.441E+00	1.408E-01	3.581E-01	9.552E-01
26	5.122E-01	3.723E-01	6.057E-01	9.984E-01	2.311E+00	4.325E-01	9.208E-01	2.252E+00	1.724E-01	3.988E-01	9.857E-01
27	5.966E-01	4.187E-01	6.433E-01	1.003E+00	2.114E+00	4.725E-01	9.358E-01	2.081E+00	2.124E-01	4.413E-01	1.010E+00
28	6.590E-01	4.769E-01	6.873E-01	1.009E+00	1.911E+00	5.231E-01	9.501E-01	1.895E+00	2.623E-01	4.952E-01	1.028E+00
29	7.438E-01	5.494E-01	7.654E-01	1.009E+00	1.666E+00	6.228E-01	9.659E-01	1.608E+00	3.741E-01	6.007E-01	1.043E+00
30	8.249E-01	6.494E-01	8.494E-01	1.010E+00	1.347E+00	7.425E-01	9.858E-01	1.347E+00	5.435E-01	7.213E-01	1.051E+00
31	9.172E-01	7.873E-01	9.415E-01	1.010E+00	1.122E+00	8.413E-01	9.972E-01	1.122E+00	7.923E-01	8.446E-01	1.037E+00
32	1.000E+00	1.000E+00	1.000E+00	1.000E+00	1.000E+00	1.000E+00	1.000E+00	1.000E+00	1.000E+00	1.000E+00	1.000E+00
33	1.083E+00	1.031E+00	1.017E+00	9.950E-01	9.661E-01	1.035E+00	9.915E-01	9.661E-01	1.070E+00	1.037E+00	9.721E-01
34	1.170E+00	1.041E+00	1.020E+00	9.935E-01	9.581E-01	1.044E+00	9.886E-01	9.581E-01	1.088E+00	1.047E+00	9.653E-01
35	1.251E+00	1.045E+00	1.024E+00	9.931E-01	9.544E-01	1.048E+00	9.886E-01	9.544E-01	1.097E+00	1.051E+00	9.636E-01
36	1.337E+00	1.049E+00	1.024E+00	9.931E-01	9.513E-01	1.051E+00	9.886E-01	9.513E-01	1.104E+00	1.055E+00	9.621E-01
37	1.423E+00	1.051E+00	1.025E+00	9.931E-01	9.495E-01	1.053E+00	9.886E-01	9.495E-01	1.108E+00	1.057E+00	9.638E-01
38	1.509E+00	1.050E+00	1.025E+00	9.931E-01	9.503E-01	1.052E+00	9.886E-01	9.503E-01	1.104E+00	1.055E+00	9.642E-01
39	1.593E+00	1.048E+00	1.024E+00	9.931E-01	9.514E-01	1.051E+00	9.886E-01	9.514E-01	1.104E+00	1.055E+00	9.640E-01
40	1.677E+00	1.049E+00	1.024E+00	9.930E-01	9.511E-01	1.051E+00	9.886E-01	9.511E-01	1.104E+00	1.055E+00	9.646E-01

TABLE A-4. BOUNDARY LAYER AND SHOCK LAYER DERIVED DATA (CONT'D)

PROJECT NUMBER C145VB

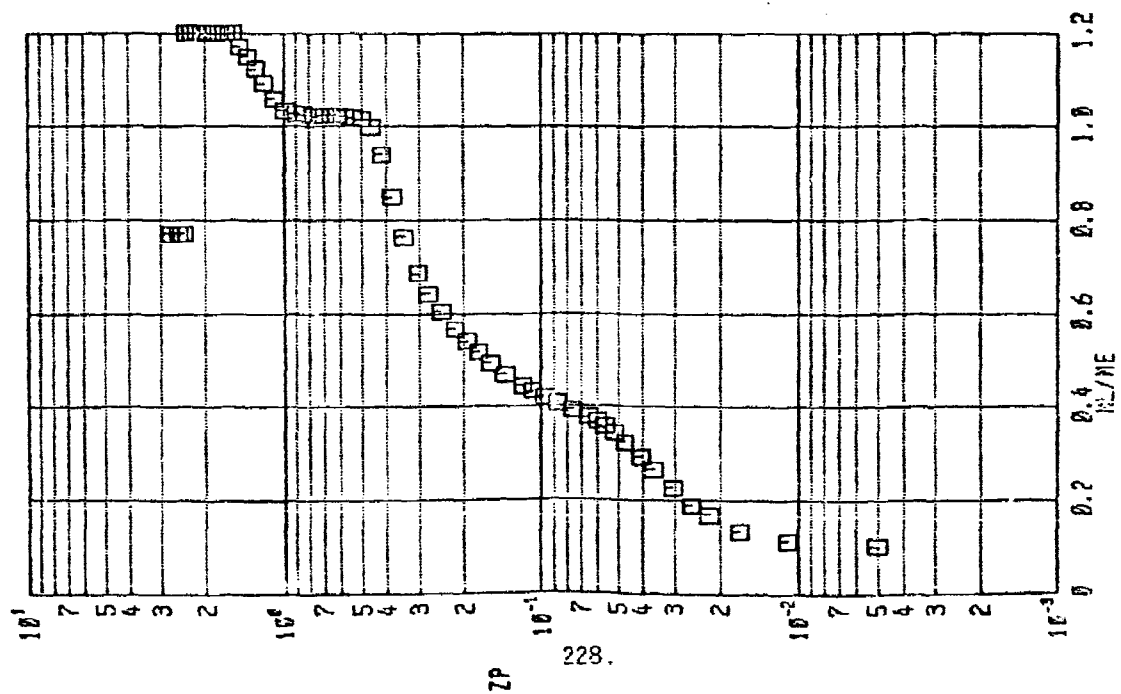
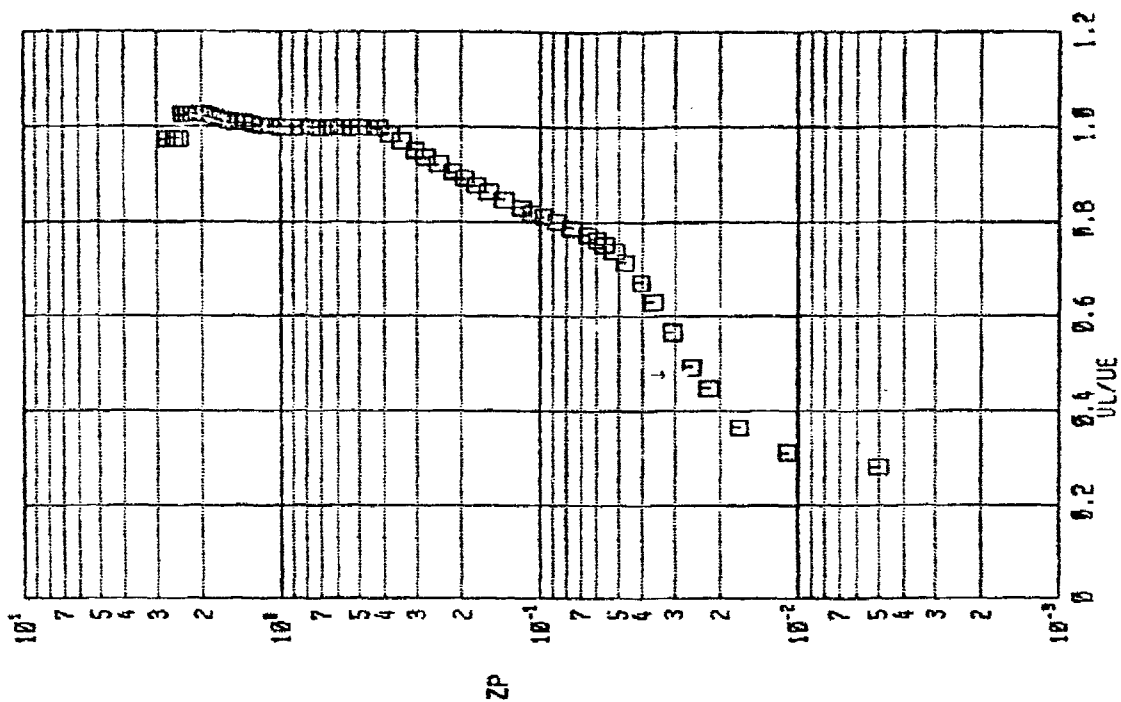
PAGE 4
 RUN 54
 ALPHA SECTOR = 1.99 DEG
 M = 7.97
 PE = 3.623E+06
 MODEL-PULL = 180.00 DEG
 CONFIGURATION 10.5/7-DEG RICONIC/SS+DS
 NOISE RADIUS, IN 0.5000
 TRIP .06 MACHINED
 FLAP NONE

DATA TYPE: 3. SURVEY-PP AND TT
 BOUNDARY LAYER INTEGRAL EVALUATION

POINT	ZF/DEL	PP/PPF	ML/ME	TTL/TTE	TL/TE	RHOL/RHOE	UL/UR	MUTL/MUTE	REL/REE	RETL/RETE	DITTL/DITTE
41	1.805E+00	1.052E+00	1.026E+00	9.928E-01	9.479E-01	1.055E+00	9.990E-01	9.479E-01	1.117E+00	1.059E+00	9.644E-01
42	1.973E+00	1.054E+00	1.028E+00	9.927E-01	9.446E-01	1.054E+00	9.991E-01	9.446E-01	1.120E+00	1.063E+00	9.639E-01
43	2.143E+00	1.072E+00	1.036E+00	9.925E-01	9.316E-01	1.074E+00	9.992E-01	9.316E-01	1.152E+00	1.078E+00	9.629E-01
44	2.354E+00	1.121E+00	1.064E+00	9.916E-01	8.937E-01	1.114E+00	1.001E+00	8.937E-01	1.254E+00	1.127E+00	9.588E-01
45	2.565E+00	1.193E+00	1.093E+00	9.904E-01	8.433E-01	1.146E+00	1.004E+00	8.433E-01	1.411E+00	1.197E+00	9.532E-01
46	2.776E+00	1.260E+00	1.124E+00	9.895E-01	8.040E-01	1.244E+00	1.006E+00	8.040E-01	1.568E+00	1.264E+00	9.488E-01
47	2.987E+00	1.319E+00	1.156E+00	9.844E-01	7.676E-01	1.302E+00	1.007E+00	7.676E-01	1.709E+00	1.321E+00	9.443E-01
48	3.204E+00	1.368E+00	1.171E+00	9.843E-01	7.418E-01	1.348E+00	1.009E+00	7.418E-01	1.832E+00	1.369E+00	9.475E-01
49	3.415E+00	1.447E+00	1.205E+00	9.806E-01	7.050E-01	1.418E+00	1.012E+00	7.050E-01	2.035E+00	1.443E+00	9.547E-01
50	3.629E+00	1.537E+00	1.242E+00	9.735E-01	6.683E-01	1.498E+00	1.015E+00	6.683E-01	2.273E+00	1.525E+00	9.700E-01
51	3.840E+00	1.627E+00	1.279E+00	9.690E-01	6.358E-01	1.573E+00	1.019E+00	6.358E-01	2.520E+00	1.605E+00	9.879E-01
52	4.050E+00	1.737E+00	1.321E+00	1.000E+00	5.997E-01	1.667E+00	1.023E+00	5.997E-01	2.843E+00	1.705E+00	1.004E+00
53	4.263E+00	1.845E+00	1.361E+00	1.003E+00	5.681E-01	1.760E+00	1.026E+00	5.681E-01	3.179E+00	1.803E+00	1.020E+00
54	4.478E+00	1.907E+00	1.394E+00	1.004E+00	5.512E-01	1.814E+00	1.027E+00	5.512E-01	3.331E+00	1.859E+00	1.025E+00
55	4.690E+00	1.901E+00	1.342E+00	1.003E+00	5.577E-01	1.804E+00	1.027E+00	5.577E-01	3.363E+00	1.854E+00	1.024E+00
56	4.901E+00	1.854E+00	1.364E+00	1.003E+00	5.656E-01	1.768E+00	1.026E+00	5.656E-01	3.207E+00	1.811E+00	1.020E+00
57	5.104E+00	1.856E+00	1.345E+00	1.003E+00	5.649E-01	1.770E+00	1.026E+00	5.649E-01	3.216E+00	1.813E+00	1.020E+00
58	5.323E+00	6.004E-01	7.727E-01	1.018E+00	1.595E+00	6.270E-01	9.758E-01	1.596E+00	3.834E-01	6.049E-01	1.107E+00
59	5.537E+00	5.999E-01	7.724E-01	1.018E+00	1.595E+00	6.268E-01	9.755E-01	1.596E+00	3.831E-01	6.047E-01	1.099E+00
60	5.959E+00	5.988E-01	7.715E-01	1.015E+00	1.594E+00	6.272E-01	9.741E-01	1.595E+00	3.831E-01	6.052E-01	1.086E+00

***** EDGE VALUES *****

DEL = 4.601E-01 INCH
 DEL* = 2.620E-01 INCH
 DEL** = 1.304E-02 INCH
 DEL3 = 2.390E-02 INCH
 DEL4 = 3.216E-04 INCH
 PUN 54
 PTE = 1.102E+01 PSTA
 ME = 6.605E+00
 TTE = 1.338E+03 DEGR
 TE = 1.376E+02 DEGR
 ME = 3.764E+03 FT/SEC
 PHOE = 4.089E-03 LRM/FT3
 RHOE = 1.553E+01 LRM/SEC-FT2
 MUTE = 1.106E-07 LRM-SEC/FT2
 REE = 3.636E+05 PER INCH
 RETTE = 5.562E+04 PER INCH
 DITTE = 6.662E+01 RTU/IN

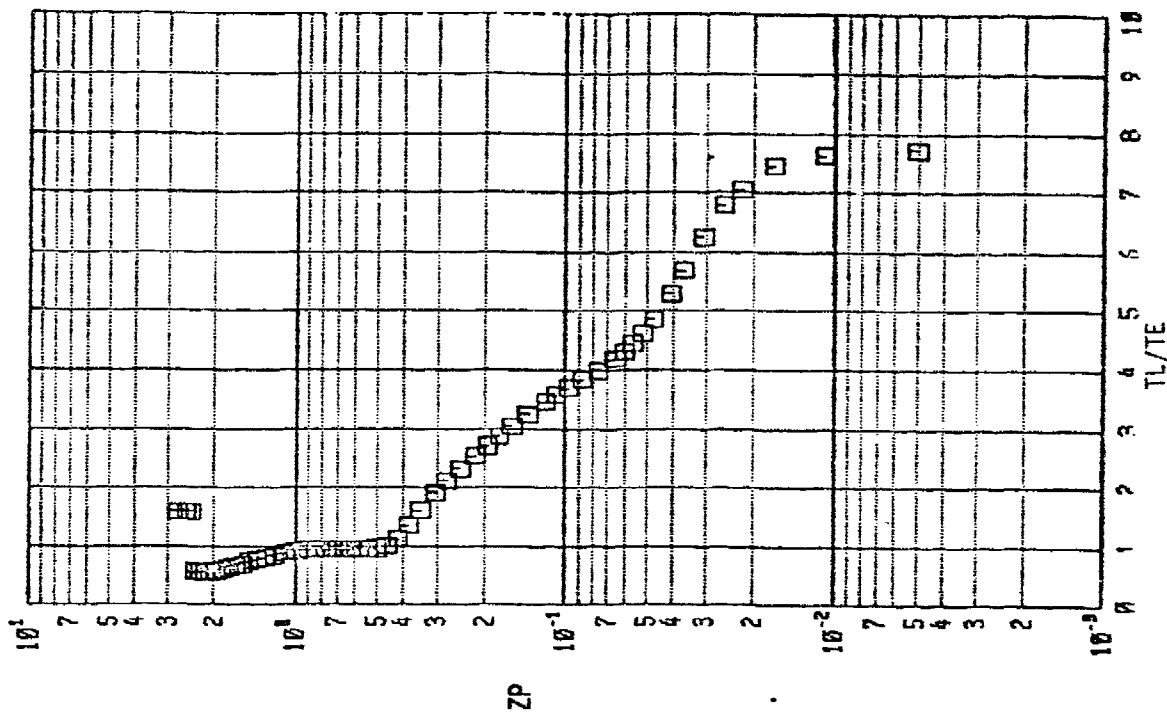
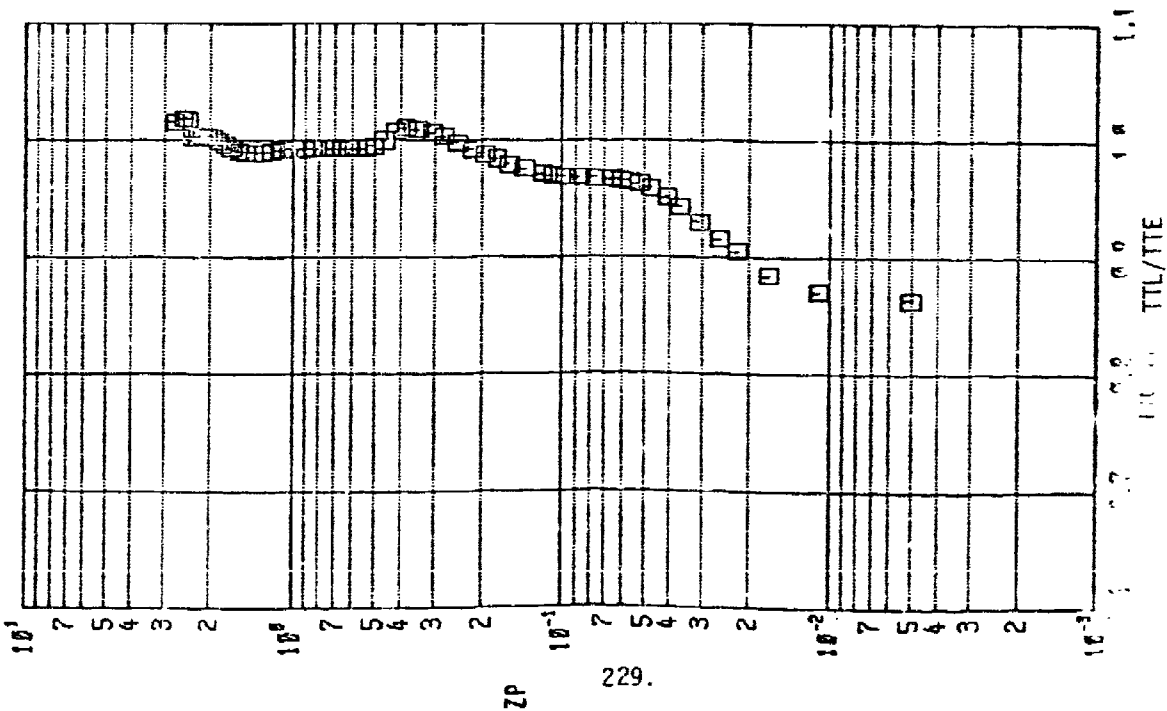


PAGE 6
14-0015-01
09:34

BOUNDARY LAYER DATA/8M0/SRI MAT

FIGURE A-16. DERIVED LOCAL MACH NUMBER AND VELOCITY DATA

RUN 054



RUN 054

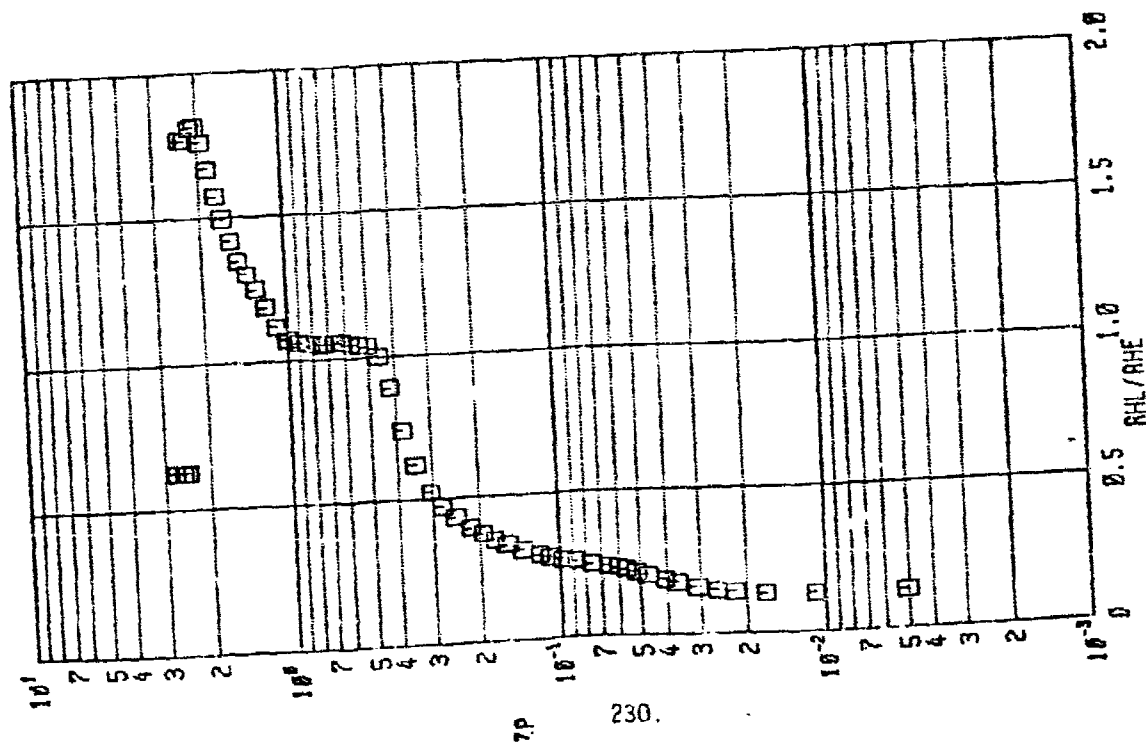
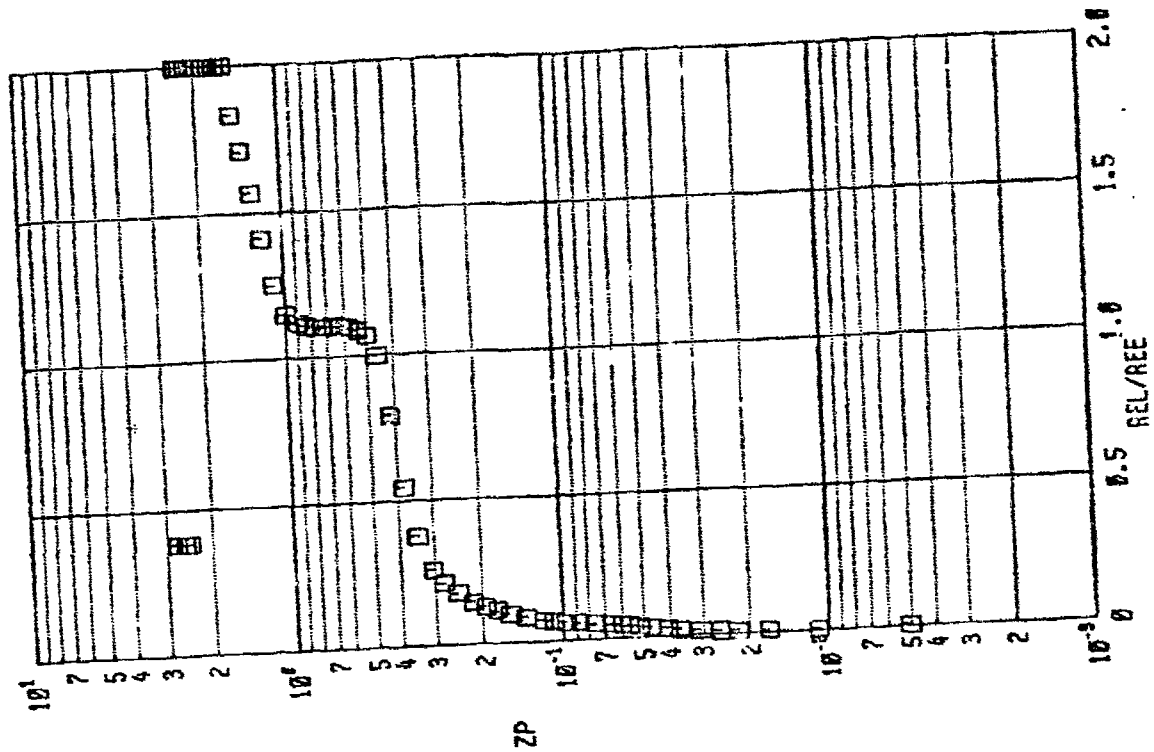
TTL/TTE

TL/TE

BOUNDARY LAYER DATA/8MO/SAT MAT

PLUG 7
14-815-01
10128

FIGURE A-17. DERIVED LOCAL STATIC AND TOTAL TEMPERATURE DATA



PRG 8
18-005-01
11.12

BOUNDARY LAYER DATA/BMD/SRI MPT

FIGURE A-18. DERIVED LOCAL DENSITY AND REYNOLDS NUMBER DATA

RUN 054

TIME COMPUTED 13/22/51
DATE RECORDED 30-APR-51
TIME RECORDED 9:31:57
PROJECT NUMBER C145VH

TABLE A-5. MACH/FLOW-ANGULARITY PROBE MEASURED DATA

ARVIN/CALSPAN FIELD SERVICES, INC.
AEDC DIVISION
VON KARMAN GAS DYNAMICS FACILITY
ARNOLD AIR FORCE STATION, TENNESSEE
END/XXI MAT PHASE 1

FLAP
NONE

TRIP
.06 MACHINED

NOSE RADIUS, IN
0.5000

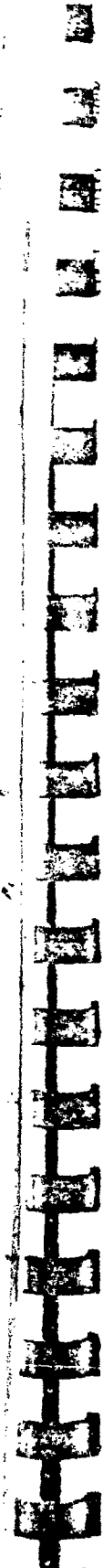
CONFIGURATION
10.5/7-DEG RICONIC/SS+DS

PAGE 1 218 ALPHA SECTOR = -8.01 DEG
RUN M = 7.97 ALPHAP = -20.01 DEG
RE = 1.627E+06 MODEL-ROLL = 180.00 DEG

DATA TYPE: 2, SURVEY-MACH/ FLOW ANGULARITY PROBE SURVEY STATION NO = 39 PNX/PT = 1.109E-03

TEST CONDITIONS AND LOCAL CONDITIONS FROM P5 OF THE MACH/FLOW ANGULARITY PROBE

POINT	PT	PT1	P	PT2	ZM	P5	P5/PT2	P5/P	P5/PNX	ML	TREC (SEC)	TOEL (SEC)
1	833.22	1352.8	0.087	7.179	0.0220	5.362	0.7459	61.49	5.80	2.03	2.34	10.0
2	833.73	1352.4	0.087	7.183	0.0482	7.121	0.9413	81.61	7.70	2.37	1.8	2.0
3	833.42	1352.3	0.087	7.181	0.0581	8.380	1.1670	96.08	9.07	2.58	7.8	2.0
4	833.15	1352.0	0.087	7.178	0.0675	9.357	1.3035	107.31	10.13	2.74	7.8	2.0
5	833.11	1351.8	0.087	7.178	0.0773	10.200	1.4719	117.06	11.05	2.86	7.8	2.0
6	833.75	1351.6	0.087	7.175	0.0877	11.000	1.5469	127.35	12.02	2.99	7.8	2.0
7	832.87	1351.4	0.087	7.174	0.0977	11.909	1.6601	136.67	12.90	3.10	7.8	2.0
8	834.12	1351.3	0.087	7.186	0.1082	12.737	1.7723	145.00	13.77	3.21	7.8	2.0
9	834.28	1351.0	0.087	7.188	0.1173	13.413	1.8661	153.61	14.50	3.30	7.8	2.0
10	834.76	1350.5	0.087	7.192	0.1171	13.609	1.9049	156.81	14.80	3.23	7.8	2.0
11	834.97	1350.3	0.087	7.193	0.1244	14.376	1.9985	164.51	15.53	3.42	7.8	2.0
12	834.84	1350.2	0.087	7.192	0.1348	14.845	2.0619	169.90	16.03	3.47	7.8	2.0
13	834.68	1350.1	0.087	7.191	0.1492	15.111	2.1009	172.94	16.39	3.51	7.8	2.0
14	835.62	1350.1	0.087	7.199	0.1666	15.412	2.1409	176.73	16.63	3.54	7.8	2.0
15	836.02	1350.0	0.087	7.202	0.1887	15.614	2.1679	178.45	16.84	3.56	7.8	2.0
16	836.11	1350.0	0.088	7.203	0.2073	15.795	2.1920	180.51	17.03	3.58	7.8	2.0
17	836.22	1349.9	0.088	7.204	0.2270	16.059	2.2242	183.49	17.32	3.62	7.8	2.0
18	836.10	1349.9	0.089	7.205	0.2483	16.460	2.2844	188.01	17.74	3.66	7.8	2.0
19	836.54	1349.9	0.089	7.206	0.2759	17.109	2.3741	195.41	18.44	3.73	7.8	2.0
20	835.09	1349.8	0.087	7.194	0.3059	17.822	2.4722	203.92	19.24	3.82	7.8	2.0
21	834.97	1349.8	0.087	7.193	0.3146	18.374	2.5542	210.26	19.84	3.88	7.8	2.0
22	835.25	1349.8	0.087	7.196	0.3735	18.825	2.6101	215.34	20.32	3.92	7.8	2.0
23	835.29	1349.8	0.087	7.196	0.4133	19.026	2.6439	217.64	20.54	3.95	7.8	2.0
24	835.19	1349.8	0.087	7.195	0.4512	19.103	2.6549	218.87	20.67	3.95	7.8	2.0
25	835.10	1349.8	0.087	7.195	0.4915	19.129	2.6586	218.87	20.66	3.96	7.8	2.0
26	835.00	1349.8	0.087	7.194	0.5294	19.138	2.6603	218.99	20.67	3.96	7.8	2.0
27	835.01	1349.8	0.087	7.194	0.5692	19.142	2.6608	219.03	20.67	3.96	7.8	2.0
28	834.64	1350.0	0.087	7.191	0.6069	19.193	2.6691	219.71	20.71	3.97	7.8	2.0
29	834.78	1350.1	0.087	7.192	0.6466	19.240	2.6753	220.22	20.74	3.97	7.8	2.0



ARVIN/CALOGAN FIELD SERVICES, INC.
AIRC DIVISION
VON KARMAN GAS DYNAMICS FACILITY
ARMED STP FORCE STATION, TENNESSEE
RND/SST MAT PHASE I

TABLE A-5. MACH/FLOW-ANGULARITY PROBE MEASURED DATA
(CONT'D)

RUN 2 218 ALPHA SECTOR = -8.01 DEG
M = 7.91 ALPHA P = -20.01 DEG
PS = 3.577E+06 MODEL-ROLL = 180.00 DEG

DATE COMPUTED 20-JUL-81
TIME COMPUTED 13:22:51
DATE RECORDED 30-APR-81
TIME RECORDED 91 3157
PROJECT NUMBER C145VB

FLAP NONE
TRIP .06 MACHINED

NOSE RADIUS, IN 0.5000

CONFIGURATION 10.5/7-DEG BICONIC/SS+DS

DATA TYPE: 2, SURVEY-MACH/ FLOW ANGULARITY PROBE

SURVEY STATION NO = 39

DATA TYPE: 2, SURVEY-MACH/ FLOW ANGULARITY PROBE

DATA TYPE: 2, SURVEY-MACH/ FLOW ANGULARITY PROBE

TEST CONDITIONS AND LOCAL CONDITIONS FROM PS OF THE MACH/FLOW ANGULARITY PROBE

POINT	PT (PSIA)	TT (DEGR)	P (PSIA)	PT2 (PSIA)	ZM (IN)	P5 (PSIA)	P5/PT2	P5/P	P5/PWK	ML	TREC (SEC)	TDEL (SEC)
30	835.32	1350.1	0.087	7.196	0.6862	19.300	2.6820	220.77	20.83	3.97	7.8	2.0
31	835.39	1350.2	0.087	7.197	0.7256	19.341	2.6874	221.22	20.88	3.98	7.8	2.0
32	835.28	1350.3	0.087	7.196	0.7646	19.381	2.6933	221.70	20.92	3.98	7.8	2.0
33	835.07	1350.5	0.087	7.194	0.8031	19.493	2.7096	223.04	21.05	4.00	7.8	2.0
34	834.94	1350.6	0.087	7.193	0.8623	19.743	2.7466	225.93	21.32	4.02	7.8	2.0
35	834.85	1350.7	0.087	7.192	0.9212	20.213	2.8103	231.34	21.83	4.07	7.8	2.0
36	834.49	1350.9	0.087	7.189	1.0184	20.983	2.9195	240.25	22.67	4.15	7.8	2.0
37	834.51	1351.1	0.087	7.190	1.1172	21.824	3.0354	249.87	23.58	4.24	7.8	2.0
38	835.05	1351.1	0.087	7.194	1.2140	22.646	3.1478	259.12	24.45	4.31	7.8	2.0
39	834.99	1351.4	0.087	7.194	1.3112	23.487	3.2449	268.76	25.36	4.40	7.8	2.0
40	834.81	1351.5	0.087	7.192	1.4084	24.285	3.3760	277.96	26.23	4.47	7.8	2.0
41	831.74	1351.7	0.087	7.192	1.5065	24.375	3.3495	279.01	26.33	4.48	7.8	2.0
42	831.54	1351.9	0.087	7.190	1.6040	21.298	2.9622	243.85	23.01	4.14	7.8	2.0
43	834.44	1352.1	0.087	7.189	1.7022	6.00	0.8352	68.76	6.44	2.16	7.8	2.0
44	834.24	1352.2	0.087	7.188	1.7999	5.994	0.8318	68.64	6.48	2.15	7.8	2.0
45	834.28	1352.3	0.087	7.188	1.8968	5.998	0.8344	68.69	6.48	2.16	7.8	2.0
46	834.14	1352.4	0.087	7.187	1.9953	5.992	0.8337	68.63	6.48	2.15	7.8	2.0
47	834.14	1352.5	0.087	7.187	1.9954	5.988	0.8332	68.59	6.47	2.15	7.8	2.0

RUN 218
PT = 833.72 PSIA
TT = 1352.8 DEGR
P = 0.0872 PSIA
RE = 3.627E+06 PER Y
MFI = 7.937E+08 LAF-SEC/PT2
DEW = -53. DEG F
V = 3882.0 FT/SEC
O = 3.881 PSIA
T = 98.6 DEGR
PT2 = 7.18 PSIA
RHO = 2.386E-03 LBM/FT3
C.R. = -0.05 IN

TIME COMPUTED 13/02/17
DATE RECORDED 30-09-81
TIME RECORDED 01.11.51
PROJECT NUMBER C145VM

TABLE A-5. MACH/FLOW-ANGULARITY PROBE MEASURED DATA
(CONT'D)

CONFIGURATION																	NOSE RADIUS, IN		TRIP		FLAP																																																																																																																																																																																																																																																																																																																																																																																																																																																																																																																																																																																																																																																																																																																																																																																																																																																																																																																																																																																																																																																																																																																																																																																																																																																																																																																																																																																																																																																																																																														
10.5/7-DEG R/CN/C/SS+DS																	0.5000		.06		MACHINED																																																																																																																																																																																																																																																																																																																																																																																																																																																																																																																																																																																																																																																																																																																																																																																																																																																																																																																																																																																																																																																																																																																																																																																																																																																																																																																																																																																																																																																																																																														
SURVEY STATION NO. 39																																																																																																																																																																																																																																																																																																																																																																																																																																																																																																																																																																																																																																																																																																																																																																																																																																																																																																																																																																																																																																																																																																																																																																																																																																																																																																																																																																																																																																																																																																																																			
DATA TYPE 2, SURVEY-MACH/FLOW ANGULARITY PROBE																																																																																																																																																																																																																																																																																																																																																																																																																																																																																																																																																																																																																																																																																																																																																																																																																																																																																																																																																																																																																																																																																																																																																																																																																																																																																																																																																																																																																																																																																																																																			
POINT	P1	P2	P3	P4	P5	P6	P7	P8	P9	P10	P11	P12	P13	P14	P15	P16	P17	P18	P19	P20	P21	P22	P23	P24	P25	P26	P27	P28	P29	P30	P31	P32	P33	P34	P35	P36	P37	P38	P39	P40	P41	P42	P43	P44	P45	P46	P47	P48	P49	P50	P51	P52	P53	P54	P55	P56	P57	P58	P59	P60	P61	P62	P63	P64	P65	P66	P67	P68	P69	P70	P71	P72	P73	P74	P75	P76	P77	P78	P79	P80	P81	P82	P83	P84	P85	P86	P87	P88	P89	P90	P91	P92	P93	P94	P95	P96	P97	P98	P99	P100	P101	P102	P103	P104	P105	P106	P107	P108	P109	P110	P111	P112	P113	P114	P115	P116	P117	P118	P119	P120	P121	P122	P123	P124	P125	P126	P127	P128	P129	P130	P131	P132	P133	P134	P135	P136	P137	P138	P139	P140	P141	P142	P143	P144	P145	P146	P147	P148	P149	P150	P151	P152	P153	P154	P155	P156	P157	P158	P159	P160	P161	P162	P163	P164	P165	P166	P167	P168	P169	P170	P171	P172	P173	P174	P175	P176	P177	P178	P179	P180	P181	P182	P183	P184	P185	P186	P187	P188	P189	P190	P191	P192	P193	P194	P195	P196	P197	P198	P199	P200	P201	P202	P203	P204	P205	P206	P207	P208	P209	P210	P211	P212	P213	P214	P215	P216	P217	P218	P219	P220	P221	P222	P223	P224	P225	P226	P227	P228	P229	P230	P231	P232	P233	P234	P235	P236	P237	P238	P239	P240	P241	P242	P243	P244	P245	P246	P247	P248	P249	P250	P251	P252	P253	P254	P255	P256	P257	P258	P259	P260	P261	P262	P263	P264	P265	P266	P267	P268	P269	P270	P271	P272	P273	P274	P275	P276	P277	P278	P279	P280	P281	P282	P283	P284	P285	P286	P287	P288	P289	P290	P291	P292	P293	P294	P295	P296	P297	P298	P299	P300	P301	P302	P303	P304	P305	P306	P307	P308	P309	P310	P311	P312	P313	P314	P315	P316	P317	P318	P319	P320	P321	P322	P323	P324	P325	P326	P327	P328	P329	P330	P331	P332	P333	P334	P335	P336	P337	P338	P339	P340	P341	P342	P343	P344	P345	P346	P347	P348	P349	P350	P351	P352	P353	P354	P355	P356	P357	P358	P359	P360	P361	P362	P363	P364	P365	P366	P367	P368	P369	P370	P371	P372	P373	P374	P375	P376	P377	P378	P379	P380	P381	P382	P383	P384	P385	P386	P387	P388	P389	P390	P391	P392	P393	P394	P395	P396	P397	P398	P399	P400	P401	P402	P403	P404	P405	P406	P407	P408	P409	P410	P411	P412	P413	P414	P415	P416	P417	P418	P419	P420	P421	P422	P423	P424	P425	P426	P427	P428	P429	P430	P431	P432	P433	P434	P435	P436	P437	P438	P439	P440	P441	P442	P443	P444	P445	P446	P447	P448	P449	P450	P451	P452	P453	P454	P455	P456	P457	P458	P459	P460	P461	P462	P463	P464	P465	P466	P467	P468	P469	P470	P471	P472	P473	P474	P475	P476	P477	P478	P479	P480	P481	P482	P483	P484	P485	P486	P487	P488	P489	P490	P491	P492	P493	P494	P495	P496	P497	P498	P499	P500	P501	P502	P503	P504	P505	P506	P507	P508	P509	P510	P511	P512	P513	P514	P515	P516	P517	P518	P519	P520	P521	P522	P523	P524	P525	P526	P527	P528	P529	P530	P531	P532	P533	P534	P535	P536	P537	P538	P539	P540	P541	P542	P543	P544	P545	P546	P547	P548	P549	P550	P551	P552	P553	P554	P555	P556	P557	P558	P559	P560	P561	P562	P563	P564	P565	P566	P567	P568	P569	P570	P571	P572	P573	P574	P575	P576	P577	P578	P579	P580	P581	P582	P583	P584	P585	P586	P587	P588	P589	P590	P591	P592	P593	P594	P595	P596	P597	P598	P599	P600	P601	P602	P603	P604	P605	P606	P607	P608	P609	P610	P611	P612	P613	P614	P615	P616	P617	P618	P619	P620	P621	P622	P623	P624	P625	P626	P627	P628	P629	P630	P631	P632	P633	P634	P635	P636	P637	P638	P639	P640	P641	P642	P643	P644	P645	P646	P647	P648	P649	P650	P651	P652	P653	P654	P655	P656	P657	P658	P659	P660	P661	P662	P663	P664	P665	P666	P667	P668	P669	P670	P671	P672	P673	P674	P675	P676	P677	P678	P679	P680	P681	P682	P683	P684	P685	P686	P687	P688	P689	P690	P691	P692	P693	P694	P695	P696	P697	P698	P699	P700	P701	P702	P703	P704	P705	P706	P707	P708	P709	P710	P711	P712	P713	P714	P715	P716	P717	P718	P719	P720	P721	P722	P723	P724	P725	P726	P727	P728	P729	P730	P731	P732	P733	P734	P735	P736	P737	P738	P739	P740	P741	P742	P743	P744	P745	P746	P747	P748	P749	P750	P751	P752	P753	P754	P755	P756	P757	P758	P759	P760	P761	P762	P763	P764	P765	P766	P767	P768	P769	P770	P771	P772	P773	P774	P775	P776	P777	P778	P779	P780	P781	P782	P783	P784	P785	P786	P787	P788	P789	P790	P791	P792	P793	P794	P795	P796	P797	P798	P799	P800	P801	P802	P803	P804	P805	P806	P807	P808	P809	P810	P811	P812	P813	P814	P815	P816	P817	P818	P819	P820	P821	P822	P823	P824	P825	P826	P827	P828	P829	P830	P831	P832	P833	P834	P835	P836	P837	P838	P839	P840	P841	P842	P843	P844	P845	P846	P847	P848	P849	P850	P851	P852	P853	P854	P855	P856	P857	P858	P859	P860	P861	P862	P863	P864	P865	P866	P867	P868	P869	P870	P871	P872	P873	P874	P875	P876	P877	P878	P879	P880	P881	P882	P883	P884	P885	P886	P887	P888	P889	P890	P891	P892	P893	P894	P895	P896	P897	P898	P899	P900	P901	P902	P903	P904	P905	P906	P907	P908	P909	P910	P911	P912	P913	P914	P915	P916	P917	P918	P919	P920	P921	P922	P923	P924	P925	P926	P927	P928	P929	P930	P931	P932	P933	P934	P935	P936	P937	P938	P939	P940	P941	P942	P943	P944	P945	P946	P947	P948	P949	P950	P951	P952	P953	P954	P955	P956	P957	P958	P959	P960	P961	P962	P963	P964	P965	P966	P967	P968	P969	P970	P971	P972	P973	P974	P975	P976	P977	P978	P979	P980	P981	P982	P983	P984	P985	P986	P987	P988	P989	P990	P991	P992	P993	P994	P995	P996	P997	P998	P999	P1000	P1001	P1002	P1003	P1004	P1005	P1006	P1007	P1008	P1009	P1010	P1011	P1012	P1013	P1014	P1015	P1016	P1017	P1018	P1019	P1020	P1021	P1022	P1023	P1024	P1025	P1026	P1027	P1028	P1029	P1030	P1031	P1032	P1033	P1034	P1035	P1036	P1037	P1038	P1039	P1040	P1041	P1042	P1043	P1044	P1045	P1046	P1047	P1048	P1049	P1050	P1051	P1052	P1053	P1054	P1055	P1056	P1057	P1058	P1059	P1060	P1061	P1062	P1063	P1064	P1065	P1066	P1067	P1068	P1069	P1070	P1071	P1072	P1073	P1074	P1075	P1076	P1077	P1078	P1079	P1080	P1081	P1082	P1083	P1084	P1085	P1086	P1087	P1088	P1089	P1090	P1091	P1092	P1093	P1094	P1095	P1096	P1097	P1098	P1099	P1100	P1101	P1102	P1103	P1104	P1105	P1106	P1107	P1108	P1109	P1110	P1111	P1112	P1113	P1114	P1115	P1116	P1117	P1118	P1119	P1120	P1121	P1122	P1123	P1124	P1125	P1126	P1127	P1128	P1129	P1130	P1131	P1132	P1133	P1134	P1135	P1136	P1137	P1138	P1139	P1140	P1141	P1142	P1143	P1144	P1145	P1146	P1147	P1148	P1149	P1150	P1151	P1152	P1153	P1154	P1155	P1156	P1157	P1158	P1159	P1160	P1161	P1162	P1163	P1164	P1165	P1166	P1167	P1168	P1169	P1170	P1171	P1172	P1173	P1174	P1175	P1176	P1177	P1178	P1179	P1180	P1181	P1182	P1183	P1184	P1185	P1186	P1187	P1188	P1189	P1190	P1191	P1192	P1193	P1194	P1195	P1196	P1197	P1198	P1199	P1200	P1201	P1202	P1203	P1204	P1205	P1206	P1207	P1208	P1209	P1210	P1211	P1212	P1213	P1214	P1215	P1216	P1217	P1218	P1219	P1220	P1221	P1222	P1223	P1224	P1225	P1226	P1227	P1228	P1229	P1230	P1231	P1232	P1233	P1234	P1235	P1236	P1237	P1238	P1239	P1240	P1241	P1242	P1243	P1244	P1245	P1246	P1247	P1248	P1249	P1250	P1251	P1252	P1253	P1254	P1255	P1256	P1257	P1258	P1259	P1260	P1261	P1262	P1263	P1264	P1265	P1266	P1267	P1268	P1269	P1270	P1271	P1272	P1273	P1274	P1275	P1276	P1277	P1278	P1279	P1280	P1281	P1282	P1283	P1284	P1285	P1286	P1287	P1288	P1289	P1290	P1291	P1292	P1293	P1294	P1295	P1296	P1297	P1298	P1299	P1300	P1301	P1302	P1303	P1304	P1305	P1306	P1307	P1308	P1309	P1310	P1311	P1312	P1313	P1314	P1315	P1316	P1317	P1318	P1319	P1320	P1321	P1322	P1323	P1324	P1325	P1326	P1327	P1328	P1329	P1330	P1331	P1332	P1333	P1334	P1335	P1336	P1337	P1338	P1339	P1340	P1341	P1342	P1343	P1344	P1345	P1346	P1347	P1348	P1349	P1350	P1351	P1352	P1353	P1354	P1355	P1356	P1357	P1358	P1359	P1360	P1361	P1362	P1363	P1364	P1365	P1366	P1367	P1368	P1369	P1370	P1371	P1372	P1373	P1374	P1375	P1376	P1377	P1378	P1379	P1380	P1381	P1382	P1383	P1384	P1385	P1386	P1387	P1388	P1389	P1390	P1391	P1392	P1393	P1394	P1395	P1396	P1397	P1398	P1399	P1400	P1401	P1402	P1403	P1404	P1405	P1406	P1407	P1408	P1409	P1410	P1411	P1412	P1413	P1414	P1415	P1416	P1417	P1418	P1419	P1420	P1421	P1422	P1423	P1424	P1425	P1426	P1427	P1428	P1429	P1430	P1431	P1432	P1433	P1434	P1435	P1436	P1437	P1438	P1439	P1440	P1441	P1442	P1443	P1444	P1445	P1446	P1447	P1448	P1449	P1450	P1451	P1452	P1453	P1454	P1455	P1456	P1457	P1458	P1459	P1460	P1461	P1462	P1463	P1464	P1465	P1466	P1467	P1468	P1469	P1470	P1471	P1472	P1473	P1474	P147

833

DATE COMPUTED 20-JUL-81
TIME COMPUTED 13:22:52
DATE RECORDED 30-APR-81
TIME RECORDED 91 3:57
PROJECT NUMBER C145VH

TABLE A-5. MACH/FLOW-ANGULARITY PROBE MEASURED DATA
(CONT'D)

ARVIN/CALSPAN FIELD SERVICES, INC.
AERC DIVISION
VON KARMAN GAS DYNAMICS FACILITY
ARNDOLF AIR FORCE STATION, TENNESSEE
PHD/SAI MAT PHASE I

PAGE 4	CONFIGURATION										NOSE RADIUS, IN		TRIP		FLAP			
RUN 218	10.5/7-DEG RICONIC/SS+08										0.5000		.06 MACHINED		NONE			
M = 7.97	ALPHAP = -20.01 DEG																	
RE = 1.627E+06	MODEL-POGL = 180.00 DEG																	
DATA TYPE: 2, SURVEY-MACH/FLOW ANGULARITY PROBE														SURVEY STATION NO = 39				
POINT	P1	P2	P3	P4	P5	P1F	P2F	P3F	P4F	P5F	PAVG/PS	DPSOP	MLC	AATCA	CPHI	ALPT	PAVGPC	
	(PSIA)	(PSIA)	(PSIA)	(PSIA)	(PSIA)	(PSIA)	(PSIA)	(PSIA)	(PSIA)	(PSIA)				(DEG)	(DEG)	(DEG)		
31	5.006	3.954	1.752	2.246	19.361	0.999	1.000	1.000	1.000	1.000	0.168	0.095	3.846	10.14	207.69	-20.05	0.166	
32	5.039	3.976	1.757	2.251	19.361	1.001	1.000	1.000	1.000	1.000	0.168	0.096	3.836	10.19	207.73	-20.04	0.167	
33	5.082	4.014	1.759	2.260	19.493	1.000	1.000	1.000	1.001	1.000	0.168	0.096	3.838	10.26	207.82	-20.04	0.167	
34	5.170	4.103	1.775	2.280	19.743	0.999	1.000	1.000	1.001	1.000	0.169	0.098	3.837	10.37	208.23	-20.03	0.167	
35	5.254	4.263	1.831	2.306	20.213	0.999	1.000	1.002	1.001	1.000	0.169	0.098	3.824	10.36	209.76	-20.02	0.168	
36	5.371	4.567	1.954	2.355	20.983	1.000	1.000	1.004	1.001	1.000	0.170	0.097	3.783	10.26	212.92	-20.03	0.169	
37	5.504	4.872	2.094	2.424	21.624	1.000	1.000	1.004	1.002	1.000	0.171	0.096	3.741	10.12	215.67	-20.05	0.169	
38	5.648	5.170	2.226	2.498	22.646	1.000	1.000	1.002	1.001	0.999	0.171	0.096	3.707	10.06	218.09	-20.07	0.170	
39	5.786	5.499	2.366	2.517	23.497	1.000	0.999	1.002	1.001	1.000	0.172	0.096	3.675	10.04	220.80	-20.07	0.171	
40	5.920	5.810	2.510	2.607	24.285	1.000	1.001	1.001	1.001	1.000	0.173	0.096	3.641	10.02	223.26	-20.06	0.173	
41	5.981	5.920	2.561	2.628	24.376	1.000	1.000	1.000	1.000	1.000	0.175	0.097	3.597	10.06	223.90	-20.05	0.174	
42	6.108	6.371	2.638	2.651	21.298	0.998	0.992	1.001	0.928	1.010	0.204	0.165	3.595	16.21	251.98	-20.03	0.203	
43	6.170	6.018	2.671	2.711	6.005	0.999	0.824	0.498	0.724	1.002	0.265	0.309	4.792	28.71	184.74	-19.99	0.251	
44	6.161	6.847	0.240	0.772	5.994	1.000	0.954	0.514	0.931	1.000	0.253	0.324	6.361	29.44	181.11	-20.03	0.246	
45	6.157	6.831	0.238	0.783	5.998	1.001	0.964	0.601	0.983	0.999	0.251	0.327	6.900	29.39	180.73	-20.03	0.246	
46	6.157	6.830	0.230	0.786	5.997	0.994	1.003	0.717	0.998	1.000	0.250	0.328	6.966	29.41	180.63	-20.04	0.246	
47	6.157	6.842	0.297	0.785	5.988	1.001	0.993	0.926	0.998	1.001	0.254	0.322	6.135	29.43	180.85	-20.04	0.246	
RUN 218	PT = 833.22 PSIA										V = 3882.0		FT/SEC					
	TT = 1352.8 DEGR										O = 3.881		PSIA					
	P = 0.0872 PSIA										T = 98.6		RFR					
	RE = 1.627E+06 PFF FT										PT2 = 7.18		PSIA					
	MU = 7.937E-08 LHM-SEC/PT2										RHD = 2.386E-03		LRM/FT3					
	DEN = -53.0 DEGR										C.R. = -0.05		IN					

V = 3882.0 FT/SEC
O = 3.881 PSIA
T = 98.6 RFR
PT2 = 7.18 PSIA
RMD = 2.386E-03 LBW/FT3
C.R. = -0.05 IN

PT = 833.22 PSIA
TT = 1352.8 DEGR
P = 0.0872 PSIA
RE = 1.627E+06 PEF FT
MU = 7.937E-08 UNP-SFC/PT2
DENS = -53. DEG F

TABLE A-5. MACH/FLOW-ANGULARITY PROBE MEASURED DATA (CONT'D)

DATE COMPUTED 20-JUL-81
TIME COMPUTED 12:22:15
DATE RECORDED 30-APR-81
TIME RECORDED 9: 31:57
PROJECT NUMBER C145VR

10.5/7-DEG RICONIC/SS+DS															
NOSE RADIUS, IN															
0.5000															
TRIP															
.06 MACHINED															
FLAP															
NONE															
CONFIGURATION															
10.5/7-DEG RICONIC/SS+DS															
NOSE RADIUS, IN															
0.5000															
TRIP															
.06 MACHINED															
FLAP															
NONE															
KNOCK(1-5) = 0.057 0.080 0.061 0.050 0.047															
APC(1-5) = 0.100 0.100 0.100 0.100 0.100															
TIME	P11/	P21/	P31/	P41/	P51/	TNP1	TNP2	TNP3	TNP4	TNP5	KP1	KP2	KP3	KP4	KP5
TIME	P1F	P2F	P3F	P4F	P5F	(SEC)	(SEC)	(SEC)	(SEC)	(SEC)					
1	0.997	0.998	1.003	0.998	0.991	2.756	3.217	5.050	6.681	1.960	-0.003	0.027	0.016	-0.000	0.004
2	0.999	0.995	1.011	0.992	0.994	2.686	2.883	5.617	6.121	1.482	0.007	0.034	0.037	0.047	0.019
3	0.990	0.992	1.041	0.986	0.987	2.635	2.615	6.597	5.531	1.261	0.014	0.051	0.051	0.046	0.021
4	0.996	0.996	1.027	0.992	0.996	2.552	2.501	7.403	5.255	1.110	0.006	0.048	0.070	0.042	0.009
5	0.997	0.999	0.960	1.002	0.996	2.472	2.482	6.433	5.288	1.036	0.022	0.016	0.052	0.029	-0.000
6	0.999	0.996	0.999	1.001	0.998	2.403	2.412	6.250	5.349	0.953	0.004	0.038	0.095	0.045	-0.007
7	0.997	0.994	1.005	0.999	0.997	2.345	2.320	6.353	5.311	0.888	0.017	0.045	0.028	0.026	-0.004
8	0.999	0.996	0.996	0.997	0.998	2.292	2.222	6.193	5.223	0.832	-0.003	0.049	0.151	0.074	0.003
9	1.002	0.997	0.963	0.997	0.997	2.260	2.145	5.972	5.152	0.789	-0.000	0.031	-0.051	0.042	0.005
10	0.996	0.996	0.996	0.998	0.995	2.241	2.112	5.852	5.116	0.772	-0.001	-0.002	0.011	-0.012	0.000
11	0.996	0.988	0.976	0.993	0.994	2.216	2.043	5.624	5.050	0.736	0.044	0.048	0.047	0.054	0.005
12	0.996	0.992	0.976	0.994	0.996	2.194	1.994	5.403	4.905	0.713	0.034	0.048	0.050	0.059	0.008
13	0.997	0.995	0.985	0.997	0.998	2.183	1.965	5.254	4.963	0.701	0.015	0.043	0.040	-0.006	0.001
14	0.996	0.995	0.983	0.995	0.998	2.159	1.931	5.095	4.921	0.688	0.020	0.056	0.054	0.031	0.016
15	0.996	0.996	0.993	0.997	0.994	2.130	1.908	5.019	4.890	0.679	0.030	0.054	0.049	0.034	0.005
16	0.994	0.998	0.996	0.997	1.000	2.097	1.869	4.980	4.858	0.672	0.023	0.073	0.027	0.063	-0.003
17	0.994	0.997	0.997	0.996	0.999	2.057	1.865	4.951	4.810	0.660	0.065	0.069	0.027	0.058	0.001
18	0.994	0.996	0.996	0.993	0.999	2.008	1.838	4.914	4.736	0.644	0.029	0.052	0.048	0.049	0.002
19	0.994	0.994	0.994	0.991	0.999	1.947	1.787	4.847	4.636	0.620	0.050	0.065	0.063	0.043	0.005
20	0.997	0.994	0.991	0.992	0.999	1.901	1.736	4.761	4.546	0.595	0.026	0.041	0.084	0.064	0.018
21	0.997	0.995	0.990	0.994	0.999	1.871	1.692	4.668	4.491	0.577	0.015	0.030	0.050	0.040	0.006
22	0.996	0.997	0.989	0.996	0.999	1.841	1.653	4.558	4.442	0.563	0.007	0.057	0.041	0.057	0.001
23	1.001	1.000	0.996	0.998	1.000	1.828	1.634	4.516	4.411	0.554	0.024	0.005	0.080	0.089	0.001
24	1.000	0.998	1.000	0.999	1.000	1.811	1.623	4.509	4.393	0.556	-0.001	0.048	-0.014	0.050	0.011
25	0.999	0.998	1.001	0.999	1.000	1.798	1.615	4.514	4.379	0.555	0.002	0.004	-0.036	0.035	0.000
26	0.999	0.998	1.001	1.000	1.000	1.787	1.604	4.519	4.380	0.554	0.008	0.014	0.070	0.013	0.001
27	0.999	0.999	1.001	0.999	1.000	1.777	1.600	4.532	4.374	0.554	0.036	0.000	-0.019	-0.010	0.000
28	0.999	0.998	1.002	1.000	1.000	1.763	1.592	4.552	4.370	0.553	0.035	0.051	0.045	0.023	-0.002
29	0.999	0.997	1.001	0.999	0.999	1.749	1.581	4.560	4.361	0.551	0.004	0.040	0.024	0.001	-0.001

DATE COMPUTED 30-JUN-81
TIME COMPUTED 13122154
DATE RECORDED 30-APR-81
TIME RECORDED 91 3157
PROJECT NUMBER C145VB

TABLE A-5. MACH/FLOW-ANGULARITY PROBE MEASURED DATA
(CONT'D)

ARVIN/CALSPAN FIELD SERVICES, INC.
AEDC DIVISION
VON KARMAN GAS DYNAMICS FACILITY
ARMONIA AFB FORCE STATION, TENNESSEE
BMO/SBI MAT PHASE I

PAGE 6
RUN 218 ALPHA SECTOR = -8.01 DEG
M = 7.97 ALPHAP = -20.01 DEG
RE = 3.627E+06 MODEL=ROLL = 180.00 DEG

CONFIGURATION
MOSE RADIUS, IN 0.5000
TRIP .06 MACHINED
FLAP NONE

DATA TYPE: 2, SURVEY-MACH/FLOW ANGULARITY PROBE
PRESSURE STABILIZATION STATISTICS

POINT	TIME HR:MIN:SEC	P1P	P2P	P3P	P4P	P5P	TNP1	TNP2	TNP3	TNP4	TNP5	KP1	KP2	KP3	KP4	KP5
30	91 12:30	0.999	0.998	1.000	1.000	1.000	1.738	1.571	4.559	4.357	0.550	-0.003	-0.003	0.014	-0.011	0.003
31	91 12:43	1.001	0.998	0.999	1.000	1.000	1.734	1.561	4.550	4.356	0.549	0.013	0.037	0.071	0.003	0.002
32	91 12:55	1.000	0.998	0.998	0.999	1.000	1.725	1.552	4.535	4.346	0.548	0.003	0.043	-0.011	0.048	-0.003
33	91 13:18	0.999	0.999	1.000	0.998	1.000	1.709	1.539	4.533	4.331	0.545	0.013	0.020	0.021	0.066	0.026
34	91 13:21	0.999	0.996	0.996	0.998	1.000	1.679	1.505	4.494	4.294	0.537	0.004	0.035	0.046	0.055	-0.001
35	91 13:31	0.998	0.996	0.986	0.996	1.000	1.653	1.449	4.368	4.247	0.525	0.009	0.039	0.058	0.050	0.001
36	91 13:49	1.000	0.995	0.978	0.994	1.000	1.619	1.354	4.107	4.162	0.506	0.005	0.042	0.058	0.061	-0.001
37	91 14:13	0.998	0.994	0.976	0.992	0.999	1.579	1.270	3.838	4.050	0.486	0.016	0.050	0.061	0.060	0.004
38	91 14:17	0.998	0.945	0.980	0.993	0.999	1.539	1.197	3.609	3.984	0.468	0.002	0.036	0.055	0.052	-0.007
39	91 14:31	0.998	0.997	0.981	0.994	1.000	1.502	1.126	3.400	3.855	0.452	-0.004	0.018	0.062	0.074	-0.009
40	91 14:45	0.998	0.997	0.983	0.993	1.000	1.470	1.066	3.206	3.766	0.437	0.000	0.043	0.049	0.044	0.001
41	91 15:10	0.999	1.001	0.996	0.999	1.000	1.455	1.047	3.141	3.736	0.435	0.001	-0.004	0.051	0.062	-0.003
42	91 15:14	1.003	0.967	0.987	1.216	1.027	1.802	0.741	3.052	5.468	0.503	0.067	0.022	0.052	0.058	0.002
43	91 15:29	1.006	1.913	1.679	1.302	1.091	2.077	4.864	6.719	9.693	1.760	0.038	0.066	0.056	0.060	0.041
44	91 15:43	1.001	1.112	1.296	1.066	1.000	2.083	6.869	13.764	11.384	1.759	-0.000	0.043	0.055	0.056	-0.006
45	91 15:57	1.001	1.011	1.173	1.015	0.998	2.088	7.005	18.461	11.820	1.758	-0.002	0.051	0.057	0.067	0.026
46	91 16:12	1.000	0.996	1.105	1.002	1.000	2.083	7.125	22.124	11.930	1.760	0.007	-0.066	0.039	-0.100	0.003
47	91 16:27	1.001	0.961	0.921	1.002	1.002	2.088	6.959	22.124	11.960	1.763	0.010	0.321	1.407	-0.014	0.001

236.

RUN 218

PI = 833.22 PSIA
TI = 1352.8 DFGR
P = 0.8872 PSIA
RE = 3.627E+06 PER FT
MU = 7.937E-08 LBF-SEC/FT2
DWE = -53. DEG F

V = 3882.0 FT/SEC
Q = 3.681 PSIA
T = 98.6 DEGR
PT2 = 7.18 PSIA
RHO = 2.386E-03 LBM/FT3
C.R. = -0.05 IN

DATE COMPUTED 20-JUN-81
TIME COMPUTED 13122154
DATE RECORDED 30-APR-81
TIME RECORDED 91 3157
PROJECT NUMBER C145VB

TABLE A-5. MACH/FLOW-ANGULARITY PROBE MEASURED DATA (CONT'D)

FLAP
NONE

TRIP
.06 MACHINED

NOSE RADIUS, IN
0.5000

CONFIGURATION
10.5/7-DEG BICONIC/SS+DS

PAGE 7
RUN 218
ALPHA SECTOR = -8.01 DEG
ALPHA = -20.01 DEG
M = 7.97
PE = 3.627F+06
MODEL-ROLL = 190.00 DEG

DATA TYPE : 2, SURVEY-MACH/FLOW ANGULARITY PROBE
MODEL SURFACE TEMPERATURES

POINT	TC 1	TC 2	TC 3	TC 4	TC 5	TC 6	TC 7	TC 8	TC 9	TC 10	TC 11	TC 12	TC 13	TC 14	TC 15	TC 16	TC 17	TC 18	TC 19	TC 20	TC 21	TC 22	TC 23	TC 24	TC 25	TC 26	TC 27	TC 28	TC 29	TC 30	TC 31	TC 32	TC 33	TC 34	TC 35	TC 36	TC 37	TC 38	TC 39	TC 40	TC 41	TC 42	TC 43	TC 44	TC 45	TC 46	TC 47	TC 48	TC 49	TC 50	TC 51	TC 52	TC 53	TC 54	TC 55	TC 56	TC 57	TC 58	TC 59	TC 60	TC 61	TC 62	TC 63	TC 64	TC 65	TC 66	TC 67	TC 68	TC 69	TC 70	TC 71	TC 72	TC 73	TC 74	TC 75	TC 76	TC 77	TC 78	TC 79	TC 80	TC 81	TC 82	TC 83	TC 84	TC 85	TC 86	TC 87	TC 88	TC 89	TC 90	TC 91	TC 92	TC 93	TC 94	TC 95	TC 96	TC 97	TC 98	TC 99	TC 100	TC 101	TC 102	TC 103	TC 104	TC 105	TC 106	TC 107	TC 108	TC 109	TC 110	TC 111	TC 112	TC 113	TC 114	TC 115	TC 116	TC 117	TC 118	TC 119	TC 120	TC 121	TC 122	TC 123	TC 124	TC 125	TC 126	TC 127	TC 128	TC 129	TC 130	TC 131	TC 132	TC 133	TC 134	TC 135	TC 136	TC 137	TC 138	TC 139	TC 140	TC 141	TC 142	TC 143	TC 144	TC 145	TC 146	TC 147	TC 148	TC 149	TC 150	TC 151	TC 152	TC 153	TC 154	TC 155	TC 156	TC 157	TC 158	TC 159	TC 160	TC 161	TC 162	TC 163	TC 164	TC 165	TC 166	TC 167	TC 168	TC 169	TC 170	TC 171	TC 172	TC 173	TC 174	TC 175	TC 176	TC 177	TC 178	TC 179	TC 180	TC 181	TC 182	TC 183	TC 184	TC 185	TC 186	TC 187	TC 188	TC 189	TC 190	TC 191	TC 192	TC 193	TC 194	TC 195	TC 196	TC 197	TC 198	TC 199	TC 200	TC 201	TC 202	TC 203	TC 204	TC 205	TC 206	TC 207	TC 208	TC 209	TC 210	TC 211	TC 212	TC 213	TC 214	TC 215	TC 216	TC 217	TC 218	TC 219	TC 220	TC 221	TC 222	TC 223	TC 224	TC 225	TC 226	TC 227	TC 228	TC 229	TC 230	TC 231	TC 232	TC 233	TC 234	TC 235	TC 236	TC 237	TC 238	TC 239	TC 240	TC 241	TC 242	TC 243	TC 244	TC 245	TC 246	TC 247	TC 248	TC 249	TC 250	TC 251	TC 252	TC 253	TC 254	TC 255	TC 256	TC 257	TC 258	TC 259	TC 260	TC 261	TC 262	TC 263	TC 264	TC 265	TC 266	TC 267	TC 268	TC 269	TC 270	TC 271	TC 272	TC 273	TC 274	TC 275	TC 276	TC 277	TC 278	TC 279	TC 280	TC 281	TC 282	TC 283	TC 284	TC 285	TC 286	TC 287	TC 288	TC 289	TC 290	TC 291	TC 292	TC 293	TC 294	TC 295	TC 296	TC 297	TC 298	TC 299	TC 300	TC 301	TC 302	TC 303	TC 304	TC 305	TC 306	TC 307	TC 308	TC 309	TC 310	TC 311	TC 312	TC 313	TC 314	TC 315	TC 316	TC 317	TC 318	TC 319	TC 320	TC 321	TC 322	TC 323	TC 324	TC 325	TC 326	TC 327	TC 328	TC 329	TC 330	TC 331	TC 332	TC 333	TC 334	TC 335	TC 336	TC 337	TC 338	TC 339	TC 340	TC 341	TC 342	TC 343	TC 344	TC 345	TC 346	TC 347	TC 348	TC 349	TC 350	TC 351	TC 352	TC 353	TC 354	TC 355	TC 356	TC 357	TC 358	TC 359	TC 360	TC 361	TC 362	TC 363	TC 364	TC 365	TC 366	TC 367	TC 368	TC 369	TC 370	TC 371	TC 372	TC 373	TC 374	TC 375	TC 376	TC 377	TC 378	TC 379	TC 380	TC 381	TC 382	TC 383	TC 384	TC 385	TC 386	TC 387	TC 388	TC 389	TC 390	TC 391	TC 392	TC 393	TC 394	TC 395	TC 396	TC 397	TC 398	TC 399	TC 400	TC 401	TC 402	TC 403	TC 404	TC 405	TC 406	TC 407	TC 408	TC 409	TC 410	TC 411	TC 412	TC 413	TC 414	TC 415	TC 416	TC 417	TC 418	TC 419	TC 420	TC 421	TC 422	TC 423	TC 424	TC 425	TC 426	TC 427	TC 428	TC 429	TC 430	TC 431	TC 432	TC 433	TC 434	TC 435	TC 436	TC 437	TC 438	TC 439	TC 440	TC 441	TC 442	TC 443	TC 444	TC 445	TC 446	TC 447	TC 448	TC 449	TC 450	TC 451	TC 452	TC 453	TC 454	TC 455	TC 456	TC 457	TC 458	TC 459	TC 460	TC 461	TC 462	TC 463	TC 464	TC 465	TC 466	TC 467	TC 468	TC 469	TC 470	TC 471	TC 472	TC 473	TC 474	TC 475	TC 476	TC 477	TC 478	TC 479	TC 480	TC 481	TC 482	TC 483	TC 484	TC 485	TC 486	TC 487	TC 488	TC 489	TC 490	TC 491	TC 492	TC 493	TC 494	TC 495	TC 496	TC 497	TC 498	TC 499	TC 500	TC 501	TC 502	TC 503	TC 504	TC 505	TC 506	TC 507	TC 508	TC 509	TC 510	TC 511	TC 512	TC 513	TC 514	TC 515	TC 516	TC 517	TC 518	TC 519	TC 520	TC 521	TC 522	TC 523	TC 524	TC 525	TC 526	TC 527	TC 528	TC 529	TC 530	TC 531	TC 532	TC 533	TC 534	TC 535	TC 536	TC 537	TC 538	TC 539	TC 540	TC 541	TC 542	TC 543	TC 544	TC 545	TC 546	TC 547	TC 548	TC 549	TC 550	TC 551	TC 552	TC 553	TC 554	TC 555	TC 556	TC 557	TC 558	TC 559	TC 560	TC 561	TC 562	TC 563	TC 564	TC 565	TC 566	TC 567	TC 568	TC 569	TC 570	TC 571	TC 572	TC 573	TC 574	TC 575	TC 576	TC 577	TC 578	TC 579	TC 580	TC 581	TC 582	TC 583	TC 584	TC 585	TC 586	TC 587	TC 588	TC 589	TC 590	TC 591	TC 592	TC 593	TC 594	TC 595	TC 596	TC 597	TC 598	TC 599	TC 600	TC 601	TC 602	TC 603	TC 604	TC 605	TC 606	TC 607	TC 608	TC 609	TC 610	TC 611	TC 612	TC 613	TC 614	TC 615	TC 616	TC 617	TC 618	TC 619	TC 620	TC 621	TC 622	TC 623	TC 624	TC 625	TC 626	TC 627	TC 628	TC 629	TC 630	TC 631	TC 632	TC 633	TC 634	TC 635	TC 636	TC 637	TC 638	TC 639	TC 640	TC 641	TC 642	TC 643	TC 644	TC 645	TC 646	TC 647	TC 648	TC 649	TC 650	TC 651	TC 652	TC 653	TC 654	TC 655	TC 656	TC 657	TC 658	TC 659	TC 660	TC 661	TC 662	TC 663	TC 664	TC 665	TC 666	TC 667	TC 668	TC 669	TC 670	TC 671	TC 672	TC 673	TC 674	TC 675	TC 676	TC 677	TC 678	TC 679	TC 680	TC 681	TC 682	TC 683	TC 684	TC 685	TC 686	TC 687	TC 688	TC 689	TC 690	TC 691	TC 692	TC 693	TC 694	TC 695	TC 696	TC 697	TC 698	TC 699	TC 700	TC 701	TC 702	TC 703	TC 704	TC 705	TC 706	TC 707	TC 708	TC 709	TC 710	TC 711	TC 712	TC 713	TC 714	TC 715	TC 716	TC 717	TC 718	TC 719	TC 720	TC 721	TC 722	TC 723	TC 724	TC 725	TC 726	TC 727	TC 728	TC 729	TC 730	TC 731	TC 732	TC 733	TC 734	TC 735	TC 736	TC 737	TC 738	TC 739	TC 740	TC 741	TC 742	TC 743	TC 744	TC 745	TC 746	TC 747	TC 748	TC 749	TC 750	TC 751	TC 752	TC 753	TC 754	TC 755	TC 756	TC 757	TC 758	TC 759	TC 760	TC 761	TC 762	TC 763	TC 764	TC 765	TC 766	TC 767	TC 768	TC 769	TC 770	TC 771	TC 772	TC 773	TC 774	TC 775	TC 776	TC 777	TC 778	TC 779	TC 780	TC 781	TC 782	TC 783	TC 784	TC 785	TC 786	TC 787	TC 788	TC 789	TC 790	TC 791	TC 792	TC 793	TC 794	TC 795	TC 796	TC 797	TC 798	TC 799	TC 800	TC 801	TC 802	TC 803	TC 804	TC 805	TC 806	TC 807	TC 808	TC 809	TC 810	TC 811	TC 812	TC 813	TC 814	TC 815	TC 816	TC 817	TC 818	TC 819	TC 820	TC 821	TC 822	TC 823	TC 824	TC 825	TC 826	TC 827	TC 828	TC 829	TC 830	TC 831	TC 832	TC 833	TC 834	TC 835	TC 836	TC 837	TC 838	TC 839	TC 840	TC 841	TC 842	TC 843	TC 844	TC 845	TC 846	TC 847	TC 848	TC 849	TC 850	TC 851	TC 852	TC 853	TC 854	TC 855	TC 856	TC 857	TC 858	TC 859	TC 860	TC 861	TC 862	TC 863	TC 864	TC 865	TC 866	TC 867	TC 868	TC 869	TC 870	TC 871	TC 872	TC 873	TC 874	TC 875	TC 876	TC 877	TC 878	TC 879	TC 880	TC 881	TC 882	TC 883	TC 884	TC 885	TC 886	TC 887	TC 888	TC 889	TC 890	TC 891	TC 892	TC 893	TC 894	TC 895	TC 896	TC 897	TC 898	TC 899	TC 900	TC 901	TC 902	TC 903	TC 904	TC 905	TC 906	TC 907	TC 908	TC 909	TC 910	TC 911	TC 912	TC 913	TC 914	TC 915	TC 916	TC 917	TC 918	TC 919	TC 920	TC 921	TC 922	TC 923	TC 924	TC 925	TC 926	TC 927	TC 928	TC 929	TC 930	TC 931	TC 932	TC 933	TC 934	TC 935	TC 936	TC 937	TC 938	TC 939	TC 940	TC 941	TC 942	TC 943	TC 944	TC 945	TC 946	TC 947	TC 948	TC 949	TC 950	TC 951	TC 952	TC 953	TC 954	TC 955	TC 956	TC 957	TC 958	TC 959	TC 960	TC 961	TC 962	TC 963	TC 964	TC 965	TC 966	TC 967	TC 968	TC 969	TC 970	TC 971	TC 972	TC 973	TC 974	TC 975	TC 976	TC 977	TC 978	TC 979	TC 980	TC 981	TC 982	TC 983	TC 984	TC 985	TC 986	TC 987	TC 988	TC 989	TC 990	TC 991	TC 992	TC 993	TC 994	TC 995	TC 996	TC 997	TC 998	TC 999	TC 1000	TC 1001	TC 1002	TC 1003	TC 1004	TC 1005	TC 1006	TC 1007	TC 1008	TC 1009	TC 1010	TC 1011	TC 1012	TC 1013	TC 1014	TC 1015	TC 1016	TC 1017	TC 1018	TC 1019	TC 1020	TC 1021	TC 1022	TC 1023	TC 1024	TC 1025	TC 1026	TC 1027	TC 1028	TC 1029	TC 1030	TC 1031	TC 1032	TC 1033	TC 1034	TC 1035	TC 1036	TC 1037	TC 1038	TC 1039	TC 1040	TC 1041	TC 1042	TC 1043	TC 1044	TC 1045	TC 1046	TC 1047	TC 1048	TC 1049	TC 1050	TC 1051	TC 1052	TC 1053	TC 1054	TC 1055	TC 1056	TC 1057	TC 1058	TC 1059	TC 1060	TC 1061	TC 1062	TC 1063	TC 1064	TC 1065	TC 1066	TC 1067	TC 1068	TC 1069	TC 1070	TC 1071	TC 1072	TC 1073	TC 1074	TC 1075	TC 1076	TC 1077	TC 1078	TC 1079	TC 1080	TC 1081	TC 1082	TC 1083	TC 1084	TC 1085	TC 1086	TC 1087	TC 1088	TC 1089	TC 1090	TC 1091	TC 1092	TC 1093	TC 1094	TC 1095	TC 1096	TC 1097	TC 1098	TC 1099	TC 1100	TC 1101	TC 1102	TC 1103	TC 1104	TC 1105	TC 1106	TC 1107	TC 1108	TC 1109	TC 1110	TC 1111	TC 1112	TC 1113	TC 1114	TC 1115	TC 1116	TC 1117	TC 1118	TC 1119	TC 1120	TC 1121	TC 1122	TC 1123	TC 1124	TC 1125	TC 1126	TC 1127	TC 1128	TC 1129	TC 1130	TC 1131	TC 1132	TC 1133	TC 1134	TC 1135	TC 1136	TC 1137	TC 1138	TC 1139	TC 1140	TC 1141	TC 1142	TC 1143	TC 1144	TC 1145	TC 1146	TC 1147	TC 1148	TC 1149	TC 1150	TC 1151	TC 1152	TC 1153	TC 1154	TC 1155	
-------	------	------	------	------	------	------	------	------	------	-------	-------	-------	-------	-------	-------	-------	-------	-------	-------	-------	-------	-------	-------	-------	-------	-------	-------	-------	-------	-------	-------	-------	-------	-------	-------	-------	-------	-------	-------	-------	-------	-------	-------	-------	-------	-------	-------	-------	-------	-------	-------	-------	-------	-------	-------	-------	-------	-------	-------	-------	-------	-------	-------	-------	-------	-------	-------	-------	-------	-------	-------	-------	-------	-------	-------	-------	-------	-------	-------	-------	-------	-------	-------	-------	-------	-------	-------	-------	-------	-------	-------	-------	-------	-------	-------	-------	-------	-------	-------	--------	--------	--------	--------	--------	--------	--------	--------	--------	--------	--------	--------	--------	--------	--------	--------	--------	--------	--------	--------	--------	--------	--------	--------	--------	--------	--------	--------	--------	--------	--------	--------	--------	--------	--------	--------	--------	--------	--------	--------	--------	--------	--------	--------	--------	--------	--------	--------	--------	--------	--------	--------	--------	--------	--------	--------	--------	--------	--------	--------	--------	--------	--------	--------	--------	--------	--------	--------	--------	--------	--------	--------	--------	--------	--------	--------	--------	--------	--------	--------	--------	--------	--------	--------	--------	--------	--------	--------	--------	--------	--------	--------	--------	--------	--------	--------	--------	--------	--------	--------	--------	--------	--------	--------	--------	--------	--------	--------	--------	--------	--------	--------	--------	--------	--------	--------	--------	--------	--------	--------	--------	--------	--------	--------	--------	--------	--------	--------	--------	--------	--------	--------	--------	--------	--------	--------	--------	--------	--------	--------	--------	--------	--------	--------	--------	--------	--------	--------	--------	--------	--------	--------	--------	--------	--------	--------	--------	--------	--------	--------	--------	--------	--------	--------	--------	--------	--------	--------	--------	--------	--------	--------	--------	--------	--------	--------	--------	--------	--------	--------	--------	--------	--------	--------	--------	--------	--------	--------	--------	--------	--------	--------	--------	--------	--------	--------	--------	--------	--------	--------	--------	--------	--------	--------	--------	--------	--------	--------	--------	--------	--------	--------	--------	--------	--------	--------	--------	--------	--------	--------	--------	--------	--------	--------	--------	--------	--------	--------	--------	--------	--------	--------	--------	--------	--------	--------	--------	--------	--------	--------	--------	--------	--------	--------	--------	--------	--------	--------	--------	--------	--------	--------	--------	--------	--------	--------	--------	--------	--------	--------	--------	--------	--------	--------	--------	--------	--------	--------	--------	--------	--------	--------	--------	--------	--------	--------	--------	--------	--------	--------	--------	--------	--------	--------	--------	--------	--------	--------	--------	--------	--------	--------	--------	--------	--------	--------	--------	--------	--------	--------	--------	--------	--------	--------	--------	--------	--------	--------	--------	--------	--------	--------	--------	--------	--------	--------	--------	--------	--------	--------	--------	--------	--------	--------	--------	--------	--------	--------	--------	--------	--------	--------	--------	--------	--------	--------	--------	--------	--------	--------	--------	--------	--------	--------	--------	--------	--------	--------	--------	--------	--------	--------	--------	--------	--------	--------	--------	--------	--------	--------	--------	--------	--------	--------	--------	--------	--------	--------	--------	--------	--------	--------	--------	--------	--------	--------	--------	--------	--------	--------	--------	--------	--------	--------	--------	--------	--------	--------	--------	--------	--------	--------	--------	--------	--------	--------	--------	--------	--------	--------	--------	--------	--------	--------	--------	--------	--------	--------	--------	--------	--------	--------	--------	--------	--------	--------	--------	--------	--------	--------	--------	--------	--------	--------	--------	--------	--------	--------	--------	--------	--------	--------	--------	--------	--------	--------	--------	--------	--------	--------	--------	--------	--------	--------	--------	--------	--------	--------	--------	--------	--------	--------	--------	--------	--------	--------	--------	--------	--------	--------	--------	--------	--------	--------	--------	--------	--------	--------	--------	--------	--------	--------	--------	--------	--------	--------	--------	--------	--------	--------	--------	--------	--------	--------	--------	--------	--------	--------	--------	--------	--------	--------	--------	--------	--------	--------	--------	--------	--------	--------	--------	--------	--------	--------	--------	--------	--------	--------	--------	--------	--------	--------	--------	--------	--------	--------	--------	--------	--------	--------	--------	--------	--------	--------	--------	--------	--------	--------	--------	--------	--------	--------	--------	--------	--------	--------	--------	--------	--------	--------	--------	--------	--------	--------	--------	--------	--------	--------	--------	--------	--------	--------	--------	--------	--------	--------	--------	--------	--------	--------	--------	--------	--------	--------	--------	--------	--------	--------	--------	--------	--------	--------	--------	--------	--------	--------	--------	--------	--------	--------	--------	--------	--------	--------	--------	--------	--------	--------	--------	--------	--------	--------	--------	--------	--------	--------	--------	--------	--------	--------	--------	--------	--------	--------	--------	--------	--------	--------	--------	--------	--------	--------	--------	--------	--------	--------	--------	--------	--------	--------	--------	--------	--------	--------	--------	--------	--------	--------	--------	--------	--------	--------	--------	--------	--------	--------	--------	--------	--------	--------	--------	--------	--------	--------	--------	--------	--------	--------	--------	--------	--------	--------	--------	--------	--------	--------	--------	--------	--------	--------	--------	--------	--------	--------	--------	--------	--------	--------	--------	--------	--------	--------	--------	--------	--------	--------	--------	--------	--------	--------	--------	--------	--------	--------	--------	--------	--------	--------	--------	--------	--------	--------	--------	--------	--------	--------	--------	--------	--------	--------	--------	--------	--------	--------	--------	--------	--------	--------	--------	--------	--------	--------	--------	--------	--------	--------	--------	--------	--------	--------	--------	--------	--------	--------	--------	--------	--------	--------	--------	--------	--------	--------	--------	--------	--------	--------	--------	--------	--------	--------	--------	--------	--------	--------	--------	--------	--------	--------	--------	--------	--------	--------	--------	--------	--------	--------	--------	--------	--------	--------	--------	--------	--------	--------	--------	--------	--------	--------	--------	--------	--------	--------	--------	--------	--------	--------	--------	--------	--------	--------	--------	--------	--------	--------	--------	--------	--------	--------	--------	--------	--------	--------	--------	--------	--------	--------	--------	--------	--------	--------	--------	--------	--------	--------	--------	--------	--------	--------	--------	--------	--------	--------	--------	--------	--------	--------	--------	--------	--------	--------	--------	--------	--------	--------	--------	--------	--------	--------	--------	--------	--------	--------	--------	--------	--------	--------	--------	--------	--------	--------	--------	--------	--------	--------	--------	--------	--------	--------	--------	--------	--------	--------	--------	--------	--------	--------	--------	--------	--------	--------	--------	--------	--------	--------	--------	--------	--------	--------	--------	--------	--------	--------	--------	--------	--------	--------	--------	--------	--------	--------	--------	--------	--------	--------	--------	--------	--------	--------	--------	--------	--------	--------	--------	--------	--------	--------	--------	--------	--------	--------	---------	---------	---------	---------	---------	---------	---------	---------	---------	---------	---------	---------	---------	---------	---------	---------	---------	---------	---------	---------	---------	---------	---------	---------	---------	---------	---------	---------	---------	---------	---------	---------	---------	---------	---------	---------	---------	---------	---------	---------	---------	---------	---------	---------	---------	---------	---------	---------	---------	---------	---------	---------	---------	---------	---------	---------	---------	---------	---------	---------	---------	---------	---------	---------	---------	---------	---------	---------	---------	---------	---------	---------	---------	---------	---------	---------	---------	---------	---------	---------	---------	---------	---------	---------	---------	---------	---------	---------	---------	---------	---------	---------	---------	---------	---------	---------	---------	---------	---------	---------	---------	---------	---------	---------	---------	---------	---------	---------	---------	---------	---------	---------	---------	---------	---------	---------	---------	---------	---------	---------	---------	---------	---------	---------	---------	---------	---------	---------	---------	---------	---------	---------	---------	---------	---------	---------	---------	---------	---------	---------	---------	---------	---------	---------	---------	---------	---------	---------	---------	---------	---------	---------	---------	---------	---------	---------	--

DATE COMPUTED 200304-81
TIME COMPUTED 13122155
DATE RECORDED 30-APR-81
TIME RECORDED 9:3157
PROJECT NUMBER C145VB

TABLE A-5. MACH/FLOW-ANGULARITY PROBE MEASURED DATA
(CONT'D)

PAGE 8		CONFIGURATION										NOSE RADIUS, IN		TRIP		FLAP	
RUN 218		10.5/7-DEG RICONIC/SS+DS										0.5000		.06		MACHINED	
M = 7.97		ALPHA SECTOR = -8.01 DEG															
RE = 3.677E+06		ALPHAP = -20.01 DEG															
		MODEL-ROLL = 180.00 DEG															
DATA TYPE 1 2, SURVEY-MACH/FLOW ANGULARITY PROBE																	
MODEL SURFACE TEMPERATURES																	
POINT	TG 1	TG 2	TG 3	TG 4	TG 5	TG 6	TG 7	TG 8	TG 9	TG 10	TG 11	TG 12	TG 13	TG 14	TG 15	TG 16	TG 17
18	1209.	1186.	1193.	1134.	1134.	1160.	1081.	1016.	1016.	1016.	1016.	1016.	1016.	1016.	1016.	1016.	1016.
19	1209.	1186.	1193.	1134.	1134.	1160.	1081.	1016.	1016.	1016.	1016.	1016.	1016.	1016.	1016.	1016.	1016.
20	1209.	1186.	1193.	1134.	1134.	1160.	1081.	1016.	1016.	1016.	1016.	1016.	1016.	1016.	1016.	1016.	1016.
21	1209.	1186.	1193.	1134.	1134.	1160.	1081.	1016.	1016.	1016.	1016.	1016.	1016.	1016.	1016.	1016.	1016.
22	1209.	1186.	1193.	1134.	1134.	1160.	1081.	1016.	1016.	1016.	1016.	1016.	1016.	1016.	1016.	1016.	1016.
23	1209.	1186.	1193.	1134.	1134.	1160.	1081.	1016.	1016.	1016.	1016.	1016.	1016.	1016.	1016.	1016.	1016.
24	1209.	1186.	1193.	1134.	1134.	1160.	1081.	1016.	1016.	1016.	1016.	1016.	1016.	1016.	1016.	1016.	1016.
25	1209.	1186.	1193.	1134.	1134.	1160.	1081.	1016.	1016.	1016.	1016.	1016.	1016.	1016.	1016.	1016.	1016.
26	1209.	1186.	1193.	1134.	1134.	1160.	1081.	1016.	1016.	1016.	1016.	1016.	1016.	1016.	1016.	1016.	1016.
27	1209.	1186.	1193.	1134.	1134.	1160.	1081.	1016.	1016.	1016.	1016.	1016.	1016.	1016.	1016.	1016.	1016.
28	1209.	1186.	1193.	1134.	1134.	1160.	1081.	1016.	1016.	1016.	1016.	1016.	1016.	1016.	1016.	1016.	1016.
29	1209.	1186.	1193.	1134.	1134.	1160.	1081.	1016.	1016.	1016.	1016.	1016.	1016.	1016.	1016.	1016.	1016.
30	1209.	1186.	1193.	1134.	1134.	1160.	1081.	1016.	1016.	1016.	1016.	1016.	1016.	1016.	1016.	1016.	1016.
31	1209.	1186.	1193.	1134.	1134.	1160.	1081.	1016.	1016.	1016.	1016.	1016.	1016.	1016.	1016.	1016.	1016.
32	1209.	1186.	1193.	1134.	1134.	1160.	1081.	1016.	1016.	1016.	1016.	1016.	1016.	1016.	1016.	1016.	1016.
33	1209.	1186.	1193.	1134.	1134.	1160.	1081.	1016.	1016.	1016.	1016.	1016.	1016.	1016.	1016.	1016.	1016.
34	1209.	1186.	1193.	1134.	1134.	1160.	1081.	1016.	1016.	1016.	1016.	1016.	1016.	1016.	1016.	1016.	1016.

ARVIN/CALSPAN FIELD SERVICES, INC.
AEC DIVISION
VON KARMAN GAS DYNAMICS FACILITY
ARNOLD AFB FORCE STATION, TENNESSEE
BWO/SAT NAT PHASE I

ARVIN/CALSPAN TYPED SUBMITS, INC.
AEDC DIVISION
VON KARMAN GAS DYNAMICS FACILITY
ARNOLD AIR FORCE STATION, TENNESSEE
RND/SET MAT PHASE 1

TABLE A-5. MACH/FLOW-ANGULARITY PROBE MEASURED DATA
(CONT'D)

PAGE 9
RUN 21P ALPHA SECTOR = -8.01 DEG
M = 7.97 ALPHA = -20.01 DEG
PE = 3.627E+06 MODEL-ROLL = 180.00 DEG
FLAP NONE

COMPUTED 131215Z
DATE RECORDED 30-APR-81
TIME RECORDED 91 3157
PROJECT NUMBER C145VB

DATA TYPE : 2, SURVEY-MACH/FLOW ANGULARITY PROBE
MODEL SURFACE TEMPERATURES

POINT	TG 1	TG 2	TG 3	TG 4	TG 5	TG 6	TG 7	TG 8	TG 9	TG 11	TG 12	TG 13	TG 14	TG 15	TG 16	TG 102	TG 106	TG 110	TG 114	TG 118	TG 120	TG 122
	DEGR	DEGR	DEGR	DEGR	DEGR	DEGR	DEGR	DEGR	DEGR	DEGR	DEGR	DEGR	DEGR	DEGR	DEGR	DEGR	DEGR	DEGR	DEGR	DEGR	DEGR	DEGR
25	1208.	1185.	1193.	1135.	1135.	1159.	1080.	1016.	1016.	1016.	1016.	1016.	1016.	1016.	1016.	1016.	1016.	1016.	1016.	1016.	1016.	1016.
36	1208.	1185.	1193.	1135.	1135.	1159.	1080.	1016.	1016.	1016.	1016.	1016.	1016.	1016.	1016.	1016.	1016.	1016.	1016.	1016.	1016.	1016.
37	1209.	1185.	1193.	1135.	1135.	1159.	1080.	1016.	1016.	1016.	1016.	1016.	1016.	1016.	1016.	1016.	1016.	1016.	1016.	1016.	1016.	1016.
38	1209.	1185.	1193.	1135.	1135.	1159.	1080.	1016.	1016.	1016.	1016.	1016.	1016.	1016.	1016.	1016.	1016.	1016.	1016.	1016.	1016.	1016.
39	1209.	1185.	1193.	1135.	1135.	1159.	1080.	1016.	1016.	1016.	1016.	1016.	1016.	1016.	1016.	1016.	1016.	1016.	1016.	1016.	1016.	1016.
40	1209.	1185.	1193.	1135.	1135.	1159.	1080.	1016.	1016.	1016.	1016.	1016.	1016.	1016.	1016.	1016.	1016.	1016.	1016.	1016.	1016.	1016.
41	1209.	1185.	1193.	1135.	1135.	1159.	1080.	1016.	1016.	1016.	1016.	1016.	1016.	1016.	1016.	1016.	1016.	1016.	1016.	1016.	1016.	1016.
42	1209.	1185.	1193.	1135.	1135.	1159.	1080.	1016.	1016.	1016.	1016.	1016.	1016.	1016.	1016.	1016.	1016.	1016.	1016.	1016.	1016.	1016.
43	1209.	1185.	1193.	1135.	1135.	1159.	1080.	1016.	1016.	1016.	1016.	1016.	1016.	1016.	1016.	1016.	1016.	1016.	1016.	1016.	1016.	1016.
44	1209.	1185.	1193.	1135.	1135.	1159.	1080.	1016.	1016.	1016.	1016.	1016.	1016.	1016.	1016.	1016.	1016.	1016.	1016.	1016.	1016.	1016.
45	1209.	1185.	1193.	1135.	1135.	1159.	1080.	1016.	1016.	1016.	1016.	1016.	1016.	1016.	1016.	1016.	1016.	1016.	1016.	1016.	1016.	1016.
46	1209.	1185.	1193.	1135.	1135.	1159.	1080.	1016.	1016.	1016.	1016.	1016.	1016.	1016.	1016.	1016.	1016.	1016.	1016.	1016.	1016.	1016.
47	1209.	1185.	1193.	1135.	1135.	1159.	1080.	1016.	1016.	1016.	1016.	1016.	1016.	1016.	1016.	1016.	1016.	1016.	1016.	1016.	1016.	1016.

239.

RUN 21P

PT = 833.22 PSIA
TT = 1352.8 DEGR
P = 0.0872 PSIA
RE = 3.627E+06 PFP FT
MU = 7.937E-04 LRP-SEC/FT2
DFWE = -53. DEGR

V = 3882.0 FT/SEC
Q = 3.881 PSIA
T = 98.6 DEGR
PT2 = 7.18 PSIA
RHO = 2.386E-03 LRP/FT3
C.P.E = -0.05 IN

ARVIN/CALAPAN FIELD SERVICES, INC.
AFSC DIVISION
VON KARMAN GAS DYNAMICS FACILITY
ARNOLD AIR FORCE STATION, TENNESSEE
6ND/5AT MAT PHASE I

TABLE A-6. MACH/FLOW-ANGULARITY DERIVED DIRECTIONAL DATA

PROJECT NUMBER C145VB

PAGE 1
RUN 218
M = 7.97
RE = 3.627E+06
ALPHA SECTOR = -8.01 DEG
ALPHAP = -20.01 DEG
MODEL-ROBL = 180.00 DEG

TRIP
.06 MACHINED
FLAP
NONE

DATA TYPE: 2, SURVEY-MACH/FLOW ANGULARITY PROBE SURVEY STATION NO = 39 PMX/PT= 0.111E-02

CONFIGURATION

NOSE RADIUS, IN
0.5000

NOSE RADIUS, IN
0.5000

TRIP
.06 MACHINED
FLAP
NONE

PROJECT NUMBER C145VB

VELOCITY VECTORS
THETA = -29.00 DEG
PSIO = 3.30 DEG
PHIO = -5.00 DEG

POINT	MLC	ATCA (DEG)	CPHI (DEG)	UP/VL	VP/VL	WP/VL	UF/VL	VF/VL	WF/VL	UM/VL	VM/VL	WM/VL
1	1.87	12.13	196.04	0.9777	-0.0581	-0.2020	0.9526	-0.0190	0.3037	0.9990	-0.0190	-0.0405
2	2.24	11.19	196.27	0.9810	-0.0543	-0.1862	0.9478	-0.0138	0.3187	0.9996	-0.0138	-0.0248
3	2.55	11.56	195.21	0.9797	-0.0526	-0.1933	0.9501	-0.0127	0.3117	0.9994	-0.0127	-0.0322
4	2.81	11.88	194.19	0.9786	-0.0505	-0.1995	0.9523	-0.0112	0.3055	0.9992	-0.0112	-0.0386
5	3.08	10.66	195.58	0.9828	-0.0497	-0.1781	0.9453	-0.0083	0.3261	0.9998	-0.0083	-0.0170
6	3.08	10.57	197.15	0.9830	-0.0541	-0.1753	0.9442	-0.0125	0.3291	0.9998	-0.0125	-0.0138
7	3.27	10.67	198.25	0.9827	-0.0580	-0.1759	0.9442	-0.0164	0.3289	0.9998	-0.0164	-0.0140
8	3.39	10.44	199.72	0.9835	-0.0611	-0.1705	0.9423	-0.0190	0.3342	0.9998	-0.0190	-0.0083
9	3.47	10.16	201.15	0.9843	-0.0636	-0.1645	0.9401	-0.0209	0.3402	0.9998	-0.0209	-0.0020
10	3.49	10.05	201.77	0.9847	-0.0647	-0.1620	0.9392	-0.0218	0.3425	0.9998	-0.0218	0.0005
11	3.56	9.73	203.30	0.9856	-0.0668	-0.1552	0.9368	-0.0232	0.3492	0.9997	-0.0232	0.0076
12	3.59	9.47	204.54	0.9864	-0.0684	-0.1497	0.9348	-0.0242	0.3544	0.9996	-0.0242	0.0132
13	3.60	9.33	205.30	0.9868	-0.0695	-0.1465	0.9335	-0.0251	0.3576	0.9995	-0.0251	0.0166
14	3.61	9.20	206.16	0.9871	-0.0705	-0.1435	0.9324	-0.0258	0.3604	0.9995	-0.0258	0.0197
15	3.61	9.22	206.37	0.9871	-0.0712	-0.1436	0.9324	-0.0265	0.3604	0.9995	-0.0265	0.0197
16	3.62	9.31	206.22	0.9868	-0.0715	-0.1452	0.9330	-0.0269	0.3589	0.9995	-0.0269	0.0181
17	3.64	9.42	205.97	0.9855	-0.0717	-0.1472	0.9337	-0.0273	0.3571	0.9995	-0.0273	0.0161
18	3.67	9.52	205.55	0.9862	-0.0713	-0.1492	0.9344	-0.0271	0.3551	0.9995	-0.0271	0.0140
19	3.73	9.59	205.42	0.9860	-0.0715	-0.1505	0.9349	-0.0275	0.3539	0.9995	-0.0275	0.0127
20	3.80	9.60	205.77	0.9860	-0.0725	-0.1501	0.9347	-0.0284	0.3543	0.9995	-0.0284	0.0132
21	3.85	9.55	206.58	0.9861	-0.0743	-0.1485	0.9340	-0.0300	0.3560	0.9994	-0.0300	0.0150
22	3.87	9.52	207.32	0.9862	-0.0759	-0.1469	0.9333	-0.0315	0.3576	0.9994	-0.0315	0.0167
23	3.87	9.54	207.53	0.9862	-0.0766	-0.1469	0.9333	-0.0322	0.3576	0.9993	-0.0322	0.0167
24	3.87	9.60	207.50	0.9860	-0.0770	-0.1479	0.9336	-0.0327	0.3567	0.9993	-0.0327	0.0158
25	3.86	9.67	207.37	0.9858	-0.0773	-0.1492	0.9341	-0.0331	0.3555	0.9993	-0.0331	0.0145
26	3.86	9.76	207.51	0.9855	-0.0783	-0.1504	0.9344	-0.0343	0.3545	0.9993	-0.0343	0.0134
27	3.85	9.86	207.30	0.9852	-0.0785	-0.1522	0.9350	-0.0346	0.3528	0.9993	-0.0346	0.0116
28	3.85	9.96	207.20	0.9849	-0.0793	-0.1538	0.9356	-0.0356	0.3514	0.9993	-0.0356	0.0101
29	3.85	10.05	207.30	0.9846	-0.0801	-0.1551	0.9360	-0.0364	0.3501	0.9993	-0.0364	0.0088
30	3.85	10.12	207.36	0.9844	-0.0808	-0.1560	0.9363	-0.0372	0.3493	0.9993	-0.0372	0.0079
31	3.85	10.14	207.69	0.9844	-0.0818	-0.1558	0.9361	-0.0382	0.3496	0.9992	-0.0382	0.0082
32	3.84	10.19	207.63	0.9842	-0.0823	-0.1566	0.9364	-0.0388	0.3489	0.9992	-0.0388	0.0075
33	3.84	10.26	207.82	0.9840	-0.0831	-0.1576	0.9367	-0.0398	0.3480	0.9992	-0.0398	0.0065
34	3.83	10.37	208.23	0.9837	-0.0852	-0.1587	0.9369	-0.0419	0.3471	0.9991	-0.0419	0.0056
35	3.82	10.36	209.76	0.9837	-0.0892	-0.1561	0.9357	-0.0457	0.3408	0.9989	-0.0457	0.0085
36	3.78	10.26	212.92	0.9840	-0.0968	-0.1495	0.9328	-0.0526	0.3565	0.9985	-0.0526	0.0158
37	3.74	10.12	215.67	0.9844	-0.1075	-0.1428	0.9300	-0.0577	0.3631	0.9981	-0.0577	0.0230
38	3.71	10.06	218.09	0.9846	-0.1078	-0.1375	0.9276	-0.0625	0.3683	0.9976	-0.0625	0.0287
39	3.68	10.04	220.80	0.9847	-0.1139	-0.1320	0.9250	-0.0681	0.3738	0.9971	-0.0681	0.0347
40	3.64	10.02	223.26	0.9847	-0.1192	-0.1267	0.9225	-0.0729	0.3789	0.9965	-0.0729	0.0404

TABLE A-6. MACH/FLOW-ANGULARITY DERIVED DIRECTIONAL DATA (CONT'D)

PROJECT NUMBER C145VB

VON KARMAN GAS DYNAMICS FACILITY
ARMEDIC AIR FORCE STATION, TENNESSEE
RHO/SAT MAT PHASE I

FLAP
NONE

TRIP
.06 MACHINED

NOSE RADIUS, IN
0.5000

CONFIGURATION
10.5/7-DEG RICONIC/SS+DS

PAGE 2
RUN 218
M = 7.97
RE = 3.627E+00
ALPHA SECTOR = -8.01 DEG
ALPHAP = -20.01 DEG
MUDEL-POINT = 180.00 DEG

DATA TYPE: 2, SURVEY-MACH/FLOW ANGULARITY PROBE
SURVEY STATION NO = 39
PHX/PT = 0.111E-02

PHIO = -5.00 DEG

VELOCITY VECTORS
THETA0 = -79.00 DEG
PSIN = 3.30 DEG
WP/VL

POINT	M/LC	ARTCA (DEG)	CPHI (DEG)	UP/VL	VP/VL	WP/VL	UF/VL	VF/VL	WF/VL	UM/VL	VM/VL	WM/VL
41	3.60	10.06	223.90	0.9846	-0.1211	-0.1258	0.9220	-0.0747	0.3799	0.9963	-0.0747	0.0415
42	3.60	16.21	251.98	0.9603	-0.2654	-0.0863	0.8426	-0.2162	0.4174	0.9722	-0.2162	0.0902
43	4.79	28.71	184.74	0.8771	-0.0397	-0.4797	0.9094	-0.0307	0.0127	0.9435	-0.0307	-0.3300
44	6.16	29.44	181.11	0.8709	-0.0095	-0.4914	1.0000	-0.0021	-0.0044	0.9381	-0.0021	-0.3463
45	6.90	29.39	180.73	0.8713	-0.0063	-0.4907	1.0000	0.0012	-0.0039	0.9383	0.0012	-0.3458
46	6.97	29.41	180.63	0.8711	-0.0054	-0.4911	1.0000	0.0020	-0.0045	0.9381	0.0020	-0.3463
47	6.13	29.43	180.85	0.8710	-0.0073	-0.4913	1.0000	0.0002	-0.0045	0.9381	0.0002	-0.3464

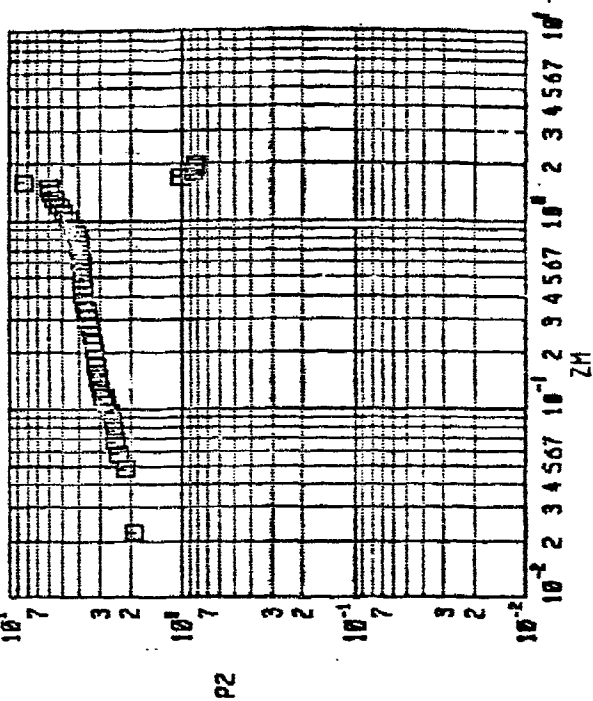
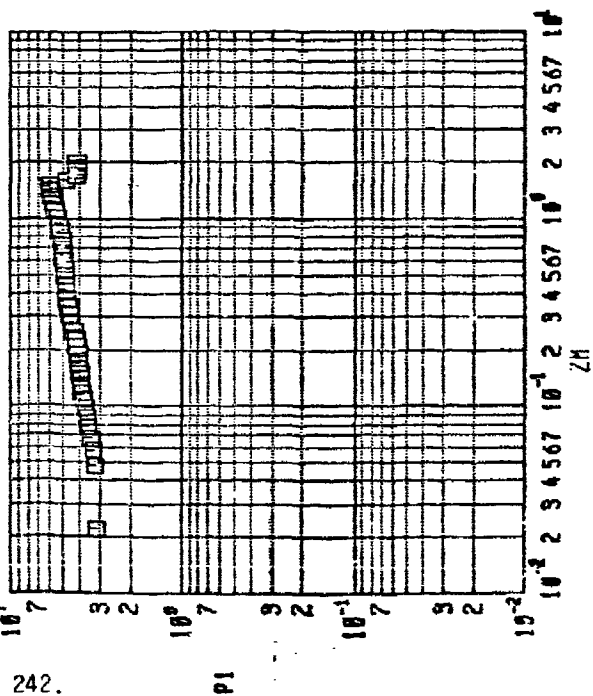
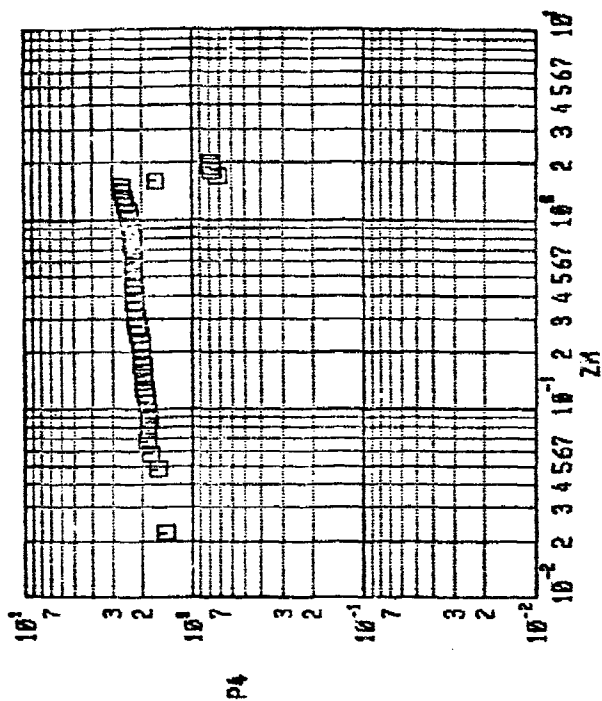
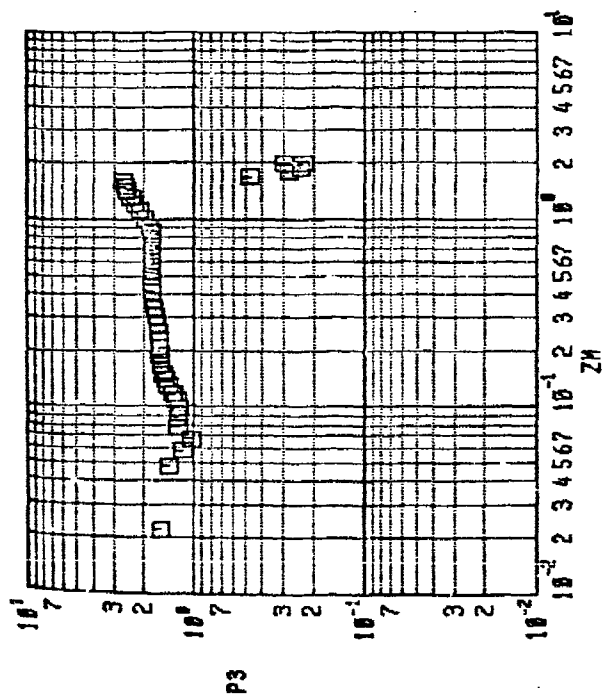
FT/SEC

V = 3892.0
Q = 3.881
T = 98.6
PT2 = 7.18
RHO = 2.386E-03
C.R. = -0.05

PT = R33.72 PSIA
TT = 1352.8 DEGR
P = 0.0872 PSIA
RE = 3.627E+06 PER FT
MU = 7.937E-08 LBF-SEC/PT2
DWE = -53. DEG F

218

RUN

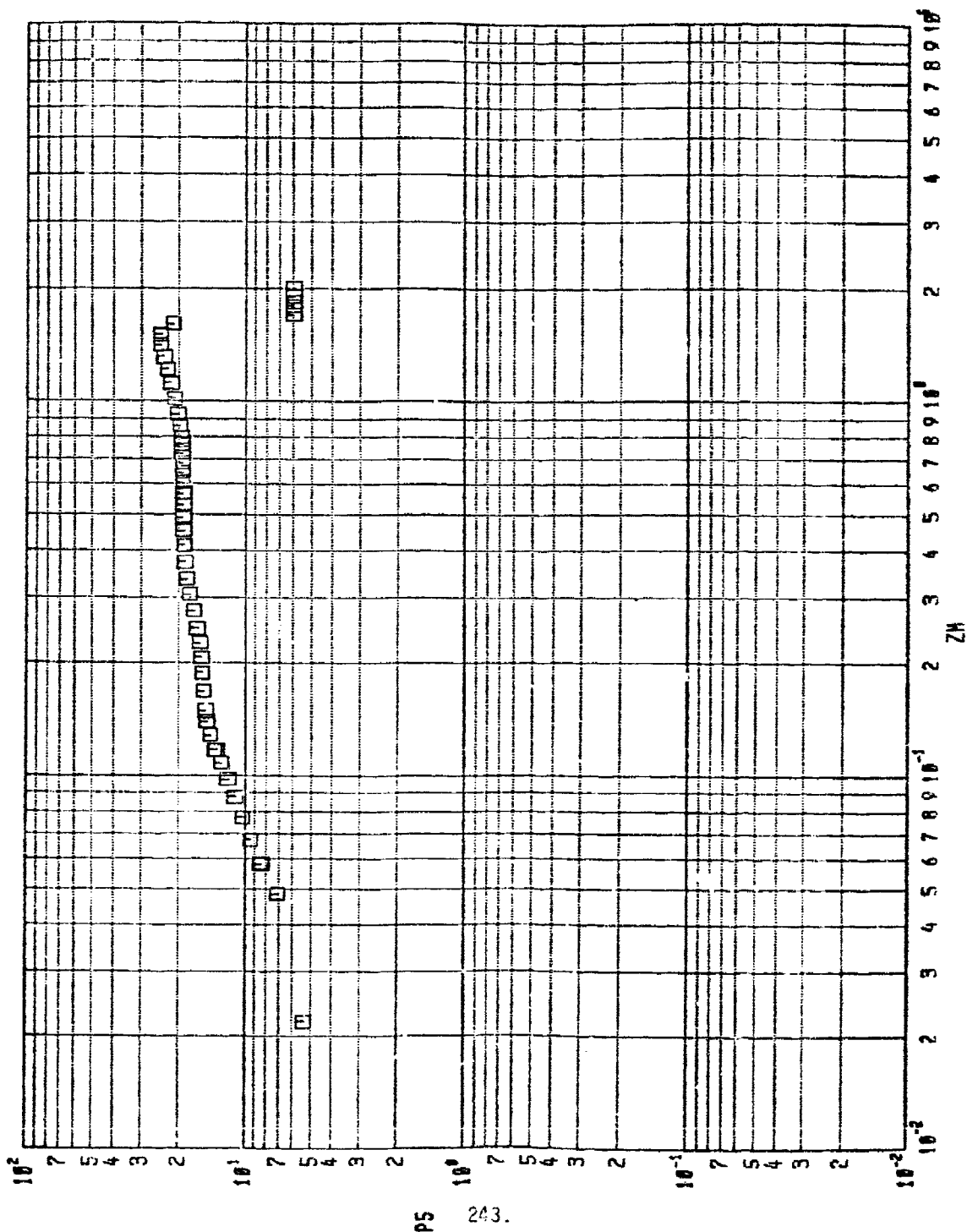


RUN 0218

BHO/SRI MAT PHASE I

FIGURE A-19. MACH/FLOW-ANGULARITY PROBE PRESSURE DATA

PAGE 1
22-JUL-4
1514



RUN 218

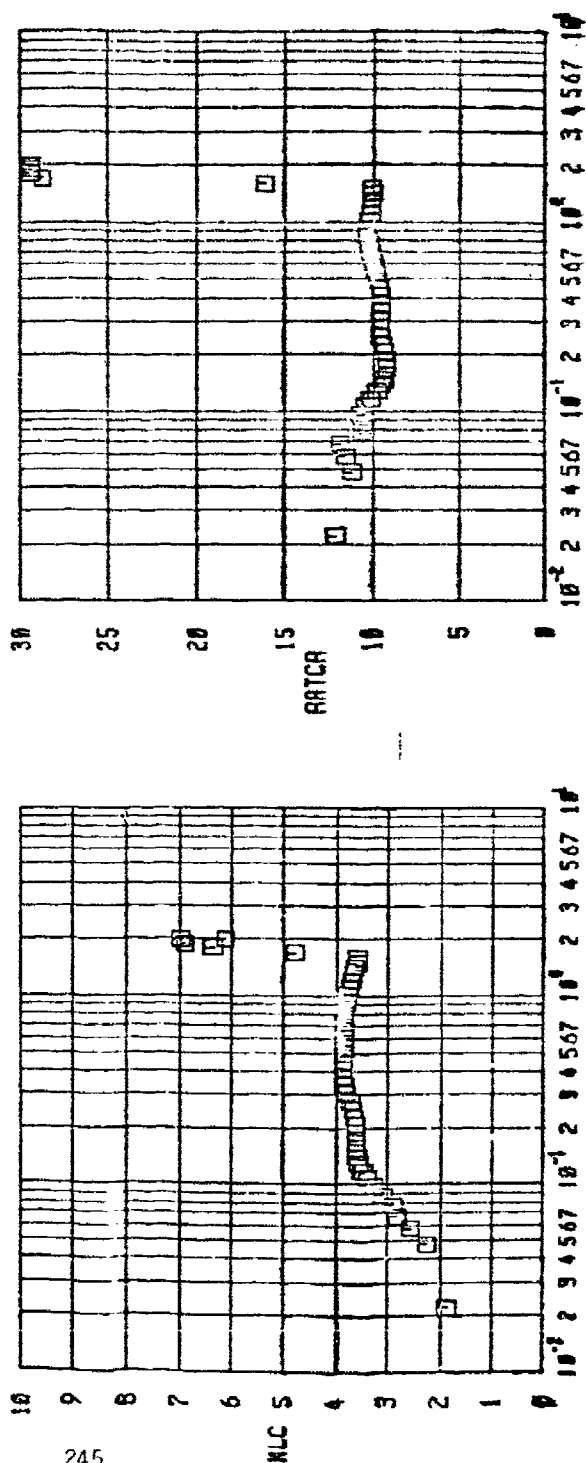
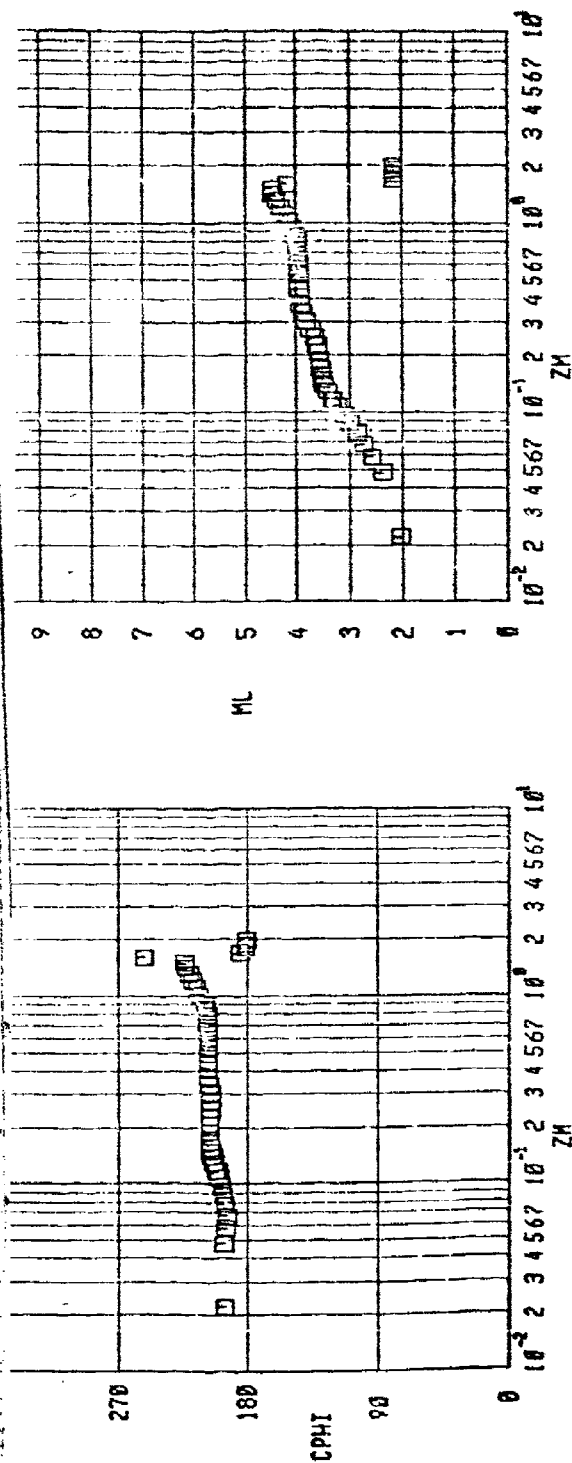
BND/SRI WRT PHASE I

FIGURE A-19. MACH/FLOW-ANGULARITY PROBE PRESSURE DATA (CONT'D)

The aerodynamic force and moment coefficients are presented in the body and wind axes. The wind axes lift and drag coefficients (CLW and CDW, respectively) were calculated using the forebody axial-force coefficient (CA). The wind axes pitching- and rolling-moment coefficients (CLMW and CLLW, respectively) were calculated using the forebody pitching-moment coefficient (CLMF). Pitching- and yawing-moment coefficients are referenced to the virtual model nose. Conic virtual model length (LM) and unsliced base area (A) were used as the reference length and area for the aerodynamic coefficients. Total axial-force coefficients (CAT) were corrected for base axial-force effects.

Pitching and yawing moment coefficients are referenced to the model base. Model base diameter (9.823 inches) and base area (75.784 inches²) were used as the reference length and area for the model aerodynamic coefficients.

Representative tabular data for a static force α sweep is shown in Table A-7 (4 pages).



RUN 0218

BMD/SAT MAT PHASE I

21-JUL-81
12:55

FIGURE A-20. MACH/FLOW-ANGULARITY DERIVED DIRECTIONAL DATA

TABLE A-7. FORCE AND MOMENT DATA

RUN	CODE	W	PT	TT	Q	P	T	PE	Z	REF. LENGTHS(CLN,CLN,CLN,CLN)
17	7	7.97	826.46	152.7	3.851	0.087	96.6	0.360E+07	75.784	33.258 33.258 33.258

CONFIDENTIAL
10.5/7 RICO

PHOSE	SLICES	FLAP	TRIP
V.5	DOUBLE	10	60M

---TUNNEL CONDITIONS AND BASE PRESSURES---

PN	ALPI	PHI	PTH	PT	TT	G	P	CAN	P81/P	P82/P	P83/P	PR4/F	P8A/P	CPBA
1	11.87	0.09	845.80	826.46	1352.7	3.851	0.087	0.0139						
2	0.87	0.09	845.96	826.54	1352.7	3.851	0.087	0.0151						
3	9.87	0.09	846.30	826.68	1352.7	3.853	0.087	0.0159						
4	8.87	0.09	846.23	826.81	1352.7	3.852	0.087	0.0165						
5	7.87	0.09	846.14	826.74	1352.7	3.852	0.087	0.0169						
6	6.88	0.09	846.12	826.72	1352.7	3.852	0.087	0.0172						
7	5.88	0.09	846.12	826.80	1352.7	3.852	0.087	0.0174						
8	4.89	0.09	846.12	826.70	1352.7	3.852	0.087	0.0175						
9	3.89	0.09	846.09	826.67	1352.7	3.852	0.087	0.0175						
10	2.90	0.10	845.96	826.55	1352.7	3.851	0.087	0.0176						
11	1.91	0.09	846.19	826.76	1352.7	3.852	0.087	0.0176						
12	0.92	0.10	846.11	826.69	1352.7	3.852	0.087	0.0176						
13	-0.08	0.11	846.12	826.70	1352.7	3.852	0.087	0.0176						
14	-1.07	0.10	845.74	826.32	1352.7	3.850	0.087	0.0176						
15	-2.06	0.10	845.89	826.47	1352.7	3.851	0.087	0.0176						
16	-3.05	0.10	845.88	826.46	1352.7	3.851	0.087	0.0175						
17	-4.05	0.11	845.86	826.44	1352.7	3.851	0.087	0.0175						
18	-5.04	0.11	845.93	826.52	1352.7	3.851	0.087	0.0174						
19	-6.03	0.11	845.81	826.40	1352.7	3.851	0.087	0.0173						
20	-6.53	0.11	845.83	826.42	1352.7	3.851	0.087	0.0172						
21	-7.02	0.11	845.81	826.39	1352.7	3.850	0.087	0.0172						
22	-7.52	0.11	845.69	826.28	1352.7	3.850	0.087	0.0171						
23	-8.02	0.11	845.84	826.43	1352.7	3.851	0.087	0.0171						
24	-8.51	0.11	845.89	826.47	1352.7	3.851	0.087	0.0170						
25	-9.01	0.11	845.83	826.42	1352.7	3.851	0.087	0.0170						
26	-9.51	0.11	845.61	826.19	1352.7	3.850	0.087	0.0170						
27	-10.00	0.11	845.61	826.20	1352.7	3.850	0.087	0.0170						
28	-10.49	0.11	845.76	826.35	1352.7	3.850	0.087	0.0171						
29	-11.08	0.11	845.80	826.38	1352.7	3.850	0.087	0.0173						

MODEL FLOWFIELD PHOTOGRAPHS TAKEN AT ALPHA = 20.34, 15.06, 9.98, 5.00, -0.10, -3.96;

ARVIN/CHASPAR FIELD SERVICE, INC.
 AEC DIVISION
 VOR KARMA GAS DYNAMICS FACILITY
 ARMED AIR FORCE STATION, TENNESSEE
 KNOX/AT MAT I FORCE TEST
 PAGE 2

TIME COMPUTED: UNAVAILABLE
 DATE RECORDED: 20-JUL-67
 TIME RECORDED: 10:51 PM
 PROJECT NUMBER: V13-41

TABLE A-7. FORCE AND MOMENT DATA (CONT'D)

RUN	CODE	M	PT	TT	Q	P	T	RE	A	REF LENGTHS(CLN,CLN,CLL)
17	7	7.97	826.46	1352.7	3.851	0.087	98.6	0.360E-07	75.784	33.258 33.258 33.258
10.5/7 RICONIC										
PN	ALPHA	BETA	PHT	CN	CLM	CLMF	CY	CLW	CLL	CAT
1	20.00	0.03	0.09	0.7707	-0.5029	-0.5030	-0.0062	0.0040	0.0001	0.1790
2	10.00	0.03	0.09	0.7226	-0.4708	-0.4710	-0.0054	0.0035	0.0001	0.1713
3	10.00	0.03	0.09	0.6706	-0.4403	-0.4405	-0.0052	0.0034	0.0001	0.1643
4	17.00	0.03	0.10	0.6318	-0.4106	-0.4108	-0.0049	0.0031	0.0001	0.1573
5	10.00	0.03	0.09	0.5874	-0.3815	-0.3817	-0.0047	0.0030	0.0000	0.1506
6	10.00	0.03	0.10	0.5446	-0.3530	-0.3531	-0.0046	0.0030	0.0000	0.1441
7	14.00	0.02	0.10	0.5024	-0.3252	-0.3254	-0.0044	0.0029	0.0000	0.1377
8	13.00	0.02	0.10	0.4617	-0.2985	-0.2987	-0.0045	0.0030	0.0000	0.1318
9	12.00	0.02	0.10	0.4213	-0.2720	-0.2722	-0.0039	0.0026	0.0000	0.1258
10	11.00	0.02	0.10	0.3821	-0.2464	-0.2466	-0.0034	0.0022	0.0000	0.1204
11	10.00	0.02	0.10	0.3434	-0.2212	-0.2214	-0.0029	0.0019	0.0000	0.1151
12	9.00	0.01	0.10	0.3054	-0.1965	-0.1967	-0.0027	0.0018	0.0000	0.1099
13	8.00	0.01	0.11	0.2659	-0.1707	-0.1709	-0.0013	0.0009	0.0000	0.1049
14	7.00	0.01	0.10	0.2279	-0.1460	-0.1462	-0.0006	0.0005	0.0000	0.1001
15	6.00	0.01	0.10	0.1919	-0.1226	-0.1228	-0.0003	-0.0001	0.0000	0.0952
16	5.00	0.01	0.10	0.1568	-0.0999	-0.1000	0.0000	-0.0003	0.0000	0.0925
17	4.00	0.01	0.11	0.1231	-0.0781	-0.0783	0.0005	-0.0003	0.0000	0.0895
18	3.00	0.00	0.11	0.0911	-0.0574	-0.0576	0.0004	-0.0002	0.0000	0.0870
19	2.00	0.00	0.11	0.0596	-0.0370	-0.0372	0.0002	-0.0001	0.0000	0.0852
20	1.50	0.00	0.11	0.0440	-0.0269	-0.0270	0.0002	-0.0001	0.0000	0.0834
21	1.00	-0.00	0.11	0.0284	-0.0167	-0.0168	0.0002	-0.0001	0.0000	0.0819
22	0.50	-0.00	0.11	0.0123	-0.0062	-0.0064	0.0002	-0.0000	0.0000	0.0816
23	0.00	-0.00	0.11	-0.0034	0.0040	0.0038	0.0001	-0.0000	0.0000	0.0816
24	-0.50	-0.00	0.11	-0.0140	0.0142	0.0140	0.0001	-0.0000	0.0000	0.0817
25	-1.00	-0.00	0.11	-0.0347	0.0244	0.0242	0.0000	0.0000	0.0000	0.0818
26	-1.50	-0.01	0.11	-0.0501	0.0344	0.0342	-0.0000	0.0001	0.0000	0.0813
27	-2.00	-0.01	0.11	-0.0657	0.0443	0.0443	-0.0000	0.0002	0.0000	0.0811
28	-3.00	-0.01	0.11	-0.0975	0.0649	0.0647	-0.0002	0.0002	0.0000	0.0810
29	-4.00	-0.01	0.11	-0.1398	0.0855	0.0853	-0.0003	0.0003	0.0000	0.0807
CA	CAR	CAT	CLL	CLW	CY	CLM	CLMF	CN	PHT	BETA
0.1651	0.0139	0.1790	0.0001	0.0040	-0.0062	-0.5029	-0.5030	0.7707	0.09	0.03
0.1562	0.0151	0.1713	0.0001	0.0035	-0.0054	-0.4708	-0.4710	0.7226	0.09	0.03
0.1484	0.0159	0.1643	0.0001	0.0034	-0.0052	-0.4403	-0.4405	0.6706	0.09	0.03
0.1408	0.0165	0.1573	0.0001	0.0031	-0.0049	-0.4106	-0.4108	0.6318	0.10	0.03
0.1337	0.0169	0.1506	0.0000	0.0030	-0.0047	-0.3815	-0.3817	0.5874	0.09	0.03
0.1269	0.0172	0.1441	0.0000	0.0030	-0.0046	-0.3530	-0.3531	0.5446	0.10	0.03
0.1204	0.0174	0.1377	0.0000	0.0029	-0.0044	-0.3252	-0.3254	0.5024	0.10	0.02
0.1143	0.0175	0.1318	0.0000	0.0030	-0.0045	-0.2985	-0.2987	0.4617	0.10	0.02
0.1082	0.0175	0.1258	0.0000	0.0026	-0.0039	-0.2720	-0.2722	0.4213	0.10	0.02
0.1028	0.0176	0.1204	0.0000	0.0022	-0.0034	-0.2464	-0.2466	0.3821	0.10	0.02
0.0975	0.0176	0.1151	0.0000	0.0019	-0.0029	-0.2212	-0.2214	0.3434	0.10	0.02
0.0923	0.0176	0.1099	0.0000	0.0018	-0.0027	-0.1965	-0.1967	0.3054	0.10	0.01
0.0873	0.0176	0.1049	0.0000	0.0009	-0.0013	-0.1707	-0.1709	0.2659	0.11	0.01
0.0825	0.0176	0.1001	0.0000	0.0005	-0.0006	-0.1460	-0.1462	0.2279	0.10	0.01
0.0766	0.0176	0.0952	0.0000	-0.0001	-0.0003	-0.1226	-0.1228	0.1919	0.10	0.01
0.0750	0.0175	0.0925	0.0000	-0.0003	0.0000	-0.0999	-0.1000	0.1568	0.10	0.01
0.0720	0.0175	0.0895	0.0000	-0.0003	0.0005	-0.0781	-0.0783	0.1231	0.11	0.01
0.0657	0.0174	0.0870	0.0000	-0.0002	0.0004	-0.0574	-0.0576	0.0911	0.11	0.00
0.0679	0.0173	0.0852	0.0000	-0.0001	0.0002	-0.0370	-0.0372	0.0596	0.11	0.00
0.0672	0.0172	0.0834	0.0000	-0.0001	0.0002	-0.0269	-0.0270	0.0440	0.11	0.00
0.0668	0.0172	0.0819	0.0000	-0.0001	0.0002	-0.0167	-0.0168	0.0284	0.11	-0.00
0.0665	0.0171	0.0816	0.0000	-0.0000	0.0002	-0.0062	-0.0064	0.0123	0.11	-0.00
0.0665	0.0171	0.0816	0.0000	-0.0000	0.0001	0.0040	0.0038	-0.0034	0.11	-0.00
0.0667	0.0170	0.0817	0.0000	-0.0000	0.0001	0.0140	0.0142	-0.0140	0.11	-0.00
0.0668	0.0170	0.0818	0.0000	0.0000	0.0000	0.0244	0.0242	-0.0347	0.11	-0.00
0.0673	0.0170	0.0813	0.0000	0.0001	-0.0000	0.0344	0.0342	-0.0501	0.11	-0.01
0.0661	0.0170	0.0811	0.0000	0.0002	-0.0000	0.0443	0.0443	-0.0657	0.11	-0.01
0.0659	0.0171	0.0810	0.0000	0.0002	-0.0002	0.0649	0.0647	-0.0975	0.11	-0.01
0.0653	0.0173	0.0807	0.0000	0.0003	-0.0003	0.0855	0.0853	-0.1398	0.11	-0.01
0.6523	0.6523	0.6523	0.6523	0.6523	0.6523	0.6523	0.6523	0.6523	0.6523	0.6523
0.6516	0.6516	0.6516	0.6516	0.6516	0.6516	0.6516	0.6516	0.6516	0.6516	0.6516
0.6508	0.6508	0.6508	0.6508	0.6508	0.6508	0.6508	0.6508	0.6508	0.6508	0.6508
0.6499	0.6499	0.6499	0.6499	0.6499	0.6499	0.6499	0.6499	0.6499	0.6499	0.6499
0.6490	0.6490	0.6490	0.6490	0.6490	0.6490	0.6490	0.6490	0.6490	0.6490	0.6490
0.6481	0.6481	0.6481	0.6481	0.6481	0.6481	0.6481	0.6481	0.6481	0.6481	0.6481
0.6473	0.6473	0.6473	0.6473	0.6473	0.6473	0.6473	0.6473	0.6473	0.6473	0.6473
0.6464	0.6464	0.6464	0.6464	0.6464	0.6464	0.6464	0.6464	0.6464	0.6464	0.6464
0.6456	0.6456	0.6456	0.6456	0.6456	0.6456	0.6456	0.6456	0.6456	0.6456	0.6456
0.6448	0.6448	0.6448	0.6448	0.6448	0.6448	0.6448	0.6448	0.6448	0.6448	0.6448
0.6441	0.6441	0.6441	0.6441	0.6441	0.6441	0.6441	0.6441	0.6441	0.6441	0.6441
0.6433	0.6433	0.6433	0.6433	0.6433	0.6433	0.6433	0.6433	0.6433	0.6433	0.6433
0.6422	0.6422	0.6422	0.6422	0.6422	0.6422	0.6422	0.6422	0.6422	0.6422	0.6422
0.6398	0.6398	0.6398	0.6398	0.6398	0.6398	0.6398	0.6398	0.6398	0.6398	0.6398
0.6390	0.6390	0.6390	0.6390	0.6390	0.6390	0.6390	0.6390	0.6390	0.6390	0.6390
0.6385	0.6385	0.6385	0.6385	0.6385	0.6385	0.6385	0.6385	0.6385	0.6385	0.6385
0.6377	0.6377	0.6377	0.6377	0.6377	0.6377	0.6377	0.6377	0.6377	0.6377	0.6377
0.6369	0.6369	0.6369	0.6369	0.6369	0.6369	0.6369	0.6369	0.6369	0.6369	0.6369
0.6345	0.6345	0.6345	0.6345	0.6345	0.6345	0.6345	0.6345	0.6345	0.6345	0.6345
0.6299	0.6299	0.6299	0.6299	0.6299	0.6299	0.6299	0.6299	0.6299	0.6299	0.6299
0.6202	0.6202	0.6202	0.6202	0.6202	0.6202	0.6202	0.6202	0.6202	0.6202	0.6202
0.6099	0.6099	0.6099	0.6099	0.6099	0.6099	0.6099	0.6099	0.6099	0.6099	0.6099
0.5873	0.5873	0.5873	0.5873	0.5873	0.5873	0.5873	0.5873	0.5873	0.5873	0.5873
0.5045	0.5045	0.5045	0.5045	0.5045	0.5045	0.5045	0.5045	0.5045	0.5045	0.5045

DATE COMPUTED 07-JUL-81
TIME RECORDED 09149:10
DATE RECORDED 20-JUL-81
TIME RECORDED 101 5139
PROJECT NUMBER V43B-21

TABLE A-7. FORCE AND MOMENT DATA (CONT'D)

ARRIVE/CRISPAN FIELD SERVICES, INC.
AEDC DIVISION
VON KARMAN GAS DYNAMICS FACILITY
ARNOLD AIR FORCE STATION, TENNESSEE
RNO/SFI PART 1 FORCE TEST
PAGE 3

RUN	CODE	M	PT	TT	Q	P	RE	A	REF LENGTHS(CLM,CUN,CIL)
17	7	7.97	826.46	1352.7	3.451	0.007	98.6	0.360E+07	75.784 33.258 33.258
--- WIND AXES ---									
PN	ALPHA	BETA	PHT	CLM	CLMW	CCW	CLNW	CULW	CDW (L/D)W
1	20.00	0.03	0.09	0.6678	-0.5030	-0.0059	0.0038	0.0011	0.4187
2	10.00	0.03	0.09	0.6323	-0.4710	-0.0052	0.0033	0.0009	0.3829
3	10.00	0.03	0.09	0.5576	-0.4405	-0.0050	0.0032	0.0009	0.3502
4	17.00	0.03	0.10	0.5630	-0.4108	-0.0048	0.0031	0.0008	0.3194
5	16.00	0.03	0.09	0.5282	-0.3817	-0.0046	0.0029	0.0007	0.2905
6	15.00	0.03	0.10	0.4932	-0.3531	-0.0045	0.0029	0.0007	0.2635
7	14.00	0.02	0.10	0.4584	-0.3254	-0.0043	0.0028	0.0006	0.2383
8	13.00	0.02	0.10	0.4242	-0.2987	-0.0044	0.0029	0.0006	0.2152
9	12.00	0.02	0.10	0.3896	-0.2722	-0.0039	0.0025	0.0005	0.1935
10	11.00	0.02	0.10	0.3555	-0.2466	-0.0033	0.0022	0.0004	0.1738
11	10.00	0.02	0.10	0.3212	-0.2214	-0.0029	0.0019	0.0003	0.1556
12	9.00	0.01	0.10	0.2872	-0.1967	-0.0026	0.0017	0.0002	0.1390
13	8.00	0.01	0.11	0.2511	-0.1709	-0.0013	0.0009	0.0001	0.1234
14	7.00	0.01	0.10	0.2161	-0.1462	-0.0005	0.0004	0.0000	0.1096
15	6.00	0.01	0.10	0.1827	-0.1228	0.0004	0.0001	-0.0000	0.0982
16	5.00	0.01	0.10	0.1496	-0.1000	0.0006	-0.0003	-0.0000	0.0884
17	4.00	0.01	0.11	0.1178	-0.0783	0.0005	-0.0003	-0.0000	0.0805
18	3.00	0.00	0.11	0.0873	-0.0576	0.0004	-0.0002	-0.0000	0.0743
19	2.00	0.00	0.11	0.0572	-0.0372	0.0002	-0.0001	0.0000	0.0700
20	1.50	0.00	0.11	0.0473	-0.0270	0.0002	-0.0001	0.0000	0.0683
21	1.00	-0.00	0.11	0.0272	-0.0168	0.0002	-0.0001	0.0000	0.0673
22	0.50	-0.00	0.11	0.0117	-0.0064	0.0002	-0.0000	0.0000	0.0666
23	0.00	-0.00	0.11	-0.0034	0.0038	0.0001	-0.0000	0.0000	0.0665
24	-0.50	-0.00	0.11	-0.0184	0.0140	0.0001	-0.0000	0.0000	-0.0509
25	-1.00	-0.00	0.11	-0.0335	0.0242	0.0000	0.0000	0.0000	-0.0471
26	-1.50	-0.01	0.11	-0.0483	0.0342	-0.0000	0.0001	0.0000	-0.0486
27	-2.00	-0.01	0.11	-0.0633	0.0443	-0.0002	0.0002	-0.0000	-0.0703
28	-3.00	-0.01	0.11	-0.0937	0.0647	-0.0002	0.0002	-0.0000	-0.0749
29	-4.00	-0.01	0.11	-0.1245	0.0853	-0.0003	0.0002	-0.0000	-0.0813

DATE COMPUTED 27-JUN-8
TIME COMPUTED 09:49:11
DATE RECORDED 20-JUL-8
TIME RECORDED 10:513
PROJECT NUMBER V43B-21

TABLE A-7. FORCE AND MOMENT DATA (CONT'D)

REF LENGTHS(CLM,CLN,CLL)
33.258 33.258 33.258

A
75.784 0.360E+07 98.6 T RE

P
0.087 3.851 0

PT 1352.7 7.97 826.46 7

17

CONFIG 10.5/7 PICONIC
PROSE 0.5
SLICFS DOUBLE
FLAP 10
TRIP 60M

-- FLAP DIFFERENTIAL, BODY AXES --

PH	ALPHA	BETA	PHI	OCN	DCLN	DCY	DCLL	DCAT
1	20.00	0.03	0.09	0.0948	-0.0925	-0.0006	0.0004	0.0253
2	19.00	0.03	0.04	0.0888	-0.0868	-0.0000	0.0000	0.0234
3	18.00	0.03	0.09	0.0836	-0.0816	0.0002	-0.0001	0.0219
4	17.00	0.03	0.10	0.0790	-0.0769	0.0003	-0.0001	0.0205
5	16.00	0.03	0.09	0.0736	-0.0717	0.0003	-0.0002	0.0191
6	15.00	0.03	0.10	0.0688	-0.0668	0.0003	-0.0001	0.0178
7	14.00	0.02	0.10	0.0640	-0.0620	0.0002	-0.0001	0.0166
8	13.00	0.02	0.10	0.0593	-0.0579	-0.0001	0.0001	0.0156
9	12.00	0.02	0.10	0.0550	-0.0535	0.0002	-0.0000	0.0142
10	11.00	0.02	0.10	0.0516	-0.0495	0.0001	0.0000	0.0131
11	10.00	0.02	0.10	0.0478	-0.0457	0.0003	-0.0002	0.0120
12	9.00	0.01	0.10	0.0440	-0.0423	0.0003	-0.0001	0.0110
13	8.00	0.01	0.11	0.0400	-0.0379	0.0004	-0.0002	0.0101
14	7.00	0.01	0.10	0.0355	-0.0336	0.0004	-0.0002	0.0088
15	6.00	0.01	0.10	0.0313	-0.0295	0.0008	-0.0005	0.0078
16	5.00	0.01	0.10	0.0273	-0.0256	0.0010	-0.0006	0.0066
17	4.00	0.01	0.11	0.0236	-0.0221	0.0009	-0.0005	0.0057
18	3.00	0.00	0.11	0.0207	-0.0191	0.0009	-0.0006	0.0048
19	2.00	0.00	0.11	0.0181	-0.0165	0.0008	-0.0005	0.0041
20	1.50	0.00	0.11	0.0167	-0.0152	0.0009	-0.0006	0.0037
21	1.00	-0.00	0.11	0.0154	-0.0140	0.0009	-0.0006	0.0035
22	0.50	-0.00	0.11	0.0140	-0.0127	0.0008	-0.0005	0.0031
23	0.00	-0.00	0.11	0.0127	-0.0115	0.0009	-0.0005	0.0028
24	-0.50	-0.00	0.11	0.0119	-0.0106	0.0009	-0.0006	0.0026
25	-1.00	-0.00	0.11	0.0108	-0.0097	0.0009	-0.0005	0.0022
26	-1.50	-0.01	0.11	0.0101	-0.0089	0.0009	-0.0005	0.0020
27	-2.00	-0.01	0.11	0.0097	-0.0084	0.0007	-0.0005	0.0020
28	-2.50	-0.01	0.11	0.0083	-0.0072	0.0009	-0.0005	0.0016
29	-3.00	-0.01	0.11	0.0076	-0.0065	0.0007	-0.0004	0.0015

ACUREX CORPORATION
ATTN: Chuck Nardo
485 Clyde Avenue
Mountain View CA 94040

AEDC/DOT
Arnold AFS TN 37389

Aerospace Corp
ATTN: Al Robertson
P.O. Box 95085
Los Angeles, CA 90045

AFOSR/NA
Bolling AFB DC 20332

AFWAL/FIMG
Wright-Patterson AFB OH 45433

Arete Association
ATTN: Steve Lubard
P.O. Box 350
Encino, CA 91316

AVCO CORPORATION
ATTN: Noel Thyson
201 Lowell Street
Wilmington MA 01887

Ballistic Missile Defense Adv Tech Cntr
ATTN: Jim Papadopoulos (ATC-M)
P.O. Box 1500
Huntsville AL 35807

CALSPAN CORPORATION-AEDC
ATTN: Billy Griffith
Arnold AFS TN 37389

Calspan Corporation
Advanced Technology Cenbter
ATTN: Mike Holden
P.O. Box 400
Buffalo NY 14225

DRDAR-LCA-FB (Tom Hoffman)
US Army ARRADCOM
Dover NJ 07801

General Dynamics - Convair
ATTN: Archie Gay
P.O. Box 80847
San Diego, CA 92138

GENERAL ELECTRIC COMPANY/RESO
ATTN: Robert Neff
3198 Chestnut Street
Philadelphia PA 19101

Lockheed Missiles and Space Company
ATTN: Gerald Chrusciel
Dept 81-11
P.O. Box 504
Sunnyvale, CA 94086

Martin Marietta Corporation
ATTN: John Carmichael
P.O. Box 5837
Orlando FL 32805

MCDONNELL DOUGLAS ASTRONAUTICS COMPANY
ATTN: Jim Xerikos
5301 Bolsa Avenue
Huntington Beach CA 92647

Montana State University
ATTN: A. Demetriades
Bozeman MT 59714

NASA Langley Research Center
ATTN: Dennis Bushnell
Hampton VA 23665

NASA Ames Research Center
ATTN: Paul Kutler
Moffett Field, CA 94035

Naval Surface Weapons Center
ATTN: Frank Moore
Dahlgren VA 22448

Naval Surface Weapons Center
ATTN: Carson Lyons
White Oak Laboratory
Silver Springs MD 20910

PDA ENGINEERING
ATTN: Jim Dunn
1560 Brookhollow Drive
Santa Ana CA 92705

SANDIA LABORATORIES
ATTN: Al Bustamonte
P.O. Box 5800
Albuquerque NM 87185

TRW Defense & Space Systems Group
ATTN: M.J. Gyetvay, Bldg 88, rm 1012
One Space Park
Redondo Beach CA 90278

TRW/E & DS - Ballistic Missile Div
ATTN: L. Cassel
ATTN: Tony Lin
P.O. Box 1310
San Bernardino CA 92402

Virginia Polytechnic Institute
Blacksburg VA 24060
ATTN: Clark Lewis